

St. Petersburg State University of Information Technologies,
Mechanics and Optics
A.F. Ioffe Physical Institute of RAS, St. Petersburg

Book of abstracts

XIV International Feofilov symposium
on spectroscopy of crystals
doped with rare earth and transition metal ions



Sankt -Petersburg
2010

УДК 550.4: 543.42
ББК Д318
Т 67

XIV Международный Феофиловский симпозиум по спектроскопии кристаллов, активированных ионами редкоземельных и переходных металлов / Тезисы докладов (Санкт-Петербург, октябрь, 18-21, 2010). – СПб: СПбГУ ИТМО, 2010. – 183 стр.

Book of abstracts XIV International Feofilov symposium on spectroscopy of crystals doped with rare earth and transition metal ions (Sankt-Petersburg October 18-21, 2010)

This book contains the abstracts of the talks submitted to the XIV International Feofilov Symposium on Spectroscopy of Crystals Doped with Rare Earth and Transition Metal Ions held October 18-21, 2010 in St. Petersburg, Russia. The XIV-th Feofilov symposium continues a sequence of symposia started in 1965. The first nine symposia were held as national meetings. The X-th (St. Petersburg, 1995), XI-th (Kazan, 2001), XII-th (Ekaterinburg 2004) and XIII-th (Lake Baikal 2007) symposia, as well as the current one, were held with international participation.

The presented invited, oral and poster talks cover all aspects of theoretical and experimental studies of the phenomena related to the f- and d- ions in condensed matter. Relevant areas of research include condensed matter physics, material sciences and new techniques of such research.

Main topics of the symposium are: f- and d- ions in crystalline and non-crystalline insulators and semiconductors, energy transfer, electron-phonon interaction, dynamics and relaxation of excited states, charge transfer phenomena and charge ordering, cooperative processes, coherent phenomena, optical - microwave spectroscopy, spectroscopy of magneto-concentrated crystals, spectroscopy of nanocrystals, probing of organic and bio-materials, nonlinear spectroscopy, solid-state lasers, scintillators, phosphors, crystal chemistry aspects of developing new materials.

©Санкт-Петербургский государственный
университет информационных технологий,
механики и оптики, 2010
©Издательство СПбГУ ИТМО, 2010

ISBN 978-5-7577-0359-6.

Sponsored by

Russian Foundation for Basic Research

The non-profit Dynasty Foundation

Symposium Honorary Chairs:

Vladimir N. Vasiliev
Vyacheslav V. Osiko

SPb SU ITMO, St. Petersburg
A.M Prokhorov GPI RAS, Moscow

Symposium Chairs:

Alexander A. Kaplyanskii
Nikolay V. Nikonorov

A.F. Ioffe PTI RAS, St. Petersburg
SPb SU ITMO, St. Petersburg

Program Committee

T.T. Basiev
G. Boulon
G.N. Gerasimov
V.L. Ermolaev
S.P. Feofilov
A.A. Kaminskii
A.A. Kaplyanskii
S.Z. Malkin
V.G. Maslov
S.B. Mirov
A.E. Nikiforov
Yu.V. Orlovskii
E.A. Radzhabov
A.I. Ryskin
V.A. Smirnov
A.M. Tkachuk

Moscow - co-chair
Lyon
St. Petersburg
St. Petersburg
St. Petersburg
Moscow
St. Petersburg - co-chair
Kazan
St. Petersburg
Birmingham, AL
Ekaterinburg
Moscow
Irkutsk
St. Petersburg
Moscow
St. Petersburg

Local Organizing Committee

A.S. Rokhmin
E.B. Brui
A.B. Kutsenko

SPb SU ITMO, St. Petersburg – chair
SPb SU ITMO, St. Petersburg – vice-chair
PTI, St. Petersburg – vice-chair

Symposium Schedule

Monday, October 18

TIME	EVENT
14:00 – 19:00	Symposium Social Program, bus tour to Tsarskoe Selo (Katherine's Palace and park)

Tuesday, October 19

TIME	EVENT
10:00 – 10:30	Symposium Opening
10:30 – 12:00	Introductory session
12:00-12:30	Coffee Break
12:30-14:00	Oral session 1
14:00-15:30	Lunch
15:30-17:50	Oral session 2
17:50-19:00	Poster Session TuP
19:00	Social Program

Wednesday, October 20

TIME	EVENT
9:30 – 11:50	Oral session 3
11:50-12:10	Coffee Break
12:10 – 14:00	Oral session 4
14:00-15:30	Lunch
15:30 – 17:50	Oral session 5
17:50-18:10	Coffee Break
18:10 – 19:10	Oral session 6
19:10-20:15	Poster Session WeP

Thursday, October 21

TIME	EVENT
9:30 – 11:50	Oral session 7
11:50-12:10	Coffee Break
12:10 – 14:00	Oral session 8
14:00-15:30	Lunch
15:30 – 17:50	Oral session 9
17:50-18:10	Coffee Break
18:10 – 19:10	Oral session 10
19:10	Symposium Closing

TUESDAY, October 19

TUESDAY, October 19

10:00 – 10:30

SYMPOSIUM OPENING

10:00 Vladimir N. Vasiliev, *Rector of St. Petersburg University of ITMO*
Alexander A. Kaplyanskii, *academic of A.F.Ioffe PTI RAS, St. Petersburg*
Nikolay V. Nikonorov, *professor of St. Petersburg University of ITMO*

10:30 – 12:00

INTRODUCTORY SESSION

- 10:30 [Tu-I-1] COLOR CENTERS IN FLUORITE CRYSTALS: THE HISTORY AND PRESENT STATE
A.I. Ryskin, A.S. Shcheulin, A.E. Angervax
- 11:00 [Tu-I-2] RARE EARTH DOPANT SEGREGATION IN OPTICAL CERAMICS
G. Boulon^{1,2}, W. Zhao^{1,3}, S. Anghel^{1,4}, C. Mancini¹, D. Amans¹, T. Epicier⁵, V. Chani², A. Yoshikawa²
¹Physical Chemistry of Luminescent Materials (LPCML), University of Lyon, France
²IMRAM, Tohoku University, Japan
³University of Science and Technology of China, China
⁴Institute of Applied Physics, Republic of Moldova
⁵Matériaux, Ingénierie et Sciences (MATEIS), Université de Lyon, France
- 11:30 [Tu-I-3] NEW NANOGLASSCERAMICS DOPED WITH RARE EARTH AND TRANSITION METAL IONS: OPTICAL, SPECTRAL AND LUMINESCENT PROPERTIES
N. Nikonorov¹, V. Aseev¹, A. Ignatiev¹, A. Kim¹, E. Kolobkova², P. Shershnev¹, A. Sidorov¹, V. Tsekhomsky¹
¹ St. Petersburg University of Information Technologies, Mechanics, and Optics, Russia
²St. Petersburg State Technological Institute (Technical University), Russia

COFFEE BREAK

2:30-14:00

ORAL SESSION 1

- 12:30 [Tu-I-4] FLUORESCENCE AND VISIBLE UPCONVERSION IN HEAVILY DOPED $\text{LiNd}_x\text{La}_{1-x}\text{P}_4\text{O}_{12}$ NANOCRYSTALLINE POWDERS
W. Strek, L. Marciniak, A. Bednarkiewicz, A. Lukowiak, R.J. Wiglusz, D. Hreniak
Institute of Low Temperature and Structure Research, Polish Academy of Sciences, Wroclaw, Poland
- 13:00 [Tu-O-5] ENERGY TRANSFER PROBE FOR CHARACTERIZATION OF LUMINESCENT PHOTONIC CRYSTALS MORPHOLOGY
Yu.V. Orlovskii, T.T. Basiev, E.V. Samsonova, N.A. Glushkov
Prokhorov General Physics Institute RAS, Russia

TUESDAY, October 19

- 13:20 [Tu-O-6] MICRO-LUMINESCENCE SPECTROSCOPY OF Xe OPTICAL CENTER IN DIAMOND
Y.A. Dziashko¹, A.M. Zaitsev¹, Mengbing Huang², A.A. Gorokhovskiy¹
¹CUNY – The College of Staten Island and The Graduate Center, USA,
²The University at Albany, The State University of New York, USA
- 13:40 [Tu-O-7] LASER PIEZOSPECTROSCOPY OF Sm³⁺ IONS IN FLUORITE EPITAXIAL LAYERS
S.V.Gastev¹, V.A.Chernyshev², J.K.Choi³, A.V.Krupin¹, N.S.Sokolov¹, A.D. Nazemnykh²
¹Ioffe Physical-Technical Institute of the Russian Academy of Sciences, Russia
²Ural State University, Russia
³University of Canterbury, New Zealand

14:00 - 15:30 LUNCH

15:30-17:50

ORAL SESSION 2

- 15:30 [Tu-I-8] QUANTUM LIGHT STORAGE IN RARE-EARTH DOPED CRYSTALS: LARGE MULTIPLEXING CAPACITY OF TM:YAG.
T. Chanelière, M. Bonarota, V. Damon, R. Lauro, J. Ruggiero, R.C. Tongning, J.-L. Le Gouët
Laboratoire Aimé Cotton, France
- 16:00 [Tu-I-9] DECOHERENCE IN “MOLECULE MAGNETS” AND “SPIN-ORBIT” QUBITS
B. Barbara
Institut Néel-CNRS and INAC-CEA, Grenoble
- 16:30 [Tu-O-10] CRITICAL PHENOMENA AND FEMTOSECOND ORDERING DYNAMICS ASSOCIATED WITH ELECTRONIC AND SPIN ORDERED PHASES IN YVO₃ AND GdVO₃
R.V. Yusupov^{1,2}, D. Mihailovic², C. Colin^{3,4}, G.R. Blake³, T.T.M. Palstra³
¹Kazan Federal University, Russia
²Jozef Stefan Institute, Slovenia
³University of Groningen, The Netherlands
⁴Institut Neel, France
- 16:50 [Tu-O-11] SITE-SELECTIVE SPECTROSCOPY OF BaF₂:Yb³⁺ CRYSTALS
I.E. Mumdzhi, S.L. Korableva, S.I. Nikitin
Kazan Federal University
- 17:10 [Tu-O-12] GASEOUS ENVIRONMENT-SENSITIVE FLUORESCENCE OF Ce³⁺ IMPURITY IONS IN NANOCRYSTALS
S.P.Feofilov¹, D.V.Arsentyev¹, A.B.Kulinkin¹, R.I.Zakharchenya¹, T.Gacoin², G.Mialon², R.S.Meltzer³, C.Dujardin⁴
¹A.F. Ioffe Physical-Technical Institute, Russia
²Ecole Polytechnique – CNRS, France
³Department of Physics and Astronomy, University of Georgia, USA
⁴Université Lyon 1 69622 Villeurbanne, France

TUESDAY, October 19

- 17:30 [Tu-O-13] SPECTROSCOPIC AND LASER PROPERTIES OF TRIVALENT YTTERBIUM IONS IN ZnWO₄ CRYSTAL
E.V. Pestryakov¹, V.V. Petrov¹, V.I. Trunov¹, A.V. Kirpichnikov¹, M.A. Merzliakov¹, E.N. Galashov², V.N. Shlegel², J.V. Vasiliev²
¹ Institute of Laser Physics SB RAS, Russia
² Institute of Inorganic Chemistry SB RAS, Russia
- 17:50-19:00** **POSTER SESSION TuP**
- [Tu-P-1] LUMINESCENCE OF CO-DOPE α -ZnAl₂S₄ SPINEL TYPE SINGLE CRYSTALS
S. Anghel^{1,2}, G. Boulon², L. Kulyuk¹, S. Klokishner¹, K. Sushkevich³
¹Institute of Applied Physics, Republic of Moldova
²Physical Chemistry of Luminescent Materials, University of Lyon, France
³Moldavian State University, Republic of Moldova
- [Tu-P-2] MECHANISMS OF THE LOCAL STRUCTURAL TRANSITION OF MnO₄²⁻ MOLECULAR ION IN THE K₃Na(CrO₄)₂ FERROELASTIC
H.R. Asatryan, V.S. Vikhnin, T.I. Maksimova, M. Maczka, J. Hanuza**
Ioffe Physical Technical Institute of RAS, Russia.
*Institute for Low Temperature and Structure Research PAS, Poland
- [Tu-P-3] RESOLVED HYPERFINE STRUCTURE IN OPTICAL SPECTRA OF KY₃F₁₀:Ho³⁺
E.P. Chukalina, D.S. Pytalev
Institute of Spectroscopy, RAS, Russia
- [Tu-P-4] EXCITONS IN THE THIN FILMS OF Zn_{1-x}Mn_xO (X=0–0.06)
V. I. Sokolov¹, A. V. Druzhinin¹, N. B. Gruzdev¹, A. Dejneka², O. Churpita², Z. Hubicka², L. Jastrabik², V. Trepakov^{2,3}
¹ Institute of Metal Physics UD RAS, Russia
² Institute of Physics, Czech Republic
³ Ioffe Institute RAS, Russia
- [Tu-P-5] TIME-RESOLVED SPECTROSCOPY OF Ce³⁺-DOPED ALKALI GADOLINIUM PHOSPHATES
G. Stryganyuk^{1,2}, T. Shalapska¹, I. Pashyk¹, A. Voloshinovskii¹, A. Krasnikov³, S. Zazubovich³
¹Ivan Franko National University of Lviv, Ukraine
²Institute for Scintillation Materials, NAS of Ukraine, Ukraine
³Institute of Physics, University of Tartu, Estonia
- [Tu-P-6] SELFQUENCHING IN Tm-DOPED SODIUM-YTTRIUM DOUBLE FLUORIDE CRYSTALS (Tm:NYF)
S.E. Ivanova¹, A.M. Tkachuk^{1,2}, A. Mirzaeva², F. Pellé³
¹ University of Information Technology, Mechanics and Optics, Russia
² Scientific Production Corporation “S.I. Vavilov State Optical Institute”, Russia
³LCMCP UMR7574 CNRS - Université P&M Curie-ENSCP, France
- [Tu-P-7] ANOMALOUS LUMINESCENCE IN CaF₂:Yb²⁺ CRYSTAL FROM AB INITIO CALCULATIONS
A. Myasnikova, E. Radzhabov, A. Mysovsky
Vinogradov Institute of Geochemistry SB RAS, Russia,

TUESDAY, October 19

- [Tu-P-8] SPECTRAL AND LUMINESCENT PROPERTIES AND ENERGY TRANSFER OF LEAD-FLUORINE NANOGLASSERAMICS DOPED WITH ERBIUM AND YTTERBIUM
V. Aseev^{1}, E. Kolobkova², N. Nikonorov¹, E. Korchagin¹, V. Golubkov³, K. Moskaleva¹*
¹ Saint-Petersburg University of Information Technologies, Mechanics, and Optics, Russia
² Saint-Petersburg State Technological Institute (Technical University), Russia,
³ Institute of Silicate Chemistry of RAS, Russia
- [Tu-P-9] OPTICAL AND RADIO FREQUENCY OPTICALLY DETECTED EPR SPECTROSCOPY OF Sm³⁺ IN Cs₂NaYF₆ CUBIC CRYSTAL
M.L. Falin¹, K.I. Gerasimov¹, B.Z. Malkin², N.M. Khaidukov³
¹ Kazan Physical-Technical Institute of RAS, Russia
² Kazan Federal University, , Russia
³ Institute of General and Inorganic Chemistry of RAS, Russia
- [Tu-P-10] UPCONVERSION LUMINESCENCE IN Er³⁺/Yb³⁺ CODOPED Y₂CaGe₄O₁₂
I.I. Leonidov, V.G. Zubkov, A.P. Tyutyunnik, N.V. Tarakina, L.L. Surat
Institute of Solid State Chemistry, UB RAS, Ekaterinburg, Russia
- [Tu-P-11] PERCOLATION THRESHOLD FOR MAGNETIC BINDING IN THE STRUCTURE OF THE HALDANE CHAIN NIKELATES R₂BaNiO₅
V.A. Panfilov, A.V. Potapov, S.A. Klimin
Institute of spectroscopy RAS, Troitsk Moscow region, Russia
- [Tu-P-12] SPECTRAL AND DECAY TIME PROPERTIES OF Pr, Tb, Eu DOPED Gd₂O₂S CERAMICS
P.A. Rodnyi¹, E.I. Gorokhova², S.B. Eron'ko², V.A. Demidenko², S.B. Mikhrin¹, S.D. Gain¹
¹ St. Petersburg State Technical University, Russia
² Scientific Research and Technological Institute of Optical Material Science, S. I. Vavilov State Optical Institute All-Russia Science Center, Russia
- [Tu-P-13] PHOTOINDUCED RECHARGING Pb²⁺ → Pb³⁺ IN FERROELECTRIC LEAD GERMANATE
V.A. Vazhenin, A.N. Ivachev, M.Yu. Artyomov, A.P. Potapov
Research Institute of Physics and Applied Mathematics, Ural State University, Russia
- [Tu-P-14] IDENTIFICATION OF THE DEEP LEVEL DEFECTS IN BULK ALN: EPR STUDIES
V.A. Soltamov, I.V. Ilyin, A.A. Soltamova, E.N. Mokhov, P.G. Baranov
Ioffe Physical-Technical Institute, Russia
- [Tu-P-15] RARE EARTH FLUORIDE SPECIES IN ZEOLITE HOSTS
M. Lezhnina^{1,2}, U. Kynast¹
¹ Department of Chemical Engineering, Applied Materials Sciences, University of Applied Sciences Muenster, Germany
² on leave from Mari State Technical University, Department of Physics, Russia

TUESDAY, October 19

- [Tu-P-16] LASER SPECTROSCOPY OF TWO CENTRE OF Eu^{3+} IN SILICATE WITH APATITE STRUCTURE
A.M. Karpov, M.G. Zuev
Institute of Solid State Chemistry, Ural Branch Russian Academy of Science
- [Tu-P-17] CALCULATION OF Sm^{3+} OPTICAL SPECTRA IN $\text{CaF}_2:\text{Sm}$ STRAINED EPITAXIAL LAYERS ON SILICON
V.A. Chernyshev¹, A.E. Nikiforov¹, A.D. Nazemnykh¹, S.V. Gastev², N.S. Sokolov²
¹Ural State University, Russia
²Ioffe Physical-Technical Institute, Russia
- [Tu-P-18] LUMINESCENT PROPERTIES OF Am IN YTTRIUM ALUMINUM GARNET
Ya. V. Kuznetsova¹, B. E. Burakov², A. N. Trofimov¹, V. P. Usacheva¹, M. V. Zamoryanskaya¹
¹ Ioffe Physical-Technical Institute, Russia
² V. G. Khlopin Radium Institute, Russia
- [Tu-P-19] A TRANSIENT OPTICAL ABSORPTION SPECTROSCOPY OF $\text{Li}_6\text{Re}(\text{BO}_3)_3$ CRYSTALS
I.N. Ogorodnikov¹, N.E. Poryvay¹, I.N. Sedunova¹, A.V. Tolmachev², R.P. Yavetskiy², V.Yu. Yakovlev³
¹ Ural State Technical University, Russia
² STC Institute for Single Crystals, NAS of Ukraine, Ukraine
³ Tomsk Polytechnic University, Russia
- [Tu-P-20] ER CENTERS IN KTaO_3 : OPTICAL AND EPR SPECTROSCOPY STUDY
A.P. Skvortsov¹, V.A. Trepakov^{1,2}, N.K. Poletaev¹, Z Potucek², V.V. Laguta², L. Jastrabik²
¹ Ioffe Physico-Technical Institute RAS, Russia
² Institute of Physics AS CR, Czech Republic
- [Tu-P-21] LUMINESCENT PROPERTIES OF LANTHANIDE CARBOXYLATES UNDER TUNABLE DISTORTIONS OF Ln^{3+} COORDINATION POLYHEDRON
K. Zhuravlev¹, V. Tsaryuk¹, V. Zolin¹, A. Vologzhanina²
¹ V.A. Kotelnikov Institute of Radioengineering and Electronics of RAS, Russia,
² A.N. Nesmeyanov Institute of Organoelement Compounds of RAS, Russia
- [Tu-P-22] PRESSURE DEPENDENCE OF CRYSTAL, ORBITAL, AND MAGNETIC STRUCTURES OF LaMnO_3 AND $\text{LaMn}_{0.5}\text{Ga}_{0.5}\text{O}_3$
L.E. Gonchar^{1,2}, A.E. Nikiforov¹, Yu.V. Leskova¹, A.A. Firsin¹, D.P. Kozlenko³*
¹Ural State University, Russia;
²Ural State University of Railway Transport, Russia
³ Frank Laboratory of Neutron Physics, Russia

TUESDAY, October 19

- [Tu-P-23] NEAR-BAND GAP ELECTRONIC STRUCTURE OF THE TETRAGONAL RARE-EARTH AND BISMUTH CUPRATES
R.V. Pisarev¹, V.V. Pavlov¹, A.M. Kalashnikova^{1,3}, A.S. Moskvina²
¹A. F. Ioffe Physical-Technical Institute of RAS, Russia
²Ural State University, Russia
³Radboud University Nijmegen, The Netherlands
- [Tu-P-24] SUPER-HYPERFINE STRUCTURE OF EPR SPECTRA OF IMPURITY IONS WITH 4f AND 5f ELECTRONS IN DOUBLE FLUORIDES LiRF₄ (R=Y, Lu, Tm)
L.K. Aminov, A.A. Ershova, S.L. Korableva, I.N. Kurkin, B.Z. Malkin, A.A. Rodionov
Kazan Federal University, Russia
- [Tu-P-25] STRUCTURAL PHASE TRANSFORMATION AND PARAMAGNETIC RESONANCE OF THE Mn⁴⁺, Mn²⁺, Fe³⁺, Cr³⁺ AND Gd³⁺ CENTERS IN LANTHANUM GALLATE.
V.A. Vazhenin, V.B. Guseva, A.V. Fokin, A.P. Potapov, M.Yu. Artyomov
Research Institute of Physics and Applied Mathematics, Ural State University, Russia
- Tu-P-26] PULSE EXCITATION OF CERIUM DOPED CRYSTALS
V.I. Baryshnikov, A.V. Bolondz, D.V. Sannikova
Irkutsk State Railway University, Russia.
Irkutsk Filial of Laser Physics Institute at SB RAS, Russia.
Applied Physics Institute of Irkutsk State University, Russia.
- [Tu-P-27] CATHODOLUMINESCENT PROPERTIES OF YAG:Nd³⁺
K.N. Guliaeva, A.N. Trofimov, M.V. Zamoryanskaya
Ioffe Physical-Technical Institute, Russia
- [Tu-P-28] EPR STUDY OF THE VANADIUM DOPED FORSTERITE CRYSTAL
R.V. Yusupov¹, I.N. Subacheva¹, A.A. Rodionov¹, N.I. Silkin¹, V.B. Dudnikova², V.F. Tarasov³, E.V. Zharikov^{4,5}, M.Kh. Salakhov¹
¹Kazan Federal University, Russia
²Vernadsky Institute of Geochemistry and Analytical Chemistry of the Russian Academy of Sciences, Russia
³Zavoisky Physical-Technical Institute of the Kazan Scientific Center of the Russian Academy of Sciences, Russia
⁴Mendeleev University of Chemical Technology of Russia, Russia
⁵Prokhorov General Physics Institute of the Russian Academy of Sciences, Russia
- [Tu-P-29] LUMINESCENCE STUDY IN {Bi,Gd}₃(Ga,Ti)₅O₁₂ SINGLE CRYSTALLINE FILMS
N.V. Vasilieva¹, D.A. Spassky², Yu.V. Ryabchikov³, A.V. Platonova⁴, V.V. Radoshkin¹, V.N. Kolobanov⁴, V.G. Plotnichenko⁵
¹Prokhorov General Physics Institute RAS, Russia
²Skobeltsyn Institute of Nuclear Physics, M.V. Lomonosov Moscow State University, Russia
³Lebedev Physical Institute RAS, Russia
⁴Faculty of Physics, M.V. Lomonosov Moscow State University, Russia
⁵Fiber Optics Research Center RAS, Russia

TUESDAY, October 19

[Tu-P-30]

PHONON-ASSISTED MAGNETIC ABSORPTION IN LOW-DIMENSIONAL MAGNETIC SYSTEMS. OPTICAL DATA ON $\text{Gd}_2\text{BaNiO}_5$

S.A. Klimin¹, A.B. Kuzmenko², M.N. Popova¹, B.Z. Malkin³

¹ Institute of Spectroscopy RAS, Russia

² DPMC, University of Geneva, Switzerland

³ Kazan Federal University, Russia

19:00 Social Program

WEDNESDAY, October 20

WEDNESDAY, October 20

9:30 – 11:50

ORAL SESSION 3

- 9:30 [We-I-14] RARE EARTH DOPED NANOPARTICLES FOR HIGH RESOLUTION IMAGING
F. Pellé¹, L. Caillat¹, A. Tadili¹, B. Hajj², D. Chauvat², J. Zyss²
¹ LCMCP UMR7574 CNRS/UMPC/Chimie ParisTech, France
² LPQM, UMR 8537 CNRS, France;
- 10:00 [We-I-15] RADIATIVE PROPERTIES OF THE NANOCRYSTALS DOPED WITH LANTHANIDE AND TRANSITION METAL IONS
K.K. Pukhov, T.T. Basiev, Yu.V. Orlovskii
A.M. Prokhorov General Physics Institute RAS, Russia
- 10:30 [We-O-16] VISIBLE LUMINESCENCE OF NANOCRYSTALS
T.A.Kudykina, A.I.Pervak.
University “Ukraina”, Department of Engineering Technologies, Ukraine
- 10:50 [We-O-17] EPR OF IMPURITY d-ION COMPLEXES IN THE FLUORITE TYPE CRYSTALS: PECULIARITIES CAUSED BY THE JAHN-TELLER EFFECT ON TRIPLY DEGENERATED GROUND ORBITAL STATE
V.A. Ulanov^{1,2}, M.M. Zaripov², A.D. Siraev¹
¹Kazan State Energetic University,
²Zavoisky Physical Technical Institute RAS
- 11:10 [We-O-18] OPTICAL STUDIES OF THE UNIAXIAL STRESS-INDUCED ALIGNMENT OF JAHN-TELLER Cr²⁺ CENTERS IN KZnF₃ CRYSTAL
S.I. Nikitin, I.N. Subacheva, R.V. Yusupov
Kazan Federal University
- 11:30 [We-O-19] PHOTOLUMINESCENCE AND PHOTOLUMINESCENCE EXCITATION SPECTROSCOPY OF ZnO DOPED WITH Co AND Ni
V.I. Sokolov¹, V.A. Pustovarov², N.B. Gruzdev¹, V.T. Surikov³
¹ Institute of Metal Physics UD RAS, Russia
² Ural Federal University the name after The First President of Russia B.N. Yeltzin, Russia,
³ Institute of Chemistry of Solid State, Russia

COFFEE BREAK

WEDNESDAY, October 20

12:10 – 14:00

ORAL SESSION 4

- 12:10 [We-I-20] SPECTROSCOPY AND LASER OSCILLATIONS IN LOW PHONON CRYSTALS AND CERAMICS
T.T. Basiev, M.E. Doroshenko, A.M. Prokhorov
General Physics Institute RAS, Russia.
- 12:40 [We-O-21] RESEARCH OF CIRCADIAN RESPONSE FOR WHITE LIGHTING WITH Ce³⁺-DOPED GLASS PHOSPHOR AND UV/BLEU LEDS
L. Andrade^{1,2}, S. Lima¹, A. Novatski^{1,2}, A. Steimacher^{1,2}, M.P. Belançon^{3,2}, A. Neto³, A. Bento³, M. Baesso³, Y. Guyot², G. Boulon²
¹Grupo de Espectroscopia Óptica e Fototérmica, Universidade Estadual de Mato Grosso do Sul, Brazil
²Physical Chemistry of Luminescent Materials (LPCML), University of Lyon, France
³Departamento de Física, Universidade Estadual de Maringá, Brazil
- 13:00 [We-O-22] Ce(III)- AND Ce(IV)-RELATED SPECTRAL COMPONENTS OBSERVABLE IN THE UV ABSORPTION SPECTRA OF PHOTO-THERMO-REFRACTIVE GLASS MATRICES
A.M. Efimov, A.I. Ignatiev, N.V. Nikonorov, E.S. Postnikov
St. Petersburg State University of Information Technologies, Mechanics, and Optics
- 13:20 [We-O-23] 5d-4f EMISSION AND SCINTILLATION PROPERTIES OF SrF₂-Pr³⁺ AND SrF₂-Ce³⁺ CRYSTALS
R. Shendrik, E. Radzhabov
Vinogradov Institute of Geochemistry, Russia
- 13:40 [We-O-24] PUMP-PROBE EXPERIMENTS WITH CaF₂:Ce³⁺+Yb³⁺ CRYSTALS
A.S. Nizamutdinov, S.A. Kirysheva, V.V. Semashko, A.K. Naumov, S.L. Korableva, E.Yu. Gordeev
Kazan State University, Russia

14:00-15:30 LUNCH

15:30 – 17:50

ORAL SESSION 5

- 15:30 [We-I-25] CLUSTER THEORY OF THE CHARGE TRANSFER EXCITATIONS IN STRONGLY CORRELATED OXIDES
A.S. Moskvina
Ural State University, Russia
- 16:00 [We-I-26] INDUCTIVE-RESONANT THEORY OF NONRADIATIVE TRANSITIONS IN LANTHANIDE AND TRANSITION METAL IONS
E.B. Sveshnikova, V.L. Ermolaev
St. Petersburg State University of Information Technologies, Mechanics, and Optics, Russia
- 16:30 [We-O-27] PHOTOCONDUCTIVITY MEASUREMENTS IN Ce³⁺-DOPED FLUORIDES
L. Nurtdinova¹, V. Semashko¹, Y. Guyot², S. Korableva¹, M.-F. Joubert²
¹Kazan State University,
²Université Claude-Bernard Lyon 1

WEDNESDAY, October 20

- 16:50- [We-O-28] EFFECT OF IONIZING RADIATION ON STRUCTURE AND VALENCE STATE OF IMPURITY CHROMIUM IONS IN SYNTHETIC FORSTERITE AS STUDIED BY TUNABLE HIGH-FREQUENCY EPR SPECTROSCOPY
D.A. Akhmetzyanov¹, V.B. Dudnikova², A.A. Konovalov¹, V.F. Tarasov¹, E.V. Zharikov^{3,4}
¹Zavoisky Physical-Technical Institute of the Kazan Scientific Center of the Russian Academy of Sciences, Russia
²M.V. Lomonosov Moscow State University, Russia
³Mendeleev University of Chemical Technology of Russia, Russia
⁴Prokhorov General Physics Institute of the Russian Academy of Sciences, Russia
- 17:10 [We-O-29] CATHODOLUMINESCENCE STUDY OF Y(Ta,Nb)O₄:Tb³⁺-BASED POWDER PHOSPHORS
A.N. Trofimov¹, M.V. Zamoryanskaya¹, M.V. Nazarov², S.V. Andreev³, A.A. Zaytsev³
¹Ioffe Physical-Technical Institute, Russia,
²Department of Materials Science and Engineering, Gwangju Institute of Science and Technology, Republic of Korea
³St Petersburg Academic University — Nanotechnology Research and Education Centre
- 17:30 [We-O-30] THE FORMATION OF STABLE DIVALENT STATE OF Yb IONS IN THE CRYSTAL Na₄Y₆F₂₂: Ce³⁺, Yb³⁺ AFTER ACTION BY INTENSIVE UV IRRADIATION
D.I. Tselischev, A.K. Naumov, E.Yu. Koryakina, E.Yu. Gordeev, V.V. Semashko, S.L. Korableva
Kazan (Volga region) Federal University, Russia

COFFEE BREAK

18:10 – 19:10

ORAL SESSION 6

- 18:10 [We-O-31] CATHODOLUMINESCENCE OF WIDE GAPE CRYSTALS DOPED WITH RARE EARTH IONS
M.V. Zamoryanskaya, A.N. Trofimov, K.N. Guliaeva
Ioffe Physical Technical Institute, Russia
- 18:30 [We-O-32] ADIABATIC POTENTIAL IN ZNSE:Fe²⁺ CRYSTAL RECONSTRUCTED IN AN ULTRASONIC EXPERIMENT
V.V. Gudkov¹, I.V. Zhevstovskikh²
¹Ural Federal University, Russia
²Institute for Metal Physics, Ural Department of the Russian Academy of Sciences, Russia
- 18:50 [We-O-33] TERAHERTZ EPR-SPECTROSCOPY OF Fe²⁺ IONS IN THE NATURAL AND SYNTHETIC FORSTERITE
G.S. Shakurov, T.A. Shcherbakova, V.A. Shustov
Kazan Physical-Technical Institute RAS, Russia

WEDNESDAY, October 20

19:10-20:15

POSTER SESSION WeP

[We-P-31]

OPTICAL SPECTRUM OF Yb^{3+} IMPURITY CLUSTER IN CaF_2

V.A. Chernyshev, A.E. Nikiforov, V.P. Volodin

Ural State University, Russia

[We-P-32]

THE ORIGIN OF THE 1.6 eV ABSORPTION BAND IN THE RARE-EARTH HEXAGONAL MANGANITES RMnO_3 AND $\text{YMn}_{1-x}\text{Ga}_x\text{O}_3$

A.M. Kalashnikova,^{1,5} S.A. Basun,¹ A.S. Moskvina,² A.A. Nugroho,^{3,4} T.T.M. Palstra,⁴ Th. Rasing⁵, R.V. Pisarev¹

¹Ioffe Physical-Technical Institute, Russia

²Ural State University, Russia

³Solid State Materials Laboratory, Zernike Institute for Advanced Materials, University of Groningen, The Netherlands

⁴Faculty of Mathematics and Natural Sciences, Institut Teknologi Bandung, Indonesia

⁵Radboud University Nijmegen, Institute for Molecules and Materials, The Netherlands

[We-P-33]

TERBIUM LOW-LYING ENERGY LEVELS IN PYROCHLORE STRUCTURE $(\text{Tb}_x\text{R}_{1-x})_2\text{Ti}_2\text{O}_7$ STUDIED BY OPTICAL SPECTROSCOPY

M.V. Narozhny¹, S.A. Klimin¹, M.N. Popova¹, T. Lummen², P.H.M. van Loosdrecht², G. Dhalenne³

¹Institute for spectroscopy RAS, Russia

²Material Science Center, University of Groningen, the Netherlands

³Laboratoire de Physico-Chimie de l'État Solide, Université Paris-Sud, France

[We-P-34]

COHERENCE TIMES AND RABI OSCILLATIONS OF Cr^{5+} IONS IN CaWO_4

E.I. Baibekov, I.N. Kurkin, M.R. Gafurov, R.M. Rakhmatullin, G.V. Mamin

Kazan Federal University, Russia

[We-P-35]

UPCONVERSION LUMINESCENCE IN YTTERBIUM-SENSITIZED PRASEODYMIUM-DOPED LEAD-FLUORINE NANOGLASSERAMICS

K. Moskaleva¹, V. Aseev¹, E. Kolobkova², N. Nikonov, E. Korchagin¹, V. Golubkov³,

¹Saint-Petersburg University of Information Technologies, Mechanics, and Optics, Russia

²Saint-Petersburg State Technological Institute (Technical University), Russia,

Institute of Silicate Chemistry of RAS, Russia

WEDNESDAY, October 20

- [We-P-36] SPECTROSCOPIC, LASER INVESTIGATIONS AND CONCENTRATION QUENCHING OF TWO Yb³⁺-DOPED OH- FREE CALCIUM ALUMINOSILICATE LASER GLASSES
A. Steimacher^{1,2}, M.P. Belançon^{1,2}, A.N. Medina¹, L. Baesso¹, L.H.C. Andrade^{2,3}, S. Lima^{2,3}, R. Peretti², A.M. Jurdyc², A. Brenier², Y. Guyot², G. Boulon^{2}*
¹Departamento de Física, Universidade Estadual de Maringá, Brazil
²Physical Chemistry of Luminescent Materials (LPCML), University of Lyon, France
³Grupo de Espectroscopia Óptica e Fototérmica, Universidade Estadual de Mato Grosso do Sul, Brazil
- [We-P-37] MULTIFREQUENCY EPR STUDY OF Dy³⁺ IONS IN RbPb₂Cl₅
G.S. Shakurov¹, I.I. Fazlizhanov¹, V.A. Shustov¹, A.G. Okhrimchuk², N.V. Lichkova³, V.N. Zagorodnev³
¹Kazan Physical-Technical Institute of RAS, Russia
²Fiber Optics Research Center of RAS, Russia.
³Institute of Microelectronics Technology of RAS, Russia
- [We-P-38] LI-DOPING INDUCED GREAT ENHANCEMENT OF UPCONVERSION LUMINESCENCE IN Y₂O₃:Yb³⁺,Tm³⁺
M. Yin, J. Zhao, X. Wei, Y. Chen, W. Zhang
Hefei National Laboratory for Physical Sciences at Microscale, Department of Physics, University of Science and Technology of China, China
- [We-P-39] SPECTRAL AND LUMINESCENT PROPERTIES OF LEAD-FLUORINE NANOSTRUCTURED GLASSERAMICS DOPED WITH ERBIUM
V. Aseev^{1}, E. Kolobkova², N. Nikonorov¹, A. Yasukevich³, N. Kuleshov³, K. Moskaleva¹*
¹ Saint-Petersburg University of Information Technologies, Mechanics, and Optics, Russia
²Saint-Petersburg State Technological Institute (Technical University), Russia
³Research institute of optical material and technologies BNTU, Belarus
- [We-P-40] MONTE-CARLO SIMULATION OF ENERGY TRANSFER PROCESSES FOR INHOMOGENEOUS ACTIVATOR DISTRIBUTION
V.M. Sitdikov, N.V. Nikonorov, A.K. Przhevuskii
St. Petersburg State University of Information Technologies, Mechanics and Optics, Russia
- [We-P-41] OPTICAL SPECTROSCOPY OF THE CHAIN NICKELATE Sm₂BaNiO₅:CRYSTAL-FIELD INTERACTIONS AND MAGNETIC ORDERING
A.S. Galkin¹, S.A. Klimin¹, E.P. Chukalina¹, M.N. Popova¹, B.V. Mill²
¹ Institute of Spectroscopy RAS, Russia
² Moscow State University, Physics Department, Russia

WEDNESDAY, October 20

- [We-P-42] TWO-PHOTON PICOSECOND ABSORPTION DYNAMICS IN MeWO₄ CRYSTALS (ME=Zn, Pb, Ca, Sr, Ba)
V.I. Lukanin, D.S. Chunaev, A.Ya. Karasik
Prokhorov General Physics Institute RAS
- [We-P-43] ACCUMULATION OF EXCITATION ENERGY NANOPARTICLES FROM Ln(III) COMPLEXES AT DYE MOLECULE ADMIXTURE.
V.L. Ermolaev^{}, E.B. Sveshnikova, S.S.Dudar[']*
St. Petersburg State University of Information Technologies, Mechanics and Optics, Russia
- [We-P-44] TEMPERATURE DEPENDENCES OF THE SECOND RANK PARAMETERS b_2^0 AND P_2^0 FOR THE ODD ISOTOPES Gd³⁺ IN PbMoO₄ AND YVO₄
A.D. Gorlov, D.A. Gorlov
Institute of Physics and Applied Mathematics,
Ural State University, Russia
- [We-P-45] INTERCONFIGURATIONAL 4fⁿ - 4fⁿ⁻¹ 5d SPECTRA OF Pr³⁺ AND Tm³⁺ IN LiLuF₄ HOST
B.Z. Malkin¹, O.V. Solovyev¹, V.N. Makhov², G. Stryganyuk³, M. Kirm⁴, E. Garcia Villora⁵, K. Shimamura⁵
¹ Kazan Federal University, Russia
² P.N. Lebedev Physical Institute, Russia
³ Institute for Scintillation Materials NAS of Ukraine, Ukraine
⁴ Institute of Physics, University of Tartu, Estonia
⁵ Advanced Materials Lab., NIMS, Japan
- [We-P-46] ESA AND ACTIVATOR IONS PHOTOIONIZATION SPECTRA INVESTIGATIONS OF Ce:YLF AND Ce:LiLuF₄ SINGLE CRYSTALS
V.V. Pavlov, V.V. Semashko, A.K. Naumov, S.L. Korableva, L.A. Nurtdinova, A.S. Nizamutdinov
Kazan (Volga Region) Federal University, Russia
- [We-P-47] PHOTOLUMINESCENCE OF Zn_{1-x}Ni_xO SOLID SOLUTIONS WITH NaCl-TYPE SYMMETRY
V.I. Sokolov¹, V.A. Pustovarov², A.N. Baranov³, P.S. Sokolov³, N.B. Gruzdev¹
¹ Institute of Metal Physics UD RAS, Russia
² Ural Federal University the name after The First President of Russia B.N. Yeltzin, Russia,
³ M.V.Lomonosov Moscow State University, Russia
- [We-P-48] OPTICAL AND FAR-INFRARED SPECTROSCOPY OF MULTIFERROIC EuFe₃(BO₃)₄
T.N. Stanislavchuk^{1,2}, K.N. Boldyrev², M.N. Popova², B.Z. Malkin³
¹ Moscow Institute of Physics and Technology (State University), Russia
² Institute for Spectroscopy, RAS, Russia
³ Kazan Federal University, Russia
- [We-P-49] ELECTRON PARAMAGNETIC RESONANCE OF Dy³⁺ IONS IN A PbGa₂S₄ SINGLE CRYSTALS
H.R. Asatryan, V.A. Khramtsov, D.V. Kramushchenko, A.A. Gurin
Ioffe Physical Technical Institute of RAS, Russia

WEDNESDAY, October 20

- [We-P-50] FIRST-PRINCIPLES CALCULATIONS OF HYPERFINE INTERACTIONS IN IONS CRYSTALS
O.A. Anikeenok
Kazan State University, Russia
- [We-P-51] THE CHARGE TRANSFORMATION OF CHROMIUM ION IMPURITY UNDER LIGHT AND THERMAL ANNEALING IN SrTiO₃ SINGLE CRYSTALS STUDIED BY EPR
A.G. Badalyan¹, P. Galinetto², A.S. Gurin¹, M.C. Mozzati², V.A. Trepakov^{1,3}, J. Rosa³, L. Jastrabik³
¹ Ioffe Physical-Technical Institute, Russia
² Dipartimento di Fisica "A. Volta, Università di Pavia, CNISM-1-27100 Pavia, Italy
³ Institute of Physics, AS CR, Czech Republic
- [We-P-52] THE INVESTIGATION OF PHOTOCHROMISM IN CaF₂, SrF₂, BaF₂.
T.Y. Sizova, E.A. Radzhabov
The Vinogradov Institute of Geochemistry, Siberian Branch of Russian Academy of Sciences, Russia
- [We-P-53] SILICATE PHOTOLUMINOPHOR FOR CONVERSION OF RADIATION OF NITRIDE LIGHT-EMITTING DIODES
N.P. Soshchin, V.N. Lichmanova, V.A. Bol'shuhin
Science-Research Institute "Platan", Russia
- [We-P-54] EPR STUDY OF SOLID SOLUTION La_{1-0.33y}Ba_{0.33y}Mn_yAl_{1-y}O₃ (y = 0.02; 0.04; 0.10)
*R.R. Andronenko, S.I. Andronenko**
Institute of Silicate Chemistry RAN, Russia
*Kazan State University, Russia
- [We-P-55] SPIN DYNAMICS AND LOW SYMMETRY EFFECTS IN Gd³⁺ EPR SPECTRA OF SINGLE CRYSTAL OF EuAlO₃
*S.I. Andronenko**, *R.R. Andronenko*
Institute of Silicate Chemistry, Russia
*Physics Department, Kazan State University, Russia
- [We-P-56] ADDITIVE COLORATION OF CaF₂:Sm CRYSTALS
A.S. Shcheulin, T.S. Semenova, M.A. Petrova, L.F. Koryakina, A.E. Angervax, A.I. Ryskin
- [We-P-57] SPECTROSCOPIC PROPERTIES OF COLOR CENTERS IN CRYSTALS KY₃F₁₀: Ce AND KY₃F₁₀: Ce, Yb
E.Yu. Koryakina, A.K. Naumov, D.I. Tselitchev, S.L. Korableva, V.V. Semashko
Kazan (Volga region) Federal University, Kazan, Russia

WEDNESDAY, October 20

[We-P-58]

SPECTROSCOPY OF AN ION Ce^{+3} AS PROBE OF THE
COMPOSITION MULTILIGANDE GARNETS

N.P. Soshchin

The East-Chinese normal University, Shanghai, Peoples Republic Of
China

THURSDAY, October 21

THURSDAY, October 21

- 9:30 – 11:50** **ORAL SESSION 7**
- 9:30 [Th-I-34] PARALLEL BETWEEN RARE EARTH-TRAPPED EXCITON AND CHARGE TRANSFER IN RARE EARTH DOPED CRYSTALS
C. Pedrini¹, A. Belsky¹, A. Petrosyan², R.V. Sargsyan², I. Kamenskikh³
¹ Université de Lyon, Université Lyon 1, CNRS, UMR5620, France
² Institute for Physical Research, Laboratory of Crystal Growth of Luminescent Materials, Armenia
³ M.V.Lomonosov Moscow State University, Physics Department, Synchrotron Radiation Laboratory, Russia
- 10:00 [Th-O-35] LUMINESCENT PROPERTIES OF RARE EARTH IONS IN NANOSCALED LAYER STRUCTURES
M. Lezhnina^{1,2}, M. Bentlage¹, U. Kynast¹
¹ Department of Chemical Engineering, Applied Materials Sciences, University of Applied Sciences Muenster, Germany
² on leave from Mari State Technical University, Department of Physics, Russia
- 10:30 [Th-O-36] 5d-4f EMISSION OF Nd³⁺, Er³⁺, Tm³⁺, Gd³⁺ IONS IN ALKALINE EARTH FLUORIDES
E.A. Radzhabov, E.A. Prosekina
Vinogradov Institute of Geochemistry, Russian Academy of Sciences, Russia
- 10:50 [Th-O-37] LUMINESCENCE AND RECOMBINATION PROCESSES IN Li₆Gd_xY_{1-x}(BO₃)₃:Eu BULK CRYSTALS
I.N. Ogorodnikov¹, N.E. Poryvay¹, I.N. Sedunova¹, A.V. Tolmachev², R.P. Yavetskiy²
¹ Ural State Technical University, Russia
² STC Institute for Single Crystals, NAS of Ukraine, , Ukraine
- 11:10 [Th-O-38] LOW-TEMPERATURE STUDY OF INTRINSIC ELECTRONIC EXCITATIONS IN WIDE-GAP MATERIALS USING LUMINESCENT RE³⁺ AND Cr³⁺ IMPURITY IONS
Ch. Lushchik, I. Kudryavtseva, T. Kärner, A. Lushchik, F. Savikhin, E. Vasil'chenko
Institute of Physics, University of Tartu, Estonia
- 11:30 [Th-O-39] LASER-RELATED SPECTROSCOPY OF Ce³⁺:SrAlF₅ CRYSTALS
A.N. Yunusova, A.S. Nizamutdinov, V.V. Semashko, A.K. Naumov, S.L. Korableva, M.A. Marisov
Kazan Federal University, Russia

COFFEE BREAK

THURSDAY, October 21

12:10 – 14:00

ORAL SESSION 8

- 12:10 [Th-I-40] ZERO-PHONON LINES: NOVEL MANIFESTATIONS OF VIBRONIC INTERACTIONS IN IMPURITY CENTERS OF SOLIDS
V. Hizhnyakov
Institute of Physics, University of Tartu, Estonia
- 12:40 [Th-O-41] EXPERIMENTAL AND THEORETICAL RESEARCH OF LiF:Cu
A.S. Paklin, A.S. Mysovsky, A.A. Shalaev
- 13:00 [Th-O-42] NON-CONDON OPTICAL SPECTRA OF IMPURITY CENTERS IN CRYSTALS AT FINITE TEMPERATURES: THEORY AND EXPERIMENT
O.V. Solovyev¹, V.N. Makhov², G. Stryganyuk³, M. Kirm⁴
¹Kazan Federal University, Russia
²P.N. Lebedev Physical Institute, Russia
³Institute for scintillation materials, NAS of Ukraine, Ukraine
⁴Institute of Physics, University of Tartu, Estonia
- 13:20 [Th-O-43] RAMAN, INFRARED, AND VIBRONIC SPECTRA OF YbAl₃(BO₃)₄
K.N. Boldyrev¹, B.N. Mavrin¹, L.N. Bezmaternykh²
¹Institute of spectroscopy RAS, Russia
²Kirensky Institute of Physics, Russia
- 13:40 [Th-O-44] EXCHANGE-INDUCED MAGNETIC DIPOLE MECHANISM OF MAGNON SIDEBAND IN KCuF₃
M.V. Eremin^{1}, J. Deisenhofer², M. A. Fayzullin¹, Ch. Kant², A. Loidl²*
¹Kazan State University, Russia;
²Institute for Physics, Augsburg University, Germany

14:00-15:30 LUNCH

15:30 – 17:50

ORAL SESSION 9

- 15:30 [Th-I-45] HIGH-RESOLUTION SPECTROSCOPY OF RARE-EARTH ORTHOBORATES: CRYSTAL-FIELD AND ANISOTROPIC f-d EXCHANGE INTERACTIONS DEFECTS
M.N. Popova
Institute of Spectroscopy, RAS, Russia
- 16:00 [Th-I-46] PARTICULAR FEATURES OF ELECTRONIC STRUCTURE IN MULTIFERROIC OXIDES
R.V. Pisarev
Ioffe Physical-Technical Institute, Russian Academy of Sciences, Russia
- 16:30 [Th-O-47] SPECTROSCOPIC STUDY OF MULTIFERROIC TbMn₂O₅
E.P. Chukalina¹, M.N. Popova¹, M.A. Kaschenko^{1,2}, R.V. Pisarev³
¹Institute of Spectroscopy of RAS, Russia
²Moscow Institute of Physics and Technology, Russia
³Ioffe Physical-Technical Institute of RAS, Russia

THURSDAY, October 21

- 16:50 [Th-O-48] LUMINESCENCE AND ENERGY TRANSFER IN $\text{RE}^{3+}:\text{Kpb}_2\text{Cl}_5$ CRYSTALS AT UV EXCITONIC AND RE DIRECT EXCITATION
S.E. Ivanova¹, A.M. Tkachuk^{1,2}, F. Pellé³, L.I. Isaenko⁴, M.-F. Joubert⁵, Y. Guyot⁵
¹ University of Information Technology, Mechanics and Optics, Russia
² Scientific Production Corporation “S.I. Vavilov State Optical Institute”, Russia
³ LCMCP UMR7574 CNRS - Université P&M Curie-ENSCP, France
⁴ Institute of Mineralogy & Petrography SB RAS, Russia
⁵ LPCML, UMR 5620 du CNRS, Université Lyon 1, France
- 17:10 [Th-O-49] UPCONVERSION ABSOLUTE EFFICIENCY IN Er DOPED CALCIUM-YTTRIUM DOUBLE FLUORIDE CRYSTAL
S. Ivanova¹, F. Pellé², A.M. Tkachuk^{1,3}
¹ University of Information Technology, Mechanics and Optics, St. Petersburg, Russia
² LCMCP UMR 7574 CNRS - Université P&M Curie-ENSCP, France
³ Scientific Production Corporation “S.I. Vavilov State Optical Institute”, Russia
- 17:30 [Th-O-50] INFLUENCE OF THE ADDITIONAL EXCITED STATES ON ENERGY TRANSFER PROCESSES IN LANTHANIDE-CONTAINING COMPOUNDS
L.N. Puntus¹, K.A. Lyssenko², I.S. Pekareva¹
¹ Laboratory of Molecular Nanoelectronics, Institute of Radioengineering & Electronics, Russian Academy of Sciences, Russia
² X-ray Structural Center, A.N. Nesmeyanov Institute of Organoelement Compounds, Russian Academy of Sciences, Russia

COFFEE BREAK

18:10 – 19:10

ORAL SESSION 10

- 18:10 [Th-O-51] THE MANY-PARTICLE KINETICS OF THE HOPPING LUMINESCENCE QUENCHING IN DISORDERED SOLID SOLUTIONS
S.G. Fedorenko¹, Yu.V. Orlovskii², E.V. Samsonova²
¹ Institute of Chemical Kinetics and Combustion SB RAS, Russia
² Prokhorov General Physics Institute RAS, Russia

THURSDAY, October 21

- 18:30 [Th-O-52] PHOTOINDUCED COMPLEXES IN $\text{KTa}_{0.988}\text{Nb}_{0.012}\text{O}_3$ CRYSTALS: EPR STUDY
I.N. Subacheva¹, A.A. Rodionov¹, R.V. Yusupov¹, V.A. Trepakov^{2,3}, P.P. Syrnikov², A.I. Gubaev⁴, M.Kh. Salakhov¹
¹Kazan Federal University, Russia
²Ioffe Physical-Technical Institute, RAS, Russia
³Institute of Physics, ASCR, Czech Republic
⁴Basel University, Switzerland
- 18:50 [Th-O-53] ANOMALOUS LINE SHAPE OF EPR SPECTRA OF IMPURITY Ho^{3+} ION IN SYNTHETIC FORSTERITE
K.M. Salikhov¹, A.A. Sukhanov¹, V.F. Tarasov¹, R.B. Zaripov¹, E.V. Zharikov^{2,3}
¹Zavoisky Physical-Technical Institute of the Kazan Scientific Center of the Russian Academy of Sciences, Russia
²Mendeleev University of Chemical Technology of Russia, Russia
³Prokhorov General Physics Institute of the Russian Academy of Sciences, Russia
- 19:10 SYMPOSIUM CLOSING**

[We-O-28]

Effect of ionizing radiation on structure and valence state of impurity chromium ions in synthetic forsterite as studied by tunable high-frequency EPR spectroscopy

D.A. Akhmetzyanov¹, V.B. Dudnikova², A.A. Konovalov¹, V.F. Tarasov¹,
E.V. Zharikov^{3,4}

¹*Zavoisky Physical-Technical Institute of the Kazan Scientific Center of the Russian Academy of Sciences, Sibirskii trakt 10/7, Kazan, 420029 Russia*

²*M.V. Lomonosov Moscow State University, Leninskie Gory, Moscow, 119991 Russia*

³*Mendeleev University of Chemical Technology of Russia, Miusskaya pl. 9, Moscow, 125047 Russia*

⁴*Prokhorov General Physics Institute of the Russian Academy of Sciences, Vavilova ul. 38, Moscow, 119991, Russia*

Chromium-doped forsterite is well-known as a material for efficient tunable laser generation in the range of 1236-1300 nm. Recently tunable laser generation in the range of 1030–1180 nm was obtained on forsterite co-doped with chromium and lithium [1]. The aim of this work was to study the effect of ionizing radiation on the structure and valence state of paramagnetic centers formed by impurity chromium ions in synthetic forsterite. Samples were grown by the Czochralski method in the neutral argon or oxidizing atmosphere, irradiated with gamma-rays and high-energy electrons and studied by tunable high-frequency EPR spectroscopy.

Impurity chromium ions in forsterite form various types of paramagnetic centers differing by the valence of the chromium ions, their position in the forsterite crystal lattice and the type of the charge compensation upon heterovalent substitution.

The use of the quasi-optical waveguide and backward wave oscillators as a source of the microwave radiation allows one to obtain a two-dimensional pattern of magnetic field dependences of resonance frequencies for various transitions of chromium paramagnetic centers in the frequency range of 65 – 270 GHz at magnetic fields of 0 – 0.5 T [2]. It is shown that in non-irradiated samples there are single Cr²⁺ and Cr³⁺ ions substituting the Mg²⁺ ion in the forsterite crystal lattice and associate of Cr³⁺ ions with paramagnetic center. It is established that under ionizing radiation a small amount of Cr³⁺ ions transforms into Cr²⁺ ions. As a result, there appears a new type of associates, associate of Cr²⁺ ion with paramagnetic center. The integral intensities of the resonance transitions between electron levels of this associate are significantly lower than those of the single Cr²⁺ ion. Both associates are non-Kramers centers with an integer electron spin, though the electron spin of the Cr³⁺ ion is half-integer and that of the Cr²⁺ ion is integer.

Magnetic properties of these associates, their possible structure and effect of the ionizing radiation are discussed.

The work is partially supported by the RFBR grant 09-07-97006 and the grant of the President of the Russian Federation NSh -6267.2010.2

1. A.V. Gaister, E.V. Zharikov, V.F. Lebedev, A.S. Podstsvkin, S.Yu. Tenyakov, A.V. Shestakov, I.A. Shcherbakov, *Quantum Electronics*, 34, (8), 693-694 (2004)
2. V.F. Tarasov, G.S. Shakurov, *Appl. Magn. Reson.* 2, 571-576 (1991)

[Tu-P-24]

Super-hyperfine structure of EPR spectra of impurity ions with 4f and 5f electrons in double fluorides LiRF₄ (R=Y, Lu, Tm)

L.K. Aminov, A.A. Ershova, S.L. Korableva, I.N. Kurkin, B.Z. Malkin, A.A. Rodionov

Kazan Federal University, Kremlevskaya 18, 420008 Kazan, Russia

EPR spectra of double fluorides LiYF₄, LiLuF₄ and LiTmF₄ single crystals doped by rare-earth ions (Ce³⁺, Nd³⁺, Yb³⁺ -4fⁿ electrons) and U³⁺ ions (5f³ electrons) have been investigated on Bruker ESP 300 spectrometer at the frequency $\nu \approx 9.4$ GHz in the temperature range of 5 – 25 K. Note, that LiTmF₄ is Van Vleck paramagnet. The effective g-values of ions slightly differ in these crystals and for LiYF₄ they equal to: Ce³⁺ - $g_{\parallel} = 2.737$, $g_{\perp} = 1.475$; Nd³⁺ - $g_{\parallel} = 1.987$, $g_{\perp} = 2.554$; Yb³⁺ - $g_{\parallel} = 1.331$, $g_{\perp} = 3.917$; U³⁺ - $g_{\parallel} = 1.149$, $g_{\perp} = 2.508$.

The aim of the present work is the search and study of the super-hyperfine structure (SHFS) in the above mentioned systems. The results are the following.

Ce³⁺. The SHFS in single crystals LiYF₄:Ce and LiLuF₄:Ce was not found at $\mathbf{B}||c$. At $\mathbf{B}\perp c$ (and arbitrary orientation in *ab* plane) the SHFS is observed and consists of 5 components spaced by intervals ~ 0.9 mT = 18.6 MHz. In single crystals LiTmF₄, on the contrary, the SHFS of EPR was found only at $\mathbf{B}||c$. The number of the observed SHFS components also equals to 5 with intensity relation 1:4:6:4:1 and the interval between lines ~ 1.06 mT = 41 MHz.

Nd³⁺. The SHFS in single crystals LiYF₄:Nd and LiTmF₄:Nd is observed only at orientation $\mathbf{B}||c$. In both crystals SHFS consists of 9 components spaced by interval of ~ 0.55 mT = 15.4 MHz. In LiTmF₄ the linewidth of components is essentially greater than in LiYF₄.

Yb³⁺. In single crystals LiYF₄, LiLuF₄ and LiTmF₄ the SHFS for Yb³⁺ is observed only at orientation $\mathbf{B}||c$. The SHFS is similar for all crystals and consists of 17 components with spacing ~ 0.37 mT = 6.9 MHz.

U³⁺. In single crystals LiYF₄ and LiLuF₄ the SHFS for U³⁺ ions is observed at both orientations $\mathbf{B}||c$ and $\mathbf{B}\perp c$. At $\mathbf{B}||c$ SHFS contains up to nine components, the spacing between components being ~ 1.27 mT = 21.8 MHz. At $\mathbf{B}\perp c$ SHFS contains eleven components with spacing between components ~ 0.6 mT = 21.1 MHz. In single crystals LiTmF₄ the SHFS of U³⁺ is observed only at $\mathbf{B}||c$, the spectra being strikingly different from those of Li(Lu,Y)F₄:U³⁺. In LiTmF₄ the EPR spectrum consists of 5 components with intensity relation 1:4:6:4:1 spaced by interval ~ 3.68 mT = 62.5 MHz (at ~ 6 K). Each of 5 components has the finer structure analogous to that in SHFS of Li(Lu,Y)F₄:U³⁺.

SHFS of Li(Lu,Y)F₄: Ce³⁺, Nd³⁺, Yb³⁺ and U³⁺ is evidently due to two fours of fluorine ions forming the nearest coordination spheres of these ions. The largest contribution to SHFS of U³⁺ and Ce³⁺ in the LiTmF₄ crystal is coming from Tm³⁺ ions of the fourth coordination sphere, which becomes possible due to highly enhanced, strongly anisotropic nuclear gyromagnetic tensor of thulium ions in the crystal. All characteristic features of the complex EPR spectra of rare-earth ions and U³⁺ ions introduced in double fluorides are qualitatively described by existing theories of super-hyperfine interactions and Van Vleck paramagnetism.

[We-I-21]

Research of circadian response for white lighting with Ce³⁺-doped glass phosphor and UV/blue LEDs

L. Andrade^{1,2}, S. Lima¹, A. Novatski^{1,2}, A. Steimacher^{1,2},
M.P. Belançon^{3,2}, A. Neto³, A. Bento³, M. Baesso³, Y. Guyot², G. Boulon^{2*}

¹*Grupo de Espectroscopia Óptica e Fototérmica, Universidade Estadual de Mato Grosso do Sul, UEMS, Dourados, MS, Brazil*

²*Physical Chemistry of Luminescent Materials (LPCML), University of Lyon, UCBLyon1, UMR 5620 CNRS, 69622 Villeurbanne, France*

³*Departamento de Física, Universidade Estadual de Maringá,, Maringá, PR, Brazil*

*E-mail: georges.boulon@univ-lyon1.fr

We are dealing with research of luminescent materials able to produce appropriated white light (WL), which is useful for light sources, combining a coated luminescent phosphor material, onto a blue or UV InGaN or GaN-based light-emitting diodes (LEDs) chip. Among many materials [1-4], especially Ce³⁺ ion is interesting for phosphors due its short life time (about 50ns), broad emission band centered in the range of 350 to 550nm assigned to the allowed electronic transition 5d→4f, and high quantum efficiency [5]. Although Ce³⁺:YAG, as either crystal or more recently ceramic, shows interesting properties for WL generation [6], this crystal has some disadvantages: it is expensive, difficult growing, demands high optimal Ce³⁺ concentration (~ 2 at.%) leading to fast luminescence quenching, the low color rendering index due to its weak emission intensities band in the red region [7]. There are few Ce³⁺-doped crystals emitting a broad emission band in the yellow region such as: Ce³⁺/Li⁺: Sr₃SiO₅, Ce³⁺: SrY₂O₄ and garnet structure materials as Ce³⁺: Y₃Al₅O₁₂, Ce³⁺: Tb₃Al₅O₁₂, Ce³⁺: Lu₃Al₅O₁₂, and Ce³⁺: Y₃Al₂Ga₃O₁₂.

We report the broad yellow emission band under blue excitation LEDs (405nm) in Ce³⁺-doped Low Silica Calcium Aluminum Silicate glass (Ce³⁺:LSCAS), easy to synthesize with shaping in casting procedures and with low cost production. The emission coordinates has been analyzed in the CIE 1931 x-y chromatic diagram showing that Ce³⁺:LSCAS presents WL emission close to the ideal WL point under excitation by blue LED. For the compared crystals, blue emission is very weak or even does not exist. The analyzed glass dispenses the use of a strong complementary blue light to obtain the WL. Besides, it permits to increase the thickness of the emission layer over the blue LED chip and thus increasing its emission efficiency. The blue emission of the Ce³⁺:LSCAS glass, that can be also easily obtained by a commercial UV LED, is very interesting for the regulation of the circadian rhythms control of humans. The two emissions can be obtained simultaneously in this glass. This is a great advantage for this material when compared with crystals. The possibility to use only one coat phosphor over two excitation sources should be an ideal solution to overcome the drawback found in WL LEDs-multi-phosphors based and to reach the natural day light simulation [8].

[1] E. F. Schubert and J.K. Kim. Science 308(2005)1274

[2] Z. Lei, G. Xia, L. Ting, G. Xiaoling, L. q. Ming, S. Guangdi. Microelectron. J.38(2007)1

[3] H. S. Jang and D. Y. Jeon. Appl Phys. Lett. 90(2007)041906-1

[4] D. Zhao, S. Seo and B. Bae. Adv. Mater. 19(2007)3473

[5] W. M. Yen, M. Raukas, A. A. Basun, W. van Schaik and H. Happek. J. Lumines. 69(1996)287

[6] E Zych, C Brecher and J Glodo. J. Phys.-Condes. Matter 12 (2000)1947

[7] H. S. Jang, W. B. Im, D. C. Lee, D. Y. Jeon and S. S. Kim. J. Lumines. 126(2007)371

[8] L. H. Andrade, S. M. Lima, A. Novatski, A. Steimacher, A. M. Neto, A. C. Bento, M. L. Baesso, Y. Guyot, G. Boulon, Applied Physics Letters L09-03690 (2009) and ECS Transactions (Electrochemical Society), Volume: 25, Issue: 9, Pages 237 - 246 (2009)

[We-P-54]
EPR study of solid solution $\text{La}_{1-0.33y}\text{Ba}_{0.33y}\text{Mn}_y\text{Al}_{1-y}\text{O}_3$
($y = 0.02; 0.04; 0.10$)

R.R. Andronenko, S.I. Andronenko*

Institute of Silicate Chemistry RAN, nab. Makarova 2, St-Petersburg, 199034, Russia

**Kazan State University, Kremlevskaya 18, Kazan, 420008, Russia*

Solid solution $\text{La}_{1-0.33y}\text{Ba}_{0.33y}\text{Mn}_y\text{Al}_{1-y}\text{O}_3$ ($y = 0.02; 0.04; 0.10$), prepared following ceramic technology, was investigated by EPR method at 77 K and 300 K.

Observed EPR spectra were interpreted as belonging to Mn^{2+} ions (at $T=77$ K $g = 2.04$; linewidth $\Delta H_{pp}=64 \times 10^{-4}$ T) and Mn^{4+} ions (at $T=77$ K, $g = 1.97$; $\Delta H_{pp} = 76 \times 10^{-4}$ T); as well as belonging to clusters of magnetically coupled Mn ions corresponding to broad line with linewidth at $T=77$ K $\Delta H_{pp} = 500 \times 10^{-4}$ T. The interpretation was based on rigorous simulation of experimental EPR spectra with software, which uses exact diagonalization of spin –Hamiltonian matrix. The dilution of Mn ions in solid solution of $\text{La}_{0.67}\text{Ba}_{0.33}\text{MnO}_3$ in diamagnetic LaAlO_3 , enable to investigate cluster formation and spin dynamics of Mn ions in such diluted system. In the system under investigation with Ba^{2+} ions, compared to system with Sr^{2+} ion, which has small ionic radius, EPR lines belonging to localized Mn ions are more intensive at room temperature and, in the same time, broad lines, belonging to Mn clusters, are very intense. The temperature dependence of linewidth, consistent with that in concentrated compounds, was observed. The clusters of $\text{La}_{0.67}\text{Ba}_{0.33}\text{MnO}_3$, diluted in LaAlO_3 , keep to some extent magnetic properties of initial manganite even at doping level of $y = 0.02$, and role of such clusters increased here compared to $\text{La}_{1-0.33y}\text{Sr}_{0.33y}\text{Mn}_y\text{Al}_{1-y}\text{O}_3$ [1].

In the samples, where, La^{3+} ion was partly substituted by Ba^{2+} ion ($x=0.33$), at 77 K isolated manganese ion were observed only at low concentration of Mn ($y=0.02$), in the same time at $y=0.04$ and 0.10 amount of clusters increases in great extent, what corresponds to the predominance of wide line ($\Delta H_{pp} = 500 \times 10^{-4}$ T)[2]. Observed EPR spectra at 300 K exhibit localized state of manganese ions along with clusters at all three concentration of manganese. Since, in investigated samples compared with Sr containing solid solutions, ferromagnetic interactions are much stronger in low temperature region, which is correlated with formation of the clusters, such as $\text{Mn}^{3+} - \text{Mn}^{4+} - \text{Mn}^{3+}$. These clusters include significant amount of manganese ions, while at $T = 300$ K, localized states play more important role.

Considerable difference in EPR spectra of samples of $\text{La}_{1-0.33y}\text{Ba}_{0.33y}\text{Mn}_y\text{Al}_{1-y}\text{O}_3$ and $\text{La}_{1-0.33y}\text{Sr}_{0.33y}\text{Mn}_y\text{Al}_{1-y}\text{O}_3$, as well with EPR spectra of $\text{LaAl}_{1-x}\text{Mn}_x\text{O}_3$ [3], clearly show, that Ba and Sr ions are included in magnetic clusters and these ions modify magnetic properties of these manganese clusters. Therefore, even at strong dilution in such systems, manganese clusters keep “the memory” about initial concentrated compounds, $\text{La}_{0.67}\text{Ba}_{0.33}\text{MnO}_3$ and $\text{La}_{0.67}\text{Sr}_{0.33}\text{MnO}_3$, respectively.

[1]. Andronenko S.I., Andronenko R.R., Zagrebel'ny O.A., Chezhina N.V., EPR study of compounds in the $\text{LaAlO}_3 - \text{Ln}_{0.67}\text{Sr}_{0.33}\text{MnO}_3$ system, *Glass Physics and Chemistry*, 2009, **35**(6), 652 -659.

[2]. Andronenko. S.I., Andronenko R.R., Zagrebel'ny O.A., EPR study of compounds in the $\text{LaAlO}_3 - \text{Ln}_{0.67}\text{Ba}_{0.33}\text{MnO}_3$ system, *Glass Physics and Chemistry*, 2010, **36**, accepted.

[3]. Dante C., Marco F., Giuliano M., Manlio O. and Piero P., $\text{LaAl}_{1-x}\text{Mn}_x\text{O}_3$ perovskite-type oxide solid solutions: structural, magnetic and electronic properties, *Phys. Chem. Chem. Phys.*, 2003, **5**(7),1467-1473.

[We-P-55]

Spin dynamics and low symmetry effects in Gd³⁺ EPR spectra of single crystal of EuAlO₃

R.R. Andronenko, S.I. Andronenko*

Institute of Silicate Chemistry RAN, nab. Makarova 2, St-Petersburg, 199034, Russia

**Kazan State University, Kremlevskaya 18, Kazan, 420008, Russia*

RAIO₃ (R = rare earth) single crystals, characterized by perovskite structure at and below room temperature, are interesting due to their phosphorescence and luminescence properties as well as for their use as laser materials. They also have the potential to provide high capacitance replacement for silicon dioxide gate dielectrics. A relevant detailed EPR study of the Gd³⁺ ion in a LaNbO₄ crystal was reported by Misra and Andronenko [1], which is also characterized by a low (C₂) point symmetry of the Gd³⁺ ion, similar to that in La₂Si₂O₇ [2].

Europium aluminate (EuAlO₃) is dielectric Van Vleck paramagnetic and its paramagnetism is due to the admixture, to the ground state, of levels of the ⁷F₁ term split by the orthorhombic field into three singlets (281,359, and 479 cm⁻¹). The influence of this term ⁷F₁ on Gd³⁺ EPR linewidth was investigated [3], however, low symmetry effects were not considered that time.

Electron paramagnetic resonance (EPR) studies on a single crystal of Van Vleck compound EuAlO₃ with the Gd³⁺ ion substituting for the Eu³⁺ ion, were carried out at X-band (9.4 GHz) over the 77 – 400 K temperature range. At these temperatures the single crystals of EuAlO₃ had the space symmetry group D_{4h}^{16} and rare-earth ions located at the Gd³⁺ sites had the point symmetry group C_s.

The asymmetry exhibited by the Gd³⁺ EPR line positions for the orientations of the external magnetic field about the Z and Y magnetic axes in the ZY plane was ascribed to the existence of monoclinic site symmetry at the site of the Gd³⁺ ion, as confirmed by the significant values of the spin-Hamiltonian (SH) parameters g_{yz} , b_2^{-1} , b_4^{-m} (m = 1, 3), b_6^{-m} (m = 1, 3, 5), estimated by fitting all EPR line positions observed at room temperature for the orientation of the magnetic field in the magnetic ZX and ZY planes using a rigorous least-square fitting procedure.

The novel features of the EPR study of the Gd³⁺ ion in EuAlO₃ crystal presented in this paper are as follows:

- (i) The SH parameters (b_n^m) for the Gd³⁺ ion situated at a Eu³⁺ site have been estimated accurately at 77 and 295 K. Additional set of EPR lines was observed, most likely from Eu²⁺ ions.
- (ii) Temperature dependence of Gd³⁺ linewidth was investigated and interpreted in the terms of “life-time” broadening.
- (iii) It was found, that dynamical dipolar and exchange interactions of impurity Gd³⁺ ions and host Eu³⁺ ions are responsible for EPR Gd³⁺ linewidth broadening.

[1]. Misra. S.K., Andronenko S.I., and Chemekova T. Yu., Variable temperature X-band EPR of Gd³⁺ in LaNbO₄ and PrNbO₄ crystals: Low-symmetry effect, influence of host and impurity paramagnetic ions on linewidth, and onset of antiferromagnetism, Phys. Rev. B, 2003, 67(21), 214411 (1-7).

[2]. Misra S. K. and Andronenko S. I., A variable temperature X-band EPR study of the Gd³⁺ ion in a La₂Si₂O₇ crystal characterized by monoclinic site symmetry, Applied Magnetic Resonance, 2007, 32(3), 377-384.

[3]. Andronenko S.I., Koroleva L.N., Bondar' I.A., and Ioffe V.A., Influence of levels of the ⁷F₁ term of Eu³⁺ on the ESR spectra of Gd³⁺ in EuAlO₃, Sov. Phys. Solid State, 1982, 24(5), 881 – 882.

[Tu-P-1]

Luminescence of co-dope α -ZnAl₂S₄ spinel type single crystals

S. Anghel^{1,2}, G. Boulon², L. Kulyuk¹, S. Klokishner¹, K. Sushkevich³

¹*Institute of Applied Physics, Academiei Str.5, Chisinau, MD-2028, Republic of Moldova*

²*Physical Chemistry of Luminescent Materials, University of Lyon, Claude Bernard Lyon1 University, UMR 5620 CNRS, La Doua, 69 622 Villeurbanne, France*

³*Moldavian State University, str. A. Mateevici 60, Chisinau, MD-2009, Republic of Moldova*

Optical properties of the metal transition-doped spinel structure have been studied elsewhere mainly with oxide compounds due to their potentially large area of implementation as the active media for solid-state lasers and a variety of interesting electrical, magnetic, and optical properties. The authors of this paper are currently dealing mostly with the investigations of the metal transition-doped sulphide spinel compounds.

The purpose in this work is the study of the radiative properties of the Co-doped α -ZnAl₂S₄ wide band-gap semiconductor. Bulk Co-doped α -ZnAl₂S₄ crystals with impurity concentration 0.1-0.5 at.% were grown by a closed tube vapor method with halogen as a transport agent. The X-ray diffraction measurements confirmed that the ZnAl₂S₄: Co samples was crystallized in the spinel structure with O_h ($Fd3m$) symmetry.

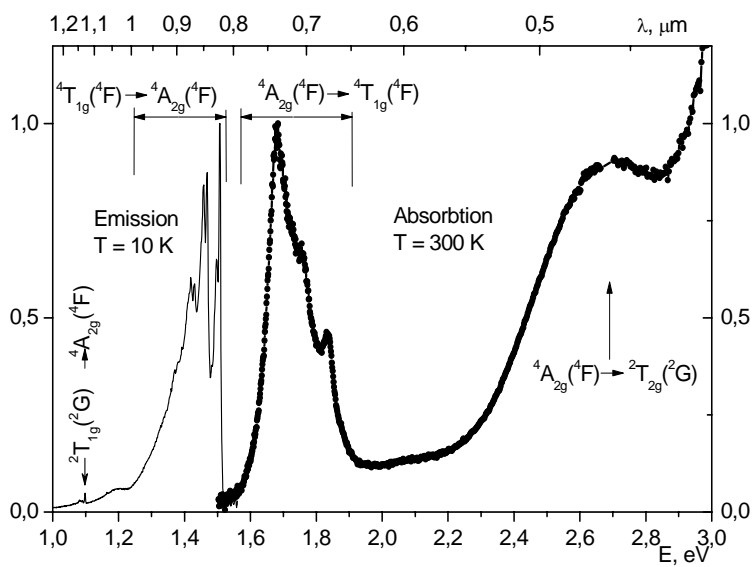


Fig.1 Absorption and emission spectra at different temperatures

The absorption spectra measured at room temperature in the wavelength range 320–2000 nm consist of at least four bands centered at 478, 705, 738 and 769nm, the last one being the most prominent. The excitation of the photoluminescence (PL) was provided by an OPO system at three wavelengths: $\lambda_{ex1}=496$ nm, $\lambda_{ex2}=533$ nm, and $\lambda_{ex2}=670$ nm (in the region of the absorption spectral bands). The PL measurements were carried out in the temperature range $T=10$ -300K.

The observed absorption and emission spectra (Fig.1) are assigned to electron transitions in the tetrahedral complex consisting of a Co²⁺-ion and four ligands of the sulfur atoms. The Co²⁺ ion has the d⁷ configuration and the energy level structure of the Co²⁺ ion in a tetrahedral site is similar to the level structure of d³ ions in octahedral sites. According to the Tanabe-Sugano diagrams, the bands at the 705, 738, and 769 nm detected in absorption spectrum, which are placed almost in the same spectral region as in other sulfurous compounds doped with Co²⁺ [1-2], are assigned to the transition from the ground state $^4A_{2g}(^4F)$ to the triple degenerated $^4T_{1g}(^4P)$ excited level.

An energy diagram is suggested to explain the temperature behavior of the observed PL spectra under different wavelengths of optical excitation.

- [1] Kim H-G and Kim W-T 1990 Optical absorption of ZnGa₂S₄ and ZnGa₂S₄:Co²⁺ crystals *Physical Review B* **41** 8541
 [2] Oh S K, Song H J, Kim W T, Kim H G, Lee C I, Park T Y, Jin M S and Yoon C S 2000 Impurity optical absorption of Co²⁺-doped MgAl₂S₄ and CaAl₂S₄ single crystals *Journal of Physics and Chemistry of Solids* **61** 1243-7

[We-P-50]

First-principles calculations of hyperfine interactions in ions crystals

O.A. Anikeenok

Kazan State University, Kremlevskaya, 18, Kazan 420008, Russian Federation
E-mail: Oleg.Anikeenok@ksu.ru

In Refs. [1,2] the secondary-quantization method is developed on the basis of partially non-orthogonal orbitals. For the first-principles calculations it is necessary to isolate some finite-domain V around of impurity ion, where all interactions should be write accurately and rest crystal consider in ions approximation. Arbitrary operator in V in orthonormalized multiparticle basis $|\{\xi\}\rangle$ according to Ref. [1] is determined as

$$H_{\Psi} = \sum_{n=0}^{\infty} c_n [Q, \bar{H}]^{(2n)}, \quad c_n = \frac{E_{2n}}{2^{2n} \times (2n)!}, \quad |\{\xi\}\rangle = \prod_{\xi} a_{\xi}^+ |0\rangle, \quad (1)$$

where H_{Ψ} is determined on the functions $|\{\xi\}\rangle$. E_{2n} in (1) are Euler number ($E_0 = 1, E_2 = -1, E_4 = 5, E_6 = -61, E_8 = 1385, E_{10} = -50521, \dots$). Series with c_n coefficient are convergent. \bar{H}, Q is detemined in [1,2], a_{ξ}^+ (a_{ξ}) is the creation (annihilation) operators for electron in V satisfy the conventional relations for Fermi operators.

The calculations two-center and one-center matrix elements of the Coulomb interaction between an electron and infinite ionic crystal lattice are necessary in present approach. There is no any estimation of these matrix elements. Let the orbital is taken in the Gaussian expansion form (GTO). Then these matrix elements can be calculated accurately using the approach of paper [3]. Let the ion with q_j charge is in the site \mathbf{r}_j . For example the interaction p_x - electron of this ion with the infinite crystal lattice can be written as

$$E_j(p_x) = \frac{3\pi^{\frac{1}{2}}}{8} \sum a_i a_k \left(\frac{1}{\alpha_{ik}} \right)^{\frac{5}{2}} \left[\frac{4\pi}{v_c} \sum_{\mathbf{g}} \left(\frac{\mathbf{g}_x^2}{2\alpha_{ik}} - 1 \right) \frac{G_j(\mathbf{g})}{\mathbf{g}^2} \exp\left(-\frac{\mathbf{g}^2}{4\alpha_{ik}} \right) + \frac{4}{3} q_j \left(\frac{\alpha_{ik}}{\pi} \right)^{\frac{1}{2}} \right] \quad (2)$$

$G_j(\mathbf{g})$ is the structure factor of the crystal [3], \mathbf{g} is the vector of reciprocal lattice, $\alpha_{ik} = \alpha_i + \alpha_k$ is the sum exponents of Gauss exponent, v_c - volume of the unit cell.

Transferred hyperfine interactions (THFI) for Yb^{3+} ions in CsCaF_3 and Cs_2NaYF_6 single crystals are considered. Experiment shows that the relevant parameters for two studied matrices differ, in spite of the fact that the nearest environment of the rare earth ion is nearly identical. A first-principles theoretical analysis is performed for the THFI parameters of the first coordination shell of F^- ions. Several mechanisms of metal ion-ligand coupling are considered and it is found that one of them, ligand polarization, explains the difference observed for the THFI parameters in Cs_2NaYF_6 and CsCaF_3 . Processes include the so-called core polarization of central ion are used in parametric approach [4]. In present study we considered these processes of our method.

[1] O. A. Anikeenok, Phys. Solid State **45**, 854 (2003).

[2] M. L. Falin, O. A. Anikeenok, V. A. Latypov, N. M. Khaidukov, F. Callens, H. Vrielinck, A. Hoefstaetter, Phys. Rev. B **80**, 174110 (2009).

[3] O. A. Anikeenok, MRSej **11**, 1 (2009).

[4] M. L. Falin, M. V. Eremin, H. Bill, D. Lovy, Appl. Magn. Reson. **9**, 329 (1995).

[We-P-49]

Electron paramagnetic resonance of Dy³⁺ ions in a PbGa₂S₄ single crystals

H.R. Asatryan, V.A. Khramtsov, D.V. Kramushchenko, A.A. Gurin

*Ioffe Physical Technical Institute of RAS, Politekhnicheskaya 26,
St. Petersburg, 194021, Russia. E-mail: hike.asatryan@mail.ioffe.ru*

Electron paramagnetic resonance (EPR) spectra of the rare-earth Dy³⁺ ions in a lead thiogallate (PbGa₂S₄) single crystal were studied in this report. The crystals were synthesized by Bridgeman-Stokbarger technique. EPR spectra were studied in the X-band in the large temperature range 4 – 300 K on JEOL standard radio spectrometer.

On the basis of a detailed study of the hyperfine structure of observed EPR lines in the lead thiogallate crystals, activated by dysprosium we can unambiguously assert that spectra belong to Dy³⁺ ions. Spectra consist of the intense line and two groups of low-intensity lines, each of which has of six equidistant lines. Naturally occurring dysprosium, besides its even isotope with zero nuclear spin ($I=0$), also has two odd isotopes, each of which has nuclear spin $I=5/2$. The natural abundance of these isotopes (¹⁶¹Dy and ¹⁶³Dy) is equal to 19.0 and 24.9 %, respectively, and the ratio of the nuclear magnetic moments ¹⁶¹Dy/¹⁶³Dy is equal to 1.41. The experimental spectrum looks exactly as one would expect for Dy³⁺. Two groups of six lines each are the components of the hyperfine structure for the odd isotopes, and the intense central line belongs to the even isotope. The ratio of the distances between the lines of the hyperfine structure in each group corresponds to the ratio of the nuclear magnetic moments of the odd isotopes, and the ratios of intensities of the lines in the spectrum corresponds to the natural abundances of the isotopes.

The EPR spectra belong to the Dy³⁺ ions in the ground state corresponding to the lower Stark sublevel G₇ of the ⁴H_{15/2} term. Because of the large splitting between the Stark components the excited state is not observed in the X-band. The spectra are anisotropic and can be described by the spin Hamiltonian of axial symmetry with an effective spin $S = 1/2$. The average value of the g tensor corresponds to the G₇ state in a cubic field. From comparison of experimental angular dependences of g-factors with the calculated values of the known G₆ and G₇ levels for the free atom it is shown that the lowest level of Dy³⁺ ion in PbGa₂S₄ single crystals is G₆.

There are three types of various paramagnetic centers of Dy³⁺ ions, denoted as Dy1, Dy2 and Dy3. Dysprosium ions are assumed to substitute for lead ions in the PbGa₂S₄ crystal lattice. The observation of three nonequivalent paramagnetic centers corresponds to the three structural positions Pb1, Pb2 and Pb3 of the lead ions in lead thiogallate lattice [1]. From experimental integral intensities ratio it is obtained that the Dy1, Dy2 concentration is approximately five times lesser than Dy3 centers. The hyperfine coupling constants for two odd isotopes and main values of g-tensor for all paramagnetic centers are found. The strong angular dependence of the EPR line width of Dy³⁺ ion, qualitatively corresponding to the increasing in the separation between components of the hyperfine structure in the EPR spectra is apparently due to the unresolved superhyperfine structure from the ligands.

This study was supported by Russian academy of sciences programs: «Spin-Dependent Effects in the Solids and Spintronics»; «The Supporting of Innovations and Developments»; «Fundamental investigation of nanotechnologies and nanomaterials», also by the RBRF project № 09-02-01409.

[1]. V.N. Kamenshchikov, V.A. Stefanovich, Z.P. Gad'mash, V.I. Sidey, L.M. Suslikov.
Sov. Phys. Solid State, **49** (2) 338 (2007).

[Tu-P-2]

Mechanisms of the local structural transition of MnO_4^{2-} molecular ion in the $\text{K}_3\text{Na}(\text{CrO}_4)_2$ ferroelastic

H.R. Asatryan, V.S. Vikhnin, T.I. Maksimova, M. Maczka*, J. Hanuza*

*Ioffe Physical Technical Institute of RAS, Politekhnikeskaya 26,
St. Petersburg, 194021, Russia. E-mail: hike.asatryan@mail.ioffe.ru*

**Institute for Low Temperature and Structure Research PAS, Wroclaw, Poland*

Structural Local Transition (LST) could be treated as spontaneous alteration and reconstruction of local center potential from single well to multi-well one or vice versa. SLT phenomenon takes place in the framework of temperature, external pressure or other type external parameter changes. SLTs were detected mainly due to EPR studies on the examples of classical insulators on the one hand and crystals with matrix structural phase transitions on the other. Here SLT were detected on the example of the crystals with matrix structural phase transitions: ferroelastic $\text{K}_3\text{Na}(\text{CrO}_4)_2$ doped with molecular ions MnO_4^{2-} .

The electron spin resonance saturation effects for the paramagnetic molecular impurity ion MnO_4^{2-} were observed. When analyzing the ESR saturation effects, we used also the data on temperature dependence of the ESR integrated intensities [1] near the local structural transition. This is primarily a sharp increase of the ESR integrated intensity with a decrease of temperature in a fairly narrow range: ($T < 4\text{K}$). The integrated intensity sharply increased by a factor of about 2.7. This behavior corresponds to qualitative change in the nature of the vibronic states, which is active in LST.

Based on experimental data on the ESR saturation effects and phenomenological expression for the temperature and spin-lattice relaxation time dependence of the ESR intensity we conclude the following. *First*, we have to deal with local transition from low symmetry state to high symmetry one when temperature lowering [1]. *Second*, the SLT phenomenon is appearing at low temperature region is rather far from the region of two ferroelastic matrix phase transitions with critical temperatures at 239 K and at 150 K. As a result, such a behavior suppresses strong enough mutual influence of these different type transitions and puts obstacles in the direct way of the SLT realization. *Third*, different type coexisting impurity centers related to coexisting of different EPR-spectra all corresponding to molecular paramagnetic ion MnO_4^{2-} are realizing in the case.

It is shown in the present work that all these peculiarities could be explained by multi-well anharmonic Jahn-Teller (JT) approach. Two different soft quasi-local JT-modes, temperature dependent both, are topical in the case. Their successive condensation induces two different type mechanisms of the SLT.

This study was supported by Russian academy of sciences programs: «Spin-Dependent Effects in the Solids and Spintronics»; «The Supporting of Innovations and Developments», also by the RBRF project № 09-02-01409 and by the DPS Program “Fundamental Spectroscopy”.

References

[1] V.S. Vikhnin, H.R. Asatryan, T.I. Maksimova et al, Phys. Sol. State, V.50, N.9, p. 1642 (2008)

[Tu-P-8]

Spectral and luminescent properties and energy transfer of lead-fluorine nanoglassceramics doped with erbium and ytterbium

V. Aseev^{1*}, E. Kolobkova², N. Nikonorov¹, E. Korchagin¹, V. Golubkov³, K. Moskaleva¹

¹ Saint-Petersburg University of Information Technologies, Mechanics, and Optics, 49 Kronverksy ave., Saint-Petersburg, 197101, Russia

² Saint-Petersburg State Technological Institute (Technical University) 26, Moskovskiy ave, Saint-Petersburg, 190013, Russia,

Institute of Silicate Chemistry of RAS, Adm. 2, Makarova emb., Saint-Petersburg, 19903, Russia

*E-mail: Aseev@oi.ifmo.ru

Lead-fluoride nano-glassceramics doped with ytterbium-erbium have been developed and synthesized. The size of crystalline phase achieved up to 40 nm. Spectral and luminescence properties of nano-glassceramics in visible, near IR spectral range and energy transfer from ytterbium to erbium have been investigated. The entry of RE ions in crystalline phase resulted in a broadening emission spectra and changing the energy transfer ratio. Ytterbium-erbium doped nano-glassceramics are promising candidates for different photonics applications, sensors, fiber and waveguide lasers.

Currently, transparent nano-glassceramics are of great interest for the modern element base of photonics. Because they stay at intermediate state between crystalline materials and glasses, these ceramics combine the best properties of crystals (high mechanical and thermal strength) and glasses (possibilities of pressing and molding, pulling optical fibers, and carrying out ion exchange to fabricate waveguide structures). If the dopants (erbium, neodymium, etc.) enter the crystalline phase, the spectral, luminescence and laser characteristics of glassceramics become close to those of laser crystal analogues. Glassceramics are heterogeneous structures formed upon annealing of glass due to the growth of crystalline phase in a glassy matrix

In the present work, samples of glass composition $30\text{SiO}_2\text{-}18\text{PbF}_2\text{-}7.5\text{Al}_2\text{O}_3\text{-}5\text{ZnF}_2\text{-}29\text{CdF}_2\text{-}3\text{YF}_3$ doped with different erbium concentration (0.05-0.5 mol %) and constant ytterbium concentration (5 mol%) have been developed and synthesized. In these systems, the crystalline phase is precipitated upon heat treatment. Rare-earth ions play a role of nucleation centers. An X-ray diffraction analysis of the samples after the secondary heat treatment showed that the crystalline phase has a composition of PbYOF_3 . In case of erbium glassceramics the lattice constant was 5.75 Å and in case of ytterbium - 5.67Å. Secondary heat treatment results to growing of mixed crystalline phase which contained ytterbium and erbium ions simultaneously. Increase of time treatment results in the increase of size of nanocrystals up to 30-40 nm.

Spectral and luminescence properties of virgin and thermal treated samples have been investigated in visible (0.4-0.8 μm) and near (1.5 μm) IR- ranges. It was shown that the luminescence lifetime at 1.5 μm and energy transfer from ytterbium to erbium probabilities changed during the treatment. The entry of rare-earth ions in crystal phase results in the widening of emission spectra because of fluoride surrounding. The thermal treatment results in appearance of Stark structure in absorption and luminescence spectra and their deformation.

[We-P-39]

Spectral and luminescent properties of lead-fluorine nanostructured glassceramics doped with erbium

V. Aseev^{1*}, E. Kolobkova², N. Nikonorov¹, A. Yasukevich³, N. Kuleshov³, K. Moskaleva¹

¹ Saint-Petersburg University of Information Technologies, Mechanics, and Optics, 49 Kronverksy ave., Saint-Petersburg, 197101, Russia

² Saint-Petersburg State Technological Institute (Technical University) 26, Moskovskiy ave, Saint-Petersburg, 190013, Russia,

³ Research institute of optical material and technologies BNTU, 65 b17 Nezavisimosti ave., Minsk 220013, Belarus

*E-mail: Aseev@oi.ifmo.ru

Lead-fluoride nano-glassceramics doped with erbium have been developed and synthesized. The size of crystalline phase achieved up to 40 nm. Spectral and luminescence properties of nano-glassceramics in visible, near and middle IR spectral range have been investigated. It was shown, that emitting probabilities of different transitions changed during thermal treatment. The entry of erbium ions in crystalline phase resulted in a broadening of emission spectra. Erbium doped nano-glassceramics are promising candidates for different photonics applications, sensors, fiber and waveguide lasers.

Currently, transparent nano-glassceramics are of great interest for the modern element base of photonics. Because they stay at intermediate state between crystalline materials and glasses, these ceramics combine the best properties of crystals (high mechanical and thermal strength) and glasses (possibilities of pressing and molding, pulling optical fibers, and carrying out ion exchange to fabricate waveguide structures). If the dopants (erbium, neodymium, etc.) enter the crystalline phase, the spectral, luminescence and laser characteristics of glassceramics become close to those of laser crystal analogues. Glassceramics are heterogeneous structures formed upon annealing of glass due to the growth of crystalline phase in a glassy matrix

In the present work, samples of glass composition $30\text{SiO}_2-18\text{PbF}_2-7.5\text{Al}_2\text{O}_3-5\text{ZnF}_2-29\text{CdF}_2-3\text{YF}_3$ doped with different erbium concentration (1-3 mol %) have been developed and synthesized. In these systems, the crystalline phase is precipitated upon heat treatment. Rare-earth ions play a role of nucleation centers. An X-ray diffraction analysis of the samples after the secondary heat treatment showed that the crystalline phase has a composition of PbYOF_3 . In case of erbium glassceramics the lattice constant was 5.75 Å. Increase of time treatment results in the increase of size of nanocrystals up to 30-40 nm.

Spectral and luminescence properties of virgin and thermal treated samples have been investigated in visible (0.4-0.8 μm) and near (1.5 μm) and middle (3 μm) IR- ranges. It was shown that the emitting probabilities of different transitions changed during the treatment. The entry of rare-earth ions in crystal phase results in widening of emission spectra because of fluoride surrounding. For spectral range around 1,5 μm we demonstrated the increase of emission spectra width for Er-doped glass-ceramics from 59 nm for the virgin glass up to 71 nm for the nano-glassceramic. The thermal treatment results in appearance of Stark structure in absorption and luminescence spectra and their deformation.

[We-P-51]

The Charge Transformation of Chromium Ion Impurity under light and thermal annealing in SrTiO₃ Single Crystals Studied by EPR

A.G. Badalyan¹, P. Galinetto², A.S. Gurin¹, M.C. Mozzati², V.A. Trepakov^{1,3}, J. Rosa³,
L. Jastrabik³

¹ *Ioffe Physical-Technical Institute, Politekhnicheskaya 26, 194021, St.Petersburg, Russia*

² *Dipartimento di Fisica "A. Volta, Università di Pavia, CNISM-I-27100 Pavia, Italy*

³ *Institute of Physics, AS CR, Na Slovance 2, 182 21, Prague 8, Czech Republic*

Functional ferroelectric oxides are the *materials-of-choice* in number applications from actuators to memory and spintronic devices. A key advantage is that their properties may be tailored by adding suitable impurities. Consequently, for improvement of compound performance a detailed knowledge of the defect structure and its impact on the materials properties is required. The problem of chromium impurity in SrTiO₃ crystal is old but the aspect of charge compensation and charge transformation is studied nowadays of a special interest with its attractive applications as resistance elements [1].

Cr-doped SrTiO₃ single crystals as grown, on thermally oxidized, and reduced were studied by means of Electron Paramagnetic Resonance (EPR) in the X-band range. The crystals were grown by the Furuuchi Chemical Corporation and contained 0.005% chromium in the melt. EPR spectra were recorded at the temperature range 4 – 300 K.

In all crystals of the Furuuchi Chemical Corporation Cr³⁺ and Cr⁵⁺ centres were observed. The temperature and angular dependences for as grown reduced and oxidized samples were performed. The linewidth of Cr³⁺ “cubic” centres were analyzed for all kinds of crystals. The strong charge compensation for impurities ions in SrTiO₃ crystals was confirmed. New axial chromium centres were founded. Possible models of the centres are discussed.

Acknowledgments.

This work has been supported by the Programs of RAS: "Spin-Dependent Effects in Solids and Spintronics"; "Support of Innovations and Elaborations"; and by the RFBR under Grants No 09-02-01409.

References

[1] F.La. Mattina, J.G. Bednorz *et. al.* Phys. Rev. B **80** (2009) 075122.

[We-P-34]
Coherence times and Rabi oscillations of Cr⁵⁺ ions in CaWO₄

E.I. Baibekov, I.N. Kurkin, M.R. Gafurov, R.M. Rakhmatullin, G.V. Mamin

Kazan Federal University, 420008 Kazan, Russian Federation

Recently, paramagnetic ions diluted in diamagnetic solid matrices have been proposed as possible qubit implementations [1]. The spin manipulation in such systems is achieved by application of short microwave (MW) pulses as part of electron spin resonance (ESR) experiments. Due to highly elaborated experimental techniques available in the field of magnetic resonance and relatively short qubit switching times such implementations are advantageous. The number of coherent single-qubit operations Q_M there may be as high as 10^4 [2].

In the present work we investigate decoherence processes responsible for the reduction of Q_M of Cr⁵⁺ ions in CaWO₄ single crystal (0.0006 at. % Cr⁵⁺). Temperature dependences of spin-lattice relaxation time T_1 and phase memory time T_M are measured in the range $T = 6-30$ K at high-frequency W and low-frequency S bands of ESR.

Since the host matrix CaWO₄ is diamagnetic, phase relaxation of Cr⁵⁺ ion arises mainly from magnetic dipole interactions with the neighbouring chromium ions. The dependence $T_M^{-1}(T)$ was calculated as the following sum:

$$T_M^{-1}(T) = \Gamma_{ID} + \Gamma_{SD}(T) + T_1^{-1}(T), \quad (1)$$

where Γ_{ID} and $\Gamma_{SD}(T)$ are the contributions from instantaneous and spectral diffusion processes, respectively [3]. A good agreement is found between the calculations employing Eq. (1) and experimental results.

In quantum computation, one needs to apply sufficient amount of successive MW pulses. Thus, apart from T_2 , the spin coherence time during the spin transition also affects Q_M . The measure of such coherence is the damping time τ_R of so-called Rabi oscillations (or transient nutations) [4]. These are quantum oscillations resulting from coherent absorption and emission of photons under the application of a long resonant MW pulse. Up to now, there is a considerable number of publications indicating anomalously fast damping of Rabi oscillations of paramagnetic impurities diluted in crystal matrices. The first observations [5] revealed the peculiar linear dependence of τ_R^{-1} on Rabi frequency $\Omega_R/2\pi$:

$$\tau_R^{-1} = \frac{1}{2}T_M^{-1} + \beta\Omega_R, \quad (2)$$

The first term in Eq. (2) is explained in the framework of Bloch model. However, to the best of our knowledge, there is still no satisfactory explanation of the term linear in Ω_R . For the values of Ω_R used in experiments, the second term in Eq. (2) usually exceeds the first one. The damping of transient nutations might in principle indicate some unclear decoherence process occurring in the presence of resonant MW field, and that would drastically decrease the coherence time of Cr⁵⁺ ions during the spin transitions and reduce the value of Q_M .

In the present work the damping of Rabi oscillations of Cr⁵⁺ ions in CaWO₄ single crystal is detected at both high- and low-frequency bands. The results of our measurements agree with Eq. (2), with $\beta = 0.11$ (W band) and $\beta = 0.009$ (S band).

In order to reveal the mechanism of the damping, we develop a model of transient nutations in the presence of MW field inhomogeneity inside the resonator. Relations between the damping time of Rabi oscillations, Rabi frequency and the size of the crystal sample placed at the centre of TE₀₁₁ mode cylindrical resonant cavity are obtained. A good agreement is found between calculated and measured decays of average longitudinal magnetization (Fig. 1). The decay pattern has essentially non-exponential, rather Lorentzian shape.

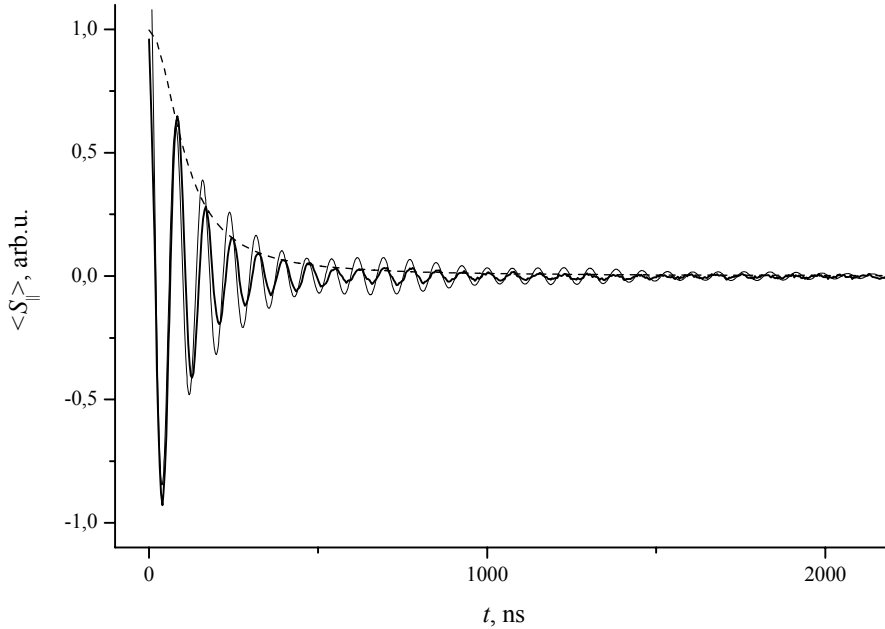


Fig. 1. Rabi oscillations obtained at the central ESR line of Cr⁵⁺ ion in CaWO₄ at *W* band. $\Omega_R = 8 \cdot 10^7 \text{ s}^{-1}$. Experimental data, the results of calculations, and the fit to the expression $\langle S_{\square}(0) \left(1 + (t/\tau_R)^2 \right)^{-1}$ are represented by thick solid, thin solid and dashed lines, respectively.

Bridged loop-gap resonant cavities and smaller sample dimensions are suggested to lower spin dephasing during transient nutations. Since during the nutations each individual spin state remains coherent, the field inhomogeneity does not affect Q_M . It is believed that the model developed here is applicable to recent observations of anomalous damping of Rabi oscillations in other magnetically diluted solids.

This work was partially supported by RFBR (grant N09-02-00930).

- [1] D. P. DiVincenzo, *Science* **270**, 255 (1995).
- [2] R. M. Rakhmatullin, I. N. Kurkin, G. V. Mamin, S. B. Orlinskii, M. R. Gafurov, E. I. Baibekov, B. Z. Malkin, S. Gambarelli, S. Bertaina, B. Barbara, *Phys. Rev. B* **79**, 172408 (2009).
- [3] K.M. Salikhov, S.A. Dzuba, and A.M. Raitsimring, *J. Magn. Res.* **42**, 255 (1981).
- [4] I. I. Rabi, *Phys. Rev.* **51**, 652 (1937).
- [5] R. Boscaino, F. M. Gelardi, J. P. Korb, *Phys. Rev. B* **48**, 7077 (1993).

[Tu-I-9] Decoherence in “molecule magnets” and “spin-orbit” qubits

B. Barbara

Institut Néel-CNRS and INAC-CEA, Grenoble

Rabi oscillations have been recently observed for the first time in Single Molecular Magnets (SMMs) ¹ and Rare-Earth ions (REs) ²⁻⁴.

The SMM qubit system consists in the well-known “nanometer $S=1/2$ “ V_{15} clusters embedded in a self-organized non-magnetic environment. Despite huge Hilbert space dimension (10^{15}), coherence times on the μs scale at He temperatures are observed and analyzed, showing an interplay between intramolecular (nuclear spins) and inter-molecular (electronic spins) decoherence. These qubits, of nanometer size, could be self-organized in supramolecular networks and addressed selectively.

The Rare-Earth qubits systems consist in paramagnetic ions (Gd^{3+} , Ho^{3+} , Er^{3+} , Yb^{3+} ...) diluted in a nonmagnetic matrix ($YLiF_4$, $CaWO_4$...). Despite spin-lattice coupling, coherence times reaching several tens μs at He temperatures have been observed and studied vs fields orientations evidencing a strong anisotropy of Rabi frequencies (isolated spin $1/2$ qubits are isotropic). This result, due to the effect of crystal-field in the presence of strong spin-orbit coupling, is quantitatively interpreted without free parameter. It could be used for new types of spin manipulations through applied field vectors. As for SMMs, decoherence has been studied on the basis of the spin-bath model ⁵.

Beyond the decoherence by the “natural” spin-bath, both types of qubits show a much stronger decoherence in the presence of microwaves, by what we call the “driven spin bath”, which is analyzed semiquantitatively (good order of magnitude).

[1] Bertaina S., Gambarelli S., Tkachuk A., Kurkin I., Malkin B., Stepanov A., and Barbara B., *Nature nanotechnology* 2, 39-42 (2007).

[2] Bertaina S., Gambarelli S., Mitra T., Tsukerblat B., Müller A., and Barbara B., *Nature* 453, (7192), 203-205 (2008).

[3] Bertaina S., Shim J.H., Gambarelli S., Malkin B. Z., and Barbara B., *Physical Review Letters* 103, 22, 226402 (2009).

[4] Bertaina S., Gambarelli S., Mitra T., Tsukerblat B., Müller A., and Barbara B., submitted.

[5] Prokofev N and Stamp P., *Journal of Low Temperature Physics* 104, 143 (1996).

[Tu-P-26]
Pulse excitation of cerium doped crystals

V.I.Baryshnikov, A.V.Bolondz, D.V.Sannikova

*Irkutsk State Railway University,
15 Chernyshevskogo, Irkutsk, 664074, Russia.
Irkutsk Filial of Laser Physics Institute at SB RAS,
130 a, Lermontova, Irkutsk, 664033, Russia.
Applied Physics Institute of Irkutsk State University,
20 Gagarin Blvd, Irkutsk, 664003, Russia. E-mail: vib@api.isu.ru*

The yield (η) of cathode-luminescence (CL) and X-ray-luminescence (XL) of Ce^{3+} ions in $Ce:LaF_3$ crystals corresponds with their concentration: $\eta = 0,1\%$ at Ce^{3+} 0,1 wt. %; $\eta = 0,01\%$ – Ce^{3+} 0,01 wt. %; $\eta = 0,001\%$ – Ce^{3+} 0,001 wt. %. It is explained by regular potential U^* in a vicinity of ions Ce^{3+} as $(La^{3+} - 5p^6, Ce^{3+} - 5p^6)$. In this case induced by radiation pulse a hot electrons (e) and holes (h) at coherent migration interact equally with ions of intrinsic substance and Ce^{3+} ions [1].

However an anomaly high the yield of emission (η) of nanosecond CL and XL of Ce^{3+} ions observes in crystals $Ce:YAlO_3$; $Ce:Y_3Al_5O_{12}$; $Ce:Y_2SiO_5$; $Ce:YLiF_4$; $Ce:LiLuF_4$, etc at concentration of $Ce^{3+} < 0,1$ wt. %. At that in a vicinity of ions Ce^{3+} potential U^* , formed by s -, p -, d -subgroups of valent electronic shell, as function from $(r + a)$ is irregular, Bloh principle is broken and therefore hot e and h effectively transfer energy to Ce^{3+} defects [1]. At that in these crystals η of Ce^{3+} CL and XL achieves $\sim 10\%$ at concentration of Ce^{3+} ions about 0,1 wt. %.

In the indicated group of crystals at the power N_2 -laser, x-ray and electron beam excitation of Ce^{3+} ions is found the "slowing" of lifetime of Ce^{3+} CL and XL. At 300 K in $Ce:Y_3Al_5O_{12}$ crystals the lifetime of Ce^{3+} PL is on 60 ns at N_2 -laser intensity about 50 kW/cm², but the lifetime of CL and XL of Ce^{3+} is to 125 ns.

At increase of intensity (I) of laser (337 nm) excitation of $Ce:Y_3Al_5O_{12}$ crystals the two-step ionization of Ce^{3+} ions take places (parabolic dependence of a photocurrent). At that are induced a hot e , but lifetime of Ce^{3+} PL is constant at $\tau = 60$ ns. In this case excitation of Ce^{3+} ions corresponds: $2h\nu \rightarrow Ce^{3+} \rightarrow Ce^{4+} + e, Ce^{4+} + e \rightarrow (Ce^{3+})^* \rightarrow h\nu(Ce^{3+}) + Ce^{3+}$ (1). At further increase I of laser excitation the dependence of a photocurrent shows on the two-photon ionization of intrinsic substance of $Ce:Y_3Al_5O_{12}$ crystals, i.e. it are induced hot e and h . At that lifetime of Ce^{3+} PL becomes equal 90 ns. From here with the account reaction (1) the excitation of Ce^{3+} CL, XL and PL with $\tau = 90 - 125$ ns occurs on reaction: $Ce^{3+} + e \rightarrow (Ce^{2+})^* + h \rightarrow (Ce^{3+})^* \rightarrow h\nu(Ce^{3+}) + Ce^{3+}$.

[1]. V.I. Baryshnikov, T.A. Kolesnikova, I. Kvapil. Phys. Sol. State (Rus.), 1994, V.36, № 9, p. 2788 - 2791.

Spectroscopy and laser oscillations in low phonon crystals and ceramics

T.T. Basiev*, M.E. Doroshenko

A.M. Prokhorov General Physics Institute RAS, Vavilov Str. 38, Moscow, Russia.

**E-mail: basiev@lst.gpi.ru*

Spectroscopic properties of low phonon fluoride and sulfide crystals doped with various RE³⁺ ions with heterovalent substitution of divalent matrix ions were investigated and their influence on oscillation properties of different RE³⁺ optical centers under selective optical pumping were determined.

Spectroscopic properties of Nd³⁺ ions in CaF₂ and SrF₂ crystals and ceramics were investigated. The absorption and fluorescence spectra (see Fig. 1 and Fig. 2) of different individual and clustered optical centers were observed depending on Nd³⁺ ions concentration. Two types of optical centers were found to predominate for low neodymium concentrations. The lifetimes of the high symmetry L-centers were measured and found to be two orders of magnitude longer than that for clustered M-centers (see Fig.3) at room temperature. The laser properties of SrF₂:Nd³⁺ crystal with neodymium ions concentration of 0.5 at.% containing high symmetry tetragonal optical centers together with low symmetry clustered M-centers were investigated under diode pumping. Using temperature tuning of laser diode pumping wavelength two different lines centered at about 1037 nm and 1044 nm attributed to oscillation of different optical centers were obtained (see Fig. 4).

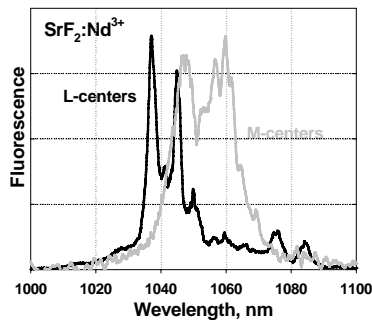


Fig. 1 Fluorescence spectra of L and M optical centers in SrF₂:Nd³⁺ crystal.

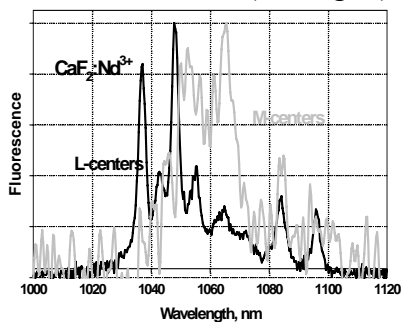


Fig. 2 Fluorescence spectra of L and M optical centers in CaF₂:Nd³⁺ crystal.

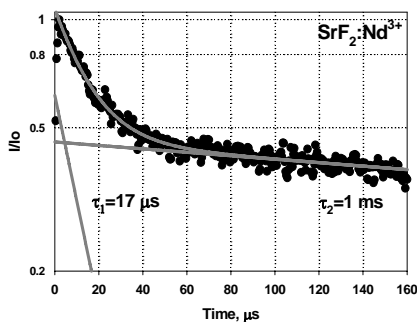


Fig. 3 Decay of L and M optical centers in SrF₂:Nd³⁺ crystal.

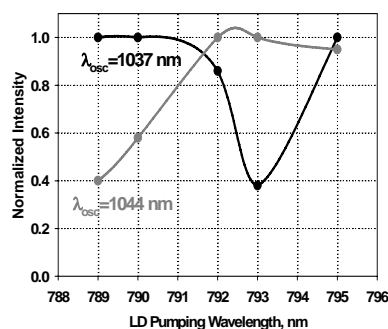


Fig. 4 Normalized intensity of oscillating lines vs LD pumping wavelength.

The investigation of spectroscopic properties of SrF₂:Yb³⁺ crystal and its solid solutions of CaF₂-SrF₂:Yb³⁺ and BaF₂-SrF₂:Yb³⁺ have shown that unlike known CaF₂:Yb³⁺ crystal all of them are characterized by less set of optical centers. Two types of Yb³⁺ optical centers namely highly symmetric cubic one and so-called low-symmetry center could be observed in SrF₂:Yb³⁺ crystal while additional tetragonal optical center could be seen in low temperature absorption spectrum of CaF₂:Yb³⁺ crystal. Using selective excitation and time resolved registration the fluorescence spectra for low-symmetry and cubic centers in SrF₂:Yb³⁺ crystal were measured and are

presented in Fig. 5. The two narrow lines at the upper graph are attributed to the fluorescence of cubic center though broad line is the residual fluorescence of low-symmetry center which can be also seen at the lower graph. In Fig.6 the fluorescence spectra of concentrated $\text{CaF}_2:\text{Yb}^{3+}$, $\text{SrF}_2:\text{Yb}^{3+}$ crystals and $\text{CaF}_2\text{-SrF}_2:\text{Yb}^{3+}$ and $\text{BaF}_2\text{-SrF}_2:\text{Yb}^{3+}$ solid solutions used in laser experiments are shown. As can be seen from the figure for concentrations of 3-4 at.% of ytterbium low-symmetry centers dominate and only broadband fluorescence could be observed in the spectrum. It should be noted that changes in the crystal field in the Ca-Sr-Ba row result in both shift of zero phonon line position (it is steadily shifted to shorter wavelengths) and changes in Stark splitting which allows to control the spectroscopic properties of Yb^{3+} ions by variation of solid solution composition. This allows to manipulate the gain properties of Yb^{3+} ions and obtain efficient lasing [1] and different tuning curves for different crystal compositions (see Fig. 7)

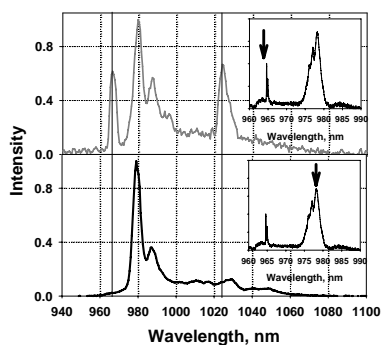


Fig.5 Fluorescence spectra of cubic (upper graph) and low-symmetry (lower graph) Yb^{3+} centers in SrF_2 crystal under selective excitation. The positions of excitation wavelengths are shown on the insertions.

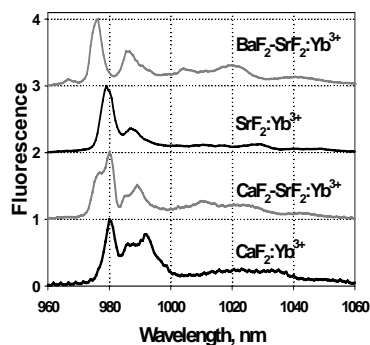


Fig.6 Fluorescence spectra of low-symmetry centers in CaF_2 and SrF_2 crystals and $\text{CaF}_2\text{-SrF}_2$ and $\text{BaF}_2\text{-SrF}_2$ solid solutions for concentrated crystals used in laser experiments.

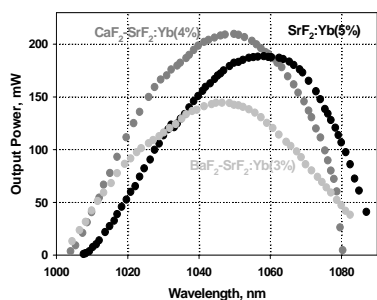


Fig. 7 Tuning curves of fluoride crystals under Laser Diode pumping.

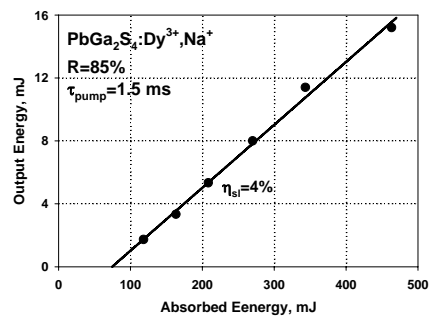


Fig. 8 Input-output characteristics of $\text{PbGa}_2\text{S}_4:\text{Dy}^{3+},\text{Na}^+$ crystal under $1.32\ \mu\text{m}$ $\text{YAG}:\text{Nd}^{3+}$ optical pumping.

The spectroscopic and oscillation properties of Dy^{3+} ions in PbGa_2S_4 and PbGa_2Se_4 crystals were also investigated and demonstrated that despite the existence of three different types of optical centers in this crystals no significant difference in spectroscopic properties of these centers could be observed. Rather efficient (slope efficiency up to 4%) laser oscillations in mid-IR spectral range were obtained for $1.32\ \mu\text{m}$ excitation by $\text{YAG}:\text{Nd}^{3+}$ and for $1.31\ \mu\text{m}$ excitation by laser diode. Long oscillation pulses up to several seconds were obtained despite self termination of both oscillating laser transitions. Possible scheme of lower laser level depopulation by pump radiation is suggested.

References:

[1]. Basiev T.T., Doroshenko M.E., Fedorov P.P., Konyushkin V.A., Kuznetsov S.V., Osiko V.V., Akchurin M.Sh., Efficient laser based on $\text{CaF}_2\text{-SrF}_2\text{-YbF}_3$ nanoceramics, *Opt. Lett.*, Vol. 33(5), pp.521-523, 2008.

[Th-O-43]
Raman, infrared, and vibronic spectra of YbAl₃(BO₃)₄

K.N. Boldyrev¹, B.N. Mavrin¹, L.N. Bezmaternykh²

¹*Institute of spectroscopy RAS, 142190, Moscow region, Troits, Russia*

²*Kirensky Institute of Physics, Siberian Branch of RAS, 660036, Krasnoyarsk, Russia*

In the YAl₃(BO₃)₄:Yb crystal, the phonon-assisted lasing was obtained at the wavelength 1130 nm with frequency tuning within 13.5 nm by changing the crystal temperature [1]. The self-frequency doubling resulted in a yellow laser radiation (560 – 570 nm) [1]. The study of the vibrational spectrum of YbAl₃(BO₃)₄ is particularly relevant in this regard. However, no comprehensive study of polarized Raman and far-infrared (FIR) spectra exist up to now but the available results are contradictory or inconsistent. In our previous work on the spectroscopy of ytterbium aluminum borate [2], preliminary results on the vibronic and unpolarized Raman spectra have been presented.

In this work, we studied the polarized Raman and FIR spectra of the YbAl₃(BO₃)₄ single crystal at room temperature. The group-theoretical analysis of the possible crystal lattice vibrations was carried out. The number of the observed vibrational modes in the spectra was in good agreement with the results of the factor-group analysis. To analyze the FIR data, we used the ReFFit program [3]. We present a list of the A₁, A₂, E_{TO}, and E_{LO} vibrational frequencies. The vibronic structure of the low-temperature absorption spectrum is compared with the reflection and Raman spectra. It was possible to identify most of the lines in the vibronic spectrum.

References

[1] P. Burns, J. Dawes, P. Dekker, J. Piper, J. Li, J. Wang, *Opt. Comm.* **207** 315 (2002).

[2] M. Popova, K. Boldyrev, P. Petit, B. Viana, L. Bezmaternykh, *J. Phys.: Condens. Matter* **20** 455210 (2008).

[3] <http://optics.unige.ch/alexey/reffit.html>

[Tu-I-2]
Rare earth dopant segregation in optical ceramics

G. Boulon^{1,2*}, W. Zhao^{1,3}, S. Anghel^{1,4}, C. Mancini¹, D. Amans¹, T. Epicier⁵,
V. Chani², A. Yoshikawa²

¹*Physical Chemistry of Luminescent Materials (LPCML), University of Lyon, UCBLyon1, UMR
5620 CNRS, 69622 Villeurbanne, France*

²*IMRAM, Tohoku University, Katahira 2-1-1, Aoba-ku, Sendai 980-8577, Japan*

³*University of Science and Technology of China, Hefei, Anhui 230026, China*

⁴*Institute of Applied Physics, Academiei Street 5, Chisinau MD-2028, Republic of Moldova*

⁵*Matériaux, Ingénierie et Sciences (MATEIS), UMR 5510 CNRS, Université de Lyon,
INSA-Lyon, 69621 Villeurbanne, France*

**E-mail: georges.boulon@univ-lyon1.fr*

New transparent polycrystalline ceramics used as optical materials can offer numerous advantages over single crystals [1-3]. Applications can be found in lasers, scintillators, (In,Ga)N-based phosphor-converted LEDs. Advantages of ceramics are low cost, sizes, high content of doping activators and ability to engineer profiles and structures. In front of such development of ceramics, there is a need to understand all mechanisms concerning the optimization of optical performances. The granular structure of ceramic materials is considered as a cause of non-uniform distribution of the doping ions across the grain boundaries and inside the grains. Thus, it is worthwhile to know more about this distribution. As a probe for this approach, we have selected Ce³⁺ and Yb³⁺ ions due to the first and last positions in the periodic table. We got Ce³⁺-doped (Gd,Y)₃Al₅O₁₂ garnet optical ceramic namely Ce³⁺-doped GYAG from Dr. H. Yagi, Dr. T. Yanagitani at Konoshima Company in Japan [4], Ce³⁺-doped YAG [5] and Yb³⁺-doped YAG [6] from Dr. Y. Shi, Prof. X. Q. Feng, Prof. Y. B. Pan at Shanghai Institute of Ceramics in China and Yb³⁺-doped Y₂O₃ from Dr. A. Ikesue, World Lab. Co., Ltd., Nagoya (Japan) [6]. We shall compare our results with those in Nd³⁺-doped YAG garnet ceramics [7]. Our main goal will be to show new experimental results from both, optical spectroscopy and spatially resolved techniques, as imaging confocal microscopy (ICM) and transmission electronic microscopy (TEM) and to interpret such data by the variation of segregation coefficients of rare earth ions in oxide optical ceramic like in growth of crystals from the melt and/or flux. The lower is the segregation coefficient of the dopant in the melt growth, the greater amount of dopant will be collected on the grain boundaries of the ceramic material[8]. It means that Yb³⁺-doped YAG or Yb³⁺-doped-Y₂O₃ laser ceramics should demonstrate better performances for application.

[1] A. Ikesue, I. Furusato, and K. Kamata, J. Am. Ceram. Soc. 78 (1995) 225-228

[2] V. Lupei, N. Pavel, and T. Taira: IEEE J. Quantum Electron. 38 (2002) 240.

[3] R.M. Yamamoto, C.D. Booley, K.P. Cutter, S.N. Fochs, K.N. LaFortune, J.M. Parker, P.H. Paks, M.D. Rotter, A.M. Rubenchik, and T.F. Soules: Proc. SPIE 6552 (2007) 655205

[4] W. Zhao, C. Mancini, D. Amans, G. Boulon, T. Epicier, Y.Min, H. Yagi, T. Yanagitani, T. Yanagida, A. Yoshikawa, Jap. J. of App. Phys. 49 (2010) 022602

[5] W. Zhao, S. Anghel, D. Amans, G. Boulon, T. Epicier, Y. Shi, X. Q. Feng, Y. B. Pan, V.Chani, A. Yoshikawa, Optical Materials, submitted on April 2010

[6] W. Zhao, S. Anghel, G. Boulon, T. Epicier, A. Ikesue, V. Chani, A. Yoshikawa, to be published

[7] M.O. Ramirez, J. Wisdom, H. Li, Y.L. Aung, J. Stitt, G.L. Messing, V. Dierolf, Z. Liu, A. Ikesue, R.L. Byer, V. Gopalan, Optics Express, 16(2008) 5966

[8] V. I. Chani, G. Boulon, W. Zhao, T. Yanagida, A. Yoshikawa, Jap. J. of App. Phys., accepted on April 13, 2010

[Tu-I-8]

Quantum light storage in rare-earth doped crystals: large multiplexing capacity of Tm:YAG.

T. Chanelière, M. Bonarota, V. Damon, R. Lauro, J. Ruggiero, R.C. Tongning, J.-L. Le Gouët

Laboratoire Aimé Cotton, CNRS-UPR 3321, Univ. Paris-Sud, Bât. 505, 91405 Orsay cedex, France

Mapping a quantum state of light into an atomic system is fundamentally interesting and may have a strong impact in the context of quantum communication and information processing [1]. Even if the first major experimental realizations involved atomic vapors during the past decade, doped solids are now considered as a valuable alternative thanks to very recent experimental developments [2]. The prospect of a quantum memory for light in solids follows a long tradition of optical storage investigation in spectral hole-burning (SHB) materials. The most promising storage protocols involve rare-earth-ion-doped crystals (REIC). They are designed in order to precisely exploit the main characteristics of these materials. For example, the large inhomogeneous broadening, as compared to a narrow homogeneous width, gives a large multiplexing capacity in the time domain. It is an original and important feature in the prospect of quantum repeaters.

As an introduction, we shall give a rapid overview of the different storage protocols and show how they are intimately related to the intrinsic properties of the REIC [3,4]. We shall briefly review the different figures of merit defining a quantum memory and present the current state of the art in REIC.

We specifically work on Tm:YAG whose coherence properties and interaction wavelength (793nm) are noticeable in that prospect [3]. Concerning the figures of merit, we more specifically focused on the retrieval efficiency [5,6]. It is intimately related to our capability of tailoring the inhomogeneous profile by SHB [6]. We also considered the multiplexing storage capacity of Tm:YAG. Thanks to an original preparation technique also based on SHB but exclusively employing a frequency-modulated diode laser, we have shown that a single spot in the crystal can store more than thousand sub-nanosecond pulses [7] (see **Fig. 1**).

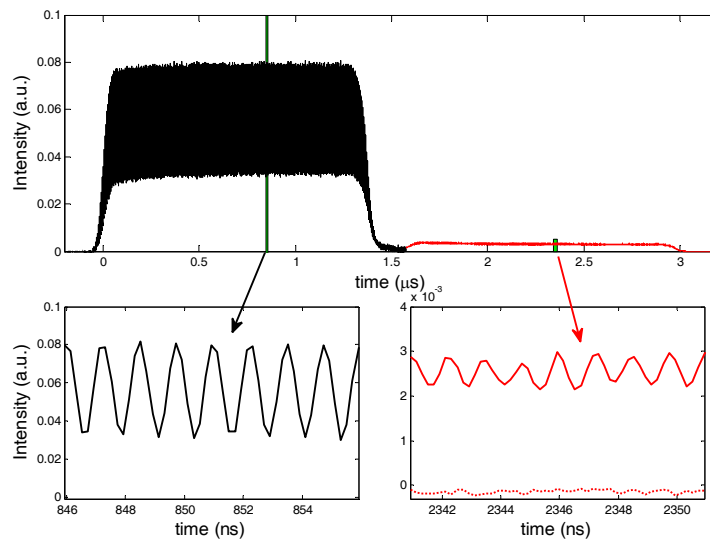


Figure 1 – Storage of a train composed of 1100 pulses (620ps duration) using the Atomic Frequency Comb protocol [5]. Left: transmitted pulse train – Right: retrieved pulses

References:

- [1] <http://quantumrepeaters.eu/>
- [2] M. P. Hedges, J. J. Longdell, Y. Li & M. J. Sellars, *Nature*, 465, 1052, (2010).
- [3] T. Chanelière, M. Bonarota, V. Damon, R. Lauro, J. Ruggiero, I. Lorgeré, and J.-L. Le Gouët, *J. Lumin.*, 130, 1572, (2010)
- [4] W. Tittel, M. Afzelius, R. Cone, T. Chanelière, S. Kröll, S. Moiseev and M. Sellars, *Laser Photonics Reviews*, 4 244, (2010).
- [5] T. Chanelière, J. Ruggiero, M. Bonarota, M. Afzelius and J.-L. Le Gouët, *New J. Phys.* 12, 023025 (2010).
- [6] M. Bonarota, J. Ruggiero, J.-L. Le Gouët, and T. Chanelière, *Phys. Rev. A* 81, 033803 (2010).
- [7] M. Bonarota, J.-L. Le Gouët, T. Chanelière, *in preparation*.

[Tu-P-17]

Calculation of Sm³⁺ optical spectra in CaF₂:Sm strained epitaxial layers on silicon

V.A. Chernyshev^{1*}, A.E. Nikiforov¹, A.D. Nazemnykh¹, S.V. Gastev², N.S. Sokolov²

¹*Ural State University, 51 Lenin av., Ekaterinburg, 620083, Russia*

²*Ioffe Physical-Technical Institute, 26 Polytechnicheskaya, St. Petersburg, 194021, Russia*

* *Corresponding author: vladimir.chernyshev@usu.ru*

Optical spectra of Sm³⁺ in CaF₂:Sm epitaxial layers grown on Si(111) by MBE method with different planar strain have been calculated. The atomic structure of the impurity centers was found by computer simulation technique in the shell model formalism of the pair potential approximation [1]. The influence of silicon substrate on CaF₂ layers were taken into account in the calculations. Impurity centers with local and non-local charge compensation have been considered.

We used a standard for the lanthanide ion ‘effective Hamiltonian’ for 4f electrons that acts only within the 4f configuration [2]. For the calculations we used programs written by Dr Michael F Reid (University of Canterbury), given to us by the author. Crystal-field parameters were calculated in the exchange charge model [3].

The work is supported by State Contract № P1462 and Program of Russian Academy of Sciences “Fundamental optical spectroscopy and its applications”. The authors would like to acknowledge Professor B.Z. Malkin (Kazan State University).

References

- [1] V.A.Chernyshev , A.V. Abrosimov, S.V. Gastev, A.V. Krupin, A.E. Nikiforov, J.K. Choi, R.J. Reeves, S.M. Sutorin and N.S. Sokolov. *J. Phys.: Cond. Mat.* **19** (2007) 395023.
- [2] Newman D.J. and Ng B. 2000 *Crystal Field Handbook* (Cambridge: Cambridge University Press) p. 290
- [3] Malkin B Z 1987 *Spectroscopy of Solids Containing Rare-Earth Ions* (Amsterdam: Elsevier Science) p.13

[We-P-31]
Optical spectrum of Yb³⁺ impurity cluster in CaF₂

V.A. Chernyshev, A.E. Nikiforov, V.P. Volodin

Ural State University, 51 Lenin av., Ekaterinburg, 620083, Russia

Most of elements in the rare-earth series, except the first few of its members, form hexamer clusters in fluorides MeF₂ (Me=Ca, Sr, Ba). Such clusters accommodate rare-earth ions, interstitial fluorines, vacancies and incorporate it into the fluorite cubic structure without modifying its structural motif. The rare-earth ion in such a cluster resides in a close to axial crystal field with its parameters differing strongly from these of single cubic and tetragonal centers. Such a crystal field in particular accounts for the large ground-state g_{\parallel} factors of paramagnetic rare-earth ions. These g -factors actually approach their limiting values.

Optical spectrum of CaF₂:Yb³⁺ were measured [1,2] at big impurity concentration (up to few percents). The spectrum of single impurity centers and clusters of Yb³⁺ in CaF₂ have been calculated in this work.

The atomic structure of the hexamer cluster and impurity centers in the hosting compound CaF₂ was established by computer simulation technique in the shell model formalism of the pair potential approximation. The crystal field and energy spectrum of the Yb³⁺ ion in single centers and cluster were calculated within the model of exchange charges [3].

An analysis of EPR spectra of Yb³⁺ ions carried out for cubic centers in CaF₂ and CdF₂ recently [4]. All energy levels were classified by presentation. It let us to determine "exchange charge" parameters for ytterbium. These parameters were used for ytterbium clusters.

The work is supported by State Contract № P1462.

References

- [1] Ito M., Gontaudier C., Guyot Y., Lebbou K., Fukuda T., Boulon G., J. Phys.: Condens. Matter, v.16, p.1501 (2004).
- [2] G. Leniec, S.M. Kaczmarek, G. Boulon, «EPR and optical properties of CaF₂:Yb single crystals», Proc. of SPIE Vol.5958, 595825, (2005) 0277-786X/05/\$15
- [3] Malkin B Z 1987 *Spectroscopy of Solids Containing Rare-Earth Ions* (Amsterdam: Elsevier Science) p.13
- [4] K.I.Gerasimov, M.L. Falin. *Phys. of the Solid State*, v. 51, № 4, p.721. (2009).

[Th-O-47]
Spectroscopic study of multiferroic TbMn₂O₅

E.P. Chukalina¹, M.N. Popova¹, M.A. Kaschenko^{1,2}, R.V. Pisarev³

¹*Institute of Spectroscopy of RAS, 142190 Troitsk, Moscow region, Russia*

²*Moscow Institute of Physics and Technology, 141700 Dolgoprudny, Moscow region, Russia*

³*Ioffe Physical-Technical Institute of RAS, 194021, St.-Petersburg, Russia*

Multiferroic TbMn₂O₅ is a member of the family of orthorhombic (space group *Pbam*) manganates RMn₂O₅ (*R*=rare earth, Y, or Bi), which demonstrates strong correlations and interplay between lattice, orbital, and magnetic degrees of freedom. Multiferroics open new potentials for device applications, e.g. such as magnetically recorded ferroelectric memory [1]. Competition between different interactions causes a cascade of phase transitions in TbMn₂O₅, see, e.g., [2,3]): at T₁=43 K the incommensurate antiferromagnetic order is settled, at T₂=38 K the ferroelectric phase transition takes place, at T₃=33 K the magnetic structure becomes commensurate, but at T₄=24 K it transforms into an incommensurate structure again. Finally, some authors report about one more phase transition (at T₅ < 10 K) which coincides with a major increase of the terbium ordered magnetic moment. Despite a large number of publications, the detailed nature of the observed phase transitions and the mechanisms leading to multiferroicity still remain unclear. To our knowledge, no spectroscopic data on Tb³⁺ ions in TbMn₂O₅ have been reported.

We have performed the broad-band optical absorption study of the Tb³⁺ *f-f* transitions in the single crystals of TbMn₂O₅. For optical measurements, thin platelets cut perpendicular to the *a*, *b*, and *c* crystallographic axes were prepared. Polarized spectra were measured in the temperature range from 3.5 to 300 K in the region of 1500-10000 cm⁻¹ using a Fourier-transform spectrometer Bruker IFS 125HR, and a closed-cycle optical cryostat Cryomech ST430 and a helium-vapour cryostat. The analysis of the spectra has delivered the energies of the Tb³⁺ crystal-field (CF) levels for the ⁷F_{6,5,4,3,2,1,0} multiplets. The temperature dependences of the peak positions and intensities of the spectral lines exhibit pronounced features at 39 and 26 K. Observed changes at T=39 K point to the appearance of several structurally inequivalent ensembles. The role of magnetoelastic and magnetoelectric interactions and of the pseudo-Stark effect is discussed. The line splittings change abruptly at 26 K and demonstrate a hysteresis-type behavior typical for a first-order phase transition. It follows from the spectra, that this phase transition is connected with the spin-reorientation. The low-temperature shape of some spectral lines points to the presence of a CF level with the energy of about 3 cm⁻¹, which explains a Schottky-type anomaly recently observed in TbMn₂O₅ [4]. We have not found in our spectra any evidence of phase transitions in the temperature range from 3.5 to 25 K.

This work was supported in part by the Russian Foundation for Basic Research (Grant №10-02-01071) and by the Russian Academy of Sciences under the Programs for Basic Research.

[1] N. Hur, S. Park, P.A. Sharma, J.S. Ahn, S. Guha, S.-W. Cheong, *Nature* **429**, 392 (2004).

[2] C. Chapon, G.R. Blake, M.J. Gutmann, S. Park, N. Hur, P.G. Radaelli, and S-W. Cheong, *Phys. Rev. Lett.*, **93**, 177402 (2004).

[3] J. Toledano, W. Schranz, and G. Krenner, *Phys. Rev. B* **79**, 144103 (2009).

[4] L.J. Chang, Y. Su, W. Schweika *et al.*, *Physica B* **404**, 2517 (2009).

[Tu-P-3]
Resolved hyperfine structure in optical spectra of $\text{KY}_3\text{F}_{10}:\text{Ho}^{3+}$

E.P. Chukalina, D.S. Pytalev

Institute of Spectroscopy, RAS, 142190, Troitsk, Moscow region, Russia

Potassium triyttrium decafluoride, KY_3F_{10} , seems to be a very attractive material for optical applications. Indeed, these crystals are chemically and thermally stable, transparent, isotropic and easy to grow. Being doped with rare earth (RE) ions, they represent a good laser medium. For instance, continuous-wave laser operation of $\text{KY}_3\text{F}_{10}:\text{Pr}^{3+}$ and $\text{KY}_3\text{F}_{10}:\text{Tm}^{3+}$ has already been demonstrated. On the other hand, RE doped materials are interesting for quantum information applications. Two hyperfine (HF) levels of a RE ion are chosen to be a quantum bit (qubit), while the third level is used to manipulate the states of this qubit by optical excitation. Such three-level Λ systems have been recently realized in several Tm^{3+} , Pr^{3+} , and Eu^{3+} doped crystals. Usually, the HF splitting is within the inhomogeneously broadened spectral profile which strongly complicates its experimental studies. There are, however, a few cases when the inhomogeneous broadening is extremely small and the HF structure can be resolved explicitly in high-resolution spectroscopy experiments (e.g., Ref. [1]). This gives a possibility to test the theoretical approaches used for HF calculations, by a direct comparison between the experimentally observed HF structure and calculated one. As for KY_3F_{10} , HF splitting of the ground multiplet $^5\text{I}_8$ of Ho^{3+} has been studied earlier by means of a submillimeter EPR spectroscopy [2].

In this work, we use an advantage of the high-resolution Fourier-transform spectroscopy to investigate $\text{KY}_3\text{F}_{10}:\text{Ho}^{3+}$ in the region of the $^5\text{I}_8 \rightarrow ^5\text{I}_{6,7}$ transitions. We show that observed fine structure of spectral lines is caused by the HF interaction that involves the electron-nuclear magnetic dipole and electric quadrupole contributions. The crystal field levels scheme of Ho^{3+} is found with assignment of the symmetries. A comparison with the EPR data is also given.

This work was partly supported by the Russian Foundation for Basic Research (Grant No 09-02-01067). D.P. acknowledges a financial support from the President of Russia (Grant No MK-1329.2010.2).

References

- [1] S. A. Klimin, D. S. Pytalev, M. N. Popova, B. Z. Malkin, M. V. Vanyunin, and S.L. Korableva, *Phys. Rev. B* **81**, 045113 (2010).
- [2] B. Z. Malkin, V. F. Tarasov, and G. S. Shakurov, *JETP Lett.* **62**, 811 (1995).

[Tu-O-6]

Micro-luminescence spectroscopy of Xe optical center in diamond

Y.A. Dziashko¹, A.M. Zaitsev¹, Mengbing Huang², A.A. Gorokhovsky¹

¹*CUNY – The College of Staten Island and The Graduate Center, 2800 Victory Blvd., Staten Island, NY 10314, USA,* ²*The University at Albany, The State University of New York, 1400 Washington Avenue, Albany, NY 12222, USA*

Various implanted ions create in diamond optically active defects which have emission lines in broad spectral regions, including visible and near-infrared. These optical centers may be used in advanced photonics and optical communication applications like single photon emitters [1] or diamond light emitting diodes [2]. Another advantage of ion implantation is the possibility to control the dose and the energy of ions, which gives a robust tool for device fabrication. On the other hand, ion implantation creates a number of radiation defects which influence properties of optical emission from the center. Our interest in the Xe-related center originated from the fact that this center is one of a few (Ni, Si, Cr) in diamond having sharp emission lines in the infrared spectral region.

We will report on and photo- and electroluminescence studies of Xe-ion implanted diamond crystals within the wide dose range of $10^{10} - 5 \times 10^{14}$ ion/cm². At low temperatures, the photoluminescence spectra featured the single zero phonon lines at 811.7 nm and a weak phonon sideband. The room temperature luminescence consists of a zero phonon line at 813 nm and a weaker line at 794 nm. Our studies concluded that vacancies are involved in the formation of this defect, it contains a single Xe ion, and is a $\langle 111 \rangle$ oriented defect [3]. These results are in agreement with the previous model calculations [4], which resulted that due to its large size, the Xe ion generates stresses and yields a stable configuration in the semi-divancy site V-Xe-V.

Probability of the emitting center generation is characterized by an important and difficult to measure conversion efficiency of implanted ions into emitting optical centers. This quantity is extremely important in search of single emitting centers and device fabrication by ion implantation. The yield is determined as a ratio of the average surface/volume density of emitting centers to the density of implanted centers. We used the method of micro-luminescence confocal mapping and statistical analyses based on a Compound Poisson distribution to determine the conversion efficiency of implanted Xe ions into emitting Xe optical centers.

With purpose to observe a single defect luminescence, we performed confocal micro-luminescence mapping of the transitional area between the Xe-ion implanted (dose of 10^{10} ion/cm²) and non-implanted regions based on changes in the 813 nm line intensity. This approach allowed us to study the luminescence transient profile through the implantation boundary and to detect and image small emitting clusters with a few Xe centers per cluster.

[1] C. Wang, C. Kurtsiefer, H. Weinfurter, B. Burchard, J.Phys. B: At. Mol. Opt. Phys. **39**, 37 (2006)

[2] A.M. Zaitsev, A.A. Bergman, A.A. Gorokhovsky, Mengbing Huang, Phys. Stat. Sol. (a) **203**, 638 (2006)

[3] A.A. Bergman, A.M. Zaitsev, Mengbing Huang and A.A. Gorokhovsky, J. of Luminescence, **129**, 1524 (2009)

[4] A.B. Anderson, E. J. Grantscharova, Phys.Rev. B **54**, 14341 (1996)

Ce(III)- and Ce(IV)-related spectral components observable in the UV absorption spectra of photo-thermo-refractive glass matrices

A.M. Efimov, A.I. Ignatiev, N.V. Nikonorov, E.S. Postnikov

St. Petersburg State University of Information Technologies, Mechanics, and Optics

The photosensitivity of Ce^{3+} ion is a physical background for developing novel glass types that are widely used in the modern photonics and optoinformatics. In particular, it is the photoionization process such as $h\nu + \text{Ce}^{3+} \rightarrow (\text{Ce}^{3+})^+ + e^-$ that is the starting point for recording the volume phase holograms on photo-thermo-refractive (PTR) glasses. However, the spectroscopic manifestations of Ce-related electronic transitions in silicate glasses (see, for example, [1,2]) are studied much less thoroughly than is the case for cerium-doped crystals. Therefore, further insight into the spectroscopic behaviour of Ce(III) and Ce(IV) valence states in these glasses is of great interest for practice.

Glass samples based on a typical $\text{Na}_2\text{O-ZnO-Al}_2\text{O}_3\text{-NaF-SiO}_2$ PTR glass matrix doped with CeO_2 up to 0.02 mol% were synthesized. The optical density spectra for samples down to 0.2 mm thick were recorded in the $(2.8\text{-}5.0)\times 10^4 \text{ cm}^{-1}$ (360-200 nm) region with Varian Cary 500 double-beam spectrophotometer. The natural absorption coefficient spectra calculated from the optical density spectra and reflection loss were processed with the dispersion analysis method based on the convolution model for the complex dielectric function of glasses (see, for example, [3]), this method being now the most powerful tool for deconvoluting the complicated poorly resolved spectra of glasses into the constituent bands.

It was shown with the dispersion analysis that:

(1) A seemingly single band centered around $3.3\times 10^4 \text{ cm}^{-1}$ (303 nm) (the one commonly assigned [1,2] to the ${}^2F_{5/2}\rightarrow 5d$ transition in the Ce^{3+} ion) is in fact an envelope. There are two or even three spectral components under the envelope, the corresponding deconvolution versions being characterized by error function magnitudes of the same order. Data presented in Table correspond to the deconvolution of the envelope into two spectral components. Thus, in spite of strong inhomogeneous broadening, the splitting of the Laporte allowed ${}^2F_{5/2}\rightarrow {}^2D_{3/2}$ and ${}^2F_{5/2}\rightarrow {}^2D_{5/2}$ transitions in Ce^{3+} ion remains to be distinguishable in the spectra of cerium-containing alkali aluminosilicate glasses including PTR ones.

(2) A quite broad band located in the $(3.7\text{-}5.0)\times 10^4 \text{ cm}^{-1}$ (200-270 nm) region commonly considered [1,2] to be a single Ce(IV) charge-transfer band is in fact an envelope of at least three spectral components - see Figure and Table (rows 3 to 5).

In accord with commonly accepted opinion that the Ce(IV) envelope is due to the charge-transfer absorption [1,2], three spectral components mentioned in Paragraph (2) should be ascribed to transitions from the ceiling of the matrix valence band to three different Ce(IV)-related energy levels. However, the problem of specifying these transitions in more detail turns out to be quite complicated because:

- (i) theoretical estimates for the locations of different energy levels for Ce(IV) valence state are not available in literature even for the purely ionic Ce^{4+} configuration;
- (ii) strictly speaking, there are no purely fourfold-charged ions in nature at all: as a rule, the (IV) valence state of any element implies an appreciable covalent contribution to chemical bonds formed.

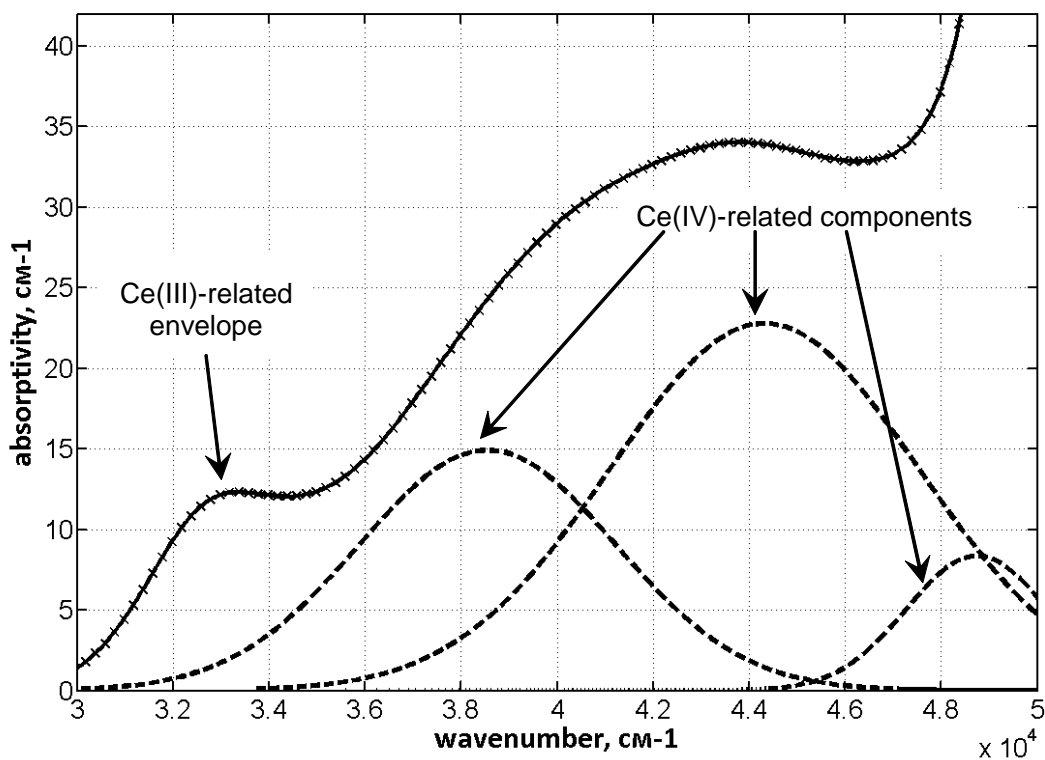


Figure. The deconvolution of the Ce(IV) charge-transfer envelope into three spectral components obtained with the dispersion analysis. Points (x) are experiment and the solid line is the fitted spectrum.

Table. Locations of the UV spectral components in the absorption spectra of cerium-doped FTR glass matrix deconvoluted with the dispersion analysis.

Cerium valence state	Spectral component notation	Spectral component locations	
		Wavenumbers, cm ⁻¹	Wavelengths, nm
Ce ³⁺	Ce ³⁺ (1)	32900	304
	Ce ³⁺ (2)	35100	285
Ce ⁴⁺	Ce ⁴⁺ (1)	38800	258
	Ce ⁴⁺ (2)	43000	233
	Ce ⁴⁺ (3)	46400	216

Therefore, further studies involving a thorough computer modeling of Ce(IV) energy level locations seem to be necessary for assigning the above three spectral components to particular Ce(IV)-related energy levels.

References

1. A. Paul, M. Mulholland, M.S. Zaman, J. Mater. Sci. 11 (1976) 2082.
2. R.C. Ropp, B. Carrol, J. Phys. Chem. 81 (1977) 1699.
3. A.M. Efimov, Optical Constants of Inorganic Glasses (CRC Press, Boca Raton, N.-Y., etc., 1995).

[Th-O-44]

Exchange-induced magnetic dipole mechanism of magnon sideband in KCuF_3

M.V. Eremin^{1*}, J. Deisenhofer², M. A. Fayzullin¹, Ch. Kant², A. Loidl²

¹Kazan State University, 420008-Kazan, Russia;

²Institute for Physics, Augsburg University, D-86135, Germany

*e-mail: Mikhail.Eremin@ksu.ru

Recently a very narrow sidebands were observed in optical absorption spectra of KCuF_3 at $T < T_N$ [1]. Its origin cannot be described by conventional mechanism [2]. For the explanation of observed sidebands in [1] we suggest the following effective operator of magnetic dipole transition

$$H_{\text{eff}}^{b \rightarrow a} = -\frac{\mu_B}{2\Delta} (\eta |H^\alpha 1_a^\alpha| \eta') J_{ab} (S_a S_b - \frac{1}{4}) \quad (1)$$

Here J_{ab} is superexchange coupling parameter of magnetic ions, Δ - energy transfer of electron from site b to site a.

The virtual process (mechanism) can be described as follows (see Fig.1). The spin down from Cu site (b) transfers to the state of ion (a) (in fact it is a cascade hopping via intermediate F ion) and then it is excited to state $|a'\rangle$ due to the interaction of the orbital momentum with magnetic field H_α and simultaneously the spin up from state $|a\rangle$ jumps to site (b). Discrete sideband structure has been formed due structure dependent factor after summation over surrounding neighbors (index b in Eq. 1) and as well to singularity in magnon density of states. These special points in DOS are displayed in Fig.2 and corresponds to $w_1 = 11.10 \text{ meV}$ and $w_2 = 15.77 \text{ meV}$. The exchange coupling constant and dispersion of magnon spectra were taken from paper about neutron scattering data [3,4].

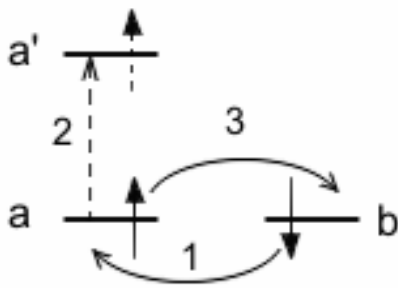


Fig.1. Virtual process scheme.

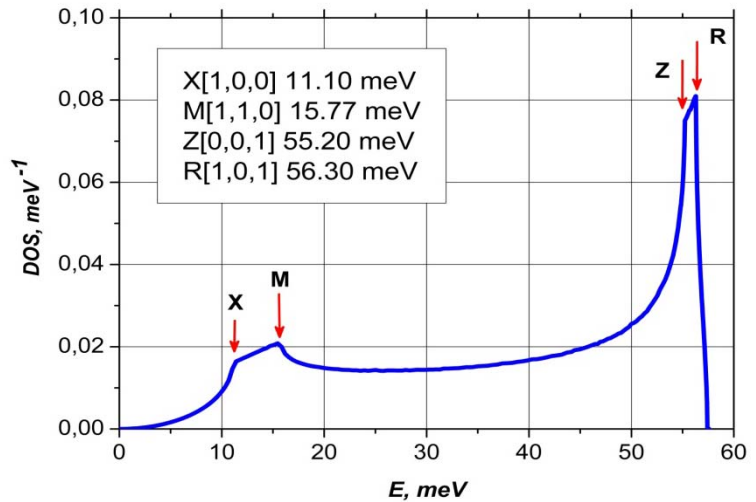


Fig.2. The calculated magnon density of states.

The operator (1) yields the correct pictures for peculiarities of polarization spectra observed in [1] and selection rules. These facts strongly supported our idea about new source (mechanism) of exciton-magnon absorption in KCuF_3 .

[1] J. Deisenhofer, I. Leonov, M.V. Eremin et al., Phys. Rev. Lett., **101**, 157406 (2008).

[2] Y. Tanabe, T. Moriya and S. Sugano, Phys. Rev. Lett., **15**, 1023 (1965)

[3] S.K. Satija, J.D. Axe, G. Shirane et al., Phys. Rev. B, **21**, 2001 (1980).

[We-P-43]

Accumulation of excitation energy nanoparticles from Ln(III) complexes at dye molecule admixture.

V.L. Ermolaev*, E.B. Sveshnikova, S.S. Dudar'

St. Petersburg State University of Information Technologies, Mechanics and Optics, St. Petersburg, 197101 Russia,

**E-mail: ermolaev@oi.ifmo.ru*

The investigation of energy migration in nanoparticles (NP) from Ln(III) complexes to some admixture is of considerable interest, because this phenomenon is applied for enhancement of the sensitivity of immuno-fluorescent analysis, using Eu(III) –label. This phenomenon examination is also essential, because the annihilation of Eu(III) exciton in nanomolecular layers of these ion diketonates results in drastic decrease of electroluminescence efficiency in devices with Eu complexes.

We have shown for the first time in 2008 [1, 2] that nanoparticles from metal complexes doped with dye molecules are formed in aqueous solutions of β -diketones, Ln(III) ions and dye molecules. The luminescence regularities were examined in such NP's. It is shown that the transfer of NP excitation energy to dye molecules takes place in such NP and causes the appearance of sensitized fluorescence (cofluorescence) of dye molecules. The formation of such NP's allows solving two problems. Firstly, it enables to increase the sensitivity of luminescent analysis of a number of dye molecules, which are widely applied as luminescent labels. Secondly, it leads to τ_{lum} decreasing of Eu(III) ions in their complexes, which are used in electroluminescent devices. The latter fact has to lead to the decrease of the probability of excited Eu(III) ion annihilation.

The NP's formed by us have radius ~ 10 nm and are made up of Eu(MBTA)₃phen, Eu(DBM)₃phen, Eu(NTA)₃phen or of the complexes of Lu(III), Gd(III) and Al(III) with the same ligands. (MBTA - *p*-methoxybenzoyltrifluoroacetone, DBM - dibenzoylmethane, NTA - 2-naphtoyltrifluoroacetone, phen - 1,10-phenantroline). All of them are doped with cationic or anionic or neutral dye molecules of different classes. The decrease of Eu(III) τ_{lum} and the appearance of delayed fluorescence of Nile blue (NB) were observed in NP's from Eu(MBTA)₃phen complexes with admixture of these dye molecules. NP's were formed in aqueous solutions having 5 μ M Eu(III), 50 μ M MBTA, 17 μ M phen and from 5 до 100 nM of this dye. The columinescence intensities (I_{cofl}) of three dyes: Nile blue (NB), Nile red (NR) and Rhodamine 6G (R6G) in NP's from Eu, Lu, Gd and Al, and the fluorescence intensities (I_{fl}) of complexes of NP's from Lu, Gd and Al complexes were compared. This comparison has shown that in NP's from Eu complexes energy transfer (ET) takes place not only from Eu(III) ions quintet states but also from excited singlet states (S_1) of complexes. It is shown [3] that at low concentrations of NB the efficiency of ET from Eu(III) to dyes is higher than from S_1 states of complexes. At dye concentration in solution > 50 nM the population of the triplet states of complexes and quintet states of Eu(III) drops due to S–S ET to dyes and S–S ET is the main path of dye sensitization. It is shown that I_{cofl} of dyes in NP's from Al(III) and Lu(III) with DBM depends almost not at all on variation of τ_{fl} complexes in 50 times, but it decreases in more than order of magnitude for NP's from Gd(DBM)₃phen complexes.

The comparison of I_{fl} of such dyes as NB, NR и R6G in H₂O under excitation of their own first absorption band and their I_{cofl} in NP's at the same dye concentrations in the region of 2-50 nM of dyes in solution has demonstrated, that the sensitivity of luminescent detection of the dye presence in aqueous solution may be enhanced by a factor of 1.5-2 order of magnitude. This study is supported by RFBR, project 10-03-00566

- [1]. Dudar' S.S., Sveshnikova E.B., Ermolaev V.L., Opt. Spectr., **104**, No. 2, 225, (2008)
- [2]. Dudar' S.S., Sveshnikova E.B., Ermolaev V.L., Opt. Spectr., **104**, No. 5, 724, (2008)
- [3]. Sveshnikova E.B., Dudar' S.S., Ermolaev V.L., High energy chemistry, **43**, No. 7, 616, (2009)

[Tu-P-9]
**Optical and radio frequency optically detected EPR spectroscopy
of Sm³⁺ in Cs₂NaYF₆ cubic crystal**

M.L. Falin¹, K.I. Gerasimov¹, B.Z. Malkin², N.M. Khaidukov³

¹*Kazan Physical-Technical Institute of RAS, Kazan 420029, Russian Federation*

^{2b}*Kazan Federal University, Kazan 420008, Russian Federation*

³*Institute of General and Inorganic Chemistry of RAS, 117907 Moscow, Russian Federation*

Unlike hexachloroelpasolites M₂ABCl₆ (M⁺, A⁺, B³⁺ are univalent and trivalent metal cations), widely studied by optical methods [1, 2], fluoroelpasolites (M₂ABF₆) doped with impurity rare earth (RE) ions have been studied much less. Fluoroelpasolites, with the cubic structure in the wide temperature interval, are perfect model systems in which the isomorphous substitution of trivalent RE ions for B³⁺ cations provides an opportunity to study optical and magnetic properties of dopants in a wide concentration range. In turn, it allows one to consider these compounds as promising materials in practice. To the best of our knowledge, we present the first communication on the investigation of the Sm³⁺ ion electronic structure in cubic Cs₂NaYF₆ single crystals using optical and magnetic resonance spectroscopy.

Cs₂NaYF₆ single crystals doped with 3.0 at. % Sm³⁺ were synthesized by the chemical reaction of alkali fluoride aqueous solutions with mixtures of Sm₂O₃ and Y₂O₃ at 750 K and pressures of 100–150 MPa.

The ground state of Sm³⁺ in Cs₂NaYF₆ is a (⁶H_{5/2}) Γ₇ Kramers doublet. In the present work magnetic resonance signals were studied by making use of a high-sensitivity technique of optically detected EPR (ODEPR) by Faraday rotation at the frequency of the rf-field about 0.8 GHz and in relatively low magnetic fields (0.14 T). In particular, ODEPR spectra were measured at the frequencies 660, 775 and 815 MHz at 2 K temperature. These spectra have shown isotropic ODEPR signals of even Sm³⁺ isotopes with g-factor of 0.363 ± 0.003. Small value of the g-factor is one of the reasons why EPR data are absent in the literature, because, to measure EPR spectra at the X band by conventional EPR technique, high magnetic fields (up to 1.8 T) are required.

From luminescence and excitation spectra measured at 77 K, energies of 22 electronic states of Sm³⁺ were obtained. The energy spectrum of Sm³⁺ in Cs₂NaYF₆ was computed by diagonalization of the Hamiltonian containing all usually considered interactions and operating in the basis consisting of all 2002 states of the 4f⁵ configuration. The total number of parameters was equal to 17. The obtained wave functions were used to calculate g-factors and probabilities of magnetic dipole optical transitions. Parameters of the crystal field were varied to fit experimental energy levels. Finally, differences between theoretical and experimental crystal field energies do not exceed 15 cm⁻¹ in the range of 0 - 20000 cm⁻¹, and calculated relative intensities of zero-phonon transitions agree well with the results of measurements. Larger deviations at higher energies above 20000 cm⁻¹ are most likely connected with the neglect of configuration mixing.

[1] P.A. Tanner *Top Curr Chem* **241**, 167 (2004)

[2] M.D. Faucher, P.A. Tanner *J. Phys.: Condens. Matter* **18**, 8503 (2006)

[Th-O-51]

The many-particle kinetics of the hopping luminescence quenching in disordered solid solutions

S.G. Fedorenko¹, Yu.V. Orlovskii², E.V. Samsonova²

¹*Institute of Chemical Kinetics and Combustion SB RAS, Novosibirsk, 630090, Russia*

²*Prokhorov General Physics Institute RAS, 38 Vavilov st., Moscow, 119991, Russia*

The kinetics of luminescence impurity quenching in solid solutions is a rather complicated process that depends essentially on the character of the interaction, and concentration of impurity centers – energy donors and acceptors chaotically distributed in the system. The necessity of performing configuration averaging over random location of impurity centers hinders considerably the theoretical description of the phenomenon. However, there are two specific cases where configuration averaging may be carried out to the end so as to obtain the solution of a many-particle problem. The first case is as follows: the donor concentration n_D is vanishingly small, and excitation decays at the same donor where it arises. Then the solution is the well-known static kinetics [1] which for dilute system of acceptors has the form: $N_0(t) = \exp\{-n_A \int d^D r [1 - e^{-w(r)t}]\}$, where n_A is the acceptor concentration, $w(r)$ is the quenching probability per unit time at the acceptor that is at the distance r from the excited donor. The second case is the hopping quenching realized when the average step $\lambda \approx n_D^{-1/3}$ of excitation migration exceeds significantly the radius of effective quenching of the excitation by acceptors. In this situation for the kinetics of luminescence quenching $N(t)$ we have the closed integral equation [2],[3]:

$$N(t) = N_0(t)R(t) - \int_0^t N_0(t')R(t')N(t-t')dt' \quad (1)$$

Here $-R(t)dt$ defines the time distribution between sequential uncorrelated excitation jumps. As is known, it is not exponential in solid solutions, and depends on the character of resonance interaction between donors. In particular, in the model taking into account the excitation return from the nearest neighbors the kinetics of the excited donor emigration is $R(t) = \exp\{-(n_D/2) \int d^D r [1 - e^{-2u(r)t}]\}$, where $u(r)$ is the probability of energy transfer per unit time between two donors separated by the distance r .

The solution of equation (1) for dipole-dipole interaction ($w(r) = C_{DA}/r^6$, $u(r) = C_{DD}/r^6$), when the functions $N_0(t)$ and $R(t)$ take the form

$$N_0(t) = \exp\{-2\Delta_A \sqrt{t}\}, \quad R(t) = \exp\{-2\Delta_D \sqrt{t}\}, \quad (2)$$

with the parameters $\Delta_A = (2/3)\pi^{3/2}(n_A \sqrt{C_{DA}})$, $\Delta_D = (\sqrt{2}/3)\pi^{3/2}n_D \sqrt{C_{DD}}$ has been given in paper [4]. The paper shows that at small $\alpha = \Delta_A/\Delta_D$ the kinetics may be represented as two independent components $N(t) = N_e(t) + N_m(t)$. The first component is determined by migration accelerated quenching at the constant rate \bar{W} depending non-linearly on donor and acceptor concentration:

$$N_e(t) = \frac{1+\alpha}{1+3\alpha} \exp(-\bar{W}t), \quad \bar{W} = \frac{2\alpha(\Delta_A + \Delta_D)^2}{1+3\alpha} \quad (3)$$

This component describes the decay of excitations arisen in the regions filled with donors, and having the possibility of effective reaching of the acceptors by a series of jumps. The second component describes all processes of non-stationary quenching beginning with the initial region of static quenching ($t \ll t_s = (1+\alpha)^2/(\Delta_A + \Delta_D)^2$) and ending with quenching of excitations at isolated

donor centers that determines the kinetics at large times:

$$N_m(t) \approx \frac{1+\alpha}{\alpha} \exp\{-2(\Delta_A + \Delta_D)\sqrt{t}\}, \quad t \gg t_f = \frac{1}{\alpha^2(\Delta_A + \Delta_D)^2} \quad (4)$$

Usually interpretation of experiment covers the first two kinetic stages: the initial static stage and the subsequent migration accelerated one. However, it is easily seen that with increasing binary parameter α the boundaries t_s and t_f approach each other, and at $\alpha \approx 1$ the interval of migration accelerated motion $t_s \ll t \ll t_f$ goes to zero leaving no room for exponential kinetics (3) at all. In our experiment the many-particle kinetics of luminescence impurity quenching beginning with the initial static region and ending with the interval of fluctuation kinetics (4) is observed for the first time. The kinetics of fluorescence quenching of the $[Y_{0.99}Tb_{0.01}(pyca)_3(H_2O)_2]nH_2O$ and $[Tb(pyca)_3(H_2O)_2]nH_2O$ vacuum dried powder where chelated complexes of the Tb^{3+} rare-earth ion appear as chromophore is measured. Due to effective energy transfer from organic ligands to the Tb^{3+} ions we measured fluorescence kinetics of the 5D_4 level of Tb^{3+} under excitation into complexing agents by pulsed nitrogen laser at 337 nm ($f = 10 \div 200$ Hz, $t_p = 2$ ns). The fluorescence kinetics decay is acquired and averaged at series of impedances coupled to the input of DC Series Tektronix oscilloscope TDS 3032B. A partial saturation of the signal at large impedances is provided. The parts of all the measured curves with best signal-to-noise ratio are used to construct the total curve. This increases the dynamic range of the measured fluorescence kinetics significantly. The complexes are liable to formation of hydrates of different structure and contain water molecules either bounded or unbounded to central ion. The Tb^{3+} ions appear as fluorescent donors, and OH ions of unbounded water appear as randomly distributed acceptors. The figure shows the experimental kinetics $I(t)$ divided by radiation decay with $\tau_R = 1.94ms$: $N(t) = I(t) / \exp(-t / \tau_R)$. In 1% sample the kinetics (upper curve) is of the Forster type (2), while in 100% sample (lower curve) besides the initial static stage a fluorescence quenching over the final measurement time range is defined by the law (4).

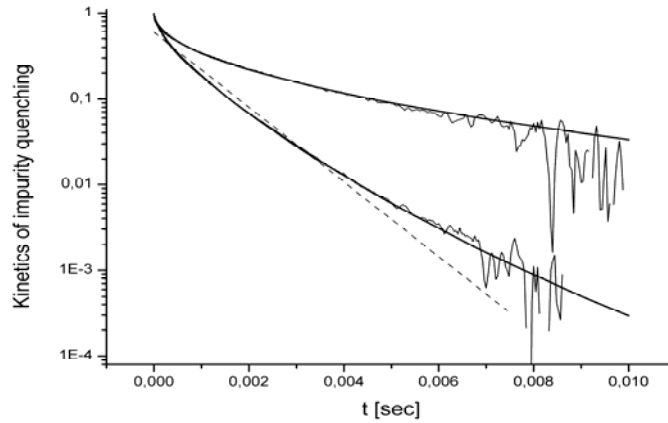


Fig. The upper curves are the static kinetics in $[Y_{0.99}Tb_{0.01}(pyca)_3(H_2O)_2]nH_2O$ (broken line – experiment, solid line – the Forster kinetics with $\Delta_A = 17 \text{ sec}^{-1/2}$). The lower curve is migration accelerated kinetics in $[Tb(pyca)_3(H_2O)_2]nH_2O$ (broken line – experiment, solid line – the solution of equation (1) with $\Delta_A = 17 \text{ sec}^{-1/2}$, and $\Delta_D = 32.7 \text{ sec}^{-1/2}$, dashed line – exponential kinetics (3)).

[1] Th. Forster, Z. Naturforsch. A 4, 321 (1949).

[2] A. I. Burshtein, Sov.Phys.JETP 35, 882 (1972).

[3] B. E. Vugmeister, Phys.Stat.Solidi B 76, 162 (1976)

[4] S. G. Fedorenko, A. I. Burshtein, A. A. Kipriyanov, Phys.Rev.B 48, 7020 (1993).

[Tu-O-12]

Gaseous environment-sensitive fluorescence of Ce³⁺ impurity ions in nanocrystals

S.P.Feofilov¹, D.V.Arsentyev¹, A.B.Kulinkin¹, R.I.Zakharchenya¹,
T.Gacoin², G.Mialon², R.S.Meltzer³, C.Dujardin⁴

¹*A.F. Ioffe Physical-Technical Institute, St. Petersburg, 194021, Russia*

²*Ecole Polytechnique – CNRS, 91128 Palaiseau, France*

³*Department of Physics and Astronomy, University of Georgia, Athens, GA 30602, USA*

⁴*Université Lyon 1 69622 Villeurbanne, France, CNRS UMR5620*

The interaction of impurity ions with the particles environment is one of the main reasons why the fluorescence of doped insulating nanoparticles may be modified compared to that of the corresponding bulk material. At the same time the general features of spectra of impurity ions in nanoparticles remain similar to those in the bulk, because the spatial extent of the localized electronic states is much smaller than the nanoparticle size. The sensitivity of the nanoparticles fluorescence to the environment makes them interesting as potential probes of different properties and processes in very different kinds of media ranging from inorganic glasses to biological objects.

Y₃Al₅O₁₂:Ce³⁺ (YAG:Ce³⁺), Sc₂O₃:Ce³⁺ and Y₂O₂S:Ce³⁺ are luminescent materials with a broad electron-phonon emission band which is due to fast (<100ns) electric dipole allowed 4f⁰5d¹ - 4f¹ radiative transition which occurs in the visible part of the optical spectrum. YAG:Ce has attracted much attention because it is used in white-light emitting LEDs for conversion of blue LED emission into the green-red spectral range.

Optically excited fluorescence of YAG:Ce³⁺, Sc₂O₃:Ce³⁺ and Y₂O₂S:Ce³⁺ nanoparticles (size 20-50 nm) was studied at different temperatures and pressures of the surrounding gaseous media (air, N₂, He). A striking new effect was observed [1]: the intensity of fluorescence of Ce³⁺ ions in nanoparticles dramatically depends on the pressure of the gas in which the powder samples are placed. The excitation power dependence of fluorescence is perfectly linear at ambient pressure whereas at 20 Pa this dependence saturates. At low (<100 Pa) gas pressures slow (seconds) fluorescent transients follow the modulations of optical excitation. It is shown that the temperature quenching of luminescence caused by laser heating cannot explain these observations.

The effects observed below 100 Pa may be explained based on a model, involving Ce³⁺ two-photon photoionization resulting in conversion to Ce⁴⁺ followed by Ce³⁺ recovery assisted by surrounding gas molecules. The pressure dependence of the fluorescence at higher pressures (10³-10⁵ Pa) is not related to photoionization; rather, the responsible processes may include modification of the surface of the particles by adsorption of gas molecules that changes the parameters of surface traps or by dehydroxylation of the surface when pumping. No pressure effects were observed in Ce³⁺ fluorescence of Sc₂O₃ of micron crystallite size; this proves that the gas pressure effect on the fluorescence of Ce³⁺ doped nanocrystals is an inherently nanoscale effect. The observed effects demonstrate the possibility of probing the pressure at the single molecule level with nanoparticles. They are important to understand for optimization of small-grain phosphor efficiency. The authors acknowledge support by RFBR grant 08-02-00907.

[1] S.P. Feofilov, D.V. Arsentyev, A.B. Kulinkin, T. Gacoin, G. Mialon, R.S. Meltzer, C. Dujardin, *J. Appl. Phys.* **107** (2010) 064308.

[We-P-41]

Optical spectroscopy of the chain nickelate $\text{Sm}_2\text{BaNiO}_5$: crystal-field interactions and magnetic ordering

A.S. Galkin¹, S.A. Klimin¹, E.P. Chukalina¹, M.N. Popova¹, B.V. Mill²

¹ *Institute of Spectroscopy RAS, Fizicheskaya 5, Troitsk 142190, Moscow region, Russia*

² *Moscow State University, Physics Department, 119899 Moscow, Russia*

$\text{Sm}_2\text{BaNiO}_5$ is interesting compound from two points of view. First, it contains Haldane chains (Ni^{2+}) that interact between each other via rare-earth ion. Second, recently magnetoelectric effect has been found in holmium nickelate $\text{Ho}_2\text{BaNiO}_5$ [1]. Magnetoelectric effect has recently attracted the considerable attention of researchers. This effect can be used in optoelectronic devices. Our investigations have shown that the presence of magnetoelectric effect results in low-temperature dynamics of energy spectra of rare-earth ions in $\text{Ho}_2\text{BaNiO}_5$ and $\text{Dy}_2\text{BaNiO}_5$ near the antiferromagnetic transition. We have undertaken the detailed spectroscopic research of $\text{Sm}_2\text{BaNiO}_5$ to get deeper insight into magnetic ordering and to find possible demonstrations of magnetoelectric effect.

In this work we have measured transmittance spectra of the polycrystalline sample $\text{Sm}_2\text{BaNiO}_5$ in a broad range of frequencies (2000-20000 cm^{-1}) and temperatures (4.2÷300K) using a Fourier-transform spectrometers BOMEM DA3.002 and BRUKER IFS 125HR and a closed-cycle helium cryostat Cryomech PT403. Positions of Sm^{3+} CF levels in the ${}^6\text{H}_{5/2}$, ${}^6\text{H}_{9/2}$, ${}^6\text{H}_{11/2}$, ${}^6\text{H}_{13/2}$, ${}^6\text{F}_{1/2}$, ${}^6\text{F}_{3/2}$, ${}^6\text{F}_{5/2}$, ${}^6\text{F}_{7/2}$, ${}^6\text{F}_{9/2}$, ${}^6\text{F}_{11/2}$ manifolds have been determined. Magnetic ordering ($T_N=57$ K) results in Kramers-doublet splittings of Sm^{3+} . The results of our spectroscopic research allow to interpret some peculiarities of magnetic properties of $\text{Sm}_2\text{BaNiO}_5$.

This work was supported by the Russian Foundation for Basic Research under grant No. 08-02-00690, and by the Russian Academy of Sciences.

References

[1] G. Nénert and T. T. Palstra, Phys. Rev. B **76** (2007) 024415.

[Tu-O-7]

Laser piezospectroscopy of Sm^{3+} ions in fluorite epitaxial layers

S.V.Gastev¹, V.A.Chernyshev², J.K.Choi³, A.V.Krupin¹, N.S.Sokolov¹, A.D. Nazemnykh²

¹*Ioffe Physical-Technical Institute of the Russian Academy of Sciences, 26 Polytechnicheskaya st., St.Petersburg, 194021 Russia*

²*Ural State University, 51 Lenin av., Ekaterinburg, 620083, Russia*

³*University of Canterbury, PB4800, Christchurch, New Zealand*

The optical piezospectroscopy is a classic method of the solid state fluorescent center investigation. However, maximal uniaxial stress, which can be applied to the bulk crystal, is limited by its mechanical strength and usually the strain does not exceed 10^{-3} . In our previous studies it was shown that planar tensile or compressive strain in fluoride epitaxial layers depending on the substrate and growth conditions can reach 10^{-2} [1,2]. It was also found that the main part of samarium ions in the layers grown by molecular beam epitaxy are Sm^{2+} and this allowed us measuring the layer planar strain by monitoring shift of photoluminescence (PL) zero-phonon line of $4f^55d \rightarrow 4f^6$ optical transition from its position in unstrained $\text{CaF}_2:\text{Sm}$ bulk crystals [2].

The Sm^{3+} ions appear in the layer in presence of interstitial F^{1-} ions serving as excess charge compensator or as a result of electron tunneling from Sm^{2+} excited state to Si conduction band [3]. There are two types of Sm^{3+} centers in CaF_2 , $A(C_{4v})$ with the neighboring F^{1-} center and the cubic (O_h) center, in which the charge compensator is remote. The centers appearing due to electron tunneling are cubic ones and they are located near the CaF_2/Si interface. In rather detailed earlier study of the Sm^{3+} centers in $\text{CaF}_2:\text{Sm}$ (0.05%) bulk crystals [4] was found that in the cubic center the lowest level of ${}^6\text{H}_{5/2}$ ground state multiplet is the Kramers's quartet and the next one is the doublet. The excited state ${}^4\text{G}_{5/2}$ multiplet has inversed energy level position, the quartet lies 400 cm^{-1} higher.

In this work, comparative study of Sm^{3+} ion optical spectra in $\text{CaF}_2:\text{Sm}$ epitaxial layers with compressive or tensile strain grown by molecular beam epitaxy on Si(111) has been carried out using laser spectroscopy. Combined excitation and emission spectroscopy (CEES) measurements of Sm^{3+} ions are performed with the Spectra-Physics dye-laser in Prof. Reeves's laboratory of Canterbury University Physics and Astronomy Department. CEES plots for 12 nm thick coherent #2303 layer measured at $T=5\text{K}$ are presented in Fig.1. In the area of ${}^6\text{H}_{5/2}(z1) \rightarrow {}^4\text{G}_{5/2}(A1)$ transition (Fig.1a) two distinct lines in the excitation spectra corresponding to the ${}^4\text{G}_{5/2}(A1) \rightarrow {}^6\text{H}_{7/2}(y2,y3)$ transitions are clearly seen. Only single line presents in the ${}^4\text{G}_{5/2}(A2)$ multiplet excitation spectra (Fig.1b). The excitation energies indicated in the figure correspond to maxima of intensity of the PL peaks. Similar pattern of ${}^4\text{G}_{5/2}$ multiplet splitting was also observed for the relaxed layers having different tensile strains (0.5% and 0.8%).

From these data one can conclude that the lower ${}^4\text{G}_{5/2}(A1)$ level is the quartet and the higher ${}^4\text{G}_{5/2}(A2)$ one is the Kramers's doublet. The quartet is split due to (111) planar strain in the layer and the doublet, which is located 400 cm^{-1} above in the bulk, is shifted for the same reason. This conclusion disagrees with the reversed order of doublet and quartet levels in this multiplet suggested in Ref. [4]. In the framework of the exchange charge model [5,6] this order is mainly determined by the sign of the crystal field parameter B^4_0 . For $\text{Sm}^{3+} O_h$ - centers in $\text{CaF}_2:\text{Sm}$ bulk crystals $B^4_0 = -2112$ [4]. The estimates of the distortions of the cubic center by the high-symmetry deformations show that these distortions should not result in change of B^4_0 parameter sign. Thus, for the present moment, there is a definite contradiction between the results of theoretic considerations and experimental data obtained in this work. The further study is underway.

This study was supported by Program of Russian Academy of Sciences “Fundamental optical spectroscopy and its applications” and State Contract P1462.

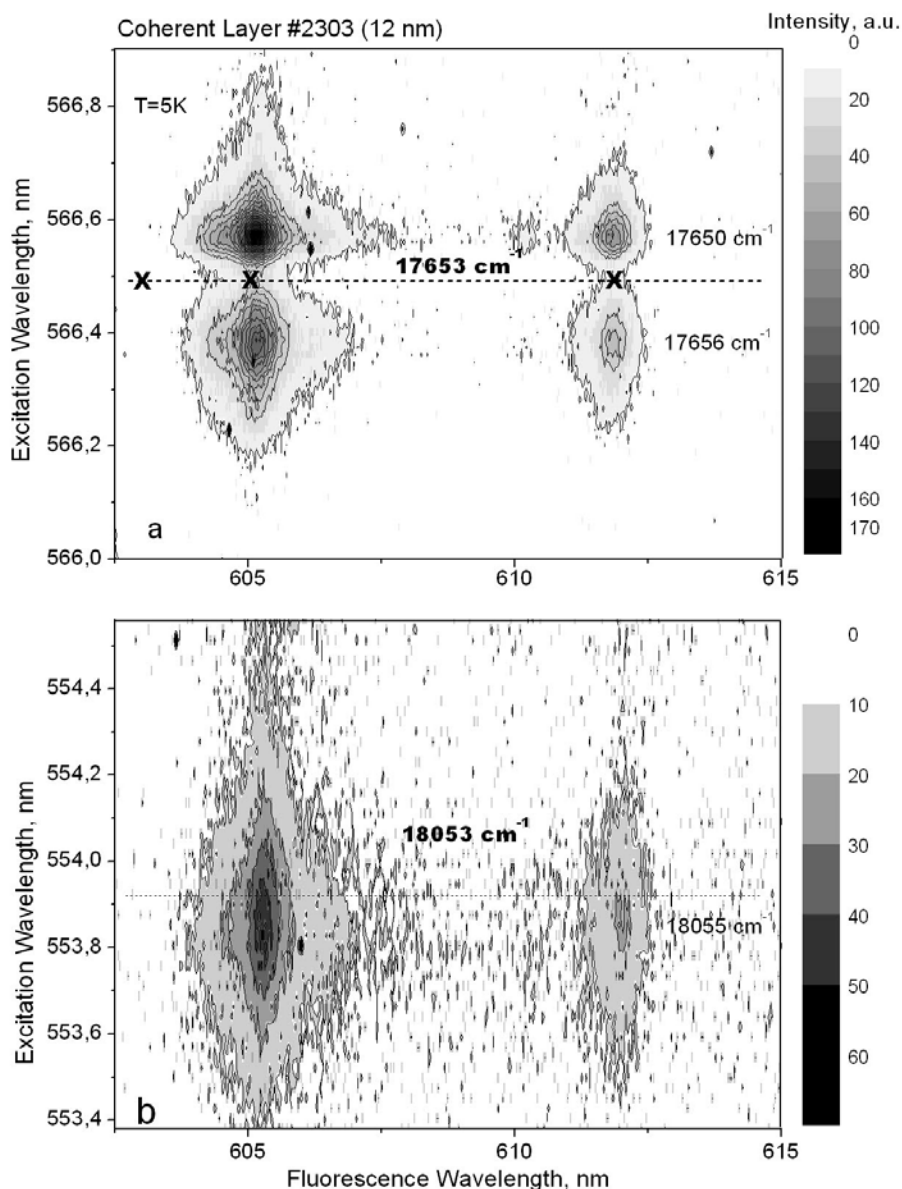


Fig.1. CEEs plot of the “cubic” Sm^{3+} center in coherent $\text{CaF}_2:\text{Sm}$ (0.1%) epitaxial layer 12 nm thickness at 5 K. a) – excitation from ${}^6\text{H}_{5/2}(\text{z1})$ to ${}^4\text{G}_{5/2}(\text{A1-low level})$ and b) – excitation to ${}^4\text{G}_{5/2}(\text{A2- high level})$. The excitation energies for $\text{Sm}^{3+} \text{O}_h$ - centers in $\text{CaF}_2:\text{Sm}$ bulk are shown by dash lines with 17653 cm^{-1} and 18053 cm^{-1} in a) and b) of the figure, respectively; the PL peak positions note in a) by sign “X” according [4].

References:

- [1] Sokolov N.S., Vigil E., Gastev S.V., Novikov S.V., Yakovlev N.L., J. Fiz. tverd. tela 31 (1989) 75 (In Russian)
- [2] Sokolov N.S., Yakovlev N.L. Proc. SPIE, 2706 (1996) 57
- [3] Gastev S.V., Alvares J.C., Vitvinsky V.V., Sokolov N.S., Khilko A.Yu. Proc. SPIE, 2706 (1996) 67
- [4] J-P.R.Wells and R.J.Reeves, Phys.Rev.B. 61, (2000), 13593.
- [5] Newman D.J. and Ng B. 2000 Crystal Field Handbook (Cambridge: Cambridge University Press) p. 290
- [6] Malkin B Z 1987 Spectroscopy of Solids Containing Rare-Earth Ions (Amsterdam: Elsevier Science) p.13

[We-P-51] Optical spectroscopy of LaGaO₃ crystal doped with Mn ions

L.R.Gilyazov, S.I.Nikitin

Kazan Federal University

In the past years, perovskite manganites have been extensively studied due to the discovery of the colossal magnetoresistance effect and rich complex phase diagram of these materials. According to most theoretical models, magnetic and transport properties of these compounds are determined by the double-exchange mechanism and vibronic interaction. It has been shown that the nature of charge-spin dynamics in these compounds can be determined on simple model mixed valence systems containing small number of ions [1]. As the first step on the way we have studied impurity centers of single Mn ions in the LaGaO₃ crystal with perovskite structure doped with Mn ions (0.5 at.%) by optical spectroscopy methods.

The LaGaO₃ crystal were grown by Czochralsky technique in slightly oxidizing atmosphere. The room temperature absorption spectrum of as-grown LaGaO₃:Mn reveals the single band with a maximum at 520 nm. Under optical excitation into the 520 nm absorption band, emission peaking at 714 nm has been observed. The emission decay is a single exponential. The absorption and emission spectra are characteristic to d³(Mn⁴⁺) ions in strong crystal field with octahedral coordination, the absorption band at 520 nm corresponds to the ⁴A₂→⁴T₂ transition and the emission band with the maximum at 714 nm correspond to the ²E→⁴A₂ transition. In the framework of strong crystal field model Racah parameter $B=855\text{ cm}^{-1}$ and crystal-field splitting parameter $Dq=1930\text{ cm}^{-1}$ of the Mn⁴⁺ center in LaGaO₃ crystal have been estimated.

In order to find manganese ions in trivalent state we annealed the crystal LaGaO₃:Mn in reducing hydrogen atmosphere. Luminescence spectrum of the annealed LaGaO₃:Mn crystal measured at 5 K is shown in Fig.1. With increasing the temperature, intensities of both emission bands decrease monotonically and at room temperature the bands completely disappear.

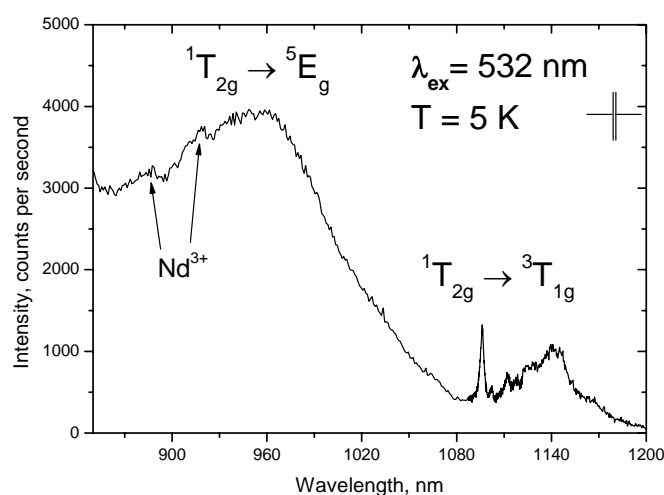


Fig.1. Luminescence spectra of the annealed LaGaO₃:Mn crystal, T= 5 K.

The excitation spectra of the luminescence bands are coincide with each other (Fig.2), the emission decay is single exponential with lifetime $\tau=416\pm 5\ \mu\text{s}$ (T=5 K) and it doesn't depend on the detection wavelength.

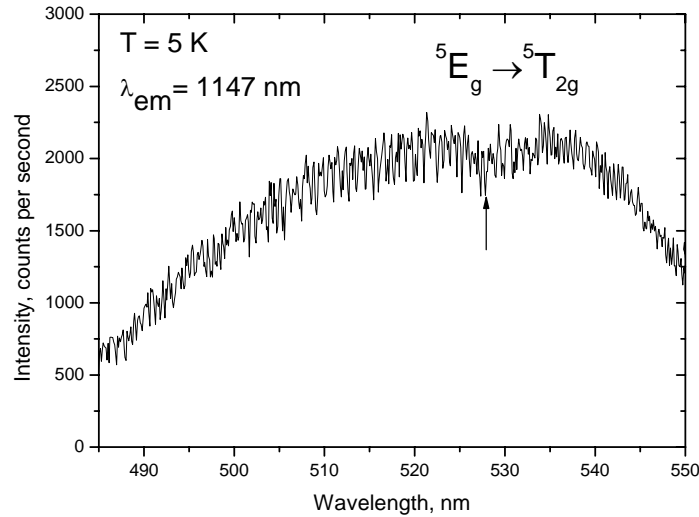


Fig.2. Excitation spectrum ($\lambda_{em}=1147$ nm) of the annealed $\text{LaGaO}_3:\text{Mn}$ crystal, $T = 5\text{K}$. Arrow indicates a dip due to the Fano antiresonance between 3E_g and ${}^5T_{2g}$ states.

The observed spectroscopic characteristics has been explained in the framework of $d^4(\text{Mn}^{3+})$ electronic configuration in strong crystal field. The band around 530 nm was assigned to a transition between the ${}^5T_{2g}$ excited state and the 5E_g ground state. A characteristic dip of this absorption band at 527 nm is caused by the Fano antiresonance mixing between the 3E_g and ${}^5T_{2g}$ energy states. Emission band at 1150 nm has a small bandwidth and a distinctive phonon sideband structure. As expected from the Tanabe-Sugano diagram this luminescence band should be assigned to ${}^1T_{2g} \rightarrow {}^3T_{1g}$ transition, because both levels have approximately the same crystal field dependence. Consequently emission band around 960 nm is assigned to ${}^1T_{2g} \rightarrow {}^5E_g$ transition. The level ${}^1T_{2g}$ is energetically lower than ${}^5T_{2g}$ level and at low temperature emissions correspond to transition from the ${}^1T_{2g}$ state to ${}^3T_{1g}$ and 5E_g states.

[1]. M.V. Eremin, S.I. Nikitin, S. Yu. Prosvirnin, N.I. Silkin and R.V. Yusupov, *Solid State Commun.* **117** 297 (2001).

[Tu-P-22]

Pressure dependence of crystal, orbital, and magnetic structures of LaMnO_3 and $\text{LaMn}_{0.5}\text{Ga}_{0.5}\text{O}_3$

L.E. Gonchar^{1,2*}, A.E. Nikiforov¹, Yu.V. Leskova¹, A.A. Firsin¹, D.P. Kozlenko³

¹*Ural State University, 620000, Ekaterinburg, Russia;*

²*Ural State University of Railway Transport, 620034, Ekaterinburg, Russia*

³*Frank Laboratory of Neutron Physics, JINR, 141980, Dubna, Russia*

**E-mail: lyudmila.gonchar@usu.ru*

The investigation of lanthanum manganite as well as other rare earth manganites is the field of great interest because the strong correlation between the crystal, charge, orbital and spin subsystems. As a consequence of this correlation one could observe the unusual properties upon external forces. The sublattice of magnetic trivalent manganese ions has the orbitally degenerated state in ideal oxygen octahedron environment. The environment distortions and other effect are intensively studied during last time. One of the interesting trends in manganites physics is the investigation of weakened orbital and magnetic correlations by doping strongly correlated manganese site by isovalent ions of orbitally non-degenerated iron or orbitally non-degenerated and non-magnetic gallium [1].

Our work is devoted to the investigation of pressure dependence of crystal structure and orbital subsystem in two manganite compounds: pure lanthanum manganite LaMnO_3 and $\text{LaMn}_{0.5}\text{Ga}_{0.5}\text{O}_3$. The pressure dependence of crystal structure is investigated experimentally and theoretically. For the theoretical description of the crystal structure of both compounds, the pair potential model with the strong electron-lattice interaction is used [2]. The same model could be used for the orbital structure simulation. For gallium doped manganite, the different models of dopant ordering are discussed. The orbital structure under external pressure is unstable.

The magnetic subsystem is described within the framework of orbitally-dependent exchange interaction model [3]. The changes of magnetic structure under the pressure are described taking into account crystal and orbital structure changes. The Neel temperature increases as a linear dependence upon pressure. Our model could explain this increase not only by Mn–O distances pressure dependence, but also by orbital component in the dependence.

The pressure effects on NMR spectra of ^{139}La are described.

[1] J.-S. Zhou, Y. Uwatoko, K. Matsubayashi, and J. B. Goodenough. Phys. Rev. B **78**, 220402 (2008)

[2] A. E. Nikiforov, S. É. Popov, and S. Yu. Shashkin, Fiz. Met. Metalloved. **87**, 16 (1999)

[3] L.E. Gontchar, A.E. Nikiforov. Phys. Rev. B **66**, 014437 (2002)

[We-P-44]

Temperature dependences of the second rank parameters b_2^0 and P_2^0 for the odd isotopes Gd^{3+} in $PbMoO_4$ and YVO_4

A.D. Gorlov, D.A. Gorlov

Institute of Physics and Applied Mathematics,

Ural State University, Ekaterinburg, Russian Federation

**E - mail: Anatoliy.Gorlov@usu.ru*

The investigations of the temperature dependences of the EPR spectrums of the odd isotopes Gd^{3+} in the crystals $PbMoO_4$ and YVO_4 carried out at $T=4.2$ K and 130-297 K show that the experimental second rank parameters of the spin-Hamiltonian defining the ground-state splitting ($|b_2^0|$) and nuclear quadrupole interaction ($|P_2^0|$) decrease in magnitude synchronously with the temperature growth. The experimental parameters b_2^0 and P_2^0 are listed in the table.

PbMoO₄					
T, K	b_2^0 (MHz)	P_2^0 (MHz)		b_2^0 / P_2^0	
		Gd^{155}	Gd^{157}		
1.8	-2500(1)		- 50,33(1)		49.67(3)
130	-2471.9(7)	-46,7(2)	-49.8(2)	52.9(3)	49.6(3)
200	-2443.7(6)	-46,4(3)	-49.3(3)	52.7(4)	49.6(3)
297	-2396.3(8)	-45,8(3)	-48.3(3)	52.3(4)	49.6(3)
YVO₄					
1.8	-1438(2)	55.052(6)	58.646(6)	- 26.12(6)	- 24.52(5)
130	-1407.3(5)	54.2(3)	57.6(3)	-25.9(2)	-24.4(2)
200	-1374.2(5)	53.1(3)	56.6(3)	-25.9(2)	-24.3(2)
297	-1322.6(6)	51.5(4)	55.1(4)	-25.8(3)	-24.1(3)

Since the b_2^0 to P_2^0 ratio is approximately constant for these crystals, it is reasonable to assume that the same fundamental mechanisms are responsible for the specific values of b_2^0 and P_2^0 .

The investigations of the hyperfine structure (HF) of the EPR spectrums of the odd isotopes Gd^{3+} and their simulations for the orientation external magnetic field normal to the major axis of the crystals show that the HF asymmetry observed is determined by the relative signs of b_2^0 and P_2^0 .

Thus our experimental results allow us to determine the theoretical model of the crystal fields used for the interpretation of the experimental data more accurately.

[We-O-32]
Adiabatic potential in ZnSe:Fe²⁺ crystal reconstructed in an ultrasonic experiment

V.V.Gudkov¹, I.V.Zhevstovskikh²

¹*Ural Federal University, 19, Mira st., Ekaterinburg, 620002 Russia*

²*Institute for Metal Physics, Ural Department of the Russian Academy of Sciences, 18, Kovalevskaya st., Ekaterinburg, 620219 Russia*

Ultrasonic experiments carried out with the use of a few zinc blende crystals doped with 3d ions have revealed anomalies in temperature dependences of attenuation α and phase velocity (see [1] and references therein). These anomalies were interpreted as manifestation of the Jahn-Teller (JT) effect [2]. Analysis of their frequency dependences [3] proved that they have a relaxation origin, moreover, almost temperature independent relaxation time $\tau(T)$ indicated the regime of static JT effect at low (i.e., liquid helium) temperatures. Among the investigated crystals, particular interest have attracted ZnSe:Fe²⁺ [4]. The ground state of the impurity ion in tetrahedral coordination is ⁵E(e³t³) and, therefore, it is an example of the most simple vibronic coupling, namely, E ⊗ e problem [5]. In this case the adiabatic potential depends upon tetragonal symmetric coordinates Q_ε, Q_σ, and it can be defined by the force constant K, linear F and quadratic G vibronic constants. Using an appropriate expression for ultrasonic attenuation [2]

$$\alpha(\omega, T) = \frac{4kNF^2 \langle Q^2 \rangle}{C\kappa_B T} \frac{\omega\tau(T)}{1 + [\omega\tau(T)]^2}, \quad (1)$$

we can determine the magnitude of F. In Eq.(1), ω is cyclic frequency of ultrasound, k is the wave number, N is the impurity concentration, $\langle Q^2 \rangle$ is factor accounting polarization of the wave and its direction of propagation, C is elastic modulus, κ_B is the Boltzmann constant. To obtain the magnitude of F one should measure attenuation at the temperature T₁ corresponding to the condition $\omega\tau(T_1) = 1$ provided the constants entering Eq.(1) are known. The procedure of T₁ determination was described in [3]. As a result,

$$F^2 = \frac{\alpha(\omega, T_1) C \kappa_B T_1}{2kN \langle Q^2 \rangle}. \quad (2)$$

After calculation, we have derived $|F| = 1.5 \times 10^{-5}$ dyn. One more parameter that can be determined in an ultrasonic experiment is the potential barrier V₀, over which the thermal activation occurs. It can be found from the temperature dependence of the relaxation time [2]. The contribution of activation process to the relaxation rate has the form of:

$$\tau(T)^{-1} = 3\nu_0 e^{-V_0 / \kappa_B T}. \quad (3)$$

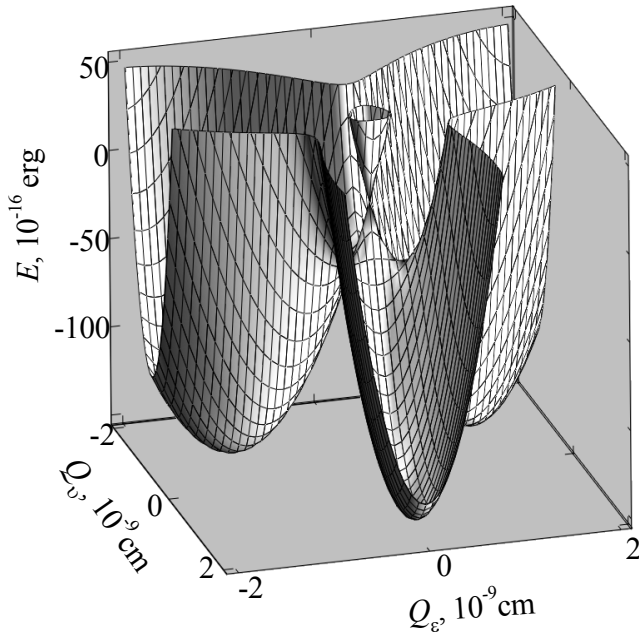
Thus, the slope of the curve $\ln[\tau(1/T)]$ at high temperatures defines the magnitude of V₀. Adiabatic potential of the E-term ground state E(Q_ε, Q_σ) written in polar coordinates (ρ, φ) as follows (see page 53 in [5]):

$$E_{\pm}(\rho, \phi) = \frac{1}{2} K \rho^2 \pm \rho [F^2 + G^2 \rho^2 + 2FG\rho \cos(3\phi)]^{1/2}. \quad (4)$$

To determine K and G , we can use the relations

$$E_{JT} = \frac{F^2}{2(K - 2|G|)}, \quad \delta = \frac{4E_{JT}|G|}{K + 2|G|}, \quad \text{and} \quad K = \mu\omega_{vib}^2, \quad (5)$$

where E_{JT} is the JT stabilization energy, δ is the height of the saddle point defined respectively the minima of the adiabatic potential, μ is the ligand mass and ω_{vib} is radial vibronic frequency.



We assume that at low temperatures all the JT complexes (Fe^{2+} and the nearest neighbors) are located in the lowest energy level broadened in general due to thermal motion. Therefore, the measured potential barrier should be: $V_0 = \delta - \frac{1}{2} \hbar\omega_{vib}$. We used the values of $V_0 = 24 \text{ cm}^{-1}$ [4], $\hbar\omega_{vib} = 70 \text{ cm}^{-1}$ [6], $\mu = 13 \times 10^{-23} \text{ g}$, and, finally, obtained: $|G| = 7.4 \times 10^3 \text{ dyn/cm}$ and $K = 2.3 \times 10^4 \text{ dyn/cm}$. The adiabatic potential calculated with these magnitudes of K , F , and G (all positive) is shown in the figure. We should note, this is the first such reconstruction whenever performed mostly on the basis of data derived in an ultrasonic experiment. The only parameter taken from the other type of experiment is the vibronic

frequency ω_{vib} .

This work was done within Russian Academy of Sciences Program (project No. 01.02.006. 13395), with partial support of the Russian Foundation for Basic Research (grant No. 09-02-01389).

[1] V.V.Gudkov, *et al*, J. Korean Phys. Soc. **53**, 63 (2008)

[2] M.D.Sturge, in *Solid State Physics*, vol.20, New York-London, Academic Press (1967), chap. The Jahn-Teller Effect in Solids, pp.92-211.

[3] V.V.Gudkov, *et al*, Phys. Rev. B, **77**, 155210 (2008).

[4] V.V.Gudkov, *et al*, Low Temp, **35**, 76 (2009).

[5] I.B.Bersuker, *The Jahn-Teller Effect in Solid State*, Cambridge University Press, Cambridge (2006).

[6] O.Mualin, *et al*, Phys. Rev. B, **65**, 035211 (2001).

[Tu-P-27]

Cathodoluminescent properties of YAG:Nd³⁺

K.N. Guliaeva, A.N. Trofimov, M.V. Zamoryanskaya

Ioffe Physical-Technical Institute, 194021, Saint-Petersburg, Russia, 26 Polytechnicheskaya st.

Yttrium-aluminum garnet doped with neodymium (YAG:Nd³⁺) crystal has a lot of applications in modern science and technology. For example, this material is used as a laser medium. Luminescent properties of YAG:Nd³⁺ in the infrared range are well studied. However, no luminescence in the visible and ultraviolet ranges is observed while exciting it with light. When excited with high-energy, such as X-ray irradiation or irradiation with an electron beam, YAG:Nd³⁺ has a rich intensive luminescence in the infrared, visible and ultraviolet ranges. It expands greatly the possibilities of its application. For example, YAG:Nd³⁺ can be used as a scintillator or X-ray phosphor.

Luminescence of YAG:Nd³⁺ in the visible and UV range has been studied earlier [1-6]. However, the interpretation of emission transitions in these works is contradictory, spectral positions of CL lines maximums differ. Therefore, our aim was to obtain cathodoluminescent properties of yttrium-aluminum garnet doped with neodymium, such as: spectral structure of emission transitions of neodymium, including the spectral position of lines and their fine structure at room temperature and at temperature of liquid nitrogen; dynamic characteristics of emission (decay and rise times of various CL lines at different temperatures); cathodoluminescent properties dependence on concentration of neodymium; degradation of cathodoluminescence of YAG: Nd³⁺ under continuous irradiation by electron beam.

The CL measurements were performed using X-ray microanalyzer Camebax Microbeam. Such experimental techniques allow to determine the composition of the sample with locality of 1 - 3 microns using electron probe microanalysis (EPMA) and analyze the luminescence from the same microvolume with excitation by electron beam. The method of EPMA was also used to investigate the composition of samples, the concentration of activators and homogeneity of their distribution. The method of local cathodoluminescence was used as the main method of research. Due to the fact that the energy of the electron beam (1-35keV) is much greater than the band gap in YAG (8eV), it becomes possible to investigate all optical transitions. The ability to vary the current of the electron beam (the excitation density) in a wide range allows to investigate the processes of saturation of emission levels. Focusing the electron beam to the size of a few tenths of a micron gives possibility for local studies of luminescent properties and visualization of the distribution of impurities (dopants) and defects [7]. Cathodoluminescent system in conjunction with a recording electronic equipment and software package allows to receive the cathodoluminescence spectra, and to observe dynamics of the emission bands (decay and rise), that allows to measure the characteristic lifetimes of excited states.

Thus, during researches the following data was obtained: cathodoluminescence spectra of yttrium-aluminum garnet with a resolution of 0.1 nm in the visible and near UV range (200-800 nm) [8], (Fig. 1,2,); cathodoluminescence times of decay of each transition after excitation; the dependence of cathodoluminescent properties of material on the concentration of neodymium (Fig. 3,4); degradation characteristics of cathodoluminescence under continuous irradiation of electron beam.

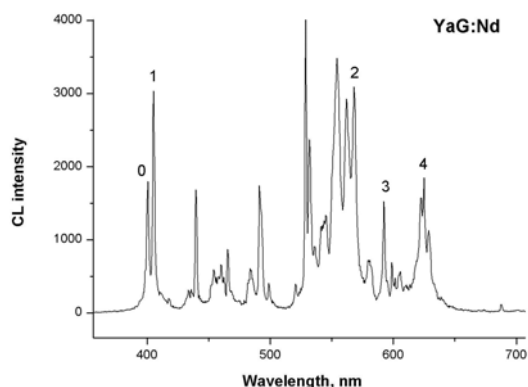


Fig.1. CL spectrum of YAG: Nd³⁺

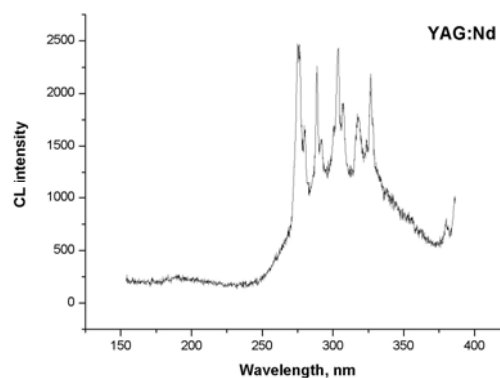


Fig. 2. Lines of CL of YAG: Nd³⁺ in UV range

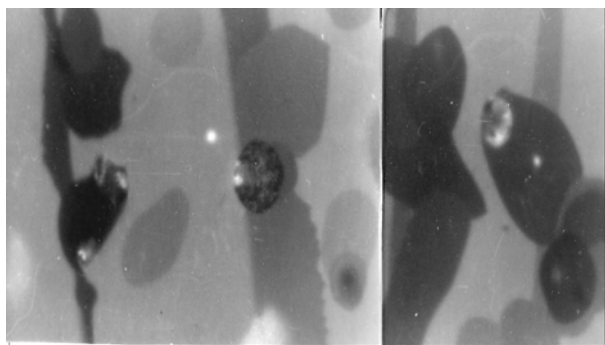


Fig. 3. CL image of YAG: Nd³⁺. In dark areas Nd³⁺ concentr. – 2-3%at., in light areas – 1-1,5%at.

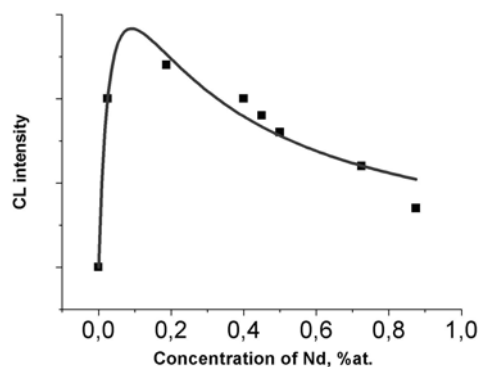


Fig. 4. Concentration dependence of emission line "1" from Fig. 1

Using received data we could interpret the spectrum of cathodoluminescence of YAG: Nd³⁺.

- [1]. A.V. Rasuleva, V. Solomonov, Solid State Physics, 2005, Volume 47, 8, 1432-1434
- [2]. S.Kh.Batygov, Yu.K.Voron'ko, N.G.Margiani, N.N.Ryskin, Advanced Solid-State Lasers, 1991, 368-370
- [3]. Yu. K. Voron'ko, E. L. Nolle, V.V. Osiko, M.I. Timoshechkin, JETP Lett, 1971, Volume 13, 125-128
- [4]. A.Niklas, W.Jelenski, Physics State Solidi (a), 1983, 77, 393
- [5]. Kolomiitsev A.I., Meylman M.L, Volodina I.S, Chukichev M.V, Smagin A.G, Bagdasarov H.S, Optics and Spectroscopy, 1984, 56, № 2, 365-367
- [6]. V.V. Randoshkih, B.I. Belovolov, N.V. Vasil'eva, K.A. Zykov-Myzin, A.M. Saletsky, N.N. Sysoev, A.N. Churkin, Quantum Electronics, 2001, 31, № 9, 799-800
- [7]. M.V. Zamoryanskaya, S.G. Konnikov, A.N. Zamoryanskiy, Instruments and Experimental Techniques, 3, p.1-8, (2004)
- [8]. Guliaeva K.N., Trofimov A.N., "Cathodoluminescence system calibration by using cathodoluminescence spectra of YAG:Nd³⁺", Thesis in book of abstracts of the sixth international conference for young scientists «Optics 2009».

[Th-I-40]

Zero-phonon lines: novel manifestations of vibronic interactions in impurity centers of solids

V. Hizhnyakov

Institute of Physics, University of Tartu, Tartu, Estonia

**E-mail: hizh@fi.tartu.ee*

An important feature of the phonon-assisted processes in impurity centres of solids at low temperatures is the existence of well-distinguishing zero-phonon transitions. These transitions determine quantum diffusion, coherent hopping of polarons and excitons, and they lead to the appearance of the zero-phonon lines (ZPLs) in optical spectra. At low temperatures the lines have very small (often natural) homogenous width and huge peak intensity. The lines are highly sensitive to the vibronic interactions in optical center allowing for a number of applications of the ZPL-based solid state spectroscopy (see, e.g. [1-3]).

The standard theory [4-6] based on the weak or moderate change of the local phonon dynamics under the electronic transition predicts the Lorentzian shape of ZPL and $\sim T^4$ and $\sim T^7$ dependences of its position and homogeneous width on temperature in the low temperature limit. However in last years a number of systems, both crystalline and amorphous have been found in which a remarkable deviations from the laws mentioned have been observed. In some of these systems the shape of the line is essentially non-Lorentzian. In amorphous solids the anomalous temperature dependence of ZPLs may be usually explained by interaction of optical centers with the continuum of the low-energy two-level (tunneling) systems. However in other systems the effects mentioned are most probably connected with strong change of the local phonon dynamics under the electronic transition. The generalizations [7-10] of the standard theory allowing one to take into account corresponding vibronic coupling and to explain the observed anomalous lines will be discussed.

- [1] K. Rebane, Impurity Spectra of Solids (Plenum Press, New York, 1970).
- [2] Y. Toyozawa, Optical Processes in Solids (Cambridge University Press, 2003).
- [3] I.S. Osad'ko, Selective Spectroscopy of Single Molecules, Springer, Berlin, 2003.
- [4] D.E. McCumber, Math. Phys. 5 (1964) 508.
- [5] M.A. Krivoglaz, Sov. Phys. Solid State 6 (1964) 1340.
- [6] G.F. Levenson, Phys. Status Solidi B 43 (1971) 739.
- [7] V. Hizhnyakov, K. Seranski, U. Schurath, Chem. Phys. 163 (1992) 249
- [8] V. Hizhnyakov, I. Tehver, Chem. Phys. Lett. 422 (2006) 299.
- [9] V. Hizhnyakov, I. Tehver, G. Benedek, EPJ B 70(4) (2009) 507.
- [10] V. Hizhnyakov, Chem. Phys. Lett. 493 (2010) 191.

Calculation of crystal-field parameters for 4f and 5d states of lanthanide ions from ab-initio calculations

L. Hu¹, M.F. Reid^{2*}, C.-K. Duan³, S. Xia¹, M. Yin¹

¹*Department of Physics, University of Science and Technology of China, Hefei, 230026, China*

²*Department of Physics and Astronomy and MacDiarmid Institute for Advanced Materials and Nanotechnology University of Canterbury, Christchurch, New Zealand*

³*Institute of Modern Physics, Chongqing University of Post and Telecommunications, Chongqing 400065, China*

**E-mail: Mike.Reid@canterbury.ac.nz*

In recent years a variety of ab-initio calculations for the $4f^N$ and $4f^{N-1}5d$ configurations of lanthanide ions in crystals have appeared [1-3]. However, these calculations are difficult to relate to standard calculations using crystal-field and “free ion” spectroscopic parameters. Furthermore, if parameters are not derived, the calculations cannot give guidance for other ions in the lanthanide series.

We have recently shown how crystal-field parameters may be deduced from the energy levels and eigenvectors from ab-initio calculations [4]. In this paper we apply this method to Ce^{3+} ions in a variety of host crystals. We obtain good agreement with published energy levels of the 4f and 5d states. Since it is impossible to fit crystal-field parameters for Ce^{3+} in low-symmetry sites we make comparisons with crystal-field parameters fitted to the energy levels other ions in the series, with generally good agreement.

[1] G. Brik and K. Ogasawara, Spectroscopy Letters, 40, (2007) 221.

[2] J. Andriessen, E van der Kolk, and P. Dorenbos, Phys. Rev. B, 76, (2007) 075124.

[3] J. Gracia, L. Seijo, Z. Barandiaran Z, et al., J. Luminescence, 128, (2008) 1248.

[4] M. F. Reid, C. K. Duan, and H. Zhou, J. Alloys Comp, 488, (2009) 591.

Calculations of energy levels, dynamics, and lifetimes of $4f^{12}5d$ states of Tm^{2+} in $SrCl_2$

R. Hughes-Currie¹, M.F. Reid^{1*}, J. Grimm², H.U. Güdel²

¹*Department of Physics and Astronomy and MacDiarmid Institute for Advanced Materials and Nanotechnology University of Canterbury, Christchurch, New Zealand*

²*Department of Chemistry and Biochemistry, University of Bern, Bern, Switzerland*

**E-mail: Mike.Reid@canterbury.ac.nz*

Over the past ten years we have used phenomenological models that extend the well-established approach to calculating energy levels for the $4f^N$ and $5f^N$ configurations of lanthanide ions to the $4f^{N-1}5d$ and $5f^{N-1}6d$ configuration [1-2].

In this paper we report on calculations for Tm^{2+} in $SrCl_2$ [3]. By calculating the energy levels and transition rates we are able to simulate the absorption spectrum and model the lifetimes of the excited states. By calculating the proportion of $5d e_g$ and t_{2g} components in the $4f^{12}5d$ states we are able to explain why some spectral features are sharp and some are broad, analogous to the case for trivalent ions [4].

[1] M. F. Reid, L. van Pieterse, R. T. Wegh, and A. Meijerink, Phys. Rev. B 62 (2000) 14744.

[2] G. W. Burdick and M. F. Reid, In K.A. Gschneidner Jr., J.C. Bunzli, V.K. Percharsky. Handbook on the Physics and Chemistry of the Rare Earths,, 2007, Volume 37, Chapter 232, pages 61-98. North Holland.

[3] J. Grimm, O. S. Wenger, K. W. Kramer, and H. U. Güdel, J. Luminescence 126 (2007) 590.

[4] L. van Pieterse, M. F. Reid, and A. Meijerink. Phys. Rev. Lett. 88 (2002) 067405.

[Tu-P-6]

Selfquenching in Tm-doped Sodium-Yttrium double fluoride crystals (Tm:NYF)

S.E. Ivanova¹, A.M. Tkachuk^{1,2}, A. Mirzaeva², F. Pellé³

¹ *University of Information Technology, Mechanics and Optics, St. Petersburg, Russia*

² *Scientific Production Corporation "S.I. Vavilov State Optical Institute", Russia*

³ *LCMCP UMR7574 CNRS - Université P&M Curie-ENSCP, Paris F-75235, France*

New low phonon energy rare earth (RE) doped sodium-yttrium double fluoride crystals $\text{RE}^{3+}:\text{Na}_{0.4}\text{Y}_{0.6}\text{F}_{2.2}$ ($\text{RE}^{3+}:\text{NYF}$) represent a particular interest for application as active media for solid-state lasers emitting in VIS and IR spectral domains not only due to the wide spectral domain of RE emission (from UV up to $\sim 3 \mu\text{m}$) but also due to inhomogeneous broadening in RE spectra in these crystals, which is a consequence of a disordered crystal structure of the $2\text{NaF}-3\text{YF}_3$ system. This property permits to obtain tuneable lasing and, from the other hand, to reduce requirements on the stability of pumping laser diode (LD) emission. The $\text{Nd}^{3+}:\text{NYF}$ crystals are known as active media, in which tuneable laser action in the region from 1.04 to 1.07 μm has been demonstrated [1]; in the double fluoride $\text{Er}^{3+}:\text{NYF}$ crystals a CW laser action at 2.8 μm was achieved under LD pumping [2].

In this work, we report on spectroscopic study and energy transfer processes of Tm³⁺ doped NYF (Tm:NYF) crystals, in order to evaluate their potential for application as an active media of solid state tunable diode-pumped lasers. The luminescence kinetics of the 1D₂, 1G₄ and 3H₄ Tm levels was investigated experimentally using selective short pulse laser excitation in crystals with Tm concentration in the range from 0.5 to 20 at. %. On the basis of spectroscopic characteristics of Tm:NYF crystals concentration selfquenching (SQ) of luminescence from these levels was studied both theoretically and experimentally on the bases of experimental and calculated characteristics of intracenter transitions. Macrorates of luminescence selfquenching were calculated within the framework of energy transfer theoretical model using the SQ microparametres obtained from the model quantum-mechanical calculation, good agreement between experimental results and calculation was achieved.

Infrared luminescence spectra of Tm:NYF crystals with various Tm concentration (0.5 – 20 at. %) were recorded, a CW Ti:sapphire laser emission at $\lambda_{\text{exc}} = 792 \text{ nm}$ (resonant with $^3\text{H}_6 \rightarrow ^3\text{H}_4$ transition) was used as an excitation source. Cascade emission of Tm ions at 1400 - 1550 nm ($^3\text{H}_4 \rightarrow ^3\text{F}_4$ transition) and at 1600 - 1900 nm ($^3\text{F}_4 \rightarrow ^3\text{H}_6$ transition) was observed in samples with low Tm concentration. It was shown, that the intensity of luminescence band at 1400 - 1550 nm decreases with increasing of Tm concentration, whereas the intensity of luminescence band at 1600 - 1900 nm increases considerably. Mechanisms of population of the $^3\text{F}_4$ level under IR pumping at $\lambda_{\text{exc}} = 792 \text{ nm}$ in NYF crystals with high Tm concentration are discussed, possible energy transfer processes influencing population of the $^3\text{F}_4$ level are considered.

References

- [1] H. Chou, P. Albers, A. Cassahno, H.P. Jenssen, Springer. Ser. Opt. Sci. **6** (9) (1986) 325
- [2] A.M. Tkachuk, S.E. Ivanova, M.-F. Joubert, Y. Guyot, and V.P. Gapontzev, "Population of Excited Erbium Levels in $\text{Er}^{3+}:\text{Na}_{0.4}\text{Y}_{0.6}\text{F}_{2.2}$ (Er:NYF) Laser Crystals", J. Alloys and Comp. **380**(1-2), 130-135 (2004)

[Th-O-48]

Luminescence and energy transfer in RE³⁺:KPB₂Cl₅ crystals at UV excitonic and RE direct excitation

S.E. Ivanova¹, A.M. Tkachuk^{1,2}, F. Pellé³, L.I. Isaenko⁴, M.-F. Joubert⁵, Y. Guyot⁵

¹ *University of Information Technology, Mechanics and Optics, St. Petersburg, Russia*

² *Scientific Production Corporation "S.I. Vavilov State Optical Institute", Russia*

³ *LCMCP UMR7574 CNRS - Université P&M Curie-ENSCP, Paris F-75235, France*

⁴ *Institute of Mineralogy & Petrography SB RAS, Russia*

⁵ *LPCML, UMR 5620 du CNRS, Université Lyon 1, France*

The RE-doped low phonon energy potassium-lead chloride crystals (RE³⁺:KPB₂Cl₅) are promising new material emitting in a wide spectral region from UV up to mid IR [1]. They have low hygroscopicity, they are transparent from 330 nm up to 20 μm, and have been demonstrated to be very advantageous active media for direct and upconversion diode-pumped lasers. Laser action in Er:KPC at both 1.7 and 4.5 μm have been demonstrated in [2].

We report on the results of comparative study of luminescence spectra and energy transfer dynamics spectroscopic study of KPB₂Cl₅ (KPC) crystals, doped with RE³⁺ ions (RE³⁺ = Nd, Er, Ho, Tm, Yb) under UV conduction band (at λ_{exc}=253 nm), excitonic (at λ_{exc}=283 nm) excitation and selective direct RE ions at UV, VIS and IR excitation. The absorption, emission spectra and luminescence dynamics were studied at low and room temperatures using time-resolved spectroscopy under selective laser excitation.

Excitation into excitonic absorption band (λ_{max}=283 nm) at low (8-20 K) temperature leads both to exciton and RE ions emission. The recombination of self-trapped exciton at low temperature is followed by broad-band emission in visible spectral range (λ_{max}~550 nm) with nanosecond decay time together with a series of narrow lines corresponding to RE ions emission, having luminescence decay rates in the ranges of micro and milliseconds. Stocks shift between absorption (λ_{max}^{abs} = 285 nm) and emission exciton (λ_{max}^{lum} ~ 550 nm) bands is explained in framework of configuration coordinate model as Frank-Condon shift between the minima positions of the ground and excited exciton states.

At room temperature RE emission lines are observed in spectral ranges which correspond to the excitonic emission ranges, in spite of the strong quenching of excitonic emission at temperature above 200 K. The conclusion was made that exciton recombination is followed by fast (>1 μs) energy transfer to impurity at wide temperature interval (20 – 300)⁰K, but energy transfer efficiency decreases with increasing temperature. Possible ways of exciton → impurity energy transfer are discussed.

In case of direct RE ions UV excitation (at λ_{exc}=355 nm), the population of lower energy levels of RE ions goes via cascade schemes and luminescence decay curves can be described as a linear combination, at least, of two exponents.

Under IR pulsed laser or CW laser diode IR excitation the RE:KPC (RE=Nd, Er, Yb) crystals exhibit upconversion luminescence in the UV, VIS and IR spectral ranges. The most intensive bands correspond to transitions from directly pumped ⁴I_{11/2} Er level and two-photon excited ⁴S_{3/2} level. Luminescence bands originating from three-photon excited ⁴G_{11/2}, ²H(G)_{9/2} and ⁴F_{5/2} levels have significantly lower intensity. The results of the luminescence dynamics analysis give evidence

of efficient ESA and nonradiative Er ↔ Er and Yb ↔ Er energy transfer processes in studied crystals. The power and concentration dependencies of erbium luminescence intensity under excitation at $^4I_{11/2}$ erbium level ($\lambda_{exc} = 980$ nm) or $^2F_{5/2}$ ytterbium level ($\lambda_{exc} = 940$ nm) permit us to conclude that the increasing of pump power density leads to the saturation of $^4I_{11/2}$ level population. It was demonstrated that co-doping of low concentrated Er:KPC crystals with Yb ions increases the efficiency of upconversion processes. The different schemes of energy transfer are discussed.

References

- [1] L.I. Isaenko, A.P. Yelissev, A.M. Tkachuk, S.E. Ivanova. In *MID-Infrared coherent sources and applications* (Springer, Series B: Physics and Biophysics, 2007), Eds. M. Ebrahimzadeh and I. Sorokina. Chapter 1.
- [2] S.R. Bowman, S.K. Searles, N.W. Jenkins, S.B. Qadri, E.F. Skelton, Josef Ganem, "New Mid-IR Laser on an Erbium activated low phonon energy crystal" In *Technical Digest of conference of Lasers and Electro-Optics, May 8-10*, (Baltimore, Maryland, USA, 2001) CLEO, CFD2, 557-558, (2001)

[Th-O-49]

Upconversion absolute efficiency in Er doped Calcium-Yttrium double fluoride crystal

S. Ivanova¹, F. Pellé², A.M. Tkachuk^{1,3}

¹*University of Information Technology, Mechanics and Optics, St. Petersburg, Russia*

²*LCMCP UMR 7574 CNRS - Université P&M Curie-ENSCP, Paris F-75235, France*

³*Scientific Production Corporation "S.I. Vavilov State Optical Institute", Russia*

The rare earth doped low phonon energy materials are well known for efficient conversion of IR radiation to the visible spectral domain. Depending on application, upconversion in these materials may play a positive or negative role. As an example, in upconversion lasers this is an essential process leading to creation of population inversion on laser transition [1]. On the contrary, in directly pumped laser media upconversion process may (i) constitute a source of losses if it leads to depopulation of initial level of laser transition or (ii) provide possibility to achieve CW laser action on self-terminating laser transition in a case when it depopulates the final laser transition level [2]. Besides laser and IR-sensor applications, upconversion processes may be used in a photon addition type photovoltaic (PV) system. In such systems, a PV cell absorbs the high-energy photons of the solar spectrum whereas the IR photons (transmitted by the semiconductor solar cell) are converted in an upconversion layer to higher energy photons and returned to the cell, e.g. using a simple mirror [3]. This leads to enhancement of light to voltage conversion efficiency of the whole system. For all these applications, detailed knowledge on the energy transfer processes, leading to upconversion, are required in order to find optimal composition of upconversion material and conditions of pumping. In spite of the fact that the upconversion processes in rare earth doped materials are extensively studied up to now, there exist a very few publications reporting on the upconversion efficiency measurements. Due to the inherent nonlinearity of up-conversion process, such measurements become a rather sophisticated procedure. Er-doped materials are especially perspective for PV applications for crystalline silicone based solar cells, which represent today the most widely applied technology.

In this paper we report on the results of absolute upconversion efficiency measurements performed for Er doped calcium-yttrium fluoride crystal $\text{Er}:\text{Ca}_{0.89}\text{Y}_{0.11}\text{F}_{2.11}$. The upconversion luminescence was excited by a CW Er glass fibre laser emitting at $1.53\ \mu\text{m}$ (IR to NIR upconversion). Luminescence signal was collected using an integrating sphere, and analysed with a calibrated spectrometer. The absolute upconversion efficiency measurements were provided in a large (up to 6 orders of magnitude) scale of pump power densities. Since upconversion efficiency depends strongly on excitation power density, such data are indispensable for comparison of materials considering their potential for applications. The setup and method for absolute upconversion efficiency measurements will be presented, along with a brief description of synthesis of studied materials.

The experimental results of the absolute upconversion efficiency measurements and the analysis of the experimental data will be presented in details. For the upconversion of IR radiation at $1.53\ \mu\text{m}$ to the VIS and NIR-range ($\sim 0.98\ \mu\text{m}$) it was shown that the luminescence spectrum and the absolute upconversion efficiency vary strongly with the pump power.

The $\text{Ca}_{0.89}\text{Y}_{0.11}\text{F}_{2.11}:\text{Er}5\%$ crystal was found to be a very efficient IR to VIS upconverter, demonstrating efficiency (i.e., ratio of power of luminescence at $\sim 0.98 \mu\text{m}$ to the absorbed IR energy at $\sim 1.53 \mu\text{m}$) up to 17% at pump power density of $\sim 100 \text{ W/cm}^2$. This value of pump power density is optimal for the IR to NIR upconversion, as the upconversion efficiency becomes lower at both lower and higher pump power densities (cf. Figure). These results will be supported by a detailed experimental and theoretical study of the energy transfer and excited state absorption processes taking place in the $\text{Ca}_{0.89}\text{Y}_{0.11}\text{F}_{2.11}:\text{Er}5\%$ crystals, which, in its turn, are linked with the structural properties of the crystal.

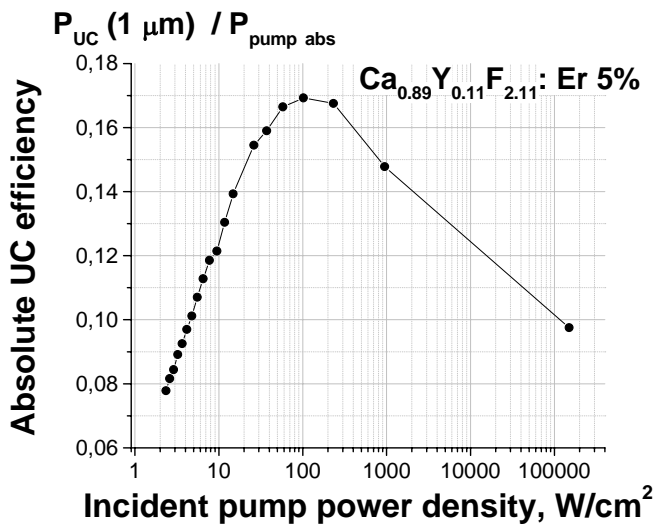


Fig.1. Absolute efficiency of $1.53 \mu\text{m} \rightarrow 0.98 \mu\text{m}$ upconversion in $\text{Ca}_{0.89}\text{Y}_{0.11}\text{F}_{2.11}:\text{Er}5\%$ crystal as a function of pump power density.

The conclusion was made that the developed experimental setup provides an efficient tool for characterisation of materials demonstrating IR to NIR upconversion. The obtained results show that the $\text{Ca}_{0.89}\text{Y}_{0.11}\text{F}_{2.11}:\text{Er}5\%$ crystal is a very efficient IR to NIR upconverter.

Part of this work was supported by the ANR, project name "THRI-PV".

References:

[1] E. Heumann, S. Bär, K. Rademaker, G. Huber et al., "Semiconductor-laser-pumped high-power upconversion laser", *Appl. Phys. Lett.* **88**, p. 061108 (2006)
 [2] A.M. Tkachuk, S.E. Ivanova, M.-F. Joubert and Y. Guyot, *J. Alloys and Comp.* **380**, pp.130-135 (2004)
 [3] T. Trupke, M. A. Green, P. Würfel, "Improving solar cell efficiencies by up-conversion of sub-band-gap light" *J. Appl. Phys.* **92**, p. 4117 (2002)

[We-P-32]

The origin of the 1.6 eV absorption band in the rare-earth hexagonal manganites $RMnO_3$ and $YMn_{1-x}Ga_xO_3$

A.M. Kalashnikova,^{1,5} S.A. Basun,¹ A.S. Moskvina,² A.A. Nugroho,^{3,4}
T.T.M. Palstra,⁴ Th. Rasing⁵, R.V. Pisarev¹

¹*Ioffe Physical-Technical Institute, 194021 St. Petersburg, Russia*

²*Ural State University, 620083, Ekaterinburg, Russia*

³*Solid State Materials Laboratory, Zernike Institute for Advanced Materials, University of Groningen, NL9747AG Groningen, The Netherlands*

⁴*Faculty of Mathematics and Natural Sciences, Institute Teknologi Bandung, 40132 Bandung, Indonesia*

⁵*Radboud University Nijmegen, Institute for Molecules and Materials, 6525AJ Nijmegen, The Netherlands*

During the last decade the interest in multiferroic materials possessing more than one type of ordering has significantly increased [1,2]. Among these, the rare-earth hexagonal manganites $RMnO_3$ are the multiferroics that combine ferroelectric and magnetic ordering [2,3], with a high ferroelectric Curie temperature and high remnant polarization. However, despite intensive studies of the ferroelectric, magnetic and magnetoelectric properties of hexa- $RMnO_3$, their electronic structure remains not fully understood.

Optical spectra of all hexagonal manganites $RMnO_3$ possess a common well-pronounced a strong absorption feature centred at the photon energy of ~ 1.6 - 1.7 eV (Fig. 1) [4-6]. In literature there are two fundamentally different interpretations of the nature of this band, suggesting its relation either

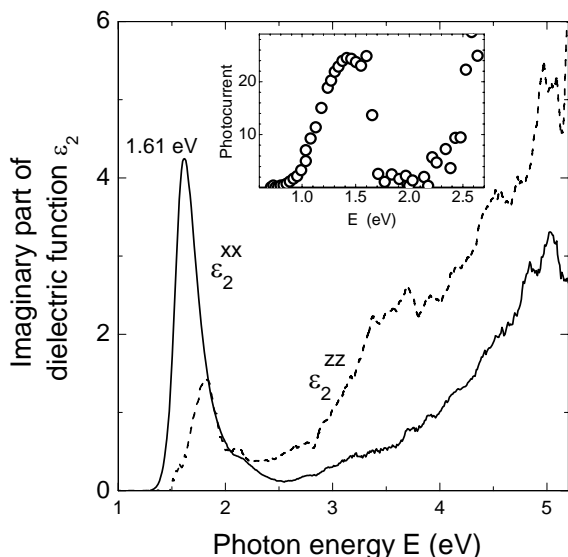


Fig. 1 Imaginary part of the dielectric function of $YMnO_3$ as a function of the photon energy for light polarized along (ϵ_2^{zz}) and perpendicular (ϵ_2^{xx}) to the hexagonal axis. Insert shows the photocurrent spectrum measured at $T=78$ K.

to the local transitions in the $3d$ shell of the Mn^{3+} ion [4] or to the charge-transfer transitions between $O2p$ valence band to the empty $3d$ levels of manganese [5]. Indeed, the electronic structure of the hexagonal manganites [7] implies both possibilities. Later, based on the spectroscopy of the hexa- $RMnO_3$ thin films and LDA+U calculations, it was suggested [6] that the strong $O2p$ - $Mn3d$ hybridization of the valence band plays a crucial role in forming the optical response in the range of 1.6-2.3 eV.

Here we report the study of the optical and photoconductivity spectra of the rare-earth hexagonal manganites $RMnO_3$ ($R=Y, Sc$ and Er) and $YGa_xMn_{1-x}O_3$. Our aim was to reveal further the nature of the electronic structure of hexa- $RMnO_3$ and, in particular, of the 1.6 eV absorption band.

By means of a spectroscopic ellipsometry we have studied the anisotropy of the observed absorption peak and have found [4] that it appears to be strongly anisotropic and is predominantly observed for the light polarized within the basal xy plane (Fig. 1(b)). Such anisotropy is characteristic for charge-transfer transitions. Moreover, the photoconductivity spectrum of the hexagonal $YMnO_3$ behaves very similar to the optical spectra. The photocurrent possesses a

pronounced peak at the photon energy of ~ 1.55 eV (see insert in Fig. 1(a)), thus suggesting the non-localized nature of the relevant absorption band.

Additional information on the nature of the 1.6 eV absorption band can be obtained from studying samples where a fraction of Mn^{3+} ions is substituted by Ga^{3+} ions [8]. In this case a significant blue shift (~ 0.14 eV) of the 1.6 eV band is observed as 30% of Ga ions are substituted for Mn ions (Fig.

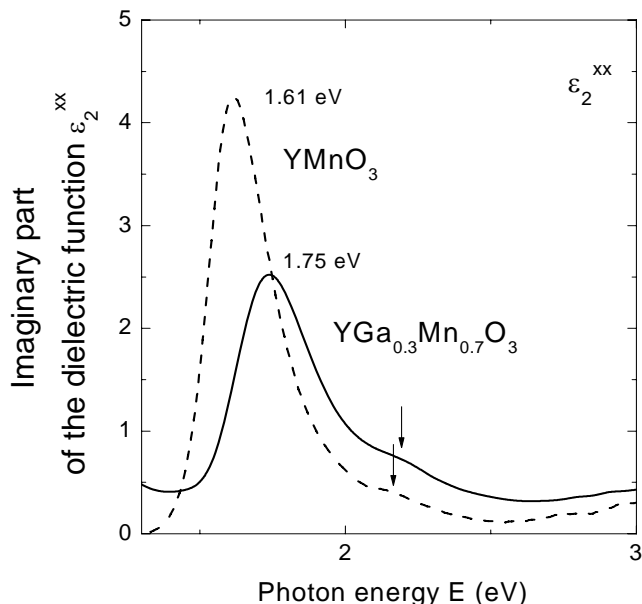


Fig. 2 Imaginary part of the dielectric function of $\text{YGa}_x\text{Mn}_{1-x}\text{O}_3$ (solid line) and YMnO_3 (dashed line) as a function of the photon energy for light polarized in the basal plane. Arrows show the position of the

2). We note that the second band centred at ~ 2.15 eV, which was also assigned in [6] to the transition from the p - d hybridized valence band, undergoes a much weaker blue shift.

Thus, on basis of the results discussed above we conclude that the origin of the strong absorption peak at 1.6 eV is indeed a non-localized charge-transfer interband transition [5,6] which involves an electron transfer from the $\text{O}^{2-}2p$ shell to the empty states of the Mn^{3+} ion.

The work was partly supported by Russian Foundation for Basic Research (grant 09-02-00070), Russian Agency for Science and Innovations (contract 02.740.11.0384), the Netherlands Organization for Scientific Research NWO, the Dutch NanoNed Initiative and EC FP7 (grant 214810-Fantomas).

- [1] M. Fiebig, *J. Phys. D: Appl. Phys.* **38**, R123 (2005).
- [2] S.-W. Cheong and M. Mostovoy, *Nature Mat.* **6**, 13 (2007).
- [3] B. B. van Aken, *et al.*, *Nature Mat.* **3**, 164 (2004).
- [4] A. B. Souchkov, *et al.*, *Phys. Rev. Lett.* **91**, 027203 (2003).
- [5] A. M. Kalashnikova and R. V. Pisarev, *JETP Lett.* **78**, 143 (2003).
- [6] W.-S. Choi, *et al.*, *Phys. Rev. B*, *Phys. Rev. B* **77**, 045137 (2008).
- [7] C. Degenhardt *et al.*, *Appl. Phys. B: Lasers Opt.* **73**, 139 (2001).
- [8] U. Adem, *et al.*, *Phys. Rev. B* **75**, 014108 (2007).

[Tu-P-16]

Laser spectroscopy of two centre of Eu^{3+} in silicate with apatite structure

A.M. Karpov, M.G. Zuev

Institute of Solid State Chemistry, Ural Branch Russian Academy of Science

RE-ions are the most popular objects for research of optical characteristics of luminescence materials. By means spectral characteristics research of activators it is possible to do conclusions about a structure of the optical centers, internal defects and presence of impurities. In this work we have divided two types of the optical centers of Eu^{3+} , in apatite-like silicates. The site-selective method has helped to identify absorption spectra and to define the nearest crystallographic environment of Eu^{3+} ions.

There are two kinds of cationic position for activators ions in apatite structure (Fig.1). The first kind 4f has nine oxygen atoms surrounding the cationic site. The second kind of site is in seven-fold coordination with six oxygen atoms in SiO_4 tetrahedral and oxygen in 2a position [1].

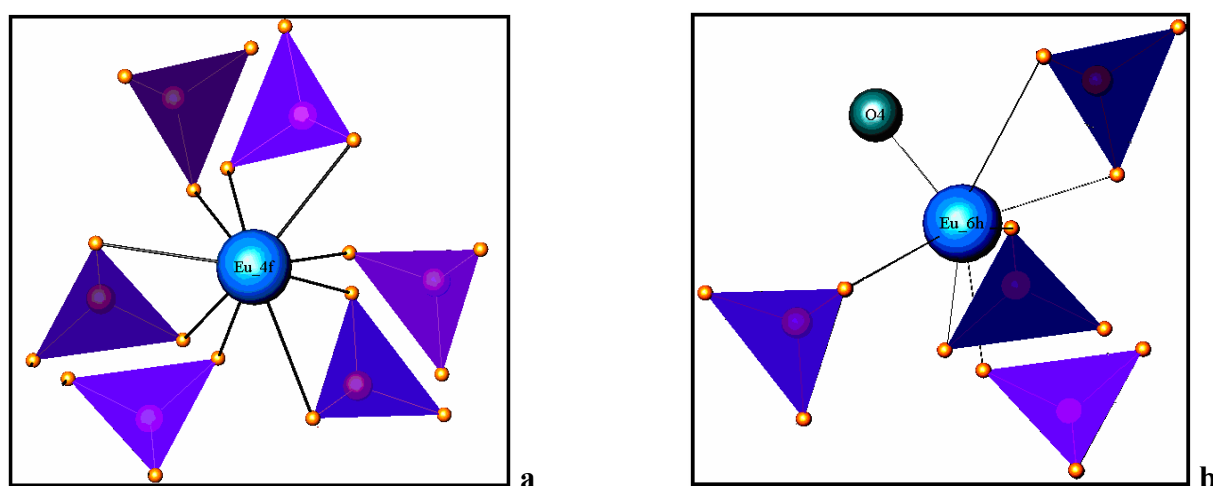
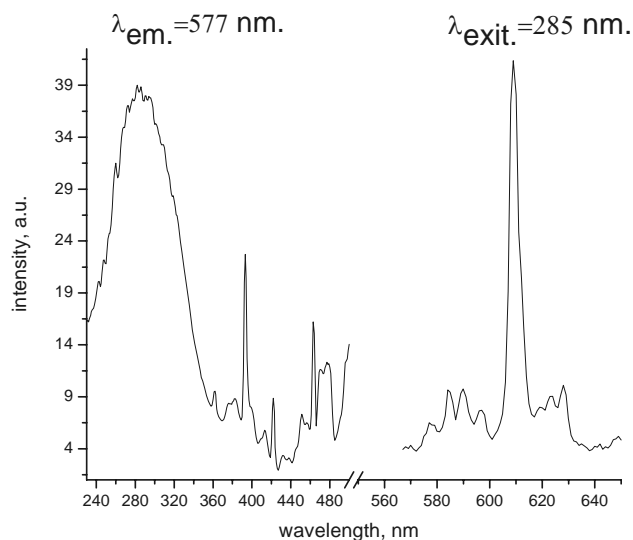


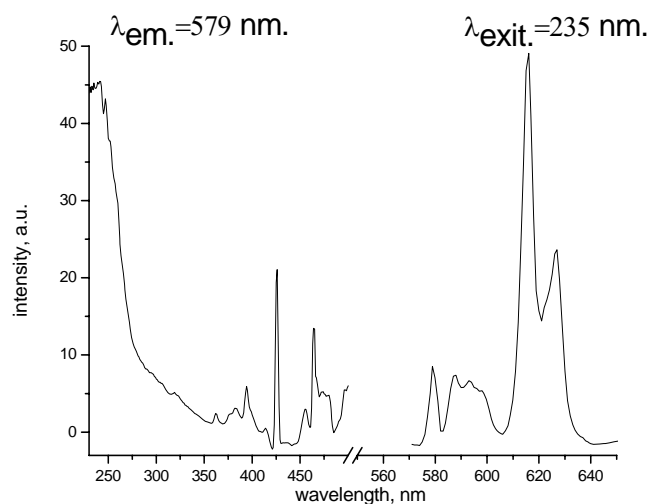
Fig.1 Local environment of Eu in two nonequivalent sites: (a) 4f position, (b) 6h position

To determine multiplet energy for each site, the excitation and emission spectra under site selective radiation were recorded for $\text{Sr}_2\text{Y}_8\text{Si}_6\text{O}_{26}: 0.15\text{Eu}$ (Fig.2). Excitation spectra have been recorded for two wavelengths $\lambda_{\text{em},1}=577$ nm, $\lambda_{\text{em},2}=579$ nm. Such values of wavelengths have been chosen not casually. At record of absorption spectra under nonselective excitation it was revealed inhomogeneously broadened peak around 579 nm. This peak corresponds to transition ${}^5\text{D}_0 - {}^7\text{F}_0$ which cannot be split [2]. The peak has been spread out with use of Gauss function, and two maximum was revealed.

From excitation spectra it is visible, that peak intensity at 464 nm is more than peak intensity at 394 nm at absorption wavelength $\lambda_{\text{em}} = 579$ nm. View a charge transfer band. The big intensity for it is observed in a spectrum with absorption wavelength $\lambda_{\text{em}} = 579$ nm. It means that in the given position the activator more ordering. It is possible to draw a conclusion that the excitation spectrum which has been removed for $\lambda_{\text{em}} = 579$ nm concern the optical centre in a 6h position. Presence near to the given position of seven ions of oxygen explains high intensity of the charge transfer band. As to position 4f, rather long bonds and presence of the defects formed at charging compensation, reduce intensity of the charge transfer band.



(a)



(b)

Fig.2 Excitation and emission spectra for two nonequivalent sites: (a) 4f position, (b) 6h position

Thus, in this investigation influence of a crystal field on the optical centers of ions Eu^{3+} in two nonequivalent positions in silicate with apatite structure has been studied. A method the site-selective luminescence was possible to divide the spectra of absorption having a different environment. The crystal field renders more intensive influence on ions Eu^{3+} in a 4f position. It is connected by that in this position, occurs considerable disordering at replacement Sr^{2+} on Eu^{3+} .

1. R. El. Ouenzerfi, G. Panczer, C. Goutaudiet, *Optical Materials*, V.16, (2001), 307.
2. P. D. Townsend, M. Khanlary, *Surface and Coating Technology* V.201, (2007), 8162

[Tu-P-30]

**Phonon-assisted magnetic absorption in low-dimensional magnetic systems.
Optical data on $\text{Gd}_2\text{BaNiO}_5$**

S.A. Klimin¹, A.B. Kuzmenko², M.N. Popova¹, B.Z. Malkin³

¹ *Institute of Spectroscopy RAS, Troitsk, Moscow region, Russia*

² *DPMC, University of Geneva, 1211 Geneva 4, Switzerland*

³ *Kazan Federal University, 420008 Kazan, Russia*

Phonon-assisted magnetic absorption is an excellent example of the interaction between vibrational and magnetic degrees of freedom. This absorption can be registered by optical spectroscopy, and low magnetic dimensionality results in some peculiarities in the spectral shape. The case of the one-dimensional (1D) chains of half-integer spins was considered theoretically [1] to explain the broad absorption band observed experimentally in Sr_2CuO_3 [2]. Recently, similar absorption was reported for CuO [3]. For the 1D chains of spins $S=1$, that exhibit properties strongly different from those of the $S=1/2$ spin chains, neither theory nor experimental data are available, to the best of our knowledge. R_2BaNiO_5 compounds are considered as model system to study 1D $S=1$ (Haldane) chains. In this work we present the optical absorption and reflection study of a $\text{Gd}_2\text{BaNiO}_5$ single crystal in a wide spectral range from 2 meV to 0.5 eV.

We present detailed information about the optical phonons in $\text{Gd}_2\text{BaNiO}_5$ along all crystallographic axes, their assignment and temperature dependences. With the aid of lattice dynamics calculation we were able to sort out three phonons of the B_{3u} -symmetry that modulate the distance Ni-O along the magnetic Haldane chains. Two of them, at 51 and at 185 cm^{-1} , demonstrate an unusual temperature behavior of frequency and halfwidth. We attribute such behavior to the interaction of these modes with a continuum of magnetic excitations. The third phonon, at 750 cm^{-1} , showing the strongest modulation of the Ni-O distance, activates magnetic absorption (phonon-assisted magnetic absorption). This absorption is a broad band which lies in the region of two-phonon absorption and is distinguished by a peculiarity at T_N in the temperature dependence of its frequency. The spectral position of this broad peak corresponds well to the energy that could be expected for phonon-assisted magnetic absorption. It equals to the sum of the phonon energy and the energy at the lower boundary of the spinon continuum at $q = \pi/2$.

This work was support in part by a Russian-Swiss collaboration program STCP-CH-RU, the Russian Foundation for Basic Research (Grant No. 08-00690-a), and by Programs of Russian Academy of Sciences.

[1] J. Lorenzana and R. Eder, *Phys. Rev. B* **55**, R3358 (1997).

[2] H. Suzuura, H. Yasuhara, A. Furusaki, N. Nagaosa, and Y. Tokura, *Phys. Rev. Lett.* **76**, 2579 (1996).

[3] SeongHoon Jung, Jooyeon Kim, E. J. Choi, Y. Sekio, T. Kimura, and J. Lorenzana, *Phys. Rev. B* **80**, 140516 (2009).

[Tu-P-38]

Impact of Yb³⁺ - co doping on spectroscopic properties dynamic of color centers in KY₃F₁₀:Ce³⁺ crystals.

E.Yu. Koryakina, A.K. Naumov, D.I. Tselishev, S.L. Korableva, V.V. Semashko

Kazan (Volga region) Federal University, Kazan, Russia

The necessity of UV tunable lasers radiation is constantly growing in various fields of science, medicine, technology, etc. Traditional methods of obtaining such radiation, such as conversion visible and infrared tunable laser radiation to the harmonic frequencies, OPO, excimer lasers etc, had always been expensive and inconvenient to use. That's why, the emerging success in the field of solid-state tunable lasers generating radiation directly into the UV spectral range with practically important output characteristics [1], gave an impetus to research a new crystalline active media for UV spectral range. Since that time, it was determined that the best matrices for UV-based active media are fluoride crystals – wide-gap dielectrics, and of rare-earth elements ions as their activators.

At present, Ce³⁺ ions activated fluoride crystals are studied most intensively. The researches revealed that in the most of these crystals under the action of intense laser pumping a formation of different type color centers (CCs) is observed as a result of absorption from the excited state (ESA) process. Initially, the presence of CCs was detected visually – the crystal was obtaining often yellow color in place exposure to intense UV radiation. Such CCs were available to study by the classical spectroscopic methods. During the study, the change of CC spectroscopic properties over time was detected, also visually was observed a weakening or complete bleaching irradiated places in the crystal.

The existence of the CC, which are formed directly after the action of pump radiation and disappear before the next pump pulse (short-lived CC), was known from indirect evidence from experiments in which the gain properties of crystals were investigated by "pump-probe" experiments. Influence of this type CC significantly decreases the output characteristics of laboratory models of lasers based on these crystals.

This paper presents the results of CC spectroscopic properties studies Ce³⁺-activated fluoride crystals.

First, in the paper described features of the original experimental setup that realizes an optical properties registration method of materials under intense laser radiation pumping like "pump-probe" experiment. In this setup as a probe beam the laser spark (laser-induced break-down of air) radiation was used. This light source has an intense continuous spectrum in the range from 200 to 800 nm with duration of emission repeating the duration laser pulse (~ 15 ns in our case). The registration part of the setup allows recording the spectrum in the range of 200-1100 nm with a spectral resolution better than 1 nm and time resolution of 1 ms.

The evolution of the CC spectra after the irradiation by intensity UV radiation was registered and the life times of long-lived CC were determined for the crystals KY₃F₁₀: Ce³⁺ (KYF:Ce) and KY₃F₁₀: Ce³⁺,Yb³⁺ (KYF:Ce,Yb).

The effect of Yb³⁺ ions on the spectroscopic properties of long-lived CC was observed in the crystal KYF:Ce,Yb. Using this setup, the spectra of short-lived color centers in the crystals KYF:Ce and KYF: Ce,Yb were investigated, and influence of Yb³⁺ ions on the formation of short-lived CC in the crystal KYF:Ce,Yb was studied.

This investigation was made in the context and under support of the Federal target program

“Scientific and research and educational personnel of innovational Russia”.

- [1] Ce³⁺-doped colquiriite a new concept of all-solid-state tunable ultraviolet laser / Dubinskii M.A., Semashko V.V., Naumov A.K., Abdulsabirov R.Yu., Korableva S.L. // J.Mod.Opt. -1993. - v.40. - N1.- pp.1-5.

[We-P-57]
**Spectroscopic properties of color centers in crystals KY₃F₁₀: Ce and
KY₃F₁₀: Ce,Yb**

E.Yu. Koryakina, A.K. Naumov, D.I. Tselishev, S.L. Korableva, V.V. Semashko

Kazan Volga Federal University, Kazan, Russia

The necessity of UV tunable lasers radiation is constantly growing in various fields of science, medicine, technology, etc. Traditional methods of obtaining such radiation, such as transformation visible and infrared tunable laser radiation to the harmonic frequencies, OPO, excimer lasers, etc had always been expensive and inconvenient to use. That's why, the emerging success in the field of solid-state tunable lasers generating radiation directly into the UV spectral range with practically meaningful output characteristics [1], gave an impetus to research new crystalline active media for UV spectral range. Since that time, it was determined that the best matrices for UV-based active media are fluoride crystals – wide-gap dielectrics, and ions of rare-earth elements as their activators.

At present, Ce³⁺ ions activated fluoride crystals are studied most intensively. The researches revealed that in the most of these crystals under the action of intense laser pumping a formation of different type color centers (CCs) is observed as a result of absorption from the excited state (ESA) process. Initially, the presence of CCs was detected visually – the crystal was obtaining often yellow color in place exposure to intense UV radiation. Such CCs were available to study by the classical spectroscopic methods. During the study, the change of CC spectroscopic properties over time was detected, also visually was observed a weakening or complete bleaching irradiated places in the crystal.

The existence of the CC, which are formed directly after the action of pump radiation and disappear before the next pump pulse (short-lived CC), was known from indirect evidence from experiments in which the gain properties of crystals were investigated – "pump-probe" experiments. Influence of this type CC significantly decreases the output characteristics of laboratory models of lasers based on these crystals.

This paper presents the results of CC spectroscopic properties studies Ce³⁺-activated fluoride crystals. The life times of long-lived CC were measured for the crystals KY₃F₁₀: Ce³⁺ (KYF:Ce) and KY₃F₁₀: Ce³⁺, Yb³⁺ (KYF:Ce,Yb) by the classical spectroscopy method. The effect of Yb³⁺ ions on the spectroscopic properties of long-lived CC was observed in the crystal KYF:Ce,Yb. By the "pump-probe" method, that used radiation of laser spark as a probe, the spectra of short-lived color centers in the crystals KYF:Ce and KYF: Ce,Yb were recorded, and influence of Yb³⁺ ions on the formation of short-lived CC in the crystal KYF:Ce,Yb was studied.

[1] Ce³⁺-doped colquiriite a new concept of all-solid-state tunable ultraviolet laser / Dubinskii M.A., Semashko V.V., Naumov A.K., Abdulsabirov R.Yu., Korableva S.L. // J.Mod.Opt. -1993. - v.40. - N1.- pp.1-5.

Visible luminescence of nanocrystals

T.A.Kudykina*, A.I.Pervak.

University "Ukraina", Department of Engineering Technologies,
 vul. Horiva, 1 Γ, Kiev-071, Ukraine, 04071.

*E-mail: tkudykina@ukr.net

A visible luminescence from a nanometer-scale solid object can be obtained just as the irradiation of radio waves by an oscillatory circuit. Such an oscillatory system has a natural frequency in the range from IR- to visible and even UV- light. In a medium with the dielectric constant ϵ and magnetic susceptibility μ , the electromagnetic wave propagates with the velocity $v = \frac{c}{\sqrt{\epsilon\mu}}$, and

the natural frequency of a layer with a thickness d is equal to $\omega_0 = \frac{c}{dn}$ (if $\mu \approx 1$, and $\epsilon \approx n^2$).

The natural frequency of a thin metal or semiconductor layer with nanometer-scale value of d (from 1 nm to 100 nm) can be in the spectral region from infrared to ultraviolet. The value of ω_0 we can find if the thickness dependence of the index of refraction $n(d)$ is known for given material.

The calculations of the thickness dependences of $n(d)$ of thin absorbing films of semiconductors and metals (fig.1,2) have shown the resonance maximum at the thicknesses

$d_{res} = \frac{\lambda_0}{\pi n(d_{res})} \cdot m; (m = 1, 2, 3, \dots)$. Here λ_0 is a wavelength of the incident light in a vacuum, and

$n(d_{res})$ is an index of refraction of a medium at a thickness d_{res} . The wavelength in crystal is equal

to $\lambda_m = \frac{2\pi d}{2}$, hence, the integer number of wavelengths is packed up on a circle with a radius

$\rho = \frac{d}{2}$. In that case, a thin film is a resonator, which reemits the incident light.

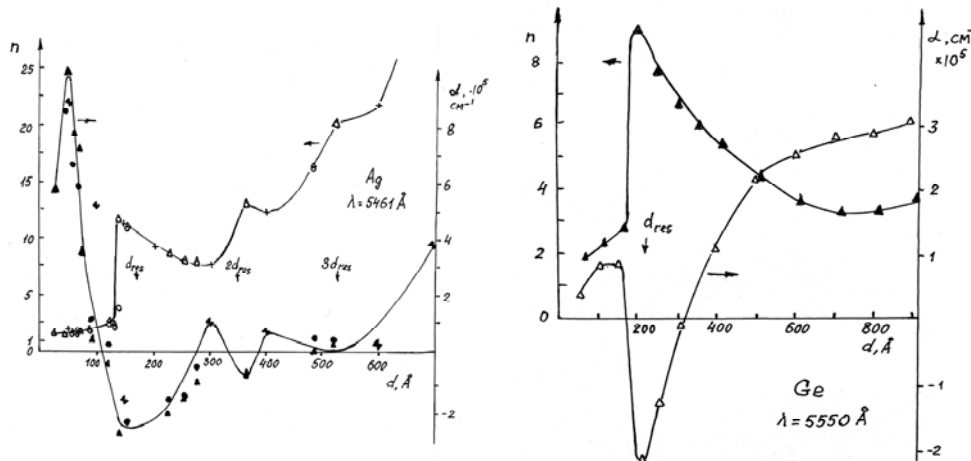


Fig.1. The calculated dimension dependences of the indices of refraction and coefficients of absorption for Ag and Ge.

In all investigated metals (Ag, Al, Fe) the indices of refraction exceed the unity, $n > 1$. It agrees with the fact that the polarization in a medium is always positive. Two independent calculations of the indices of refraction and absorption, based on the measured values of $\mathfrak{R}, \mathfrak{T}$ and $\mathfrak{R}, \mathfrak{R}'$ (\mathfrak{R} – is a reflectivity from the side of a film and \mathfrak{R}' – from the side of a substrate; \mathfrak{T} – is a transmittance)

and our formulas for wave amplitudes, give very close results (circles and triangles)[2].

The Pointing vector characterizes the emission ability of a system: $\vec{S} = \frac{c}{4\pi} \cdot [\vec{E} \times \vec{H}]$. A free thin metal film does not emit light, because an electric field in it, $E \rightarrow 0$, but the same metal film, deposited on a dielectric substrate, can emit light.

All calculated curves $n(d)$ have the resonance maxima and the curves $\alpha(d)$ (or an index of absorption $\kappa = \frac{\alpha\lambda}{4\pi}$) have the resonance minima, which correspond to the natural frequencies of the samples. Due to the dependence of $n(d)$, the natural frequencies exist in a some thickness region. There are some regions of the thicknesses, where the coefficients of absorption are negative; hence, the emission takes place. In semiconductors, the minima of the curves $\alpha(d)$ (and maxima of the curves $n(d)$) take place when d_{res} corresponds to the integer $m = 1$. In the case of silver films we see three minima which correspond to $m = 1, 2, 3$ (fig1).

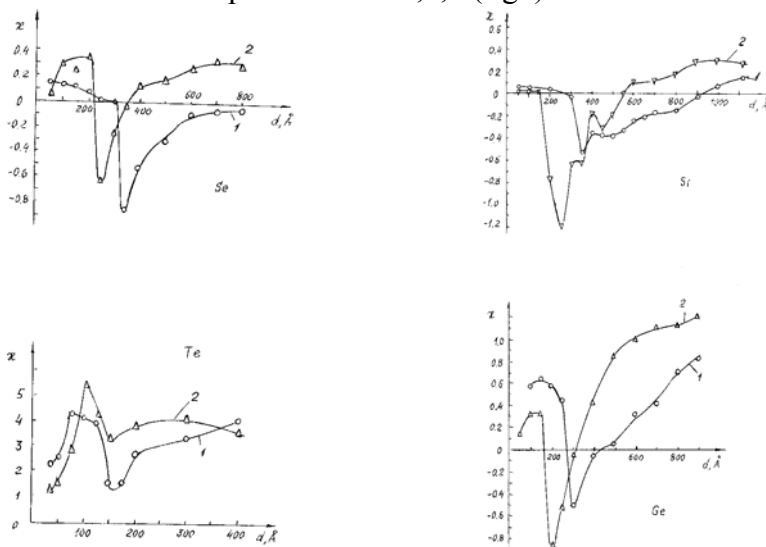


Fig.2. The calculated dimension dependences of the indices of absorption for $Se(1 - \lambda = 700nm; 2 - \lambda = 540nm)$, $Te(1 - \lambda = 700nm; 2 - \lambda = 460nm)$, $Si(1 - \lambda = 700nm; 2 - \lambda = 580nm)$, $Ge(1 - \lambda = 720nm; 2 - \lambda = 555nm)$.

A metal conductivity can be obtained as $\sigma = \frac{n\kappa \cdot \omega}{2\pi} = \frac{\alpha c n}{4\pi}$. In a thick crystal of Ag at the light wavelength $\lambda = 546.1nm$, the coefficient of light absorption is equal $\alpha \sim 10^6 cm^{-1}$ and the index of refraction $n \approx 20$, then $\sigma \approx 4.8 \cdot 10^{16} sec^{-1}$. At low frequencies the conductivity of Ag is equal to $\sigma \approx 5.4 \cdot 10^{17} sec^{-1}$, hence, we have reasonable value of conductivity for light frequency.

References

- 1.T.A.Kudykina. Phys.stat.solidi (b), **160**, 365, 1990; **165**, 591, 1991; **179**, 215, 1993; SPIE, **3573**, 324, 1998.
- 2.T.A.Kudykina, M.P.Lisitsa. Optoelectronics and Semiconductor Technics,**32**, 106, 1997.

[Tu-P-18]

Luminescent properties of Am in yttrium aluminum garnet

Ya. V. Kuznetsova¹, B. E. Burakov², A. N. Trofimov¹, V. P. Usacheva¹, M. V. Zamoryanskaya¹

¹ Ioffe Physical-Technical Institute, 26 Polytekhnicheskaya Street, 194021 St. Petersburg, Russia

² V. G. Khlopin Radium Institute, 194021, 28 2-nd Murinskiy Avenue, 194021 St. Petersburg, Russia

Ceramic waste forms based on garnet, $(Y,Gd,An)_3(Al,Ga,An)_5O_{12}$, and zircon, $(Zr,An)_2SiO_4$, where An=U, Pu, Np, Am, and Cm have been proposed for the immobilization of weapons-grade plutonium and other actinides. The lattice capacity of these materials depends on the valence state and ionic radius of the substitute ions. However, luminescence experimental data of actinide ions incorporated into wide gap crystals are very limited. Previous studies of absorption properties of AmF_3 crystals in water solution showed several narrow lines in the spectra of Am^{3+} . In this work we studied in detail luminescent properties of Am^{3+} in wide gap matrix.

Main difficulties with americium phase identification in solid state by common used methods are connected with two following peculiarities. Firstly, positions of the characteristic X-ray lines of Am and Sn are very close. Secondly, luminescent properties of Am^{3+} ion are similar to one of Eu^{3+} . In our work we used local methods such as electron probe microanalysis (EPMA) and cathodoluminescence (CL) for yttrium aluminum garnet $(Y,Am)_3Al_5O_{12}$ (YAG) investigation.

Obtaining characteristic X-ray spectra on wavelength dispersive EPMA spectrometer allowed us to determine definitely presence of Am in studied crystal (Figure 1). CL spectra of YAG:Am were obtained by $T = 77\text{ K}$ and $T = 300\text{ K}$. We assume that CL emission bands at 598 nm, 708 nm and 720 nm are caused by electron transitions between the levels 5D_0 to $^5F_{1,2}$ in Am^{3+} ion. Decay times of these bands differ slightly and were about $110 \pm 2\text{ }\mu\text{sec}$. Concentration of the Am in different parts of inhomogeneous sample was measured and concentration dependence of decay time was estimated.

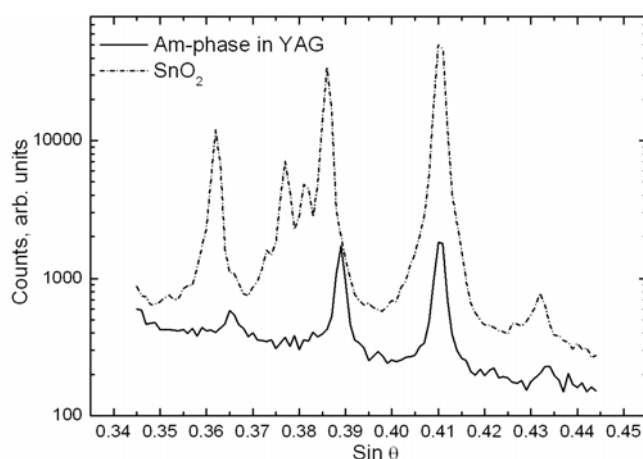


Figure 1. X-ray spectra of YAG:Am crystal and SnO_2 standard.

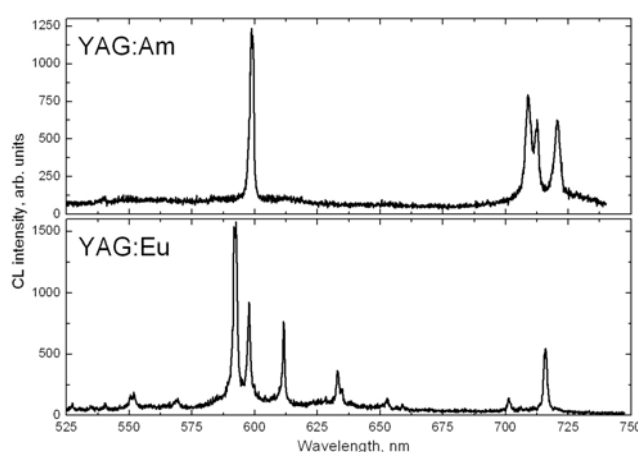


Figure 2. CL spectra of YAG:Am crystal and YAG:Eu standard ($T = 300\text{ K}$).

In paper main features of Am^{3+} luminescence are discussed.

[Tu-P-10]
Upconversion luminescence in Er³⁺/Yb³⁺ codoped Y₂CaGe₄O₁₂

I.I. Leonidov, V.G. Zubkov, A.P. Tyutyunnik, N.V. Tarakina, L.L. Surat

Institute of Solid State Chemistry, UB RAS, Ekaterinburg, Russia

Calcium yttrium tetrametagermanates Y₂CaGe₄O₁₂ doped with Er³⁺ and Er³⁺/Yb³⁺ reveal upconversion emission in visible spectral range under NIR excitation, $\lambda_{\text{ex}} = 980$ nm. The luminescence is intense enough to be seen by naked eye. For the solid solution Er_xY_{2-x}CaGe₄O₁₂ concentration dependencies for the green and red lines of the visible emission around 526 nm (²H_{11/2} → ⁴I_{15/2}), 545 nm (⁴S_{3/2} → ⁴I_{15/2}) and 670 nm (⁴F_{9/2} → ⁴I_{15/2}) show the optimal value for the sample $x = 0.2$, i.e. with 1% content of erbium ions in the lattice ($7.9 \cdot 10^{21}$ atoms/cm³). The power dependence of the visible luminescence measured at room temperature in the low-power limit indicates the well-known two-photon upconversion process. Direct intensification of the upconversion emission signals has been achieved by ytterbium sensitizing. In the Y₂CaGe₄O₁₂:Er³⁺, Yb³⁺ samples owing to energy transfer Yb³⁺ → Er³⁺ green and red emissions increase several times more. The other upconversion excitation mechanism in Y₂CaGe₄O₁₂:Er³⁺ is discussed for an 808 nm incident laser irradiation. Concerning the obtained results a scheme of excitation and emission routes involving ground/excited state absorption, energy transfer upconversion, nonradiative multiphonon relaxation processes in trivalent lanthanide ions in Y₂CaGe₄O₁₂:Er³⁺ and Y₂CaGe₄O₁₂:Er³⁺, Yb³⁺ has been proposed. In erbium doped Y₂CaGe₄O₁₂ sensitized with trivalent ytterbium under quasi-resonance $\lambda_{\text{ex}} = 1064$ nm excitation that is lower than the ytterbium ²F_{7/2} → ²F_{5/2} transition, the excitation mechanism demands the participation of optical phonons in order to compensate for the energy mismatch of ~ 850 cm⁻¹ between the pump photon and the ytterbium excitation energy. It consequently depends on the phonon occupation number in the optical host material. The population of the rare-earth activator ion emitting levels is accomplished by means of multiphonon-assisted anti-Stokes sideband excitation of the sensitizer ions, followed by successive energy transfer processes to the active emitter [1, 2]. Conditions for visible emission occurrence depending on pump power values are considered. In the low-power regime ($P_{\text{pump}} \leq 100$ mW) only NIR emission caused by the transition ⁴I_{13/2} → ⁴I_{15/2} in erbium ions has been detected [3].

This work was supported by the RFBR under grant no. 10-03-96028 r_ural_a, and grant no. 09-P-3-1009, sponsored by UB RAS.

[1] F. Auzel, Phys. Rev. B 13 (1976) 2809.

[2] A.S. Gouveia-Neto, et al. Mater. Lett. 63 (2009) 1999.

[3] V.G. Zubkov, et al. J. Lumin. 129 (2009) 1625.

[Th-O-35]

Luminescent Properties of Rare Earth Ions in Nanoscaled Layer Structures

M. Lezhnina^{1,2}, M. Bentlage¹, U. Kynast¹

¹ *Department of Chemical Engineering, Applied Materials Sciences, University of Applied Sciences Muenster, 48565 Steinfurt, Germany*

² *on leave from Mari State Technical University, Department of Physics, Yoshkar-Ola, Russia*

The term “nanoscaled” layer structures has in this contribution a two fold meaning: on one hand, it categorizes the true geometrical size of particles themselves, on the other, it refers to a gap between the layers, which will in the following be hosting luminescent species sandwiched between them. The most prominent representatives for such layered materials are clay minerals, which we intend to modify as strictly anisotropic, luminescent nanoobjects. Synthetic nanoclays of sufficient purity have become available on a commercial scale and exhibit exploitable optical and other interesting properties, the combination of which promises intriguing novel phenomena and applications.

In this work we investigated Laponite® clay doped with lanthanide ions (Ce^{3+} , Eu^{3+} , Gd^{3+} , Tb^{3+}) and intercalated metallorganic complexes. Laponite RD (a synthetic hectorite type clay), of the composition $\text{Na}_{0.7}[\text{Mg}_{5.5}\text{Li}_{0.3}\text{O}_{20}(\text{OH})_4]$, (see the fig.) can be completely exfoliated into individual disks to yield glass clear aqueous dispersions / solutions. Careful control of surface charges enables the platelets to organize to sandwich-like structures, able to accommodate a variety of guests within the interlayers. Even completely hydrophobic species can thus be rendered “soluble” in water. The sensitization required for most rare earth ions can be realised either by codoping with Ce^{3+} , by which a 35-fold increase of the Tb^{3+} emission could be accomplished. Utilization of the “antenna effect”, involving aromatic organic ligands like bipyridine [1], proved to be another feasible pathway to sensitise the luminescence in the laponites, simultaneously screening the ions against high frequency vibrations of the host, as has in analogy been reported for zeolites previously as well [2].

Due to their favourable dimensions and solubilities, these novel materials hold the promise to become valuable materials for the fabrication of, e.g., thin optical layers, immunoassays or functional polymer additives.

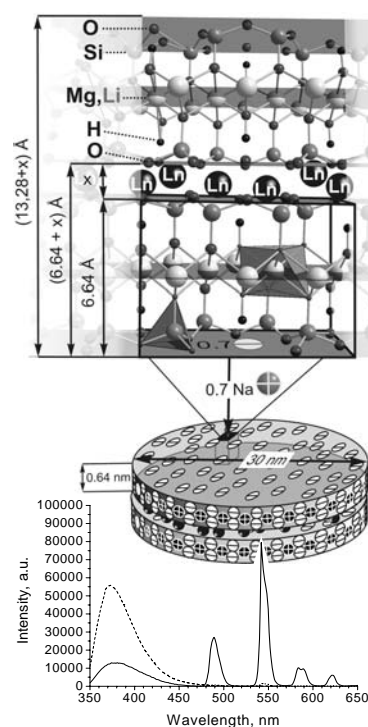


Fig. Top: Crystal Structure and geometry of Laponite. Ln^{3+} sandwiched in the interlayer (top). Bottom: Emission spectra (excitation at 310 nm) of $\text{Tb}_{0.05}\text{Na}_{0.55}$ -Laponite (dotted), $\text{Ce}_{0.05}\text{Gd}_{0.18}$ -Laponite (dashed line) and $\text{Ce}_{0.05}\text{Tb}_{0.18}$ -Laponite (solid).

[1] M. Lezhnina, E. Benavente, M. Bentlage, Y. Echevarría, E. Klumpp, U. Kynast, *Chem. Mater.*, **19**, 1098 (2007)

[2] U. Kynast, D. Sendor, *Host-Guest Systems based on nanoporous crystals*, WILEY-VCH, Weinheim, 558-583 (2003)

[Tu-P-15]
Rare earth fluoride species in zeolite hosts

M. Lezhnina^{1,2}, U. Kynast¹

¹ *Department of Chemical Engineering, Applied Materials Sciences,
University of Applied Sciences Muenster, 48565 Steinfurt, Germany*

² *on leave from Mari State Technical University, Department of Physics,
Yoshkar-Ola, Russia*

Microporous aluminosilicate frameworks are extraordinarily capable of stabilising peculiar or highly reactive species like the $S^{3\bullet-}$ radical-anion (in Ultramarine [1]), or BH_4^- [2] and BF_4^- anions [3] inside their matrix cavities. In this work we study the formation of rare earth fluorocomplexes within zeolite X (Faujasite) hosts. The fluoride environment to rare earths is of considerable interest for various luminescent processes due to the high vibrational energies ($300 - 400\text{ cm}^{-1}$) involved, and wide band gaps, thus enabling both, access to excitation in the Near Infrared, as well as in the deep UV.

Despite anticipated reactions between host and precursors, we were able to observe the formation of rare earth fluorocomplexes within the zeolite X matrix. In Eu^{3+} ions and its complexes in particular, the emission patterns are very sensitive to the structure and composition of the immediate coordination sphere. They can thus excellently provide evidence for the complex formation, additionally intrazeolite energy transfer between, e.g., Gd^{3+} and Eu^{3+} ions, can readily be probed. Of yet more significance for the present investigation are the $O \rightarrow Eu^{3+}$ charge transfer (LMCT) excitation bands, which are valuable for the discrimination between isolated fluorocomplexes and lattice oxygens complementing the Eu^{3+} coordination. At a complex load corresponding to 6 Eu^{3+} per zeolite unit cell (UC), the LMCT exhibits a fourfold excitation intensity as compared to higher loads, e.g., 14 Eu^{3+}/UC (normalized to f-f-transitions). The phenomenon is explained in terms of the formation of fluoride clusters within the zeolite supercage (\varnothing 1.2 nm) and their growth with increasing Ln^{3+} concentration (Fig. 1). In agreement with sub-nanometer sized, small fluoride agglomerates, the XRD patterns of the samples show the zeolite matrix only. Chemical analyses give a ratio $Ln^{3+}:F^- = 1:6$ within the framework, while IR spectra show the presence of NH_4^+ cations. Thus, conceivable compositions of the complexes are $(NH_4)_nLnF_{3+n}$ ($n = 1-3$). Stoichiometries with $n = 1, 2$, most likely indicate free NH_4F or Al-F species. As opposed to that, an excess of fluoride precursor (NH_4F) inevitably led to the damage of the matrix and formation of crystalline NH_4LnF_4 .

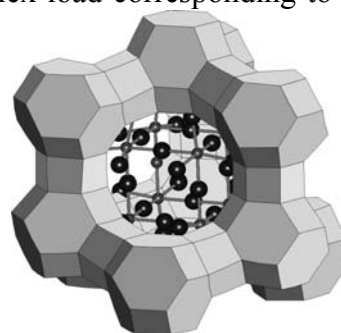


Fig. 1. Schematic representation of zeolite X embedded fluorides species

The presence of fluorocomplexes was furthermore confirmed by efficient upconversion in $[(NH_4)_nHoYbF_{3+n}]_8-X$, obtained after fluoridations. Upconversion in this system proceeds by the excitation of the spin-allowed $Yb^{3+} {}^2F_{7/2} \rightarrow {}^2F_{5/2}$ transition (980 nm), followed by two photon energy transfer to the Ho^{3+} ion, which returns to the ground state via visible emission of 544 nm (${}^5S_2 \rightarrow {}^5I_8$) or 654 nm (${}^5F_5 \rightarrow {}^5I_8$). Despite the high Ho^{3+} concentration, the low energy emission (654 nm) is unusually depreciated in this system due to the absence of cross relaxation processes between the fluoro-clusters.

[1] F. Seel, *Studies in inorganic chemistry* **5** (1984) 67.

[2] J.-Ch. Buhl, T. M. Gesing, C.H. Rüscher, *Microporous Mesoporous Mater.* **80** (2005) 57.

[3] M. M. Lezhnina, E. Jordan, S. A. Klimin, J. Loens, H. Koller, B. N. Mavrin, U. Kynast, *Z.Anorg.Allg.Chem.* **635** (2009) 450.

[We-P-42]
Two-photon picosecond absorption dynamics in MeWO₄ crystals
(Me=Zn, Pb, Ca, Sr, Ba)

V.I. Lukanin, D.S. Chunaev, A.Ya. Karasik*

Prokhorov General Physics Institute RAS, Vavilov str., 38, 119991 Moscow

**E-mail: karasik@lst.gpi.ru*

Crystalline tungstates are used as scintillation detectors of ionizing radiation, laser materials and nonlinear Raman shifters. Studies of electronic structure, excitation and relaxation processes are actual for popular divalent metal tungstate crystals MeWO₄ (Me=Zn, Pb, Ca, Sr, Ba, ...). Along with developed linear spectroscopy two-photon nonlinear spectroscopy open new possibilities on selective excitation of electronic levels in nontransparent for optical radiation conduction band of materials. In this case, a study of luminescence from excited electronic levels allows one to obtain new important results [1]. In present work we demonstrate method of the two-photon spectroscopy with direct investigation in pico - millisecond time scale a dynamics of excitation and relaxation of a self-trapped WO₄²⁻ (or W-O) molecular exciton for MeWO₄ crystals with scheelite and wolframite structure.

We used trains of 20 ps Nd:YLF powerful laser pulses for 523.5 nm excitation of the MeWO₄ crystals. Oscillograms of the radiation were measured with picosecond time resolution at input and output of the crystal using fast photodiode and digital oscilloscope. The train of output pulses with relatively high input radiation intensity was essentially deformed due to the nonlinear two-photon absorption, when two-photon sum energy (4.73 eV) corresponded to excitation band of W-O molecular complexes. A transmission of the crystal as a function of laser intensity was measured as a ratio of the output to input pulse amplitudes. For Zn, Pb tungstates a hysteresises in the dependence of absorption on laser intensity were revealed [2]. Absorption, induced by the laser radiation with tenths GW/cm² intensity, transformed the crystals at 523.5 nm wavelength to practically non-transparent state. We evaluated constants of two-photon absorption for different crystals using the measured transmission dependences.

In order to measure kinetics of excitation and absorption relaxation we along with 523.5nm picosecond pulsed radiation put in the crystal cw 632.8 nm probe radiation. At 300K we measured kinetics of the induced absorption rise and relaxation at the red wavelength. For the crystals measured rise times of a level population and following relaxation depend on a direction of a linear excitation polarization relatively optical axis of the crystals. The measured level population rise times lie in nano-microseconds range. The times of absorption relaxation have characteristic values of tenths milliseconds.

Obtained experimental results are discussed using theoretical and experimental data, in particular, on an absorption edge, the band-gap energy, one- and two-photon excitation bands for the studied crystals.

References.

1. V.B. Mikhailik, H. Kraus, D. Wahl, et al Phys.Rev. B69,205110(2004).
2. V.I. Lukanin, D.S. Chunaev, A.Ya. Karasik JETP Lett. 91(11), 615(2010)

[Th-O-38]

Low-temperature study of intrinsic electronic excitations in wide-gap materials using luminescent RE³⁺ and Cr³⁺ impurity ions

Ch. Lushchik, I. Kudryavtseva, T. Kärner, A. Lushchik, F. Savikhin, E. Vasil'chenko

Institute of Physics, University of Tartu, Riia 142, 51014 Tartu, Estonia

Low-temperature investigations of intrinsic electronic excitations (electrons e^- , holes h^+ , excitons e^0) in wide-gap materials with increasingly complicated lattice structure are being continued at the Institute of Physics, Tartu. Both, extremely pure samples and the crystals doped with various impurity ions have been studied. The migration processes of free e^- , h^+ and e^0 as well as the processes of their self-trapping or localization and subsequent recombination/decay near impurity centers reveal themselves, in particular, in the spectra of intrinsic and impurity luminescence under crystal excitation by photons, electrons and swift ions with varied energy. These processes are important for the elaboration of novel spectral transformers, scintillation detectors, selective dosimeters and radiation-resistant functional materials.

In the past s^2 -ions (Ga^+ , Ge^{2+} , In^+ , Tl^+ , Pb^{2+} , Bi^{3+}) with typical wideband emission and absorption spectra and large Stokes shift were widely used as luminescent probes in metal halides. These probes were attractive (see, e.g., [1]) for the investigation of fast excitonic processes as well as tunnel phosphorescence with the participation of self-trapped holes or anion interstitials (V_K and H centers, respectively). Rare-earth RE³⁺ ions with line spectra in a wide energy region offer several advantages over s^2 -ion, especially at the investigation of physical processes in ionic and ionic-covalent wide-gap metal oxides [2-4].

High-melting ($\sim 2800^\circ\text{C}$) magnesium oxide single crystals have been grown in Tartu for about forty years. The edge (line) emission of free excitons with large radius and small oscillator strength has been detected, while neither self-trapping of e^0 nor e^- and h^+ has been revealed in the bulk of close-packed MgO crystals using luminescent methods. Our recent measurements of the emission spectra of MgO:Cr³⁺ single crystals under excitation by synchrotron radiation at 9 K allowed to demonstrate the efficient interaction of free e^0 with Cr³⁺ impurity ions located nearby cation vacancies [5]. In MgO, the formation energy of a pair of Frenkel defects exceeds the energy gap, $E_{\text{FD}} > E_g$. Thus, the decay of e^0 or the recombination of conduction e^- and valence h^+ after their total vibration relaxation does not lead to the creation of Frenkel defects. The recombination of a sufficiently hot conduction e^- with a hole localized near an impurity or a structural defect is required for the creation of radiation defects via nonimpact mechanisms in MgO crystals. Single cation vacancies or Be²⁺ impurity ions could serve as such traps for h^+ (traps are stable up to 420 and 195 K, respectively [6]). Unfortunately, the majority of MgO crystals contains some amount of OH⁻ located nearby cation vacancies (charge compensators). Such complex hole traps are stable up to 335 K. The energy of 4.8 eV needed for the dissociation of OH⁻ can be released at the nonradiative recombination of totally relaxed e^- and h^+ . As a result, single cation vacancies serving as efficient h^+ traps are formed. It is worth noting that the creation efficiency of radiation defects (e.g., bivacancies) increases while the radiation resistance decreases in MgO samples previously exposed to a plastic stress.

The self-trapping of e^- and h^+ is also not detected in stoichiometric Al₂O₃ crystals. However, the self-trapping of e^0 takes place in Al₂O₃ at helium temperatures due to the sum of deformation potentials of e^- and h^+ [7]. The luminescence of these so-called self-shrunk excitons lies in VUV spectral region (~ 7.6 eV). The search is on for the luminescent impurities the introduction of which increases the radiation resistance of alumina and other metal aluminates against nonimpact mechanisms of Frenkel defects creation (the so-called luminescent protection) [8]. Some RE³⁺ and

transition ions (for instance, Cr^{3+} [5]) could be promising for this purpose in single crystal and fine grained Al_2O_3 .

The use of Gd^{3+} , Eu^{3+} and especially Tb^{3+} as luminescent probes allowed us to separate the mechanisms of impurity luminescence excitation connected with the direct excitation of impurity centers, excitation of oxyanions (e.g., small-radius e^0) or the formation of separated e^- and h^+ under irradiation of ionic-covalent CaSO_4 by 4-33 eV photons or 2-250 keV electrons (see also [2, 4]). It has been shown that the intensity ratio of radiative ${}^5\text{D}_4 \rightarrow {}^7\text{F}_J$ and ${}^5\text{D}_3 \rightarrow {}^7\text{F}_J$ (in more short-wavelength region) electron transitions in the phosphors containing Tb^{3+} pair centers (more properly, $\text{Tb}^{3+}\text{-Na}^+\text{-Tb}^{3+}\text{-Na}^+$ quartets, where Na^+ serve for charge compensation) depends on the excitation mechanism of impurity luminescence. In the case of high concentration of Tb^{3+} pair centers, the nonradiative resonant energy transfer (${}^5\text{D}_4 \rightarrow {}^5\text{D}_3$) from an excited Tb^{3+} to the second Tb^{3+} with its subsequent transition from the ${}^7\text{F}_6$ level in a ground state to the levels with smaller J takes place. The decay kinetics for green and blue emissions of Tb^{3+} impurity centers has been measured in the range of 10^{-9} - 10^{-2} s after excitation of a phosphor by single nanosecond pulses of 250-keV electrons. At 80 and 300 K, the rise of green emission (${}^5\text{D}_4 \rightarrow {}^7\text{F}_J$) is antipate to the decay of blue one (${}^5\text{D}_3 \rightarrow {}^7\text{F}_J$). By measuring the tunnel and recombination luminescence of Tb^{3+} pair centers, it has been determined that the probability of Tb^{3+} excitation up to ${}^5\text{D}_4$ or ${}^5\text{D}_3$ levels depends on the effective charge of complex impurity centers (partial of total charge compensation by Na^+ , F^- or cation vacancies). In pure or slightly doped CaSO_4 , the EPR demonstration of the self-trapping of h^+ (in SO_4^- form) has been confirmed. Moreover, in addition to the self-trapped h^+ and e^0 , the manifestations of the self-trapping of e^- (d states of Ca^+) at $T < 60$ K, when the efficiency of the electron-hole excitation mechanism of impurity luminescence is low, are tentatively detected. In slightly doped (~ 0.1 mol%) CaSO_4 at $T = 180$ - 400 K, e^- and h^+ are highly mobile and could migrate over a crystal.

The interaction of hot, relaxed or self-trapped e^- , and h^+ and e^0 with the lattice vibrations has been already theoretically consider by Y. Toyozawa, A. Sumi and G. Zavt for various wide-gap ionic crystals and by E. Rashba et al. for organic crystals. The thorough theoretical analysis of this complicated phenomenon in ionic-covalent metal sulphates lies ahead.

- [1] Ch. Lushchik, A. Lushchik, *Decay of Electronic Excitations with Defect Formation in Solids*. (Nauka, Moscow, 1989).
- [2] E. van der Kolk, P. Dorenbos, A.P. Vink et al., *Phys. Rev. B* **64**, 195129, 2001.
- [3] A.R. Lakschalam, S.-B. Kim, H.M. Jang et al., *Adv. Funct. Mater* **17**, 212, 2007.
- [4] I. Kudryavtseva, P. Liblik, A. Lushchik et al., *J. Lumin.* **129**, 1890, 2009.
- [5] A. Lushchik, Ch. Lushchik, T. Kärner et al., *Radiat. Meas.* **45**, 268-272, 2010.
- [6] S. Dolgov, T. Kärner, A. Lushchik, S. Nakonechnyi, *Phys. Stat. Solidi A*, 2010 (submitted).
- [7] M. Kirm, G. Zimmerer E. Feldbach, A. Lushchik et al., *Phys. Rev. B* **60**, 502, 1999.
- [8] A. Lushchik, Ch. Lushchik, P. Liblik et al., *J. Lumin.* **129**, 1894, 2009.

[We-P-45]

Interconfigurational $4f^n - 4f^{n-1} 5d$ spectra of Pr^{3+} and Tm^{3+} in LiLuF_4 host

B.Z. Malkin¹, O.V. Solovyev¹, V.N. Makhov², G. Stryganyuk³, M. Kirm⁴, E. Garcia Villora⁵,
K. Shimamura⁵

¹ *Kazan Federal University, Kremlevskaya Str. 18, 420008 Kazan, Russia*

² *P.N. Lebedev Physical Institute, Leninskii Prospect 53, Moscow 119991, Russia*

³ *Institute for Scintillation Materials NAS of Ukraine, 60 Lenin Ave., 61001 Kharkiv, Ukraine*

⁴ *Institute of Physics, University of Tartu, Riia 142, Tartu 51014, Estonia*

⁵ *Advanced Materials Lab., NIMS, 1-1 Namiki, Tsukuba, Ibaraki 305-0044, Japan*

We report on the results of experimental and theoretical studies of interconfigurational $4f^n - 4f^{n-1} 5d$ electron-vibrational transitions in UV-VUV range of impurity Pr^{3+} and Tm^{3+} ions in LiLuF_4 single crystals grown at NIMS (Japan) using Czochralski technique and CF_4 atmosphere. High-resolution (0.6 Å) time-resolved studies of the $\text{LiLuF}_4:\text{Pr}$ (0.1 mol.%) luminescence excitation and emission spectra and the $\text{LiLuF}_4:\text{Tm}$ absorption spectrum were performed using the facility of Superlumi experiment at HASYLAB (DESY, Hamburg) upon the excitation within 5-12 eV range at the temperatures 8-10 K.

Well resolved fine structures with similar shapes of the two relatively weak bands in the excitation spectrum of Pr^{3+} in the region of 6.1-6.3 eV between the absorption maxima were observed. The branching was revealed for a relaxation of excited $\text{Pr}^{3+} 4f5d$ states resulting either in the radiative $4f5d \rightarrow 4f^2$ decay or in the efficient emission originating from the 3P_0 state of the ground $4f^2$ configuration. In the spectral range from 7.5 up to 10 eV (below the edge of the proper host absorption due to $4f^{14} - 4f^{13}5d$ excitations of the Lu^{3+} ions), the absorption spectrum of the Tm^{3+} ions contains several weak or strong relatively narrow bands (with irregular fine structures and widths of about 1000 cm^{-1}) corresponding to transitions from the ground singlet sublevel of the 3H_6 multiplet of the $4f^{12}$ configuration to different sublevels of the excited mixed $4f^{11}5d$ configuration.

The $4f^n - 4f^{n-1}5d$ spectra of the Pr^{3+} and Tm^{3+} ions in the LiLuF_4 crystal have been simulated in the framework of the Condon approximation using the approach derived in [1]. Energies of the 140 and 3640 states of the $\text{Pr}^{3+} 4f5d$ and $\text{Tm}^{3+} 4f^{11}5d$ configurations, respectively, were calculated by taking into account electrostatic, spin-orbit, crystal field and electron-phonon interactions. The exchange charge model was used to calculate the electron-phonon coupling constants. Spectral densities of correlation functions for relative displacements of ions in the clusters containing the impurity rare earth ion and its nearest neighbor ligands (eight fluorine ions) were computed by making use of the parameters of the LiLuF_4 vibrational spectrum obtained in the frameworks of the rigid ion model of the lattice dynamics and accounting for the mass defect at the impurity site. The calculated envelopes of the polarized electric dipole electron-vibrational $4f^n - 4f^{n-1}5d$ transitions in the absorption and emission spectra of the Tm^{3+} and Pr^{3+} ions are compared with the experimental data. The revealed shortcomings of the cluster approximation and of the adiabatic approximation will be discussed.

[1] B.Z. Malkin, O.V. Solovyev, A.Yu. Malishev, S.K. Saikin, *J. Lumin.*, **125** (2007) 175.

[We-P-35]

Upconversion luminescence in ytterbium-sensitized praseodymium-doped LEAD-Fluorine nanoglassceramics

K. Moskaleva¹, V. Aseev¹, E. Kolobkova², N. Nikonorov, E. Korchagin¹, V. Golubkov³,

¹ Saint-Petersburg University of Information Technologies, Mechanics, and Optics, 49 Kronverksy ave., Saint-Petersburg, 197101, Russia

² Saint-Petersburg State Technological Institute (Technical University) 26, Moskovskiy ave, Saint-Petersburg, 190013, Russia,

³ Institute of Silicate Chemistry of RAS, Adm. 2, Makarova emb., Saint-Petersburg, 19903, Russia

*E-mail: x.devilberry@gmail.com

Blue, green, red, and near-infrared upconversion luminescence in the wavelength region of 480–740 nm in Pr/Yb-codoped lead–fluorine nanoglassceramic under 980 nm diode laser excitation, is presented. The dependence of the upconversion luminescence upon the Pr-concentration is also examined. Praseodymium doped nano-glassceramics are promising candidates as phosphor for white emitting diodes.

Currently, transparent nano-glassceramics are of great interest for the modern element base of photonics. Because they stay at intermediate state between crystalline materials and glasses, these ceramics combine the best properties of crystals (high mechanical and thermal strength) and glasses (possibilities of pressing and molding, pulling optical fibers, and carrying out ion exchange to fabricate waveguide structures). If the dopants (erbium, neodymium, etc.) enter the crystalline phase, the spectral, luminescence and laser characteristics of glassceramics become close to those of laser crystal analogues. Glassceramics are heterogeneous structures formed upon annealing of glass due to the growth of crystalline phase in a glassy matrix

In the present work, samples of glass composition $30\text{SiO}_2-18\text{PbF}_2-7.5\text{Al}_2\text{O}_3-5\text{ZnF}_2-29\text{CdF}_2-3\text{YF}_3$ doped with different erbium concentration (0.5-3 mol %) and constant ytterbium concentration (3 mol%) have been developed and synthesized. In these systems, the crystalline phase is precipitated upon heat treatment. Rare-earth ions play a role of nucleation centers. An X-ray diffraction analysis of the samples after the secondary heat treatment showed that the crystalline phase has a composition of PbYOF_3 . In case of praseodymium glassceramics the lattice constant was 5.81 Å and in case of ytterbium - 5.67 Å. Increase of time treatment results in the increase of size of nanocrystals up to 30-40 nm.

Spectral and luminescence properties of virgin and thermal treated samples have been investigated in visible (0.4-0.8 μm) and near (1.3 μm) IR- ranges. The thermal treatment results in appearance of Stark structure in absorption and luminescence spectra and their deformation. It was shown that the emitting probabilities of different transitions changed during the treatment. The entry of rare-earth ions in crystal phase results in increasing of upconversion luminescence intensity because of fluoride surrounding. Praseodymium doped nano-glassceramics are promising candidates as phosphor for white emitting diodes

[We-I-25]

Cluster theory of the charge transfer excitations in strongly correlated oxides

A.S. Moskvina

Ural State University, 620083, Ekaterinburg, Russia

We present a theoretical study of the optical response of strongly correlated 3d oxides such as manganites, ferrites, and cuprates with a main goal to elucidate nature of clearly visible optical features. A semi-quantitative cluster approach is developed to describe the one-center $p-d$ and two-center $d-d$ charge transfer (CT) excitations on an equal footing. The approach allows for a thorough examination of polarization properties, the role played by structural parameters, orbital mixing, spin degree of freedom, and electron-electron correlations.

Focusing on the CT excitations we present a comparative analysis of different mechanisms of the optical response in strongly correlated oxides based on the rare earth and transition metal ions, including crystal field $d-d$ and $f-f$ transitions. The discussion is focused on a large number of 0D, 1D, and 2D insulating cuprates, hexagonal and perovskite manganites to be parent systems for high- T_c and colossal magnetoresistance materials.

[Tu-O-11]

Site-selective spectroscopy of $\text{BaF}_2:\text{Yb}^{3+}$ crystals

I.E. Mumdzhi, S.L. Korableva, S.I. Nikitin

Kazan Federal University

It has been shown [1] that the clusters of Ln ions in fluorite-related solid solutions $(\text{AF}_2)_{1-x-y}(\text{Ln}'\text{F}_3)_x(\text{Ln}''\text{F}_3)_y$, where $\text{A}=\text{Ca}, \text{Sr}, \text{Ba}$; $\text{Ln}'=\text{Er}, \text{Tm}, \text{Yb}$; $\text{Ln}''=\text{Lu}, \text{Y}$; and $x \ll y=0.001-0.4$ appear to be similar in structure to the hexameric clusters, which are the basic structural units of the homologous series of fluorite-related superstructures $(\text{AF}_2)_{1-y}(\text{LnF}_3)_y$ with compositions $y=5/m$, where m is an integer in the range of 13–19. Optical spectroscopy of $\text{PbF}_2:\text{Yb}^{3+}$ crystals also evidenced the presence of Yb^{3+} centers which exhibit cooperative luminescence but its structure has not been established yet [2]. On this reason the investigation of $\text{BaF}_2:\text{Yb}^{3+}$ by the site-selective spectroscopy method has been performed.

$\text{BaF}_2:\text{Yb}^{3+}$ were grown by the Bridgman–Stockbarger method in graphite crucibles in a fluorine atmosphere. The concentrations of Yb^{3+} ions was varied from 0.03 to 0.5 wt.%. Except of well known cubic and trigonal Yb^{3+} centers other Yb^{3+} centers was also observed (Fig.1). The Stark structure of energy levels of these centers is quite different from those of cubic and trigonal centers [3]. For sample with concentration of 0.5 wt.% strong upconversion luminescence in the visible region by exciting one of the observed Yb^{3+} centers to ${}^2\text{F}_{5/2}$ manifold has been observed.

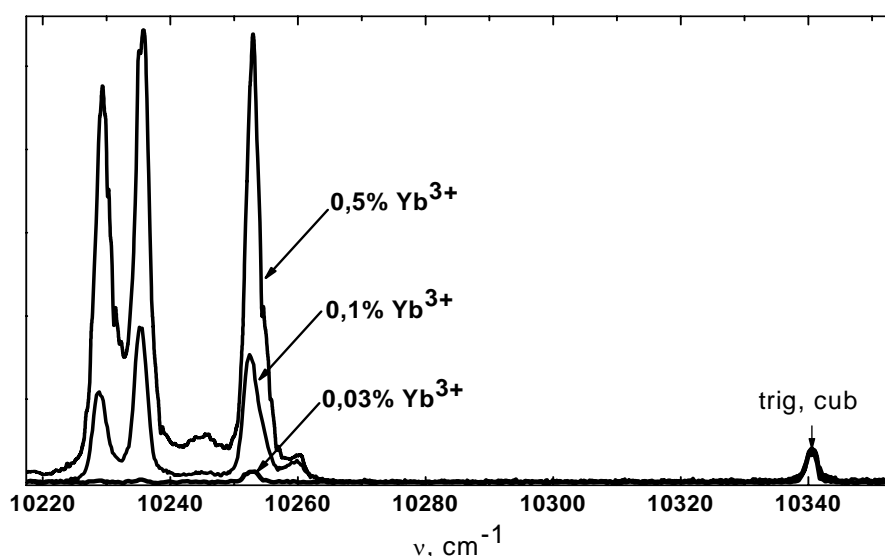


Fig.1. Luminescence spectra of $\text{BaF}_2:\text{Yb}^{3+}$ crystals with different concentrations of Yb^{3+} ions at 4.2K. All spectra are normalized on intensity of the trigonal center.

This luminescence has been unambiguously assigned to cooperative transition of the double excited pair of Yb^{3+} ions. The upconversion luminescence decay is single exponential with life time $\tau=1031 \pm 10 \mu\text{s}$ which is equal to half of life time of ${}^2\text{F}_{5/2}$ manifold $\tau=2295 \pm 8 \mu\text{s}$. Moreover the decay curve of the cooperative luminescence with rising edge has been observed when other center was excited. It has been shown that this process involve at least three Yb^{3+} ions with energy transfer from one of two excited ions to the third one and consequent cooperative transition. In addition the presents of Tm^{3+} ions excited via Yb^{3+} pair has been also observed. It should be noted that concentration of Tm^{3+} ions is much less than concentration of Yb^{3+} ions. Under site-selective

excitation of different Yb^{3+} centers the upconversion luminescence spectra of Tm^{3+} ions are different. This fact is the evidence of statistically irregular distribution of this impurity and efficient energy transfer from excited Yb^{3+} pair. And it indicates that Tm^{3+} ions are also incorporated in to the Yb^{3+} clusters.

The energy level structures of the Yb^{3+} clusters are closed to Stark structure of Yb^{3+} ions in KY_3F_{10} crystals [4], where RE ions is surrounded by eight fluorine ions, forming an antiprism site. This fact and properties of the cooperative luminescence can be explained assuming the formation of hexameric clusters with Yb^{3+} and Tm^{3+} ions in $\text{BaF}_2:\text{Yb}^{3+}$ crystals.

[1] EPR spectra and crystal field of hexamer rare-earth clusters in fluorites / S. A. Kazanskii, A. I. Ryskin, A. E. Nikiforov et al. // *Phys. Rev. B.* – 2005. – Vol. 72, - P.014127.

[2] EPR and optical study of Yb^{3+} - doped $\beta\text{-PbF}_2$ single crystals and nanocrystals of glass-ceramics / G. Dantelle, M. Mortier, Ph. Goldner, D. Vivien // *J. Phys.: Condens. Matter.* - 2006. - Vol. 18. - P. 7905-7922.

[3] Electron paramagnetic resonance and optical spectroscopy of Yb^{3+} ions in SrF_2 and BaF_2 ; an analysis of distortions of the crystal lattice near Yb^{3+} / M. L. Falin, K. I. Gerasimov, V. A. Latypov, A. M. Leushin // *J. Phys.: Condens. Matter.* - 2003. - Vol. 15. - P. 2833-2847.

[4] Spectroscopic properties, concentration quenching, and prediction of infrared laser emission of Yb^{3+} -doped KY_3F_{10} cubic crystal / M. Ito, G. Boulon, A. Bensalah et al. // *J. Opt. Soc. Am. B.* – 2007. – Vol. 24, No. 12. – P. 3023-3033.

[Tu-P-7]

Anomalous luminescence in CaF₂:Yb²⁺ crystal from ab initio calculations

A.Myasnikova^{*}, E. Radzhabov, A. Mysovsky

Vinogradov Institute of Geochemistry SB RAS, Favorsky street 1A, Irkutsk, 664033, Russia,

^{}E-mail: sasham@igc.irk.ru*

An interest to the optical properties of alkaline-earth fluoride crystals doped with rare-earth impurities is due to using these materials for various kinds of applications such as laser sources, scintillators, detection of ionizing radiation. Usually for divalent Eu²⁺ and Yb²⁺ - doped compounds df-emission (emission from 4fⁿ⁻¹5d configuration to 4fⁿ ground state) is observed. However for the some compounds (CaF₂:Eu²⁺, BaF₂:Yb²⁺ and others) the df-emission is quenched, but the strongly red-shifted ‘anomalous’ luminescence is observed [1]. The nature of the ‘anomalous’ emission is not yet known very well. At present it is accepted that the location of the 5d impurity level inside or close to the host crystal conduction band and the ‘anomalous’ emission presence are related to each other [2].

In this work we present the results of theoretical calculations of structure and optical properties of Yb²⁺ and Eu²⁺ doped CaF₂ crystal. The *ab initio* calculations have been performed in embedded-cluster approach implemented in the GUESS computer code [3]. We used 6-31G* basis set on fluorine and calcium ions and CEP-4G basis on barium, europium and ytterbium ions. To avoid the distortion of ground and excited states with the presence of positive point charges in some vicinity of QM cluster they were replaced by LANL1 ECPs. In this work the electronic structure of QM cluster has been calculated in DFT method with using modified B3LYP functional (40% of Hartree-Fock exchange and 60% of DFT exchange). Time-dependent DFT (TD DFT) method was applied for calculation of transition energies.

As a first step we calculated the equilibrium geometry of the cluster [X₁₈F₃₂]⁻⁶ (X-Ca²⁺, Ba²⁺) with rare earth impurity ions in ground state. Using this geometry we calculated the absorption energies of rare earth ions, which agree well with experimental data. After that we calculated the equilibrium geometry of the triplet state. The trapped exciton-like state model in which electron delocalized on nearest surrounding cations relatively ionized rare-earth ion will be discussed.

References

- [1] A.A. Kaplyanskii, P.P. Feofilov, Opt. Spectroscopy, 13, 129 (1962)
- [2] P. Dorenbos, J.Phys: Condens.Matter. 15, 2645 (2003)
- [3] P.V. Sushko, Surface Science. 450, 153 (2000)

[We-P-33]

Terbium low-lying energy levels in pyrochlore structure (Tb_xR_{1-x})₂Ti₂O₇ studied by optical spectroscopy

M.V. Narozhnyy¹, S.A. Klimin¹, M.N. Popova¹, T. Lummen², P.H.M. van Loosdrecht²,
G. Dhahenne³

¹*Institute for spectroscopy RAS, 142190 Troitsk, Moscow region, Russia*

²*Material Science Center, University of Groningen, 9747 AG Groningen, the Netherlands*

³*Laboratoire de Physico-Chimie de l'État Solide, Université Paris-Sud, F-91405 Orsay, France*

Compounds R₂Ti₂O₇ with pyrochlore structure show unusual magnetic properties. New type of magnetic ordering called “spin ice” was discovered in these compounds [1]. As was already shown in [2] magnetic structure is defined by single-ion anisotropy of rare earth that in its turn is determined by crystal field. The requirement for spin-ice magnetic ordering is Ising type anisotropy of the rare-earth ion. Spin ice state is observed in R₂Ti₂O₇ only for R = Dy, Ho. Tb₂Ti₂O₇ is of special interest as it does not demonstrate spin ice state, while theory predicts Ising anisotropy for Tb³⁺ ground state [2]. This peculiarity is usually explained by existence of the low-lying energetic state of Tb³⁺ ion which does not allow the realization of Ising type anisotropy. It is of interest to examine optical spectra of Tb³⁺ ion in pyrochlore structure R₂Ti₂O₇ for better understanding of terbium titanate low-temperature dynamics.

We have obtained absorption spectra for three samples of (Tb_xR_{1-x})₂Ti₂O₇ with x=1, 0.1, 0.01. First excited state of Tb³⁺ ion is located with energy ~ 1.5 meV. Other levels are situated at 10, 14 and 17 meV, in coincidence with [3]. In case of concentrated sample (x=1) strong interionic interaction leads to transformation of terbium energetic spectrum and to the mixing of ground and first excited (1.5 meV) states, thus Ising type anisotropy is not realized.

This work was supported in part by programs of RAS “Strong correlated electrons in solid states and structures” and “Quantum physics of condensed matter”.

References

[1] A.P. Ramirez, et al., Nature **399**, 333 (1999).

[2] B. Z. Malkin, A. R. Zakirov, M. N. Popova, S. A. Klimin, E. P. Chukalina, E. Antic-Fidancev, Ph. Goldner, P. Aschehoug, G. Dhahenne, Phys. Rev. B **70**, 075112 (2004).

[3] J.S. Gardner, B.D. Gaulin, A.J. Berlinsky, P. Waldron, S.R. Dunsiger, N.P. Raju, J.E. Greedan. Phys. Rev. B **64**, 224416 (2001).

[We-O-18]
**Optical studies of the uniaxial stress-induced alignment of
 Jahn-Teller Cr²⁺ centers in KZnF₃ crystal**

S.I. Nikitin, I.N. Subacheva, R.V. Yusupov

Kazan Federal University

Essential role of the orbital ordering in the electronic properties of the currently intensely studied compounds like manganites and vanadates makes the investigations of the *d*-ions with orbitally-degenerate ground state actual. Orbital ordering is a consequence of the cooperative Jahn-Teller effect. Phase diagrams of the complex transition metal oxides are rather complicated and are defined by numerous interactions: the charge, vibronic and exchange degrees of freedom are involved. In such case correct understanding of the observed phenomena demands an explicit knowledge of the corresponding energy scales. One of the approaches to obtain such information is to study the diluted dielectric crystals. Thus, the double exchange in the Cr²⁺-Cr³⁺ mixed valence pair center has been successfully studied by optical spectroscopy in the KZnF₃ crystal doped with chromium ions [1]. Spectroscopy under uniaxial stress is very informative method for evaluation of the electron-deformation and the vibronic constants respectively [2].

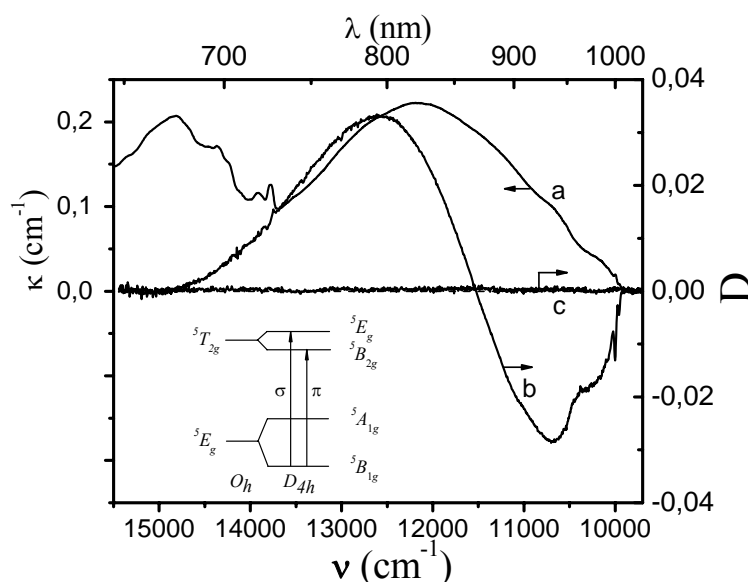


Fig.1. Absorption (a) and linear dichroism of absorption spectra of KZnF₃:Cr crystal with the stress applied along the C₄ (b) and C₃ (c) axes; $T = 4.2$ K, $P = 60$ MPa. Transitions involved and their polarization are shown; it is assumed they are electric-dipole due to interaction with the odd phonons.

Results of the spectroscopic study of Cr²⁺ ions in KZnF₃ crystal under uniaxial stress are presented in this work. Ground state ⁵E_g of the Cr²⁺ ion (electronic configuration *d*⁴) in the octahedral environment strongly interacts with the *e_g*-mode via the Jahn-Teller effect. Intense linear dichroism of absorption spectrum on the wide vibronic band corresponding to ⁵E_g → ⁵T_{2g} transition of the Cr²⁺ ions has been observed in the temperature range 2 – 80 K under uniaxial stress applied along the C₄ axis of the crystal (Fig. 1). Dichroism signal with the stress applied along C₃ axis wasn't detected. The dichroism spectrum structure (Fig. 1, b) and its huge value are determined by the orthogonally polarized transitions to ⁵E_g and ⁵B_{2g} levels which originate from the excited ⁵T_{2g} state split by Jahn-

Teller interaction and localization of the Cr^{2+} center in the minima of the ground 5E_g state under stress along C_4 axis.

Dependencies of the linear dichroism signal on pressure have been measured at 2, 4.2 and 78 K (Fig. 2). The obtained data were explained within a model taking into account occupancies of the lowest E_g and $A_{1(2)g}$ vibronic states and corresponding redistribution of the centers between the inequivalent minima of the adiabatic potential. Dichroism value within the model is determined by the expression:

$$D = \frac{I_{\parallel} - I_{\perp}}{2I_0} \propto \frac{e^{\frac{3x-1}{\tau}} \left(\cosh \frac{\Omega}{\tau} + \frac{x(1-4\sqrt{2}a)}{\Omega} \sinh \frac{\Omega}{\tau} \right) - 1}{2e^{\frac{3x-1}{\tau}} \cosh \frac{\Omega}{\tau} + 1},$$

where $x = qV_{ES}e_{\theta} / \delta$, $\tau = 2k_B T / \delta$, $\Omega = \sqrt{(4a^2 + 1)x^2 + 2x + 1}$, $a = r / q$, V_{ES} is an electron-strain interaction constant, δ – tunnel splitting, r and q – generalized reduction factors.

It is shown that while stress dependence at each temperature can well be fit within the model, the simultaneous description of the three dependencies is possible only with an account of the random strains. Fit results are shown by the solid lines in Fig. 2. In the limit of the strong vibronic coupling the values $qV_{ES} = 14100 \pm 600 \text{ cm}^{-1}$ and $\delta = 12.9 \pm 1.6 \text{ cm}^{-1}$ were obtained. Width of the Gaussian distribution of the random strains $w = (1.2 \pm 0.3) \cdot 10^{-4}$ was found.

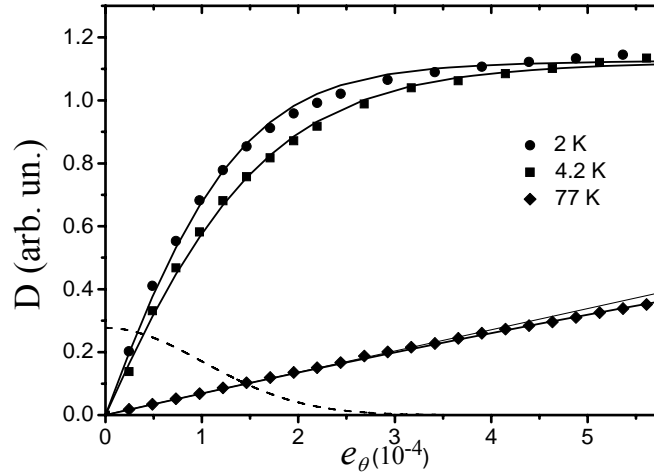


Fig.2. Dependencies of the linear dichroism signal value on pressure in $\text{KZnF}_3:\text{Cr}^{2+}$ crystal at 2 K, 4.2 K and 78 K and its fit with the proposed model; $P||C_4$. Thin line is a linear fit to the initial part of the 78 K dichroism stress dependence. Random strain value distribution is shown with the dashed line.

Additionally, it will be shown that sublinear character of the stress dependence at 78 K indicates the elongated configuration of the $[\text{CrF}_6]^{4+}$ cluster in the minima of the adiabatic potential. This result is in agreement with the SHFS structure of the Cr^{2+} EPR spectrum. We will show also that the study of the stress dependence in the limit of $k_B T \ll \delta$ is a powerful tool for determination of the octahedron distortion in the minima.

1. M.V. Eremin, S.I. Nikitin, S. Yu. Prosvirnin, N.I. Silkin and R.V. Yusupov, *Solid State Commun.* **117** 297 (2001).
2. A. V. Vinokurov, B. Z. Malkin, A. I. Pominov, and A. L. Stolov, *Fiz. Tverd. Tela (Leningrad)* **28** 381 (1986) [*Sov. Phys. Solid State* **28** 211 (1986)]

[Tu-I-3]

New nanoglassceramics doped with rare earth and transition metal ions: optical, spectral and luminescent properties

N. Nikonorov¹, V. Aseev¹, A. Ignatiev¹, A. Kim¹, E. Kolobkova², P. Shershnev¹,
A. Sidorov¹, V. Tsekhomsky¹

¹ *St. Petersburg University of Information Technologies, Mechanics, and Optics, 49 Kronverksky ave., St. Petersburg, 197101, Russia*

² *St. Petersburg State Technological Institute (Technical University) 26, Moskovskiy ave, St. Petersburg, 190013, Russia*

Four types of nanostructured glassceramics doped with rare earth and transition metal ions have been developed for photonic applications. The optical, spectral and luminescent properties of the nanoglassceramics have been compared with the characteristics of crystals and glasses.

The first material presents a laser lead-fluoride nanoglassceramics doped with Er^{3+} , Yb^{3+} , Nd^{3+} , Pr^{3+} , and Tm^{3+} . It is shown that, rare earth ions play a role of nucleation centers and precipitate in crystalline phase, for example, PbYOF_4 . Spectral, luminescent and laser properties of the nanoglassceramics have been demonstrated and compared with fluoride crystals. Possibility of utilization of the nanoglassceramics in fiber laser and amplifiers have been discussed.

The second material presents a forsterite nanoglassceramics doped with tetravalent chromium ions. Spectral and luminescent properties of the Cr^{4+} forsterite nanoglassceramics have been compared with the characteristics of forsterite single crystal and alumina-calcium glass. It was experimentally shown that tetravalent chromium ions are embedded in the forsterite nanocrystalline phase. It was found that the quantum yield of the luminescence of the forsterite nanoglassceramics is close to that for the forsterite single crystal. The results have demonstrated the possibility of synthesizing transparent nanoglassceramics doped with Cr^{4+} ions whose spectral and luminescence properties are highly competitive with those of forsterite single crystals. In this work the polarized luminescence of four-valence chromium in glasses and glassceramics was revealed for the first time. It was shown, that the degree of polarization induced by light polarized luminescence can serve as a discriminator of valence state of transitional elements in matrix. It was demonstrated that the transparent nanoglassceramics can be used for drawing optical fibers. This offers new possibilities for designing broadband optical fiber lasers and amplifiers based on the use of transition metal ions.

The third nanoglassceramics presents a glass host with precipitated nano-dimensional crystalline phase of complicated composition (CuCl/Br/I or AgCl/Br/I). The nanoglassceramics exhibits good non-linear properties. It is shown that an optical response appears in the materials when the energy density was 0.1–1 nJ/cm² while the appearance time of the response was less than 35 ps. The cause of the appearance of the nonlinear-optical response is the photogeneration of unstable color centers. These results can be used when developing nonlinear-optical media to control optical signals in integrated-optics systems, as well as for radiation limiters. Spectral and luminescent properties of the materials have been demonstrated.

The fourth material presents a glassceramics doped with silver metallic nanoparticles that play a role of nucleation centers. Nanocrystals of NaF-AgBr (20-30 nm) are grown on the centers. The nanoglassceramics are doped with Er^{3+} and Yb^{3+} ions. Spectral and luminescent properties of the materials have been demonstrated. The material combines itself three opportunities: fabrication of lasers or amplifiers, recording of volume Bragg gratings, fabrication of planar waveguides or fiber. The nanoglassceramics can be classified as optical polyfunctional material. The polyfunctional glassceramics exhibits good spectral, luminescent, and lasing characteristics, as well as

photorefractive and ion exchangeable properties. The polyfunctional glassceramics is a promising candidate for development and design of a new generation of optical elements and devices.

[We-O-24]
Pump-probe experiments with $\text{CaF}_2:\text{Ce}^{3+}+\text{Yb}^{3+}$ crystals

A. S. Nizamutdinov, S. A. Kirysheva, V. V. Semashko, A. K. Naumov, S. L. Korableva,
E. Yu. Gordeev

Kazan State University, 420008, Kremlyovskaja str., 18, Kazan, Russian Federation

Here we report on pump-probe studies of CaF_2 doped with Ce^{3+} and Yb^{3+} ions. The crystals $\text{CaF}_2:\text{Ce}^{3+}$ show advantageous spectral characteristics for tunable UV lasers application but have poor photochemical stability [1,2]. Their properties under intense UV pumping are affected by excited state absorption and color centers formation.

This work was aimed at dynamic processes investigation induced by laser radiation of UV spectral range in CaF_2 doped with Ce^{3+} and Yb^{3+} ions.

The pump-probe technique allowed us to observe nonlinear dynamic in absorption coefficient vs pumping radiation intensity in $\text{CaF}_2:\text{Ce}^{3+}+\text{Yb}^{3+}$ and spectral dependence of small signal gain coefficient in $\text{CaF}_2:\text{Ce}^{3+}+\text{Yb}^{3+}$. Optical gain was observed on $\text{CaF}_2:\text{Ce}^{3+}+\text{Yb}^{3+}$ in the range 325-335 nm for the first time. It proves Yb^{3+} coactivation antisolarant effect elaborated by us earlier[3]. Nonlinear dynamic was observed in gain coefficient vs probe intensity showing ability to control gain coefficient. Interpretation of experimental results was based on model of photodynamic processes which included recombination transitions at impurity centers of Ce^{3+} and Yb^{3+} also. Fitting procedure with numerical simulation of populations at Ce^{3+} energy levels and variation of transitions probabilities allowed us to calculate excited-state absorption cross-section of Ce^{3+} ions at pumping wavelength and recombination rates. It is shown that Yb^{3+} ions form a recombination channel with high transition rate.

[1] D. J. Pogashnik, D. S. Hamilton, Phys. Rev.B., 36, N16, (1987) 8251.

[2] R. Yu. Abdulsabirov, S. L. Korableva, A. S. Nizamutdinov, M. A. Marisov, A. K. Naumov, V. V. Semashko, Proc. SPIE, 6054, (2006) 172.

[3] V. V. Semashko, B. M. Galyautdinov, M. A. Dubinskii, R. Yu. Abdulsabirov, A. K. Naumov, S. L. Korableva, Proc. Internat. Conf. on LASERS 2000 (Albuquerque, NM, Dec. 4 - 8,2000), STS Press, McLean, VA (2001) 668.

[We-O-27]
Photoconductivity measurements in Ce³⁺-doped fluorides

L. Nurtdinova¹, V. Semashko¹, Y. Guyot², S. Korableva¹, M.-F. Joubert²

¹*Kazan State University*, ²*Université Claude-Bernard Lyon 1*

Today scientific and technological progress requires the development of the new efficient active media for lasers of ultraviolet (UV) and vacuum ultraviolet (VUV) spectral regions. And from the viewpoint of reliability, simplicity, cost, and performance solid-state active media possesses an advantage over the non-solid-state ones. Ce³⁺-activated fluoride crystals, such as Ce³⁺-doped LiYF₄ and LiLuF₄, are extensively used as UV active media for a long time and are thoroughly studied. It is well-known that in these crystals various types of photodynamic processes (PDP) arise under UV excitation involving both intra- and intercenter transitions of active ions [1]. Such processes diminish or even completely eliminate probability of laser action. Therefore in order to create an adequate model of PDP and to establish the ways to control them it is essential to know relative positions of energy levels of impurity and energy bands of the host.

Photoconductivity (PC) method allows to conduct direct investigations of PDP since it is based on registration of free charge carriers appearing in the host under UV irradiation. Joint analysis of PC data and conventional spectroscopy results provides an opportunity to determine values of physical quantities describing PDP (such as excited-state absorption and free charge carriers recombination cross-sections, etc).

There are two variations of PC measuring procedure used in the presented work. PC measurements by the use of conventional technique with attachable electrodes [2] showed that in Ce³⁺-doped LiYF₄ and LiLuF₄ crystal photocurrent appears around 300 nm and grows with shortening of wavelength. Energy dependencies of PC were obtained using microwave technique [3] in 225 – 305 nm spectral range; behavior of the dependencies changes from quadratic at longer wavelengths through linear to saturation at shorter ones. Numerical simulation based on four-level model of PDP resulted in excited-state absorption spectra with a maximum around 270 nm most probably corresponding to 5d-6s transition of Ce³⁺; physical quantities describing color centers formation, trapping and recombination processes were obtained. On the basis of the investigation results energy level diagrams for Ce³⁺:LiYF₄ and Ce³⁺:LiLuF₄ of “active ion – crystal lattice” system was proposed.

The research is supported by the Federal program “Scientific and academic and teaching staff of innovation Russia”.

1. A.S. Nizamutdinov, M.A. Marisov, V.V. Semashko, A.K. Naumov, R.Yu. Abdulsabirov, S.L. Korableva, *Physics of the Solid State*, **47**, No. 8 (2005) 1460.
2. U. Happek, S.A. Basun, J. Choi, J.K. Krebs, M. Raukas, *Journal of Alloys and Compounds*, 303– 304 (2000) 198– 206.
3. M.-F. Joubert, S. A. Kazanskii, Y. Guyot, J.-C. Gacon, and C. Pedrini, *Physical Review B* 69, 165217 (2004)

Luminescence and recombination processes in $\text{Li}_6\text{Gd}_x\text{Y}_{1-x}(\text{BO}_3)_3:\text{Eu}$ bulk crystals

I.N. Ogorodnikov¹, N.E. Poryvay¹, I.N. Sedunova¹, A.V. Tolmachev², R.P. Yavetskiy²

¹ Ural State Technical University, Mira Street, 19, Ekaterinburg 620002, Russia

² STC Institute for Single Crystals, NAS of Ukraine, Kharkov, Ukraine

Nowadays $\text{Li}_6\text{RE}(\text{BO}_3)_3$ (RE = Y, Gd, Eu) single crystals of isostructural orthoborates are being actively studied because of their great potential in thermal neutron imaging, as fast inorganic scintillators, red phosphors for plasma display panels and laser media. Substitution of gadolinium by yttrium essentially decreases the effective atomic number (Z_{eff}) of compound in the range from 46 to 26, and, consequently, its sensitivity to gamma-background. Utilization of these crystals in laser and scintillation devices implies intense processes of radiation defect formation. However, radiation-induced defects in this crystal have not been studied sufficiently so far.

All the examined $\text{Li}_6\text{RE}(\text{BO}_3)_3$ crystals were grown using Czochralski method at the Institute of Single Crystals, NAS of Ukraine (Kharkov) at the air atmosphere. The paper presents the results of a study of luminescence and recombination processes for these crystals carried out experimentally in the broad temperature range from 90 to 500 K using the luminescence and optical spectroscopy under various kinds of excitation (ultraviolet light, X-rays, the electron and ion beams), the decay kinetics measurements, and the thermally stimulated luminescence technique. Figure 1 presents an example of the obtained results on the $\text{Li}_6\text{RE}(\text{BO}_3)_3$ thermoluminescence. In addition, the computer simulations of the actual thermally stimulated processes were made.

On the bases of the obtained results, the paper discusses for these crystals the origin of the luminescence, the thermally stimulated recombination processes, the energy transport from the host lattice to luminescence centers, the origin of the radiation induced defects of the lithium sublattice, the origin of the shallow traps on the basis of these defects and a role of these shallow traps in the energy transport processes.

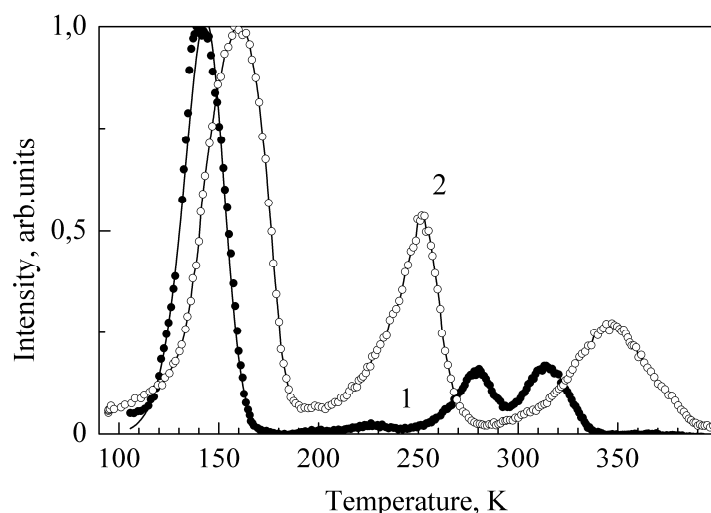


Fig.1: Glow curves of $\text{Li}_6\text{Gd}(\text{BO}_3)_3$ – (1) and $\text{Li}_6\text{Gd}_{0.5}\text{Y}_{0.5}(\text{BO}_3)_3-\text{Eu}$ – (2)

[Tu-P-19]

A transient optical absorption spectroscopy of $\text{Li}_6\text{Re}(\text{BO}_3)_3$ crystals

I.N. Ogorodnikov¹, N.E. Poryvay¹, I.N. Sedunova¹, A.V. Tolmachev², R.P. Yavetskiy²,
V.Yu. Yakovlev³

¹ *Ural State Technical University, Mira Street, 19, Ekaterinburg 620002, Russia*

² *STC Institute for Single Crystals, NAS of Ukraine, Kharkov, Ukraine*

³ *Tomsk Polytechnic University, Tomsk, Russia*

The lithium orthoborate crystals $\text{Li}_6\text{Re}(\text{BO}_3)_3$ (Re=Gd, Eu, Y) have a great potential in neutron imaging and represents a modern class of the fast inorganic scintillators that can be optimized for specific purposes, in particular, for the exothermic neutron detection. Due to considerable amount of boron atoms per elementary cell, large capture section for warm neutrons by isotope ^{10}B , great amount of emitted energy per absorbed neutron (total energy is about 2.8 MeV) borate compounds are promising materials for neutron registration in $^{10}\text{B}(n, \alpha)^7\text{Li}$ reaction. The presence of Li atoms in these crystals allows use also $^6\text{Li}(n, \alpha)^3\text{H}$ reaction, which has advantages upon detection of low energy neutrons. Besides, in composition of LGBO there are isotopes of $^{155,157}\text{Gd}$, nuclei of which have great capture section for thermal neutrons with energy below several keV.

The paper presents the results of a study of transient optical absorption (TOA) and luminescence of the crystals in the visible and ultraviolet spectral region. All the $\text{Li}_6\text{Re}(\text{BO}_3)_3$ crystals were Czochralski grown at the Institute of Single Crystals, National Academy of Sciences of Ukraine (Kharkov) in an air environment.

Measurements made by absorption optical spectroscopy with nanosecond-scale resolution established that an irradiation of these crystals by an electron beam (15 ns, 200 keV) leads to occurring a transient optical absorption. The time of optical transparency recovering comes up to 10 s at T=295 K. Slow monotonic relaxation of absorbance occurs in long time range (9 decades). We obtain that the experimental curves during 3-4 decades of the decay-time can be formally described in the (y, ln x) coordinates by a linear dependence and this TOA decay kinetics obeys a law of the interdefects tunnel recombination. The transient optical absorption of this crystal originates from optical transitions in the hole trapped centers and the optical-density relaxation kinetics is rate-limited by interdefect tunneling recombination, which involves these hole centers and the electronic Li^0 -centers representing neutral lithium atoms. At 290 K, the Li^0 -centers undergo thermally stimulated migration, which is not accompanied by carrier ejection into the conduction or valence band. The slow components of the TOA kinetics with characteristic times from a few tens of milliseconds to a few seconds can be assigned to diffusion-controlled annihilation of interstitial lithium atoms and lithium vacancies.

The paper discusses the mechanisms of creation and decay of the short-living Frenkel's pair defects in the cation sublattice of these crystals, and recombination processes with their participation.

[Tu-O-5]

Energy transfer probe for characterization of luminescent photonic crystals morphology

Yu.V. Orlovskii, T.T. Basiev, E.V. Samsonova, N.A. Glushkov

Prokhorov General Physics Institute RAS, 38 Vavilov st., Moscow, 119991, Russia

We evaluated energy transfer probe for characterization of photonic crystals morphology. It is based on measurement of direct energy transfer kinetics from excited fluorescent impurity centers (donors) to quenching acceptors randomly distributed in various restricted geometries [1]. We used photonic crystals made of inverse opals in silica (SiO₂) with voids ($D \approx 500$ nm) filled by luminescent material of chelate complexes of yttrium with pyrazine-2-carboxylic acid co-doped by Tb³⁺ [Y_{0.99}Tb_{0.01}(pyca)₃(H₂O)₂] nH₂O [2] with low donor concentration. These complexes are liable to formation of hydrates of different structure and contain water molecules either bonded or unbonded to central ion. Fluorescence quenching in lanthanide or transition metal ions in condensed phase can be described by Forster resonant mechanism of energy transfer between impurity donor and acceptor ions. The Tb³⁺ ions appear as fluorescent donors and OH⁻ ions of unbounded water molecules appear as randomly distributed acceptors. In case of low acceptor concentrations and in the absence of energy migration over the donors the fluorescence kinetics in continual approximation of embedding space at large t is described by [1, 3-5]

$$I(t) = \exp\left(-\frac{t}{\tau_R} - \gamma t^{\bar{d}/s}\right), \quad (1)$$

where τ_R the radiative lifetime; γ the macroparameter of donor – acceptor direct energy transfer; \bar{d} the Huasdorff fractal dimension of the space where acceptors are placed. Due to effective energy transfer from organic ligand to the Tb³⁺ ion we measured fluorescence kinetics of the ⁵D₄ level of Tb³⁺ under excitation into complexing agents by pulsed nitrogen laser at 337 nm. The fluorescence is detected at the ⁵D₄ → ⁷F₅ transition. The direct energy transfer kinetics $I_{\text{DET}}(t)$ can be found by division of the measured fluorescence kinetics $I(t)$ by $\exp(-t/\tau_R)$. The difficulty to find the real radiative lifetime value is that even at the late stage of the measured fluorescence kinetics the contribution from the second term of Eq.(1) is distinct from zero. However, according to Eq. (1) the energy transfer kinetics at the late disordered stage in scales of $-\log(-\ln[I(t)/\exp(-t/\tau_R)])$ vs. $\lg(t)$ has the linear dependence with the slope angle α with $\text{tg}\alpha = 3/s$. Consider τ_R as fitting parameter we tried to get the best linearization of the measured decay curve at the late stage in scales of $-\lg(-\ln[I(t)/\exp(-t/\tau_R)])$ vs. $\lg t$ (Fig. 1, curve 1) and get $\tau_R = 1.94\text{ms}$ at the slope angle α with $\text{tg}\alpha = 1/3$. Accounting that the lower energy the ⁵D₄ → ⁷F₀ and ⁵D₄ → ⁷F₁ transitions of the Tb³⁺ donor participated in the cross-relaxation with OH⁻ acceptors have reduced matrix elements of electronic transition $U^{(2)} = 0$, whereas for the other ⁵D₄ → ⁷F_J transitions $U^{(2)} \ll U^{(4)}$ and $U^{(6)}$ [6], the quadrupole transitions in donors contrarily to dipole ones are insignificant. At the same time the dipole transitions in the OH⁻ dynamic oscillators are partially allowed for $\Delta s > 1$ due to anharmonicity of lattice vibrations [7] and, hence, dipole – dipole donor – acceptor energy transfer with $s = 6$ is only possible. In this case $\text{tg}\alpha = 1/3$ indicates a reduced dimension of the medium $\bar{d} = 2 = D$ (D the Euclidian dimension of the embedding space), which can be a result of monomolecular filming of the chelate complexes inside the photonic crystal voids that confirmed by SEM image. The direct energy transfer kinetics at the late disordered stage in scales of $\ln[I(t)/\exp(-t/\tau_R)]$ vs. $t^{1/3}$ has the linear dependence with the slope angle α with $\text{tg}\alpha = \gamma_1^{(2)} = 20.3 \text{ s}^{-1/3}$. Similar measurement and analysis of the late stage of fluorescence decay curve in the [Y_{0.99}Tb_{0.01}(pyca)₃(H₂O)₂] nH₂O vacuum dried powder gives the spontaneous emission decay time, equal to that found in the opaline sample $\tau_R = 1.94\text{ms}$. However, now at the late stage the slope of the kinetics in the scales of $-\lg(-\ln[I(t)/\exp(-t/\tau_R)])$ vs. $\lg t$ is equal to α with the $\text{tg}\alpha = 1/2$ (Fig.1,

curve 3) that is an evidence of $D = 3$. In addition, we observed that linearization of the $\ln[I(t)/\exp(-t/\tau_{\text{rad}})]$ curve for the powder is much better vs. a $t^{1/2}$ scale than vs. $t^{1/3}$ with $\gamma_1^{(3)} = 35.6 \text{ s}^{-1/2}$.

To our own surprise the method is able to work at high concentrations of the Tb^{3+} donors in spite of the energy migration over them. We obtained the same results for the $[\text{Tb}(\text{pyca})_3(\text{H}_2\text{O})_2]$ nH_2O powder with 100% concentration of fluorescent donors and for the opaline sample filled by this powder (Fig.1, curves 2, 4) when we used $(1/\tau_{\text{R}} + W^{(D)})$ as a fitting parameter, where $W^{(D)}$ has a meaning of a decay rate at the migration accelerated stage of energy transfer kinetics. However, as a result of extensive literature analysis we regret to learn that there is no adequate equation for $W^{(D)}$ in existent theories of energy migration.

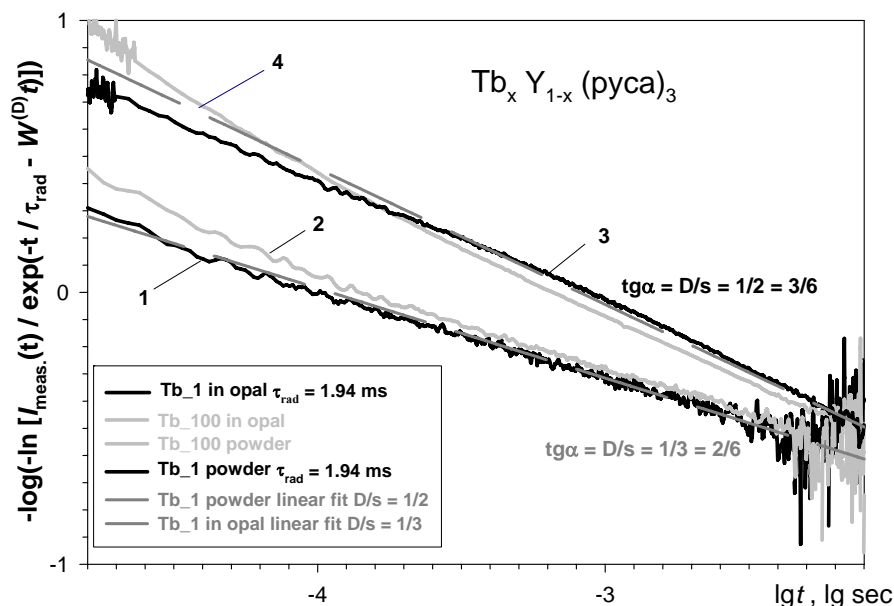


Fig.1. Direct energy transfer kinetics of chelated complexes of: 1 - yttrium co-doped by Tb^{3+} $[\text{Y}_{0.99}\text{Tb}_{0.01}(\text{pyca})_3(\text{H}_2\text{O})_2]$ nH_2O and 2 - terbium $[\text{Tb}(\text{pyca})_3(\text{H}_2\text{O})_2]$ nH_2O with 2-pyrazinecarboxylic acid embedded into inverted SiO_2 opaline matrix voids, and of: 3 – the $[\text{Y}_{0.99}\text{Tb}_{0.01}(\text{pyca})_3(\text{H}_2\text{O})_2]$ nH_2O and 4 - $[\text{Tb}(\text{pyca})_3(\text{H}_2\text{O})_2]$ nH_2O powder samples in the scales of $-\lg(-\ln [I_{\text{meas.}}(t) / \exp(-t / \tau_{\text{rad}} - Wt)])$ vs. $\lg(t)$. Dashed lines is the linear fit of curves 1 and 3 with $\text{tg}\alpha = 1/3$ and $1/2$, respectively.

[1] Th. von. Förster, Ann. Phys. **2** (1948) 55; Ztschr. Naturforsch. **A4** (1949) 321.

[2] S.V. Eliseeva, O.V. Mirzov, S.I. Troyanov, A.G. Vitukhnovsky, N.P. Kuzmina, Journal of Alloys and Compounds **374** (2004) 293

[3] B.Ya. Sveshnikov and V.I. Shirokov, Optika i Spektroskopia, **12(5)** (1962) 576

[4] M. Inokuti and F. Hirayama, J. Chem. Phys. **46** (1965) 1978

[5] P. Levitz, J. M. Drake, J. Klafter, J. Chem. Phys. **89**, (1988) 5224

[6] W.T. Carnall, H. Crosswhite, H. M. Crosswhite, Internal report of Argonne National Laboratory, Argonne (Illinois) 1975.

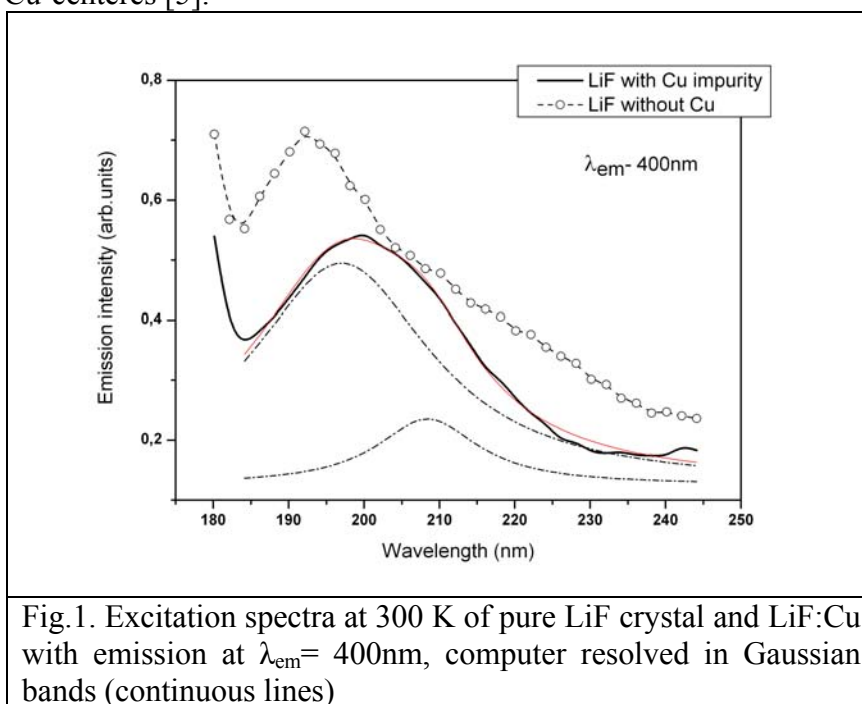
[7] V.P. Gapontzev, M.R. Sirtlanov, A.K. Gromov, A.A. Isineev, Proceedings of the International Conference on Lasers'81, Ed. C.B. Collins, 1981, pp. 763 – 768.

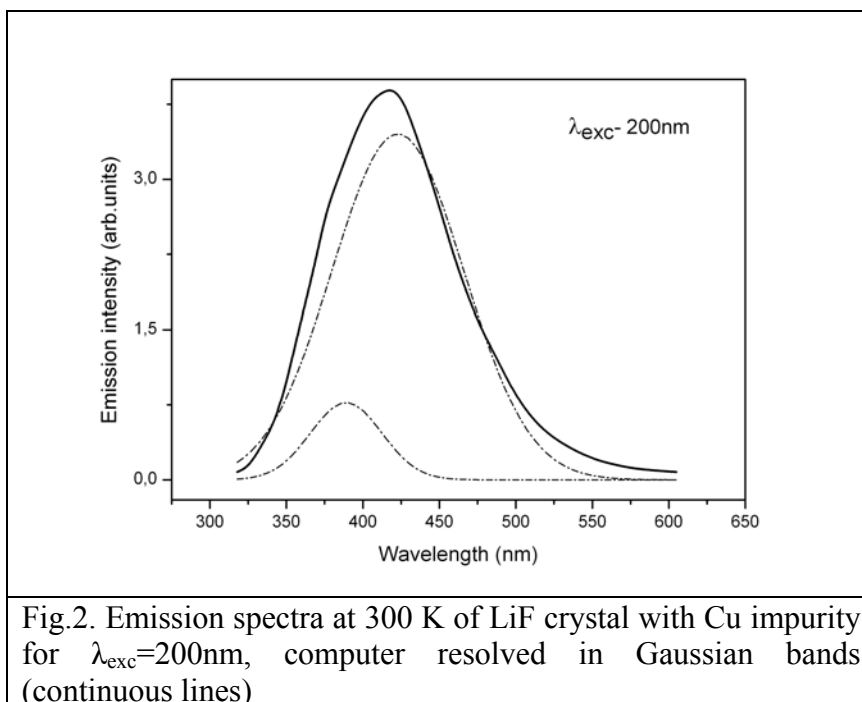
[Th-O-41] Experimental and theoretical research of LiF:Cu

A.S. Paklin, A.S. Mysovsky, A.A. Shalaev

Lithium fluoride is used as a thermoluminescent phosphor during the last 50 years [1]. Leading of LiF along other phosphors, using in thermoluminescent dosimetry, is ensured of its tissue equivalence. Thermoluminescent detector which based on LiF phosphors is chemical inertness. At last time often are used detectors LiF:Mg,Cu,P as good dosimeter of ionizing irradiations. The luminescent processes in this phosphor are not well understood. In practical dosimetry often are using detectors, are produced as powders or sintered pellets. These detectors have high sensitivity, but also they have high background signal [2,3] which are restricting measurement a small doses of irradiation. Application of monocrystalline detectors can avoid of these shortages.

We have grown monocrystalline LiF:Cu by the Czochralski method in Ar or air atmospheres in the Institute of Geochemistry SB RAS. The doping were added in pure LiF as powder CuCl with concentrations 0,5-5 wt % before growing. Chemical analysis shows concentrations of copper in crystals 0,0003-0,0018 wt %. The concentrations of copper is enough for effective thermoluminescence [4,5]. Excitation and emission spectra was measured. Probably the excitation peak (fig. 1) at 210 nm is a result of Cu impurity in LiF [5] and peak at 195 nm shows a presence of O²-centers [6]. LiF with Cu impurity and pure have grown at the same conditions. The emission spectra (fig. 2) has been resolved at two peaks 385 nm and 410 nm. The peak at 385 nm is associated with Cu-centeres [5].





We have provided *ab initio* calculations, which gave us the equilibrium geometry around the admixture Cu, which we used in various charging states. To compare the right of applying methods, we calculated the same admixtures in NaCl, KCl and NaF.

References

1. John, T.F. Calculated Energy Response of Lithium Fluoride Fingertip Dosimeters. United Kingdom Atomic Energy Establishment, Winfrith Memorandum AEEW M550 (1965)
2. Jun Zuo, Ravindra Pandey, A. Barry Kunz, Phys. Rev. B, Vol. 45, No 6, pp. 2709-2711, 1992
3. Delgado, A. and Gomez Ros, J. M. Modifications induced in the TLD-100 trap distribution during exposures at difference ambient temperatures. Radiat. Prot. Dosim. 34(1-4), 233-235 (1990)
4. R.R.Patil, S.V.Moharil, J.Phys.:Condens. Matter 7, 9925-9933, 1995
5. R.R. Patil, S.V. Moharil, Solid State Communications, Vol. 94, No. 7, pp. 573-575, 1995
6. Radzhabov E A, Phys. Status Solidi B 115 K25, 1983

[Tu-P-11]

**Percolation threshold for magnetic binding in the structure of the Haldane chain
nikelates $R_2\text{BaNiO}_5$**

V.A. Panfilov, A.V. Potapov, S.A. Klimin

Institute of spectroscopy RAS, Troitsk Moscow region, Russia

$R_2\text{BaNiO}_5$ is a family of isostructural compounds containing chains of the $S=1$ spins. The crystallographic structure fits very well for modeling the influence of the interaction between chains on magnetic properties. Y_2BaNiO_5 being the best known up-to-date Haldane system without noticeable interaction between magnetic chains provides a matrix for introducing an amount of magnetic rare-earth ions that substitute for yttrium and connect the chains. Due to the finite correlation length of Haldane chains, it is expected that a threshold amount of binding ions is needed for introducing the three-dimensional magnetic order [1].

In this work we present calculations of percolation threshold for the structure of chain nickelates. The original algorithm was checked on the simple lattices with known percolation threshold. We present the dependences of percolation threshold on the correlation length of the Haldane chain and on the possible pathways for magnetic bonds in the structure. Results of the calculations are compared with our experimental data on the magnetic ordering temperatures obtained from the analysis of the optical spectra of $(\text{Nd}_x\text{Y}_{1-x})_2\text{BaNiO}_5$.

This work was supported in part by the Russian Foundation for Basic Research (Grant No. 08-00690-a), and by Programs of Russian Academy of Sciences.

[1] J.V. Alvarez, H. Rieger, A. Zheludev, Phys. Rev. Lett. 93, 156401 (2006).

[We-P-46]

ESA and activator ions photoionization spectra investigations of Ce:YLF and Ce:LiLuF₄ single crystals

V.V. Pavlov, V.V. Semashko, A.K. Naumov, S.L. Korableva, L.A. Nurtdinova,
A.S. Nizamutdinov

Kazan (Volga Region) Federal University, Kremlyovskaja 18, Kazan, 420008, Russia
*E-mail: Vitaly655@mail.ru

Degradation of optical and laser properties of the majority of solid-state active media during operation is associated with photodynamic processes induced by high energy UV pump photons which are in resonance of activator ions 4f-5d transitions [1]. The reason of these processes is excited state absorption (ESA) of pumping radiation accompanied with ionization of activator ions and photoconductivity effects.

The aim of this work is to elaborate a new technique of ESA/photoionization (ESA/PhI) spectra investigation in the range of ground-state absorption of activator ions and study these spectra in well-known UV active media – Ce:LiLuF₄ and Ce:LiYF₄ crystals.

To study ESA/PhI spectra we propose to analyze activator ions 5d-4f fluorescence kinetics containing additional recombination component. It is possible because spectral dependence of the weight of recombination component in these kinetics is determined by the spectrum of ESA/photoionization cross section, and, therefore, depends on excitation wavelength [2].

Two techniques of fluorescence kinetic interpretation were realized. The first one is based on the fitting procedure of PDP model parameters in the rate equations systems, which describe two-photon absorption and ionization of an impurity center, formation of the color centers and pump-induced color center ionization, capture of the free carrier on impurity center etc. The second one uses an approximation of the luminescence kinetic by analytical Becquerel function [3] and allows to obtain only ESA spectra line shape. The main results are presented on fig. 1, 2 and discussed.

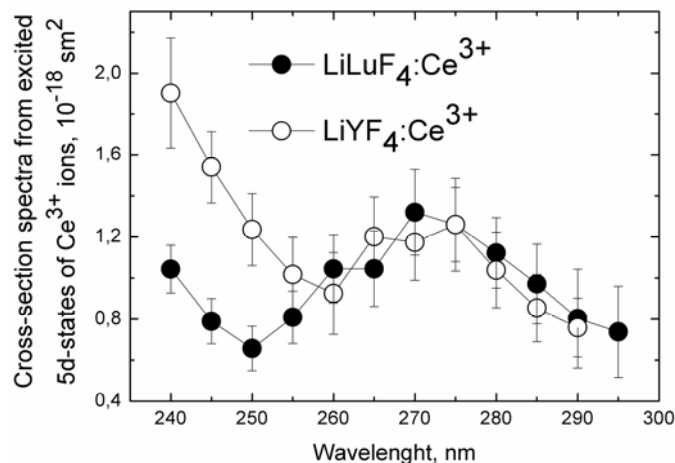


Figure 1 Nonpolarized photoionization cross-section spectra of Ce:YLF and Ce:LiLuF₄ crystals at 300 K obtained by using first technique

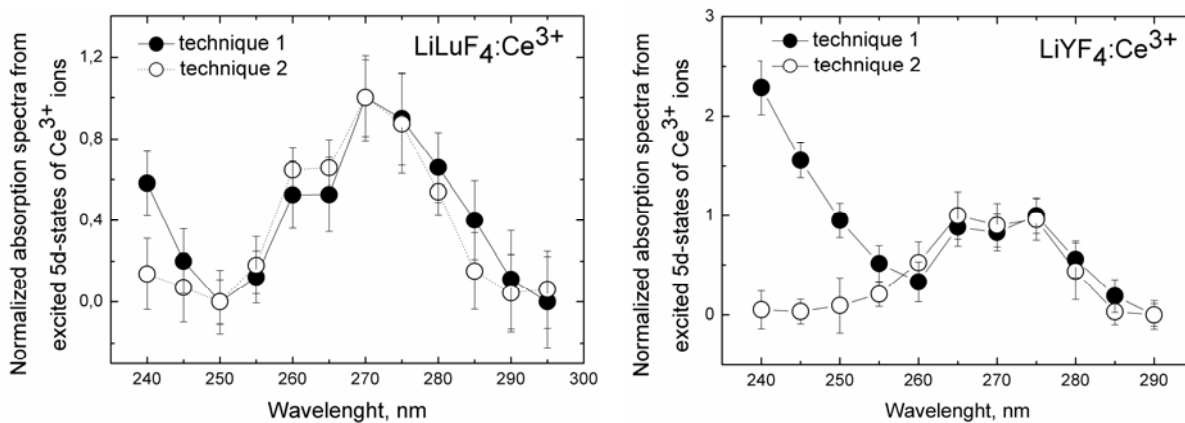


Figure 2 Nonpolarized photoionization spectra of Ce:YLF and Ce:LiLuF₄ crystals at 300 K obtained by using two interpretation techniques

ESA/photoionization cross-section spectra estimated by both techniques reveal maxima of $(\sim 1.3 \pm 0.2) \cdot 10^{-18} \text{ cm}^2$ at about 270 nm for the both crystals. Photoelectrons and holes recombination cross-section is about 10^{-16} cm^2 whereas free charge carriers trapping cross-section is about 10^{-20} cm^2 . On the basis of experimental and computed results terminal state of the ESA in these crystals was attributed to the 6s-state of Ce³⁺ partially localized in the conduction band of crystal hosts.

[1] V.V. Semashko *Phys. of Solid State*, **47**, N8, 1507-1511(2005)

[2] A. S. Nizamutdinov, V. V. Semashko, A. K. Naumov, L. A. Nurtdinova, R. Yu. Abdulsabirov, S. L. Korableva, V. N. Efimov. *Phys. of Solid State*, **50**, N9, 1648-1651 (2008)

[3] V.V. Antonov-Romanovsky, *Photoluminescence kinetics of crystals*, Nauka, Moscow (1966)

[Th-I-34]

Parallel between rare earth-trapped exciton and charge transfer in rare earth doped crystals

C. Pedrini¹, A. Belsky¹, A. Petrosyan², R.V. Sargsyan², I. Kamenskikh³

¹ *Université de Lyon, Université Lyon 1, CNRS, UMR5620, Laboratoire de Physico-Chimie des Matériaux Luminescents, F-69622 Villeurbanne Cedex, France*

² *Institute for Physical Research, Laboratory of Crystal Growth of Luminescent Materials, 0203 Ashtarak-2, Armenia*

³ *M.V.Lomonosov Moscow State University, Physics Department, Synchrotron Radiation Laboratory, 119991 Moscow, Russia*

Charge exchange processes may be observed in doped crystals leading often to a change of their luminescence properties and energy loss processes. The purpose of this presentation is to analyze charge transfer process and impurity-trapped exciton formation in few rare earth doped crystals, and to establish a parallel between the mechanism of their formation and radiative and non-radiative relaxation processes described by using configurational coordinate diagrams.

So-called charge transfer states can be formed resulting from charge exchange processes between the host valence band and the dopant rare earth RE^{n+} . Charge transfer transitions are of electron acceptor type for the rare earth impurity. Such a charge transfer center can be described as $RE^{(n-1)+} + h_{\text{bound}}$ where the hole h_{bound} is localized in the valence band and bounded to the impurity. The probability of this charge transfer process is larger in crystals doped with trivalent rare earth impurity ions RE^{3+} that are stable as RE^{2+} as well, like Eu and Yb. Examples will be given in few Eu^{3+} and Yb^{3+} doped oxide crystals.

Rare earth-trapped exciton formation $RE^{(n+1)+} + h_{\text{bound}}$ is another kind of charge exchange of electron donor type where the hole h_{bound} is localized on the rare earth. Such excitons have been observed and analyzed in fluorides doped with Eu^{2+} and Yb^{2+} that are stable as RE^{3+} , and in some oxides doped with trivalent rare earth ions that are stable in the quadrivalent state. The latter case will be illustrated through recent results obtained in calcium niobate $Ca(NbO_3)_2$ doped with Ce^{3+} , Pr^{3+} and Tb^{3+} ions.

[We-I-14]

Rare earth doped nanoparticles for high resolution imaging

F. Pellé¹, L. Caillat¹, A. Tadili¹, B. Hajj², D. Chauvat², J. Zyss²

¹ LCMCP UMR7574 CNRS/UMPC/Chimie ParisTech, Chimie ParisTech, Paris, France

² LPQM, UMR 8537 CNRS, Institut d'Alembert, ENS Cachan, Cachan, France;

Rare Earth (RE) doped nanoparticles are recognized since few years as potential optical nanoprobes for biological imaging. Due to their high photo-stability, long time observations can be achieved. Furthermore, from their particular energy level schemes, visible emissions are obtained under coherent or non coherent infrared excitation. The intensity of the upconverted emissions varies as I_{exc}^n (n, being the number of IR photons involved in the process) which allows expecting a

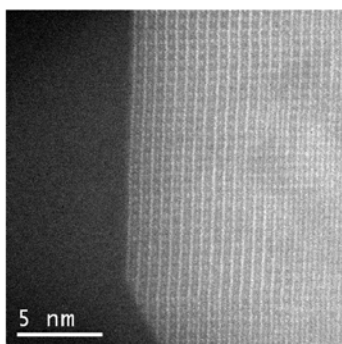


Fig.1: HRTEM image of a $Er^{3+}, Yb^{3+}:KY_3F_{10}$ nanoparticle

reduction of the fluorescent spot size using a simple experimental set up. Depending on the nature of the dopants or their respective concentration, several colors (red, green, blue) of the dopants are observed that open the way to multiplexing of signals in a way similar to the multiplexing use of quantum dots. Several tests have already demonstrated their biocompatibility [1,2]. Efficient upconversion processes are favoured in materials with a low phonon cut-off frequency i.e. halides. Among them fluorides are more appropriate due to their chemical stability. Perfect nanocrystals can be easily synthesized using soft chemistry (Fig.1).

Fluoride nanoparticles (KY_3F_{10} , LaF_3 , $NaGdF_4$) were synthesized with Er^{3+}/Yb^{3+} or Tm^{3+}/Yb^{3+} as dopants. Green and red emissions in the case of Er^{3+}/Yb^{3+} , blue and red emissions in the case of Tm^{3+}/Yb^{3+} are recorded under infrared excitation (@980nm). Single nanoparticles were studied using polarization-resolved multiphoton microscopy (Fig.2). Raster-scanned images showed an enhanced spatial resolution by a factor compatible with the square root of the number of photons involved in excitation process. Multiphoton effects with a higher number of photons involved in the infra-red excitation are envisioned.

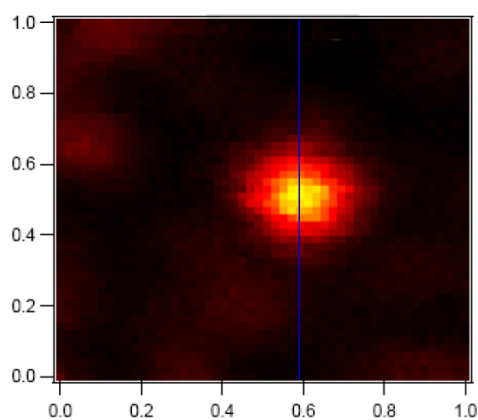


Fig.2: Multiphoton scan for a single nanoparticle

the

Acknowledgements

This work is supported by the EADS Foundation. G. Patriarche (LPN UPR20 CNRS Marcoussis, France) is acknowledged for providing HRTEM pictures.

References

- [1] Feng Wang, YongZhang, Xianping Fan and MinquanWang, *Nanotechnology*, **17**, 1527–1532 (2006).
- [2] D.K. Chatterjee, A. J. Rufaihah, Yong Zhang, Yong, *Biomaterials*, **29**, 937–943 (2008)

[Tu-O-13]

Spectroscopic and laser properties of trivalent ytterbium ions in ZnWO₄ crystal

E.V. Pestryakov¹, V.V. Petrov¹, V.I. Trunov¹, A.V. Kirpichnikov¹,
M.A. Merzliakov¹, E.N. Galashov², V.N. Shlegel², J.V. Vasiliev²

¹ *Institute of Laser Physics SB RAS, Novosibirsk, 630090, Russia*

² *Institute of Inorganic Chemistry SB RAS, Novosibirsk, 630090, Russia*

The zinc tungstate, ZnWO₄ (ZWO) crystals by a Low-Thermal Gradient Czochralskii method (LTG Cz) were grown [1]. The features of growth of single ZWO crystals doped with trivalent ytterbium ions by LTG Cz-technique have been investigated. The effect of change of the growth conditions on the crystal morphology and the capture of micro and macro-inclusions were studied. High quality and high optical transparent ZWO crystals doped with Yb(III) ions were obtained by using annealing techniques. The structure of crystal was analyzed by X-ray diffraction method.

Monoclinic structure of Yb:ZWO crystal demonstrates anisotropic optical and spectroscopic properties. Spectroscopic properties of trivalent ytterbium ions in the ZWO crystals for polarizations along *a*, *b* and *c* crystallographic axis at room and liquid nitrogen temperatures were investigated. The comparison of their spectroscopic and laser properties was performed. Fig. 1a,b,c displayed typical spectra of absorption of Yb:ZWO crystals for polarizations E//*a*, E//*b* and E//*c* at room temperature, respectively.

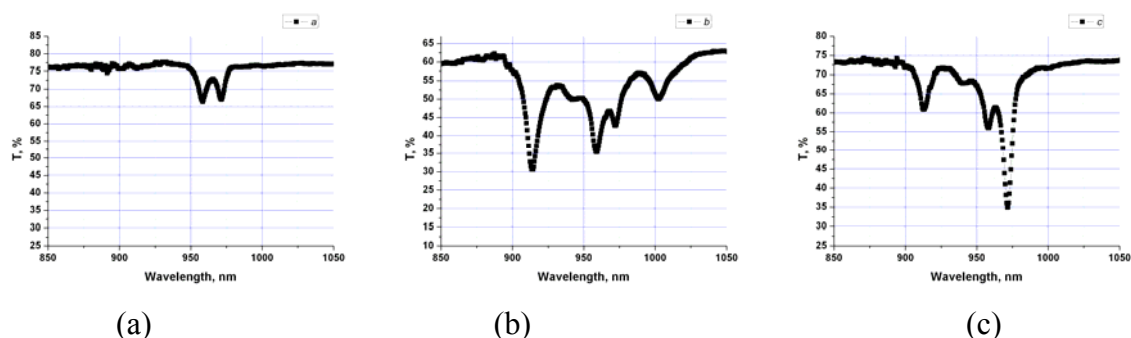


Fig.1. Polarized spectra of Yb:ZWO crystals at room temperature: a- E//*a*, b- E//*b*, c- E//*c*.

The absorption cross section for transitions between O-O levels of ground ²F_{7/2} and excitation ²F_{5/2} states of Yb(III) for E//*c* was established to be 3.5·10⁻²⁰ cm². The peak emission cross section was calculated from the emission spectra and radiative lifetime ~1.0 ms to be 2.0·10⁻²⁰ cm². Being based on the analysis of the spectroscopic data and on selection rules for intermanifold transitions the simplified schemes of energy levels in Yb:ZWO crystals have been constructed.

Calculations of gain cross sections taking into account obtained data showed prospects for diode laser pumped stimulated emission of coherent radiation in trivalent ytterbium ions in ZWO crystals in the 970-1060 nm spectral range at room temperature.

This work was performed in part under the support of Government Program “Extreme light fields” and of the RFBR grants 08-02-00965 and 09-02-12261.

[1]. E.N. Galashov, V.A. Gusev, V.N. Shlegel, J.V. Vasiliev, Crystallography Reports, v.54, 689 (2009).

Particular features of electronic structure in multiferroic oxides

R.V. Pisarev

*Ioffe Physical-Technical Institute, Russian Academy of Sciences
194021 St. Petersburg, Russia*

Multiferroics are materials which possess at least two order parameters which are mutually coupled one with another [1]. Recent theoretical studies showed that the electronic contribution to multiferroic polarization may be comparable in magnitude with the ionic contribution. In this talk we overview [2] our recent studies of electronic structure in typical multiferroics. We studied near-band-gap charge-transfer (CT) transitions in ferrites, manganites and cuprates in the spectral range from 0.6 to 5.8 eV using optical ellipsometry.

BiFeO₃ and related ferrite insulators [2]. The most prominent multiferroic among iron Fe³⁺(3d⁵) oxides is the bismuth ferrite BiFeO₃. In order to reveal particular features of its electronic structure we studied this material and other iron oxides in which Fe³⁺ ions occupy only octahedral positions. BiFeO₃ demonstrates much higher values of dielectric constants (Fig. 1a) than, such materials as α-Fe₂O₃, orthoferrites RFeO₃ (Fig.1b), or iron borates FeBO₃ and Fe₃BO₆. The second group included spinel LiFe₅O₈, garnets R₃Fe₅O₁₂, and CaFe₂O₅ where Fe³⁺ ions occupy both octahedral and tetrahedral positions. All ferrites investigated are CT insulators with the band gap determined by a dipole-forbidden *p-d* CT transition *t*_{1g}-*t*_{2g} in octahedral FeO₆ centers forming a 2.5 eV band on a tail of a strong 3.0 eV band assigned to a dipole-allowed *p-d* CT transition *t*_{2u}(π)-*t*_{2g} in octahedral FeO₆ centers. Unexpected modification of the CaFe₂O₅ spectrum in comparison to all other ferrites has been observed.

Rare earth (R) manganites RMnO₃ [3]. These materials crystallize in orthorhombic and hexagonal crystal structures where Mn³⁺(3d⁴) ions occupy octahedral sixfold and unusual fivefold positions, respectively. We studied near-band-gap electronic structure in hexagonal manganites YMnO₃ (Fig. 2), ScMnO₃, and ErMnO₃. It was found that the spectra substantially differ from the spectra of orthorhombic manganites in both the positions of spectral features and their polarization anisotropy. It was found that the optical absorption edge is determined by an abnormally strong (k~1) and narrow electric dipole transition with the center at about 1.6 eV with light polarization in the basal plane. This transition can be treated with confidence as a charge transfer from oxygen to manganese.

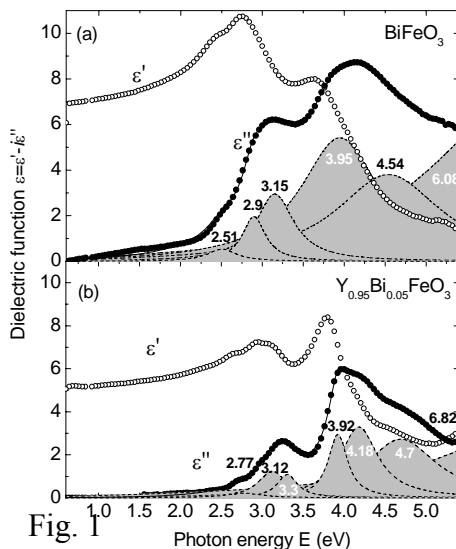


Fig. 1

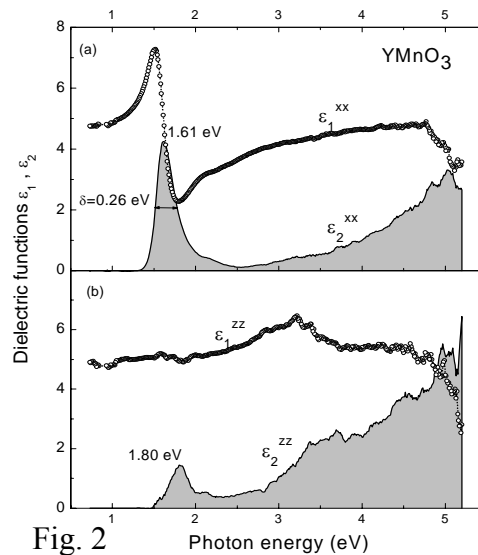


Fig. 2

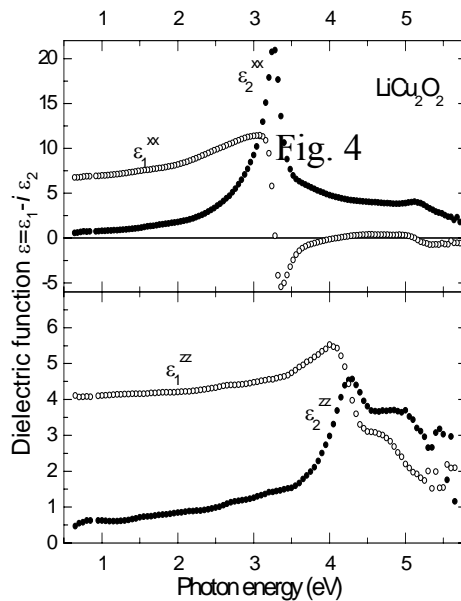
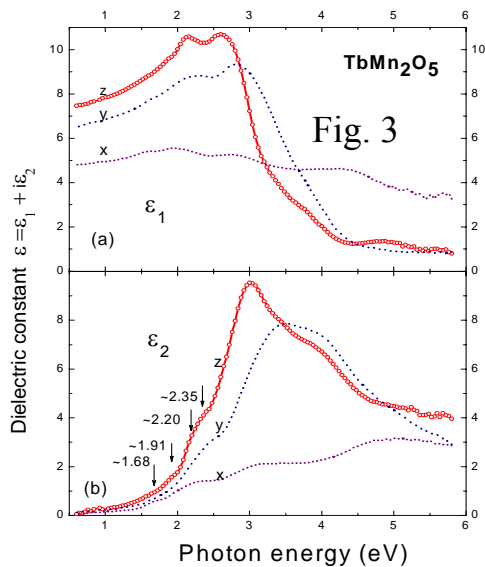
Mixed-valent manganite TbMn_2O_5 [4]. This material is an orthorhombic multiferroic. It contains the Mn^{4+} ($3d^3$) ions which strongly prefer octahedral positions (the crystal-field stabilization energy is $-12Dq$) and the Jahn-Teller Mn^{3+} ions which prefer MnO_5 pyramidal positions. Strong increase of optical response for the z and y polarizations and strong anisotropy with a relation $\epsilon_{2x} < \epsilon_{2y} < \epsilon_{2z}$ are found (Fig. 3). These findings agree with the theoretical analysis derived from the orientation of the MnO_5 pyramids in the unit cell and points to the one-center p - d CT transitions as the main contributors to the spectral weight. We argue that the CT processes are accompanied by giant electric-dipole fluctuations and therefore may be a source of large electric polarization of MnO_5 pyramids due to the parity-breaking Mn^{3+} - Mn^{4+} isotropic exchange interaction.

Mixed-valent lithium cuprate LiCu_2O_2 [5]. Among numerous transition-metals oxides_copper-based compounds hold a distinguished position. $\text{LiCu}^{1+}\text{Cu}^{2+}\text{O}_2$ crystallizes in the orthorhombic space group where the edge-sharing Cu^{2+}O_4 squares and $\text{O-Cu}^{1+}\text{-O}$ dumbbells form the basic elements of the crystalline structure. It was found that the optical response of LiCu_2O_2 in the spectral range of 0.6-5.8 eV radically differ from those of all other known Cu^{1+} and Cu^{2+} and mixed-valent oxide cuprates. An extremely strong, sharp and highly anisotropic optical feature with $\epsilon_2^{xx} = 26$ was observed at 3.27 eV (Fig. 4). Analysis showed that this feature can be explained by an exciton-type model which includes strong electron-hole correlations and a crystal-field splitting of the Cu^{1+} states. The exciton effects in LiCu_2O_2 appear strongly enhanced due to the shortening of the dumbbell lattice spacing which is the shortest one among known cuprates. These experimental results along with the model revealed previously unknown regularity in the electronic structure of the cuprates.

The work is supported by the Russian Foundation for Basic Research.

References

- [1] W. Eerenstein, N.D. Mathur, and J.F. Scott, Nature **442**, 759 (2006).
- [2] A.S. Moskvin and R. V. Pisarev, Low Temp. Phys. (2010).
- [3] R.V. Pisarev, A.S. Moskvin, A.M. Kalashnikova, and Th. Rasing, Phys.Rev. **79**, 235128 (2009).
- [4] A.M. Kalashnikova and R.V. Pisarev, JETP Lett. **78**, 143 (2003).
- [5] A.S. Moskvin and R.V. Pisarev, Phys. Rev. B **77**, 060102(R) (2008).
- [6] R.V. Pisarev, A.S. Moskvin, A.M. Kalashnikova, A.A. Bush, and Th. Rasing, Phys. Rev. B **74**, 132509 (2006).



[Tu-P-23]

Near-band gap electronic structure of the tetragonal rare-earth and bismuth cuprates

R.V. Pisarev¹, V.V. Pavlov¹, A.M. Kalashnikova^{1,3}, A.S. Moskvina²

¹*A. F. Ioffe Physical-Technical Institute of RAS, 194021 St. Petersburg, Russia*

²*Ural State University, 620083, Ekaterinburg, Russia*

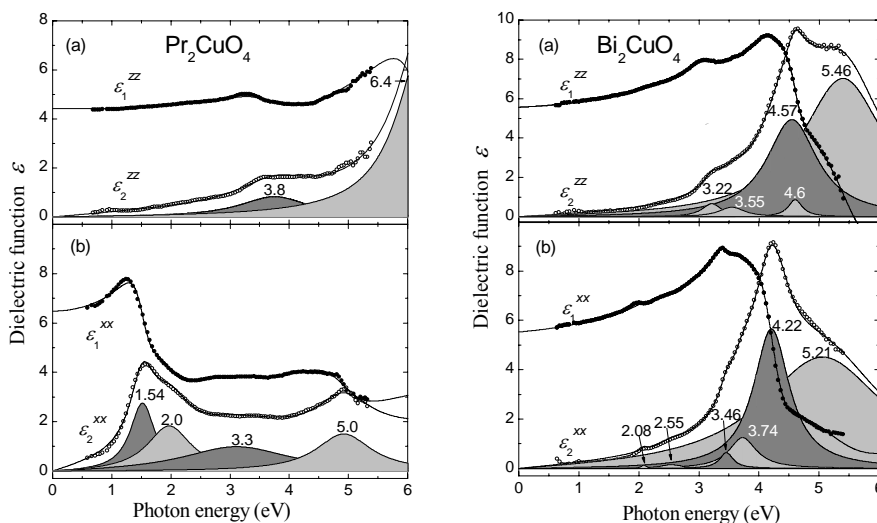
³*Radboud University Nijmegen, IMM, 6525AJ Nijmegen, The Netherlands*

Copper compounds with the general chemical formula R_2CuO_4 where R are rare earth ions and Bi, are a family of strongly correlated complex $3d$ -oxides which raised a strong interest after discovery of high T_c superconductivity in hole-doped La_2CuO_4 , and in electron-doped Nd_2CuO_4 . During last years these and relevant compounds have been actively studied. Nevertheless problems of electronic states and nature of particular physical and chemical properties of strongly correlated cuprates remain actively discussed.

Here we present complex experimental and theoretical study of optical spectra and related electronic structure of the tetragonal R_2CuO_4 ($R=Pr, Nd, Cm$) and Bi_2CuO_4 . The spectra of dielectric function of these compounds were studied by means of optical ellipsometry in a range of photon energies of 0.6-5.8 eV and analyzed in terms of a cluster model for CuO_4^{6-} complexes taking into account intra-center $p-d$ and inter-center $d-d$ charge-transfer (CT) transitions.

As a result of the study of rare-earth cuprates we found that their band gap is defined by an electric-dipole allowed CT transitions centred at 1.54-1.59 eV (Fig. 1). Optical response of Bi_2CuO_4 strongly differs from the rare-earth cuprates (Fig. 2) which we relate with strong covalency of Bi-O bonding and strong ionicity of $Cu(3d)-O(2p)$ bonding. These features are manifested in the strong intense absorption bands near 5 eV and suppression of low-energy intense intra-center $p-d$ and inter-center $d-d$ CT transitions. Regardless the strong distinctions of optical response of Pr, Nd, and Sm-cuprates, and Bi-cuprate the dielectric gap in both groups of compounds shows comparable values defined by intra-center $p-d$ CT transitions and two-center $d-d$ CT transitions.

The work was partly supported by RFBR (grant 06-02-16788), Russian Agency for Science and Innovations (contract 02.740.11.0384), NWO, NanoNed and EC FP7 Fantomas (grant 214810).



Spectra of xx - and zz – components of the dielectric function ϵ for Pr_2CuO_4 (Fig. 1) and Bi_2CuO_4 (Fig. 2).

Shaded areas show the decomposition of the spectra into Lorentz oscillators. Numbers denote the positions of separate peaks in the spectra.

[Th-I-45]

High-resolution spectroscopy of rare-earth orthoborates: crystal-field and anisotropic f-d exchange interactions defects

M.N. Popova

Institute of Spectroscopy, RAS, 142190 Troitsk, Moscow region, Russia

This presentation is devoted to the rare-earth (RE) borates $RM_3(BO_3)_4$ with $M = Al, Fe,$ and Cr , that have non centrosymmetric trigonal structure of the natural mineral huntite. It gives a brief review of a spectroscopic research on a large group of magnetic iron and chromium borates and on $YAl_3(BO_3)_4:Yb$ (YAB:Yb) which is a promising nonlinear laser material. This work was carried out by my group in collaboration with the Kazan' State University. Most of the crystals have been grown in the L.V. Kirensky Institute of Physics (Krasnoyarsk) but YAB:Yb samples came also from several other institutions in Russia, France, Italy, and Spain where different growth methods were used.

Borates with magnetic M ions (like Fe and Cr) have interesting new properties and promising new application potential connected, in particular, with magnetoelectric interactions found in these materials. We have performed a systematic study of polarized RE spectra in the $RFe_3(BO_3)_4$ single crystals, with the aim (i) to find the energies, symmetries, and, finally, wave functions and magnetic g-factors of the CF levels and to obtain a set of the CF and exchange interaction parameters for the whole series of the RE iron borates; and (ii) to study different phase transitions and, possibly, magnetoelastic and magnetoelectric interactions. Main results of this study are reviewed. The most interesting spectral peculiarities are discussed. First results on the RE chromium orthoborates are also presented. A part of the results has been published in Refs. [1-4]

Recently, in the course of the spectroscopic study of $YbAl_3(BO_3)_4$ [5], we have observed multiple additional Yb^{3+} centers. To find their nature, we study high-resolution spectra of $RA_3(BO_3)_4:Yb$ ($R=Y, Tm, Yb$) single crystals grown in different laboratories using different fluxes. We conclude that these additional centers are the Yb^{3+} ions in regular positions but in their nearest surrounding having impurities that come from the flux. Recommendations concerning growth technology are given.

This work was supported by the Russian Foundation for Basic Research (Grant № 10-02-01071) and by the Russian Academy of Sciences under the Programs for Basic Research.

- [1] M. N. Popova, T. N. Stanislavchuk, B. Z. Malkin, and L. N. Bezmaternykh, Phys. Rev. Lett., **102**, 187403 (2009); Phys. Rev. B, **80**, 195101 (2009)
- [2] M. N. Popova. Journal of Rare Earths, **27**, 607 (2009).
- [3] E.P. Chukalina, M.N. Popova, L.N. Bezmaternykh, I.A. Gudim, Phys. Lett. A **374** (2010) 1790.
- [4] E.A. Popova, N.I. Leonyuk, M.N. Popova, E.P. Chukalina, K.N. Boldyrev, N. Tristan, R. Klingeler, and B.Buechner, Phys. Rev. B, **75**, 054446 (2007)
- [5] M.N. Popova, K.N. Boldyrev, P.O. Petit, B. Viana, and L.N. Bezmaternykh, J. Phys.: Condens. Matter **20**, 455210 (2008).

[We-I-15]

Radiative properties of the nanocrystals doped with lanthanide and transition ions

K.K. Pukhov, T.T. Basiev, Yu.V. Orlovskii

A.M. Prokhorov General Physics Institute RAS, Moscow, Russia

In recent years, great interest has been expressed by researchers in the optical properties exhibited by nanomaterials, including theoretical and experimental studies of the spontaneous lifetime of optical centers in nanosized samples. A change in the spontaneous lifetime of optical centers (OCs) in nanoobjects as compared to bulk materials is of considerable interest for both fundamental physics and practical applications in the field of laser materials and phosphors. It is known that the radiative lifetimes of RE and TM ions contained in nanocrystalline dielectric are different compared to their values in the bulk crystals of the same composition and structure [1-4]. Their lifetimes depend on the effective index of refraction of a nanocomposite (n_{eff}) consisting of nanoparticles, and the substance filling the space between them [1-2]. It is of great interest to derive a formula describing the spontaneous decay rate of an excitation in a nanosized object and reveal its differences from the corresponding expression for the bulk sample.

Here we present results of the theoretical study of the radiative characteristics for the small-radius OCs (RE and TM ions) in the subwavelength ellipsoidal nanocrystals embedded in a dielectric medium.

We found that two principal physical reasons provide a basis for a change of spontaneous emission lifetime of an optical center, which moves from bulk crystal to nanocrystal. First, it is a change in photon density of states; second, it is a change of the zero-point amplitude of the electromagnetic-field modes, which are responsible for spontaneous emission. On this basis, an analytical expression is obtained for the electric-dipole radiative-decay rate of an excited OC in an ellipsoidal dielectric nanoparticles (with sizes much less than the wavelength of light) embedded in a dielectric medium. The relation of the ratio A_{nano}/A_{bulk} with refractive indexes of the nanoparticles (n_{cr}) and the medium (n_{med}) and a volume fraction x of nanoparticles in the nanocomposite (filling-factor) is established. An important result is that the ratio A_{nano}/A_{bulk} can be estimated without recourse to a particular local-field model.

In particular, the spontaneous emission rate of a two-level atom in the spherical nanoparticle is given by simple expression [5-7]

$$A_{nano}^{spher} / A_{bulk} = \frac{n_{eff}}{n_{cr}} \left[\frac{3}{2 + \varepsilon - x(\varepsilon - 1)} \right]^2 \quad (1)$$

where $\varepsilon = \varepsilon_{cr} / \varepsilon_{med} = n_{cr}^2 / n_{med}^2$. In Eq. (1) n_{eff} is given by the well-known Maxwell Garnett mixing rule [8] for the average permittivity ε_{eff} :

$$\varepsilon_{eff} = n_{eff}^2 = \varepsilon_{med} \left[1 + \frac{3x\beta}{1 - x\beta} \right] \quad (2)$$

where $\beta = (\varepsilon - 1) / (\varepsilon + 2)$. As it follows from expressions (1)-(2) the radiative rates are decreasing (increasing) if $\varepsilon = \varepsilon_{cr} / \varepsilon_{med} > 1$ ($\varepsilon = \varepsilon_{cr} / \varepsilon_{med} < 1$).

In the limit $x \rightarrow 0$ (isolated nanospheres),

$$A_{nano}^{spher} / A_{bulk} = \frac{n_{med}}{n_{cr}} \left[\frac{3}{2 + \varepsilon} \right]^2. \quad (3)$$

The derived expression (3) is consistent with both the result obtained by Yablonovitch *et al.* [9] and result derived by Chew [10].

The radiative transitions in the multilevel OCs and the applicability of the Judd-Ofelt equation for nanoparticles doped by RE ions are discussed also.

The ratio of the absorption and emission cross-sections $\sigma_{nano}/\sigma_{bulk}$ for spherical nanoparticles in dielectric medium to that in bulk crystal $\sigma_{nano}/\sigma_{bulk}$ is derived as well. Here, the functional dependence of A_{nano}/A_{bulk} and $\sigma_{nano}/\sigma_{bulk}$ ratios are found to be different. Strong increase in the radiative decay time in a nanoparticle in comparison with the bulk crystal gives rise to only a slight decrease in the corresponding cross-section for absorption and emission.

The analysis of the theoretical expressions has demonstrated that the radiative characteristics of nanoparticles differ significantly from those of a bulk crystal. By varying the volume fraction x of nanoparticles in a suspension or an aerosol, the refractive index of the medium n_{med} surrounding the nanoparticles and their morphology it is possible to control the rates of spontaneous transitions and absorption and emission cross-sections of induced transitions. Thus, it is possible to increase $\sigma\tau$ product, an important laser parameter, several times and raise a population inversion in nanocomposite laser medium. By this method, one can control the laser properties of the nanocomposite materials and, thus, to design novel laser and luminescent media with improved characteristics. The results obtained can be used in developing the fluorescence kinetic method for controlling the shape of nanoparticles and the degree of their agglomeration during subsequent applications to the synthesis of optical laser ceramic materials, control of the luminescence lifetime of nanophosphors, and observation of nanoagglomerates in organic and biological structures.

Acknowledgements

Supported in part by CRDF grant RUP2-1517-MO-06 and RFBR grants (projects no. 08-02-01058-a, 09-03-12191-ofi-m)

References

- [1] R. S. Meltzer, S. P. Feofilov, B. Tissue, H. B. Yuan, Phys. Rev. B **60**, R14012 (1999).
- [2] R. S. Meltzer, W. M. Yen, Hairong Zheng, S. P. Feofilov, M. J. Dejneka, B. Tissue and H. B. Yuan, J. Lumin. **94-95**, 217 (2001).
- [3] R. I. Zakharchenya, A. A. Kaplyanskii, A. B. Kulinkin, R.S. Meltzer, S. P. Feofilov, Phys. Solid State **45**, 2209 (2003) [Fiz. Tverd. Tela **45**, 2104 (2003)].
- [4] S. P. Feofilov, A. A. Kaplyanskii, A. B. Kulinkin, R. I. Zakharchenya, J. Lumin. **129** (12), 1689-1691 (2009).
- [5] K. K. Pukhov, T. T. Basiev and Yu. V. Orlovskii, JETP Lett. **88**, 12 (2008) [Pis'ma v Zh. Eksp. Teor. Fiz. **88**, 14 (2008)].
- [6] T. T. Basiev, Yu. V. Orlovskii, and K. K. Pukhov, Nanotechnologies in Russia **3**, 551 (2008) [Rossiiskie nanotekhnologii, **3**, 66 (2008)].
- [7] K.K. Pukhov, Yu.V. Orlovskii, T.T. Basiev, Spontaneous and stimulated transitions in impurity dielectric nanoparticles, Chapter 16, pp. 317-339, in the book Recent Optical and Photonic Technologies, Edited by Ki Young Kim, 450 pages, Open access IN-TECH Publisher, ISBN 978-953-7619-71-8, Croatia (2010)
- [8] C. Bohren and D. Huffman, *Absorption and Scattering of Light by Small Particles* (Wiley, New York, 1998).
- [9] E. Yablonovitch, T. J. Gmitter, and R. Bhat, Phys. Rev. Lett. **61**, 2546 (1988).
- [10] H. Chew, Phys. Rev. A **38**, 3410 (1988).

[Th-O-50]

Influence of the additional excited states on energy transfer processes in lanthanide-containing compounds

L.N. Puntus¹, K.A. Lyssenko², I.S. Pekareva¹

¹Laboratory of Molecular Nanoelectronics, Institute of Radioengineering & Electronics, Russian Academy of Sciences, 11-7 Mokhovaya, 125009 Moscow, Russia

E-mail: ladapuntus@gmail.com

²X-ray Structural Center, A.N. Nesmeyanov Institute of Organoelement Compounds, Russian Academy of Sciences, 28 Vavilov St, 119991, Moscow, Russia

Developing of new luminescence materials with the predetermined properties is attractive purpose for the both modern science and industry. The luminescence of lanthanide ions is widely used in different functional materials owing to its narrow bands and high quantum yield as well as relatively long-lived excited states. Moreover the introduction of lanthanide ions or their complexes into self-assembling molecular architectures leads to the obtaining such advanced luminescent materials as room temperature liquid crystals, nanoparticles, OLEDs, etc. The participation of additional excited states produced by the peculiarities of supramolecular organization of the lanthanide complexes in the luminescence sensitization of the Ln^{III} ion has been recently demonstrated [1, 2]. Indeed the strong π -stacking interaction between ligands in lanthanide chlorides with 1,10-phenantroline (phen) and 2,2'-dipyridine (bpy) proven by X-ray data promotes to the formation additional excited charge transfer state (namely SICT – stacking induced CT state).

In the frame of the research presented the energy transfer processes have been analyzed in following lanthanide systems (Ln= Nd, Eu, Tb, Er, Yb, Gd) with heterocyclic diimines: nitrates, β -diketonates containing the 2,2-paracyclophane derivatives, and 2-benzoylpyridinetes. For the analysis of these processes the absorption, luminescence, phosphorescence and vibrational spectra have been studied, as well as lifetimes of excited states of the Ln^{III} ions. Moreover for some complexes the intrinsic and overall quantum yields have been measured. Since in most cases the lanthanide systems have been characterized by X-ray technique the structural features of inner- and outer-sphere bonding pattern of the Ln^{III} ion could be analyzed in detail. For the description of the atom charges and the strength of interatomic interactions in the crystals investigated the high resolution X-ray diffraction (XRD) experiments have been performed as well. The capabilities of modern XRD technique for analysis of nature of lanthanide-ligand bonds as well as of energy estimation in different systems have been illustrated in Ln chlorides and nitrates with phen and bpy, as well as in Ln(H₂O)₉(SO₃CF₃)₃. The special attention was paid to the investigation of supramolecular organization effects on the charge distribution and their influence on the luminescent properties of lanthanide-containing complexes.

This work is supported by the Russian Foundation for Basic Research (grants N 09-03-12065, 10-03-00898, 09-03-00603)

[1] L.N. Puntus, K.A. Lyssenko, I.S. Pekareva, J.-C.G. Bunzli, *J. Phys. Chem. B.* **2009**, *113*, 9265.

[2] L. Puntus, *Helvetica Chimica Acta*, **2009**, *92*, 2552.

[3] L.N. Puntus, K.A. Lyssenko, M.Yu. Antipin, J.-C.G. Bunzli, *Inorg. Chem.* **2008**, *47*, 11095.

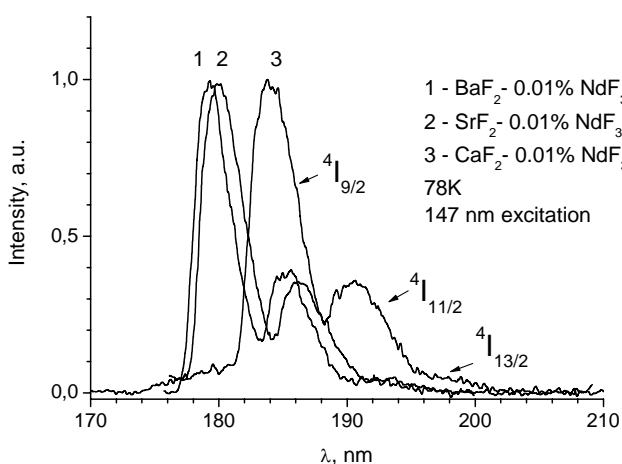
[Th-O-36]

5d-4f emission of Nd³⁺, Er³⁺, Tm³⁺, Gd³⁺ ions in alkaline earth fluorides

E.A. Radzhabov, E.A. Prosekina

Vinogradov Institute of Geochemistry, Russian Academy of Sciences, Favorskii street 1a, P.O.Box 4019, 664033 Irkutsk, Russia

Emission from the 5d to 4f shell of rare earth ions doped into ionic crystals was thoroughly studied in the last decade [1-3]. The emission was observed in vacuum ultraviolet region and has potentiality to using in lasers, scintillators or quantum cutting systems. However all measurements were done in crystals with relatively high impurity concentration [1,2]. Therefore some effects related to the emission of rare-ions aggregates could be overlooked [3].



The aim of this paper is to study the d-f emission in a wide range of rare-earth ion concentrations in alkaline-earth fluoride crystals CaF₂, SrF₂, BaF₂. Crystals were doped by MeF₃ in concentration ranging from 0.01 to 10 mol.%. Samples were excited by Xe (147 nm line) or Kr (124 nm line) resonance lamps or by an x-ray tube (Pd anode, 35 kV, 10 mA). Emission was measured by a FEU39A (160-500 nm) or solar blind FEU142 (115-350 nm) photomultipliers mounted on a VM4 grating vacuum monochromator. Resolution was near 0.2 nm.

The wavelength interval between the emission bands in CaF₂ and SrF₂ is more than thrice as large as those in SrF₂ and BaF₂ (Figure). Positions of the most intensive emission bands at 78 K are presented in Table. With increasing impurity concentration new longer wavelength bands are observed in Tm doped crystals. No Gd³⁺ 129 nm 5d-4f band were observed in SrF₂ or BaF₂ crystals.

Crystal	Tm (5d→ ³ H ₆), nm	Er (5d→ ⁴ I _{15/2}), nm	Nd (5d→ ⁴ I _{9/2}), nm
CaF ₂	168,4	166,0	183,9
SrF ₂	165,4	164,2	180,0
BaF ₂	164,6	163,7	179,2

The intensity of x-ray excited 5d-4f bands grows near 10 times with increasing impurity concentration from 0.01 up to 0.3-1 molar % and decreases above 1 molar %.

However the intensity of CaF₂-Nd 183.9 nm band remains generally the same. The highest total intensity of the 5d-4f bands still remains essentially lower than that of exciton emission in undoped crystals. The mechanisms of energy transfer will be discussed also.

References

- [1] V.N. Makhov, N.M. Khaidukov, N.Yu. Kirikova, et.al. Nucl. Instrum. Meth. A 470 (2001) 290-294
- [2] R. T. Wegh, A. Meijerink. Phys. Rev. B 60 (1999,) 10820-10830
- [3] G. Stryganyuk, G. Zimmerer, Fizika Tverdogo Tela. 50 (2008) 1570-1577

Structure and dynamics of high-energy states in lanthanide materials

M.F. Reid*

Department of Physics and Astronomy and MacDiarmid Institute for Advanced Materials and Nanotechnology University of Canterbury, Christchurch, New Zealand
*E-mail: Mike.Reid@canterbury.ac.nz

A good understanding of energy levels, transition intensities, and dynamical processes within the $4f^N$ and $5f^N$ configurations of lanthanide and actinide compounds was achieved in the 1960s, and developed further in subsequent decades. The higher-energy $4f^{N-1}5d$, charge-transfer, conduction-band, and exciton states have also been studied for decades, but interest in high-energy states became more intense over the last decade or so. This is, in part, due to the increased availability of high-resolution VUV spectra from synchrotron measurements, which has made it possible to perform analyses across the lanthanide series in a number of compounds.

The data from these experiments has been analysed in a variety of ways. We have used phenomenological models that extend the well-established approach for the $4f^N$ and $5f^N$ configuration to the $4f^{N-1}5d$ configuration [1-2]. Simple (but highly effective) models for relating the energy levels of different ions in different hosts have also been developed [3]. In addition, a variety of ab-initio calculations have appeared [4-6].

Detailed comparisons between theory and experiment are still difficult because the available experimental data mainly consist of broad bands. Designing experiments to test the predictions of ab-initio calculations of excited-state bond lengths and potential-energy surfaces provides interesting challenges.

This presentation will discuss our recent and planned experiments to probe excited-state structure and dynamics using two-colour excitation. By probing transitions between excited states with the same geometry it is possible to observe sharp-line spectra that reveal more information than the broad bands observed in one-colour spectroscopy. These techniques may be applied to a variety of excited states, including self-trapped excitons in Yb^{2+} materials [7] and $4f^{12}5d$ configurations of Tm^{2+} materials [8,9].

- [1] M. F. Reid, L. van Pieterse, R. T. Wegh, and A. Meijerink, Phys. Rev. B 62 (2000) 14744.
- [2] G. W. Burdick and M. F. Reid, In K.A. Gschneidner Jr., J.C. Bunzli, V.K. Perchinsky. Handbook on the Physics and Chemistry of the Rare Earths, Volume 37, Chapter 232 (2007) 61.
- [3] P. Dorenbos, J. Luminescence 128 (2008) 578.
- [4] G. Brik and K. Ogasawara, Spectroscopy Letters 40 (2007) 221.
- [5] J. Andriessen, E van der Kolk, and P. Dorenbos, Phys. Rev. B 76 (2007) 075124.
- [6] J. Gracia, L. Seijo, Z. Barandiaran Z, et al. , J. Luminescence 128 (2008) 1248.
- [7] C. Pedrini, M. F. Joubert, and D. S. McClure, J. Luminescence 125 (2007) 230.
- [8] E. Beurer, J. Grimm, P. Gerner, and H.U. Güdel, Inorg. Chem. 45 (2006) 9901.
- [9] J. Grimm, O.S. Wenger, K. W. Krämer and H.U. Güdel, J. Luminescence 126 (2007) 590.

[Tu-P-12]

Spectral and decay time properties of Pr, Tb, Eu doped Gd₂O₂S ceramics

P.A. Rodnyi¹, E.I. Gorokhova², S.B. Eron'ko², V.A. Demidenko², S.B. Mikhrin¹, S.D. Gain¹

¹*St.Petersburg State Technical University, Polytekhnicheskaya 29, 195251 St.Petersburg, Russian Federation*

²*Scientific Research and Technological Institute of Optical Material Science, S. I. Vavilov State Optical Institute All-Russia Science Center, Babushkina 36/1, 192171 St. Petersburg*

Gadolinium oxysulfide is particularly handy matrix for introduction of rare earth (RE) ions as activators. RE³⁺ ion, which replaces Gd³⁺ in Gd₂O₂S, is surrounded by four oxygen and three sulfur ions, it has C_{3v} point group symmetry. The excitation spectrum of Gd₂O₂S shows a peak into ⁸S_{7/2}-⁶P_j transitions of Gd³⁺ ions that are known to transfer their energy to some RE³⁺ [1]. Gd₂O₂S based materials are available mainly in powder or ceramic forms. The powder phosphors are used in medical radiographic screen systems and ceramic scintillators are profitably employed in X-ray tomography. For scintillators it is important that Gd₂O₂S has a high density, 7.34 g/cm³, and a small forbidden gap, 4.6 eV.

The present study investigates the effect of adding various RE and other elements to Gd₂O₂S ceramics on their spectral and decay time properties. Optical quality RE-doped Gd₂O₂S ceramics were sintered from powder with grain size in the range from 3 to 10 μm by the uniaxial hot pressing method. LiF powder was added before pressing to get crystal-clear and compaction of the samples. The samples were heat treated to improve their emission properties

The main characteristics of the Gd₂O₂S:RE (RE = Pr, Tb, Eu) ceramics: optical transparency, emission and excitation spectra, decay time constants, and level of afterglow have been measured under UV and/or X-ray excitations. The peculiarities of the ceramic emission spectra have been studied, in particular spectral composition depends on the heat-treating atmosphere and the activator concentration; the latter fact is due to the cross-relaxation interaction between RE ions. The main decay constants of Gd₂O₂S:Pr, Gd₂O₂S:Tb, and Gd₂O₂S:Eu ceramics have been evaluated: 3.2, 600÷700, and 450 μs, respectively.

The energies of the ground 4fⁿ levels of tri- and divalent RE ions with respect to the conduction and valence bands of Gd₂O₂S crystal have been determined. The activators exhibiting the most promise for efficient emission are Pr³⁺, Tb³⁺, and Eu³⁺. The energies of 4f-5d transitions of Pr³⁺ and Tb³⁺ ions and c charge-transfer states of Eu³⁺ ions have been determined.

The ground 4f level of the Ce³⁺ ion is near the midgap, due to which Ce³⁺ effectively captures holes from the valence band and electrons from the conduction band and significantly decreases the afterglow level of the Gd₂O₂S:RE phosphors; the last statement has been verified experimentally. The process of energy transfer from the lattice to Gd³⁺ ions and from Gd³⁺ to the Pr³⁺, Tb³⁺, and Eu³⁺ ions has been studied. The obtained results show that in dependence of pressing conditions and the thermal treatment, we can get ceramics with properties as initial powders, and with new features.

[1]. M. Raukas, K.C. Mishra, C.Peters at al., J. of Lumin., 87-89 (2000) 980-982.

[Tu-I-1]

Color centers in fluorite crystals: the history and present state

A.I. Ryskin, A.S. Shcheulin, A.E. Angervax

The lecture deals with color centers in calcium fluoride (fluorite) crystals. In late forties – early fifties of the last century their formation in the process of crystal growth hampered production of high quality fluorite crystals for optical industry. Pioneering works by Professor Feofilov result in clarification the nature and structure of these centers and in proposal the way of their elimination. Now, fluorite crystals with color centers are using as holographic material. Technique of introduction of color centers into the fluorite crystal (an “additive coloration” of the crystal) is described. There exist several types of color centers. Their transformations under optical radiation and temperature underline photochromy of additively colored fluorite crystals. The mechanism of hologram record in these crystals and their characteristics are discussed. The most important feature of holograms is their excluding high stability. This allows using these holograms for metrological purposes. In particular, holographic element based on fluorite crystal was used as a plane angle measure (the “holographic prism”). This prism may serve as a clue element of mobile and high-precision angle-measuring and angle-assignment devices. Properly recorded hologram presents one-dimensional photonic crystal. Features of luminescence of fluorite based photonic crystal are discussed.

[Th-O-53]

Anomalous line shape of EPR spectra of impurity Ho^{3+} ion in synthetic forsterite

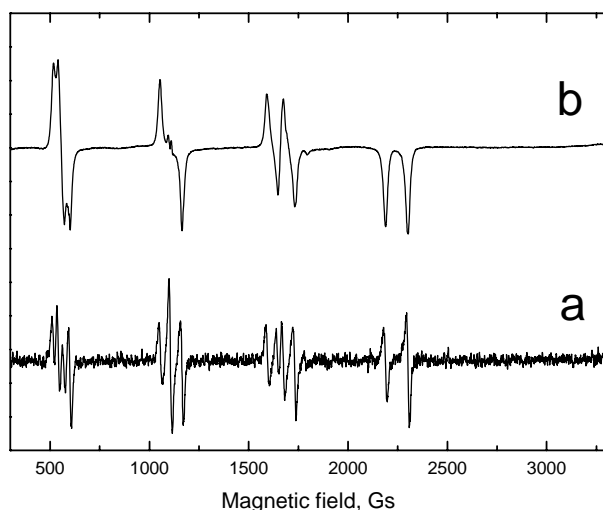
K.M. Salikhov¹, A.A. Sukhanov¹, V.F. Tarasov¹, R.B. Zaripov¹, E.V. Zharikov^{2,3}

¹Zavoisky Physical-Technical Institute of the Kazan Scientific Center of the Russian Academy of Sciences, Sibirskii trakt 10/7, Kazan, 420029 Russia

²Mendeleev University of Chemical Technology of Russia, Miusskaya pl. 9, Moscow, 125047 Russia

³Prokhorov General Physics Institute of the Russian Academy of Sciences, Vavilova ul. 38, Moscow, 119991, Russia

Impurity holmium ions in synthetic forsterite form several paramagnetic centers [1]. The zero-field splitting between two lowest electron singlet levels of a single Ho^{3+} ion is 7 GHz. These levels have a well-resolved hyperfine structure consisting of eight nuclear sublevels corresponding to the nuclear spin of the ^{165}Ho isotope $I = 7/2$. EPR spectra of the Ho^{3+} ion were recorded on X-band Bruker ELEXSYS E 580 and EMX spectrometers using the continuous-wave mode. Figure shows experimental spectra of the Ho^{3+} ion in synthetic forsterite recorded on a ELEXSYS E 580



spectrometer at different values of the microwave power; *a*, attenuation of – 60 dB; *b*, attenuation of – 10 dB. It is seen that only spectrum *a* has the line shape typical for an EPR derivative. EPR spectra recorded on an EMX spectrometer showed the conventional line shape for all values of the microwave power.

The origin of the anomalous line shape of spectrum *b* could be the difference between the resonator types used in ELEXSYS E580 and EMX spectrometers. In the former, a dielectric FlexLine resonator is used in which microwave magnetic and electric fields are not separated spatially in contrast to the conventional EPR resonator used in the EMX spectrometer. Therefore electric dipole or electric quadrupole transitions between electron-nuclear levels of the Ho^{3+} ion could be induced. The line shape dependence on temperature, orientation and position of the sample in the resonator of spectrum *b* was studied. Its anomalous line shape might result from the electric quadrupole transitions induced by the gradient of the microwave electric field.

The work is partially supported by the RFBR grant 09-07-97006 and the grant of the President of the Russian Federation NSh -6267.2010.2

[1]. A.A. Konovalov, D.A.Lis, B.Z. Malkin at al. Appl. Magn. Reson. **28**, 267-280 (2005).

[We-P-37]
Multifrequency EPR study of Dy³⁺ ions in RbPb₂Cl₅

G.S. Shakurov¹, I.I. Fazlizhanov¹, V.A. Shustov¹, A.G. Okhchimchuk², N.V. Lichkova³,
V.N. Zagorodnev³

¹*Kazan Physical-Technical Institute of RAS, 10/7 Sibirsky trakt, Kazan 420029, Russia*

²*Fiber Optics Research Center of RAS, 38 Vavilov Street, Moscow 119333, Russia.*

³*Institute of Microelectronics Technology of RAS, Chernogolovka, Moscow region, Russia*

The RbPb₂Cl₅ crystal is the structure analogue of ternary alkali lead chlorides crystals KPb₂Cl₅ that were investigated early. These materials activated by RE³⁺ ions are being intensively studied as promising mid infrared laser radiation. A monoclinic crystal lattice (Space group P2₁/c) has two different local position of Pb²⁺ that may be substitute by RE³⁺ ions. One polyhedron is tri-cap prism where Pb²⁺ ion is surrounded by nine Cl⁻. The second Pb²⁺ coordination is a distorted octahedron with one apex doubled [1]. Because of nonisomorphically substitution Pb²⁺ by Dy³⁺ charge compensation is necessary. Multifrequency EPR investigations is undertaken to clarify the position of RE ions and mechanism of charge compensation.

The measurement was performed on a Varian E-12 and wide band EPR spectrometer using backward-wave oscillators as the generators in the frequency range 37-850 GHz and usual electromagnet with magnetic field up to 1 T. All measurements were carried out at the temperature 4.2 K. We had two samples. The first crystal containing 1 at. % Dy was grown by the Bridgeman method. Also EPR signal of Dy ion was discovered in the RbPb₂Cl₅:Bi crystal. The EPR spectra were observed in the frequency region 9.5 GHz and 37-180 GHz. We identified three different signals. The first spectrum besides line from even isotopes has well resolved hyperfine structure (HFS) of ¹⁶¹Dy and ¹⁶³Dy (nuclear spin I=5/2). Magnetically non-equivalent spectra were not registered when rotation diagrams in *ab* and *ac* planes were measured. In *bc* plane EPR signals were not found. The *z*-axis of center coincides with *a*-axis of crystal and *g_z* = 15.7. The EPR spectra of this type were obtained as in X-band as on wide band spectrometer. The width of EPR lines in the RbPb₂Cl₅:Bi were less than in RbPb₂Cl₅:Dy. Second signal is a broad line with *g* ~ 4. Two magnetically non-equivalent spectra were discovered when the rotation in *bc* plane was undertaken. In *ab* plane EPR line is registered only near B || *b* direction. Third signal is narrow line with unresolved hyperfine structure. Its maximum *g*-factor is about 11. This spectrum and second one have the similar orientation dependences in *bc* plane. However second and third spectra overlap and angular dependence of third center in *bc* plane is incomplete.

Only two magnetic non-equivalent spectra are possible for both Pb²⁺ position. So second and third spectra origin from lead replaced ions. The angular diagrams for third spectrum are similar to case of Tb³⁺ in octahedral environment for KPb₂Cl₅ [2]. The broad line with same angular dependence also was discovered early but does not identified. Its origin and the nature of the first spectrum are discussed.

The work is partially supported by the RFBR grant 09-02-97008 and the grant of the President of the Russian Federation NSh – 6267.2010.2.

[1]. K. Nitsch et al. Prog.Crystal Growth and Charact. **30**, 1-22 (1995)

[2]. G.S.Shakurov et al. Appl.Magn.Reson. **26**, 579-586 (2004)

[We-O-33]

Terahertz EPR-spectroscopy of Fe²⁺ ions in the natural and synthetic forsterite

G.S. Shakurov, T.A. Shcherbakova, V.A. Shustov

Kazan Physical-Technical Institute RAS, 10/7 Sibirsky trakt, 420029 Kazan, Russia

Forsterite (Mg₂SiO₄) is the ending member of the olivine (Mg_xFe_{1-x}SiO₄) family. Early this crystal was widely investigated because of its great meaning for the terrestrial and planetary science. After discovery of the laser action on the Cr⁴⁺ spectroscopic properties of forsterite were studied in detail. Although there is a lot of EPR study of transition ions in Mg₂SiO₄, Fe²⁺ ion is not among them. Forsterite has orthorhombic symmetry (space group P_{bnn}). The Fe²⁺ ions occupy two octahedral positions with symmetry C_i (M1) and C_s (M2) and in the absence of a magnetic field the energy levels of Fe²⁺ are singlets. The splittings between singlets exceed the quanta of conventional X- and Q-band EPR spectrometers. So to study Mg₂SiO₄:Fe²⁺ high frequency EPR spectrometer is required. The preliminary study EPR of Fe²⁺ in the forsterite was done previously [1, 2].

The measurement were performed on a home-made EPR spectrometer using a set of backward-wave oscillators as the generators in the frequency range 65-1300 GHz and usual electromagnet with magnetic field up to 1 T. We studied the natural (Tajikistan) and synthetic crystals. The natural crystals were colorless and had grows faces. The synthetic Mg₂SiO₄:Cr crystal was grown in the Kuban State University (Krasnodar) and contained Fe²⁺ as the trace element. Since the cell dimension increase from forsterite (Mg₂SiO₄) to fayalite (Fe₂SiO₄), the X-ray measurements were used to determine the unite cells of the crystals. The resonance transitions for two Fe²⁺ positions were discovered. In the studied range both synthetic and in natural samples had three energy levels. Zero-Field-Splittings (ZFS) were 96.5, 580, 676.5 GHz and 112, 721, 833 GHz for M1 and M2 sites respectively. For M1 position four magnetically non-equivalent spectra were registered when rotation diagrams in *ab* and *ac* planes were measured. Angles between *a*-axis of crystal and *z*-axis projection were 12.5° and 3.5° in the *ac* and *ab* planes respectively. For M2 site single EPR line was discovered with *z*-axis coincides with the *c*-axis of the crystal. The main difference between EPR spectra in natural and synthetic crystals was lines width. Synthetic sample had more narrow EPR lines. Because the distribution Fe²⁺ ions between M1 and M2 positions intensively studied, we measured this ratio. It was found that for both synthetic and natural crystals the ratio of integrated intensity EPR lines is M1/M2 = 1/3. To determine the spectral parameters we used Spin-Hamiltonian with effective spin S=1: $H = g\beta\mathbf{B}\mathbf{S} + D(S_z^2 - S(S+1)/3) + E(S_x^2 - S_y^2)$. The calculation was performed using angular and field-frequency dependencies of EPR lines. The agreement between experiment and theory is satisfactory.

The work is partially supported by the grant of the President of the Russian Federation NSh – 6267.2010.2

[1]. V.F.Tarasov, G.S.Shakurov Optics and Spectroscopy **81**, 880 (1996)

[2]. G.S.Shakurov, T.A.Shcherbakova, V.A.Shustov, E.P.Zheglov Proceedings (abstract) 2nd Asia- Pacific EPR/ESR Symposium. Hangzhou. Chine. October 31-November 4. 1999.

[Th-P-56]
Additive coloration of CaF₂:Sm crystals

A.S Shcheulin, T.S. Semenova, M.A. Petrova, L.F. Koryakina, A.E. Angervax, A.I. Ryskin

Rare-earth ions doping calcium fluoride crystals are known to enter the lattice in the trivalent state, their excess positive charge being compensated by interstitial F⁻ ions. A conventional way to convert these ions into divalent state is the technique of additive coloration implemented by heating the doped crystals in the reduction atmosphere of metal (Ca) vapors. During this procedure chemical reactions occur on the crystal surface. As a result two fluxes (of anion vacancies and electrons) diffuse into the crystal volume. In “pure” (undoped) crystal these components recombine forming color centers. In crystals doped with rare-earths, anion vacancies recombine with interstitial F⁻ ions, while electrons are captured by inner shells of rare-earth ions thus converting them from the trivalent to divalent state. The most effective setup for performance of this procedure is so called “heat tube” that allows almost independent monitoring of two important parameters of the process, i.e. the pressure of the metal vapor and the temperature of the crystal. It was found that at the coloring temperature there occurs not only capture of electrons by Sm³⁺ ions with their conversion into divalent state but also the reverse process of thermo-ionization of Sm²⁺ ions with free electron conversion. Frenkel defects are simultaneously formed that are made up of anion vacancy and interstitial F⁻ ion. In the colored region of the crystal a certain concentration of anion vacancies and electrons is maintained, thus reducing the gradient of concentration of these components and hindering their diffusion from the surface of the sample. As a result the coloration process is slowing down significantly. Another feature of coloration of crystals doped with rare-earth ions is a sharp interface between colored and non-colored regions of the crystal compared with a fuzzy border in the pure crystal. The sharp interface indicates the threshold character of the dependence of free path length of vacancies on the degree of the rare-earth ion reduction. This threshold likely to be achieved when the concentration of compensating fluorine ions becomes comparable with that of ions formed under thermal excitation of Frenkel’s pairs. The threshold limits the advance of anion vacancies into the non-colored region of the crystal. So, the study of additive coloration of pure and Sm-doped CaF₂ crystals demonstrates the competition between the processes of formation of color centers and reduction of rare-earth ions. Experiments show the dynamic character of the latter process, which reveals itself in its reversibility. The reverse process (with respect to the reduction) of increasing the valence state of the ion, along with the formation of Frenkel defects creates a certain concentration of anion vacancies and electrons in the region of crystal colored to that moment and lowers diffusion flows from the surface into the volume. For this reason samarium substantially slows down the coloration process. This effect is accompanied by the significant narrowing of the interface between colored and non-colored regions of the crystal.

[We-O-23]

5d-4f emission and scintillation properties of SrF₂-Pr³⁺ and SrF₂-Ce³⁺ crystals

R. Shendrik*, E. Radzhabov

Vinogradov Institute of Geochemistry, Russia, Irkutsk, Favorskogo 1a, 664033,

**E-mail: shendrik@ieee.org*

At that time, scintillators are widely used in medicine, physics, and homeland security. Today, the crystals of NaJ(Tl), CsJ(Tl), CsJ(Tl), BGO, LaBr₃:Ce are the most widely used scintillation materials [1, 2].

One of the perspective scintillation materials are crystals doped with rare earth impurities. In the series of rare earths cerium (Ce) and praseodymium (Pr) have a particular place. The luminescence of Ce and Pr is fast, efficient and comparatively free of self-absorption. The primary mechanism by which the energy of e-h pair is transferred to the activator ion in the wide bandgap material is not yet clear in each of the cases studied.

In this work we study crystals of strontium fluoride doped with Ce³⁺ and Pr³⁺ by the gamma and time-resolved spectroscopy methods. We measured time-resolved spectra and decay times under X-ray pulse excitation at room and 80 K temperatures. In 5d-4f Ce³⁺ emission we found two components – fast (about 30 ns at room temperature) and slow component (about 200 ns). In contrast to Ce-doped SrF₂ in the crystals doped with Pr³⁺ the slow component in the Pr³⁺ emission was absent and we observed only two fast components (about 8 and 24 ns) at 80 K and one fast component about 32 ns at room temperature.

We measured the temperature dependence of light yield in SrF₂-Pr³⁺ in the range from room to 200 °C temperatures. Light yield of 5d-4f emission weakly depends on temperature. In Ce³⁺-doped crystals light yield is decreased with heating [3]. The presented results suggest that mechanism of transfer excitation to activator ion differs in Pr³⁺ and Ce³⁺ doped crystals. It will be discussed in our report.

References:

- [1] P. A. Rodnyi. Physical processes in inorganic scintillators. CRC Press, 1997.
- [2] Lecoq, P., Annenkov, A., Gektin, A., Korzhik, M., Pedrini, C. Inorganic Scintillators for Detector Systems. Springer, 2006.
- [3] R. Shendrik, E. Radzhabov, IEEE Trans. Nucl. Sci, vol. 57, June, 2010.

[We-P-40]

Monte-Carlo simulation of energy transfer processes for inhomogeneous activator distribution

V.M. Sitdikov, N.V. Nikonorov, A.K. Przhevuskii

St. Petersburg State University of Information Technologies, Mechanics and Optics, Russia

Monte-Carlo simulation of inhomogeneous activator ion distribution and nonradiative energy transfer process over the ensemble of optical centers have been performed. An explanation of nonmonotonic dependence of upconversion coefficient on metastable level population has been given.

Nonradiative energy transfer processes should be taken into account for development of highly-doped laser materials for mini- and micro-chip lasers and amplifiers. Such processes as up-conversion and migration of excitation lead to a reduction of the gain and quantum yield. Much attention is paid to erbium amplifiers widely applied in optical communications, because they operate near 1.5 μm which is the wavelength region of minimum fiber loss.

Statistic simulation is a convenient tool to study the up-conversion and migration of excitation. It allows both to avoid the mathematical problems arising in the theoretical analysis, and is suitable for environments with any distribution of the activator ions. This is important because the rare earth (RE) ions do not only gather in pairs but also form larger clusters including many more ions in the host glass. Since the purpose of our research was to investigate the processes of excitation transfer in laser materials with inhomogeneous activator distribution.

To study the processes of up-conversion and migration in the case of an inhomogeneous distribution of RE ions (clusters) it is proposed and implemented a simple method of clusters formation by a relaxation of the initial random ion distribution using Metropolis algorithm. It was assumed that the particles interact with repulsive forces only. The particles divided into two classes, differing only by the value of repulsion. For the particles having weak repulsive forces the decrease of relaxation temperature results in a segregation of the clusters with the shape close to spherical. The rest of particles with high repulsive forces are located into the remaining volume and do not segregate any clusters.

The processes of up-conversion, migration and radiation over the ensemble of optical centers have been performed with using of Monte-Carlo simulation technique [1]. Obtained data allowed us to interpret the nonmonotonic variation of the dependence of upconversion coefficient on metastable level population as a result of differences in the percentage of population of the metastable level inside the cluster and its environment.

The simulated data are qualitatively agree with the experimental data and can be used in the development of highly concentrated laser materials.

[1] Nikonorov N.V., Przhevuskii A.K., Chukharev A.V. Characterization of nonlinear upconversion quenching in Er-doped glasses: modeling and experiment // J. Non-Cryst. Solids. 2003. V. 324. P. 92-108.

[We-P-52]
The investigation of photochromism in CaF₂, SrF₂, BaF₂.

T.Y. Sizova, E.A. Radzhabov

*The Vinogradov Institute of Geochemistry, Siberian Branch of Russian Academy of Sciences, Favorsky Street 1A,
664033 Irkutsk, Russia*

Both irradiation and additive coloration of alkaline-earth fluorides are result in the formation of photochromic (PC) centres. Crystals in which they are present become coloured on exposure to light; the process may be reversed by heating. Optical dichroism studies have identified the centre as a complex of a dopant ion with an anion vacancy, containing two trapped electrons [1].

Absorption spectra of photochromic centers, the thermal destruction in crystals of CaF₂, SrF₂, BaF₂ doped with LaF₃, YF₃, LuF₃ have been studied at temperatures 80-600 K. The crystals were grown using Stockbarger method. The concentration of the impurity ions was 0.1-1.0 mol %.

X-ray irradiation at 80 K cause to the formation of PC⁺ centers in La, Lu and Y doped CaF₂ crystals and in a La-doped SrF₂ crystal. At temperatures in the ranges 350–450 K (in CaF₂–LaF₃) and 250–350 K (in CaF₂–YF₃), PC⁺ centers are transformed into PC centers. Photochromic color centers are also generated in the SrF₂–YF₃ crystal irradiated at room temperature, whereas the crystal irradiated at 80 K does not colored. All color centers destruct by heating of the crystals to ~600 K. In the BaF₂–YF₃ and SrF₂–LuF₃ crystals absorption bands, that are assigned to neither PC centers nor PC⁺ centers, are observed. The formation of photochromic centers are given in Table 1.

Table1.

Impurity	Irradiation coloration of CaF ₂ , SrF ₂ , BaF ₂ [2]	Additive coloration of CaF ₂ [3]	Irradiation coloration (experimental results)		
			CaF ₂	SrF ₂	BaF ₂
Y	PC	PC 80K,300K	PC ⁺ 80K PC 300K	PC 300K	not observed
La	-	PC 80K,300K	PC ⁺ 80K PC 300K	PC ⁺ 80K	not observed
Ce	-	PC 80K,300K			
Gd	-	PC 80K,300K			
Tb	-	PC 80K,300K			
Lu	-	PC 80K,300K	PC ⁺ 80K PC 300K	not observ	not observed

References

- [1] Crystals with fluorite structure ed.by Hayes, Clarendon Press, Oxford (1974)
 [2] J. R. O, Connor, J. H. Chen. Physical Review B.,**130**,1790 (1963)
 [3] D. L. Staebler, S. E. Schnatterly. Physical Review B.,**3**,516 (1971)

[Tu-P-20]

Er centers in KTaO_3 : optical and EPR spectroscopy study

A.P. Skvortsov¹, V.A. Trepakov^{1,2}, N.K. Poletaev¹, Z Potucek², V.V. Laguta², L. Jastrabik²

¹ *Ioffe Physico-Technical Institute RAS, 194 021, St-Petersburg, Russia*

² *Institute of Physics AS CR, Na Slovance 2, 182 21 Praha 8, Czech Republic*

Potassium tantalate KTaO_3 is a well known prominent representative of perovskite-type oxides, whose attractive properties can be tailored by the respective impurities and defects. Thereupon, knowledge about the structure and microscopic properties of the active impurity centers in KTaO_3 are of considerable importance.

We report on f-f optical absorption and luminescence spectra as well as EPR investigations of Er^{3+} impurity in $\text{KTaO}_3:\text{Er}$ single crystals (0.05% wt. in the charge).

The absorption spectra were recorded at 293, 77 and 2 K within the 350 – 650 nm spectral range. The structured spectra of f-f optical transitions from the $^4\text{I}_{15/2}$ ground state to excited levels of Er^{3+} ions were observed. At $T = 2$ K, the detailed studies of the optical transitions to the $^4\text{F}_{9/2}$, $^4\text{S}_{3/2}$, $^2\text{H}_{11/2}$, $^4\text{F}_{7/2}$, $^4\text{F}_{5/2}$, $^2\text{H}_{9/2}$, $^4\text{G}_{11/2}$ excited levels allowed us to determine the quantity of components for the individual transitions. Absorption spectra reveals both intense and weak absorption lines, proving the existence of at least two so called “major” and “minor” types of Er^{3+} impurity centers. The emission spectra of the $^4\text{S}_{3/2}$, $^4\text{F}_{9/2} \rightarrow ^4\text{I}_{15/2}$ transition were excited by a He-Cd laser beam (442 nm) and studied in the 12-70 K temperature range. At $T = 12$ K the emission spectra reveals more spectral lines than this is allowed theoretically for optical transitions in one type of Er centers. This indicates the presence of not less than two types of erbium centers.

In the KTaO_3 crystals of O_h^1 cubic symmetry Er^{3+} ions can occupy dodecahedral K^+ and/or Ta^{5+} octahedral lattice sites with the crystal field of cubic symmetry. Charge compensation can be satisfied by local compensation (e.g., by the formation of the adjacent oxygen vacancies with related possibly dipole complex) or non-locally. In the first case the point symmetry of Er^{3+} center decreases, in the latter – remains unchanged. The number of absorption lines observed at $T = 2$ K for the major centers exactly correspond to that theoretically possible for f-f electron transitions in Er^{3+} ions occurring the non-cubic crystal field sites. Together with the n-type conductivity, that was found in our thermo-EMF measurements, optical data leads us to suggestion that the major type of centers are Er^{3+} ions replacing K^+ . This is consistent with the ionic radii: 1.32 Å and 1.78 Å for Er^{3+} and K^+ respectively for 12 fold dodecahedral coordination position.

EPR measurements were performed at 9.2 - 9.4 GHz in the standard 3 cm wavelength range at temperatures 4.2-100 K. Below 10 K the pronounced EPR spectrum with the large linewidth (~5-6 mT) and essentially asymmetric line-shape was observed in the region of 50-140 mT. When the magnetic field is parallel to the $\langle 100 \rangle$ axes four resonance lines are revealed. With the exception of the highest-field line with $g=5.79$, which is completely isotropic, other three lines split when the magnetic field is tilted from $\langle 100 \rangle$ crystal axis suggesting orthorhombic symmetry of the corresponding center. Thus, as well as optical measurements, EPR study evidences for the presence of cubic and non-cubic Er^{3+} ($4f^{11}$) centers in KTO crystals residing in two lattice positions.

[Tu-P-4]
Excitons in the thin films of $Zn_{1-x}Mn_xO$ ($x=0-0.06$)

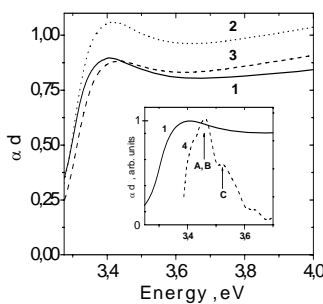
V. I. Sokolov¹, A. V. Druzhinin¹, N. B. Gruzdev¹,
A. Dejneka², O. Churpita², Z. Hubicka², L. Jastrabik², V. Trepakov^{2,3}

¹ *Institute of Metal Physics UD RAS, S. Kovalevskaya Str. 18, 620990, Yekaterinburg, Russia*

² *Institute of Physics, AS CR, v. v. i., Na Slovance 2, 18221 Praha 8, Czech Republic*

³ *Ioffe Institute RAS, 199021 St-Petersburg, Russia*

We report on optical absorption study of $Zn_{1-x}Mn_xO$ ($x=0-0.06$) films on silica substrates. This material is one of the most promising materials for optical and spin electronic devices development. Using such films we succeed to detect the absorption spectra of excitons and to determine reliably the width of the optical gap E_g . This figure presents optical absorption spectra for $Zn_{1-x}Mn_xO$



compressed films. (1- ZnO, 2 - $x = 1.8\%$, 3 - $x = 5\%$ films; film thickness $d \approx 130$ nm, $T = 300$ K). It is seen that the excitonic line is broadened and its position is shifted to higher energies in comparison to that for free exciton in ZnO (3.30 eV at 300 K, [1]). The line shift is very likely connected to the compressive strain of $Zn_{1-x}Mn_xO$ films. The large width of the absorption line, comparable with that reported in [1], is caused by simultaneous manifestation of A- and B- excitonic lines broadened due to temperature effects, presence of defects and deformation non uniformity of films. As the concentration of Mn impurity increases, excitonic line additionally broadens and shifts to

higher energies. Taking into account the exciton binding energy 60 meV allowed us to determine the dependence of the band gap on the Mn concentration. The insert on this figure indicates the shift of the excitonic line at the temperature decreasing from 300 K (curve 1) to 77,3 K (curve 4). Transformation of the absorption spectrum at the decreasing of temperature is the a reliable evidence of excitonic origin of these lines.

In $ZnSe:Mn$ and other $A^{II}B^{VI}:3d$ compounds the value of bandgap E_g decreases at the increasing of 3d- concentration from zero, at some value of concentration E_g is minimal and after that it increases. But in our case the rise of the value of E_g takes place right away at the increasing of manganese concentration above zero [2]. Therefore, the observed rise of the $E_g(x)$ value with Mn addition provides us with the reliable experimental proof that the strong hybridization condition $U/U_c > 1$ in $Zn_{1-x}Mn_xO$ is fulfilled. In addition the onset of optical absorption in $Zn_{1-x}Mn_xO$ films emerges at lower energies than that for ZnO ones. Analogous shift had been observed earlier in the spectrum of the photoluminescence excitation through deep impurity centers in $Zn_{1-x}Mn_xO$. We assume that additional absorption of $Zn_{1-x}Mn_xO$ (in comparison with ZnO) in the 3.1-3.3 eV range is a result of pushing the antibonding states out of valence band to the forbidden gap.

The work is done with the partial support of the of Russian Federal Agency for Science and Innovations (grant 02.740.11.0217)

[1] V. I. Sokolov, A. Ye. Yermakov, M. A. Uimin, A. A. Mysik, V. A. Pustovarov, M. V. Chukichev and N. B. Gruzdev, *J. of Lumin.* **129**, 1771 (2009).

[2] V. I. Sokolov, A. V. Druzhinin, N. B. Gruzdev, A. Dejneka, O. Churpita, Z. Hubicka, L. Jastrabik, V. Trepakov, *Phys.Rev. B.* **81**, 153104 (2010)

[We-P-47]

Photoluminescence of $Zn_{1-x}Ni_xO$ solid solutions with NaCl-type symmetry

V.I. Sokolov¹, V.A. Pustovarov², A.N. Baranov³, P.S. Sokolov³, N.B. Gruzdev¹

¹ Institute of Metal Physics UD RAS, S.Kovalevskaya Str. 18, 620990, Yekaterinburg, Russia

² Ural Federal University the name after The First President of Russia B.N. Yeltzin, Mira 18, 620002, Yekaterinburg, Russia,

³ M.V.Lomonosov Moscow State University, 119991, Moscow, Russia

The compound of NiO is of the materials with strong correlation. Energy level system of this material is very complicated due to strong correlations of interaction between 3d- electrons and p-electrons of oxygen and between electrons within 3d- shell. This compound is investigated for a long time by the different techniques: optical absorption, reflection, photoemission, inverse photoemission [1]. Up to date the extended experimental data collected about the occupied states of the valence band and empty states of conduction band due to the conventional and non-local charge transfer excitations. The distance between the valence and conduction bands is near 4 eV. At lower energies the charge transfer excitations are exist and not discernible in optical spectra [2]. In this paper we undertake the investigation of photoluminescence (PL) spectra of recently synthesized $Zn_{1-x}Ni_xO$ solid solutions with the symmetry of NaCl-type [3], what principally gives us the possibility to research the energy states in solid solution gap at the different x values.

Samples to the measurements are $Zn_{1-x}Ni_xO$ monocrystals with the sizes of some micrometers, which were pressed into the cellulose. PL- spectra are registrated in the region of 1.5-4 eV and in the temperature interval of 90-300 K, for the samples with x in the range (0.2-0.5). PL-spectra contain two lines: intensive line at 2.56 eV and weak line at 3.75eV; energy positions of these lines weakly change for different values of x in our range. It should be noted that two peaks in gap were registrated by inelastic X-ray scattering for NiO [2].

Preliminary we assume that these PL- peaks are due to charge transfer processes which energies practically not change.

The work is done with the support of RFBR (grant 09-0390442-Ukr_f_a) of Russian Federal Agency for Science and Innovations (grant 02.740.11.0217)

References

- [1] G.A. Sawatzky and J.W. Allen, Phys. Rev. Lett., **24**, 2339-2342 (2004)
- [2] N. Hiraoka, H. Okamura, H. Ishii, I. Jarrige, K.D.Tsuei and Y.Q. Cai, European Physical Journal B, **70**, 157-162 (2009)
- [3] A.N. Baranov, P.S.Sokolov, O.O. Kurakevich, V.A. Tafeenko, D. Trots and V.L. Solozhenko, High Pressure Research, **28**, 515-519 (2008)

[We-O-19]
**Photoluminescence and photoluminescence excitation spectroscopy of ZnO
doped with Co and Ni**

V.I. Sokolov¹, V.A. Pustovarov², N.B. Gruzdev¹, V.T. Surikov³

¹ *Institute of Metal Physics UD RAS, S.Kovalevskaya Str. 18, 620990, Yekaterinburg, Russia*

² *Ural Federal University the name after The First President of Russia B.N. Yeltzin, Mira 18,
620002, Yekaterinburg, Russia,*

³ *Institute of Chemistry of Solid State, UD RAS, Pervomayskaya Str. 91, 620041, Yekaterinburg,
Russia*

Recently the ZnO:3d are investigated very actively in order to discover the theoretically predicted ferromagnetic ordering at $T_c > 300$ K. During the researches the difference between the optical properties of ZnO:3d (especially noticeable for ZnO:Mn) and other compounds of II-VI:3d was found. T. Dietl suggests to consider ZnO:3d the insufficiently studied materials, whose properties are determined by strong d-p hybridization [1]. Convincing arguments about the strong d-p hybridization in $Zn_{1-x}Mn_xO$ were received from the observing of photoluminescence. In the photoluminescence excitation spectrum of 2.9 eV band at the energies of light quanta $\hbar\omega > E_g$ the intensity increasing is observed and we can see 3 peaks at the energies of 3.9eV, 4.5eV and 5.3eV against the background of this increasing. This spectrum differs significantly from intracentral photoluminescence excitation spectrum of Mn^{2+} ion (${}^4T_2 \rightarrow {}^6A_1$ transition) in $Zn_{1-x}Mn_xS$ where we can see the rapid decreasing at $\hbar\omega > E_g$ [2,3].

In this paper the photoluminescence (PL) and photoluminescence excitation (PLE) spectra of ZnO:Co and ZnO:Ni are presented. In PL spectra we can see the peaks, which are caused by the transitions through donor and acceptor levels of Ni^{2+} and Co^{2+} at the energies of 1.85eV, 2.20eV and 2.47eV, 2.80eV correspondently. The position of high energy edges of photoluminescence bands allows to estimate the positions of donor and acceptor levels relatively the edges of allowed bands. PLE- spectra of photoluminescence peaks have the particularities in the region of E_g and at the energies $\hbar\omega > E_g$ we can see significant increasing of excitation intensity, on the background of which some maxima are observed. This rise is analogous to the character of PLE- spectrum observed earlier for $Zn_{1-x}Mn_xO$.

Peculiarities in the PLE- spectra for $Zn_{1-x}Mn_xO$, $Zn_{1-x}Co_xO$ and $Zn_{1-y}Ni_yO$ are the evidence of the fact [1], that in the valence band of these materials the localized states appear due to the strong hybridization. Thus, the photoluminescence excitation spectroscopy gives us the unique information about the properties of ZnO:3d semiconductors. This information allows us to consider these materials as a strong correlated systems.

The work is done with the partial support of the of Russian Federal Agency for Science and Innovations (grant 02.740.11.0217)

References

- [1] T. Dietl, Phys.Rev.B, 77, 085208 (2008).
- [2] V. I. Sokolov, A. Ye. Yermakov, M. A. Uimin, A. A. Mysik, V. A. Pustovarov, M. V. Chukichev and N. B. Gruzdev, J. of Lumin. **129**, 1771 (2009).
- [3] V. I. Sokolov, A. Ye. Yermakov, M. A. Uimin, A. A. Mysik, V. A. Pustovarov, N. B. Gruzdev and V.T. Surikov, Phys. Status Solidi C, **7**, 1589 (2010)

[Th-O-42]

Non-Condon optical spectra of impurity centers in crystals at finite temperatures: theory and experiment

O.V. Solovyev¹, V.N. Makhov², G. Stryganyuk³, M. Kirm⁴

¹*Kazan Federal University, Kremlevskaya Street 18, 420008 Kazan, Russia*

²*P.N. Lebedev Physical Institute, Leninskii Prospect 53, 119991 Moscow, Russia*

³*Institute for scintillation materials, NAS of Ukraine, Lenin Ave. 60, 61001 Kharkiv, Ukraine*

⁴*Institute of Physics, University of Tartu, Riia 142, 51014 Tartu, Estonia*

Analytical expressions for non-Condon generating functions of absorption and luminescence of optical centers in crystals at finite temperatures have been derived in the adiabatic approximation. A solution of the Schrodinger equation for an electronic subsystem has been considered in the first order of the perturbation theory for a vibronic interaction linear in normal coordinates of the vibrational subsystem. The non-Condon form function of the optical transition has been obtained in the form of a convolution operator acting on the normalized Condon form function. The group-theoretical analysis shows that in the case of a symmetry forbidden electronic transition $a \leftrightarrow b$ the expression for the non-Condon form function takes the form

$$\int_0^{+\infty} \left(F^0(\Omega \mp \omega) f(\omega)(n(\omega)+1) + F^0(\Omega \pm \omega) f(\omega)n(\omega) \right) d\omega, \quad (1)$$

where the upper and lower signs relate to absorption and luminescence, respectively, $F^0(\Omega)$ is a corresponding normalized Condon form function. Distribution $f(\omega)$ equals $\text{Im} G_{\delta d(q), \delta d(q)^*}^A(\omega)$, where $\delta d(q)$ is a dynamic perturbation (linear in vibrational coordinates q) of the matrix element of the impurity center electric dipole moment d connecting the electronic states a and b ; the sign of the imaginary part should be assigned to the advanced Green's function for the vibrational coordinates; the complex coefficients, i.e. the matrix elements of the electronic operators, are factored outside the sign of the imaginary part. Distribution $n(\omega) = 1/(e^{\hbar\omega/k_B T} - 1)$ is a density of phonons with frequency ω at temperature T . At zero temperature $n(\omega) = 0$ and (1) converts into a formula obtained earlier in [1].

As follows from (1), if optical transition is forbidden in the Condon approximation due to symmetry, the non-Condon form functions of absorption and luminescence are mirror symmetric and do not contain zero-phonon lines at arbitrary temperature. This property can serve as a qualitative criterion for the interpretation of experimental data.

The developed theory was applied to simulation of the non-Condon emission spectra in the range of the symmetry forbidden transitions between the two lower electronic states of the excited Lu^{3+} ion configuration $4f^{13}5d$ and the $4f^{14}$ ground state in $\text{LiYF}_4:\text{Lu}^{3+}$ crystal. Simulation has been carried out for a set of temperatures in the range from 8 to 140 K and compared with experimental data. The measurements have been performed at the SUPERLUMI station of HASYLAB at DESY, using synchrotron radiation from the DORIS storage ring for excitation [2].

To simulate spectral envelopes for the $\text{LiYF}_4:\text{Lu}^{3+}$ crystal luminescence, we used the microscopic model of electron-phonon interaction derived in [2, 3]. Simulation involved calculations of crystal field parameters for a $5d$ electron as explicit functions of lattice ion's coordinates in the framework of the exchange charge model, numerical diagonalization of the effective impurity ion Hamiltonian containing energies of electrostatic Coulomb and exchange interactions between electrons, spin-orbit interactions and the crystal field interactions for the ground ($4f^{14}$) and excited ($4f^{13}5d$)

electronic configurations, calculations of the $5d$ -electron-phonon coupling constants, and simulations of the band shapes by making use of the realistic phonon spectrum of the host LiYF_4 lattice. Parameters of the model have been established in [2] by fitting the measured excitation spectra of the $\text{LiYF}_4:\text{Lu}^{3+}$ crystal corresponding to the allowed $4f^{14}-4f^{13}5d$ transitions in the Lu^{3+} ion. No parameters were additionally fitted in simulation of emission spectra in the range of symmetry forbidden $4f^{13}5d-4f^{14}$ transitions except for the ratio of σ - and π -polarization contributions to the spectra. Comparison of simulation results with experiment is given in Fig. 1 for the case of 60 K temperature.

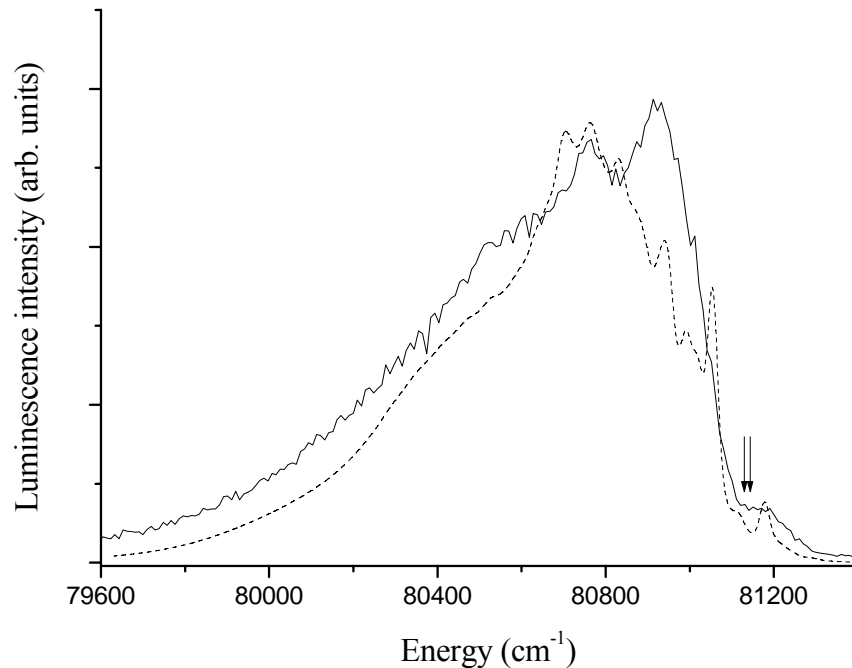


Fig. 1. Vacuum ultraviolet emission from $\text{LiYF}_4:\text{Lu}^{3+}$ (1%) single crystal excited at 60 K by 84750 cm^{-1} photons (solid curve) and simulated emission spectrum (dashed curve). Arrows mark zero-phonon energy levels (81130 and 81142 cm^{-1}).

Overall qualitative agreement between experimental data and simulation results is achieved. The developed theory explains the absence of zero-phonon lines in the $\text{LiYF}_4:\text{Lu}^{3+}$ emission spectra measured for a set of temperatures in the range from 8 to 140 K. Details of vibrational structure of the measured emission spectra are not reproduced very well by calculations (see Fig. 1). One of the reasons for the discrepancy may be the mixing of the two lower $4f^{13}5d$ electronic states of the Lu^{3+} ion by non-adiabatic phonons.

The authors are grateful to B.Z. Malkin for valuable discussions. This study was supported by the Russian Foundation for Basic Research (project № 09–02–00930).

References

- [1] O.V. Solovyev. *Physics of the Solid State*. **52**, 728 (2010).
- [2] M. Kirm et al. *Phys. Rev. B* **75**, 075111 (2007).
- [3] O.V. Solovyev, B.Z. Malkin. *J. Mol. Struct.* **838**, 176 (2007).

[Tu-P-14]

Identification of the deep level defects in bulk AlN: EPR studies

V.A. Soltamov, I.V. Ilyin, A.A. Soltamova, E.N. Mokhov, P.G. Baranov

Ioffe Physical-Technical Institute, St Petersburg, Politekhnikeskaya, 26, 194021 Russia

Aluminum nitride (AlN) is a direct-band-gap semiconductor with an energy gap of ~6.0 eV. The wurtzite polytypes of InN, GaN and AlN form a continuous alloy system whose direct bandgap range from about 0.7 eV for InN, to 3.4 eV for GaN, and 6.0 eV for AlN [1].

Transition-metal ions often encountered as trace impurities in III-nitrides form deep levels. This was shown for bulk GaN in which iron in charged state Fe^{3+} [2] and Ni^{3+} [3] as well as Mn^{2+} [4] were observed. These deep level defects can strongly affect the electrical and optical properties of material. Meanwhile, in AlN, transition-metal ions, such as Mn^{2+} [4] ions and Er^{3+} [5] have only been observed in thin films and in bulk material respectively.

In present study the electron paramagnetic resonance (EPR) at 9.4 GHz has been used to study defects in AlN bulk crystal, grown by a sublimation sandwich method [6]. Investigations revealed the presence of transition metals: Fe^{2+} ($S=2$) and some paramagnetic centers $S=3/2$, which were suggested to be Cr^{3+} and Ni^{3+} .

Conclusion about the presence of Fe^{2+} ions was made by analyzing the angular dependence of EPR spectra upon rotating the magnetic field in $(11\bar{2}0)$ plane shown in Fig.1. A distinct feature of these spectra is a strong line in the $B \perp c$ (90°) orientation that shifts to lower magnetic fields with the rotation of the crystal towards $B \parallel c$ (0°) orientation. This line is marked as L1 for $\theta = 90^\circ$. The positions of this signal in different orientations of the sample are connected in Fig. 1 with dashed line. The L1 line angular dependence is typical for $S = 2$ systems in an axial (C_{3v}) crystalline field and can be roughly described by the conventional spin Hamiltonian of the form:

$$H = g_{\parallel} \mu_B B_z S_z + g_{\perp} \mu_B (B_x S_x + B_y S_y) + D[S_z^2 - 1/3S(S+1)], \quad (1)$$

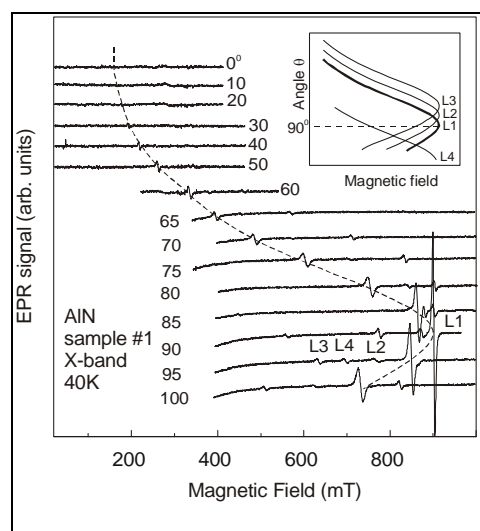


Fig. 1. Experimental X-band EPR spectra in AlN crystal at $T = 40$ K recorded in different orientations of the magnetic field with respect to the c -axis and simulated angle dependence for L1 line (dashed line). A rough sketch of the angular dependencies of the L1-L4 lines is shown in the inset.

where z is directed along the hexagonal c -axis of the crystal, parameter D characterizes the axial crystal field. The large D value leads within the $S = 2$ manifold to a splitting into the spin states $M_S=0, \pm 1, \pm 2$. The EPR spectra consist of one line which corresponds to the $M_S=-1 \leftrightarrow M_S=1$ transition within the ground state. The investigation of the angular dependence of the spectrum allowed us to find the best-fit parameters for spin Hamiltonian of Eq. (1): $g_{\parallel} = 2.003$, $g_{\perp} = 2.12$, $D = 7.93 \text{ cm}^{-1}$. Other lines of smaller intensity are clearly seen in the spectra in Fig. 1, marked as L2, L3 and L4 for $\theta = 95^\circ$. These three lines seem to belong to the same center (like L1), localized in different parts of the sample. We believe that our sample consists of at least four parts (domains) that are misaligned with respect to the c -axis. Conclusion about the presence of Cr^{3+} and Ni^{3+} was made by analyzing the angular dependence of two signals (L5 and L6 connected with lines) shown on Fig.2. The lines marked with asterisk belong to the L1 center. The signal in the region of 330 mT belongs to defects in quartz parts of cryostat and has been used as a reference signal. The HF structure of the signal could not be observed, perhaps due to the low signal intensity, so the most possible candidates should be transition metal ions with small abundance of odd isotopes with nonzero nuclear spin, i.e. $\text{Cr}^{3+}(d^3)$ or $\text{Ni}^{3+}(d^7)$.

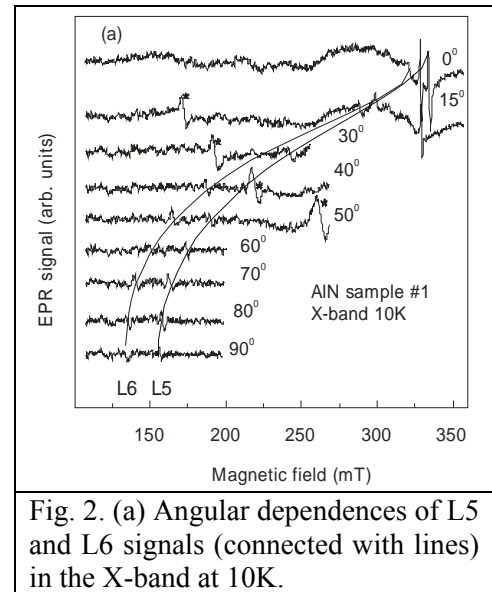


Fig. 2. (a) Angular dependences of L5 and L6 signals (connected with lines) in the X-band at 10K.

This study was supported by Ministry of education and science of the Russian Federation by the contract № 02.740.11.0108 and by Russian academy of science program «Spin-Dependent Effects in the Solids and Spintronics».

- [1] B. Monemar et al., Phys. Status Solidi B **244**, 1759 (2007).
- [2] J. Baur et al., Appl. Phys. Lett. **65**, 2211 (1994).
- [3] P.G. Baranov et al., Solid State Commun., **101**, 8, 611-615, (1997).
- [4] T. Graf et al., Phys. Rev. B **67**, 165215 (2003).
- [5] Shang Yang et al., J. Appl. Phys, **105**, 023714 (2009).
- [6] E.N. Mokhov et al., J. Cryst. Growth **281**, 93 (2005).

[We-P-58]

Spectroscopy of an ion Ce^{+3} as probe of the composition multiligande garnets

N.P. Soshchin

The East-Chinese normal University, Shanghai, Peoples Republic Of China

e-mail: soschin@mail.ru

Researches P. P. Feofilov of optical crystals activated TR^{+2} , TR^{+3} already became classical, by years interest By it constantly grows. Initially it was connected. By start of the first crystal lasers, then the periods of intensive search effective earth cathode-, roentgen- phosphors and lightconverters. Beginnings 21 centuries the explosive wave of interest is connected by a new applied direction, solid-state light (SSL) on a basis nitride InGaN-structure, supplied phosphors by converters.

Features of radiating materials for SSL are:

- Short Stockshift 60-80nm;
- High density of capacity, in 100-1000-times exceeding those standard luminescent lamps;
- Rigid demand to coloristic parameters of radiation, form of a spectrum and temperature stability of all characteristics.

Attempts to create radiating materials on the basis of compositions A_2B_6 or phosphate, silicate, vanadate, have not resulted till now to encouraging results, owing to concentration-cinetic of restrictions basic activation TR^{+3} (lifetimes 1-100 of microseconds at the contents to a matrix up to 10 % mass).

Basic for SSL are the compositions with structure Garnet $(Ln)_3(Al, Ga)_5O_{12}$, Bredigite $(Me)_8Si_4O_{16}$, and also nitride-silicate and sialons, activated mainly Ce^{+3} Eu^{+2} by ions.

Our message the basic attention is given to compositions with structure Garnet. To known structure Garnets $(Me)_3(Al, Ga)_5O_{12}$ 160 separate atoms ($Z=8$ for an elementary cell), thus replacement 64 elements are in detail described. For example, the replacement Y - Gd is accompanied lengthwave by shift of a spectrum Ce^{+3} , Y - Lu -shortwave, Y- Sc breadth of a spectrum, Al-Ga by shortwave shift. But spectral changes traditional Garnet Phosphors frequently very much are not high -25-30 nanometer, what obviously do not satisfy coloristic to the requirements SSL, a eateries on colour temperature of radiation ($T = 2500K - 9000K$) and to factor color reproduction in all seen ranging of lengths of waves.

We develop a special technique of synthesis Phosphors with garnetstructure, which it is possible is directed to change the contents all 98 ions of oxygen Tetraedr $[AlO_4]$, replacing them on heterovalence to the mechanism on ions Halogen $[F^-, Ce^-, Br^-, J^-]$ or elements of group $[N^{3-}, P^{3-}]$, and also on homovalence to the mechanism on ions S^{-2} and Se^{-2} . Arising sterical of complication at replacement income of ions, for example J^- ($rJ=2.20A$), S^{-2} ($rS=1.82A$), N^{3-} ($rN=1.48A$), P^{3-} ($rP = 1.86A$) were overcome by use special initial nanomaterials (sizes 20-30 nm) by controllable pressure ligande reagens the closed container of synthesis.

Structure one tetraedr $[AlO_4]$ could be from one up to four Ligande, for example $[AlO_4] > [AlO_{4-x-y}F_xCl_xN_yP_y]$ or $[AlO_4] > [AlO_3J_{0.5}P_{0.5}]$ at complete concervation constant catione of a skeleton

Radiation Ce^{+3} in multiligand Garnet thus was transformed he following very wide limits

Parameter of radiation	variation
Rule max	520-620 nm
Breadth of a spectrum,	98-160 nm
The form a spectral curve	Gausse or triangular
Skewness by a spectral curve	long - or shortwave 15 nm

The variation of the structure of garnet phosphors is accompanied by changes in the parameter of a crystal lattice up to a meaning from $a = 11.5 \text{ \AA}$ up to $a = 12.30 \text{ \AA}$. By the respective change of a quantum output of radiation Ce^{3+} up to size 0.92 - 0.96. It is necessary to note monocrystal of synthesized grains phosphors (diameter up to 30 micron), morphology, natural to tetragonal and their high optical transparency. The volumetric models of structure multiligand garnet tetrahedra are constructed.

Synthesized ligand-modified garnet structures already the present time provide at capacity nitride heterostructure 500mW for 455 nm light feedback cold-white LED by 5500K. At a level 130-150 lm/W, for is warm-white LED by 3500K 95-105lm/W, that essentially exceeds all parameters luminescence of lamps.

[We-P-53]

Silicate photoluminophor for conversion of radiation of nitride light-emitting diodes

N.P. Soshchin, V.N. Lichmanova, V.A. Bol'shuhin

*Science-Research Institute "Platan", Russia
e-mail: inpec@mail.ru*

It is offered to use for increase in light efficiency of radiation of structures InGaN the new silicate structure of the luminescent converter executed on the basis of silicates Ba, Sr, Ca, activated Eu^{+2} . In the message results of research of silicate photoluminophors (PL) on the basis of connections in threefold system (Ba-Sr-Ca) $8\text{Si}_4\text{O}_{16}$ ortorombic structures Bredigite, activated by ions f-elements from number Eu^{+2} , Ce^{+3} , Pr+3 are discussed. The spectrum of excitation of ion Eu^{+2} in this structure has the broadband character which long-wave part can come into visible area of a spectrum, reaching 500 nanometers and more. Visually it leads to appreciable fluorescence of samples of photoluminophors. The mechanism of long-wave excitation of the active centres depends on concentration Eu^{+2} and while up to the end it is not found out, but is already used in technical applications of these structures.

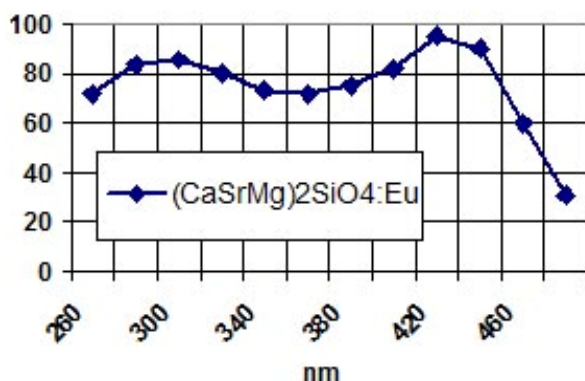


Fig 1. Typical excitation spectra silicate PL

In work it is shown, that at replacement of ion Ba^{+2} on катионы with smaller radius Sr^{+2} or Ca^{+2} there is a long-wave shift of a spectrum of radiation from $\lambda = 505\text{nm}$ to $\lambda = 580\text{nm}$, that is caused by deactivation of top radiating level Eu^{+2} . Additional doped luminescent structure Mg leads to increase of efficiency of conversion of dark blue radiation. Unusual also is sensibility activity Ce^{+3} . In relation to basic activator Eu^{+2} at a parity of their concentration from 1:50 till, promoting luminescence increase in 2 times

On the basis of the spent researches it is developed silicate PL for the luminescent converters SID providing at excitation with $\lambda = 460\text{nm}$ efficiency a luminescence more 80 lumen/watt at length of a wave radiation of 525 nanometers (it twice exceeds parametres monolithic LED).

[We-P-48]
Optical and far-infrared spectroscopy of multiferroic $\text{EuFe}_3(\text{BO}_3)_4$

T.N. Stanislavchuk^{1,2}, K.N. Boldyrev², M.N. Popova², B.Z. Malkin³

¹*Moscow Institute of Physics and Technology (State University), 141700 Dolgoprudnyj, Moscow region, Russia*

²*Institute for Spectroscopy, RAS, 142190 Troitsk, Moscow region, Russia*

³*Kazan Federal University, 420008 Kazan, Russia*

Compounds $\text{RFe}_3(\text{BO}_3)_4$ (R - rare-earth ion or Y) crystallize in the trigonal R32 structure of the natural mineral huntite. The presence of two magnetic subsystems, the rare-earth (RE) and the iron ones, results in a set of phase transitions occurring with variation of both temperature and external magnetic field [1,2]. Recently, a magnetoelectric effect was found in a number of these crystals which is of interest for possible practical applications [2]. Magnetic and magnetoelectric properties of RE iron borates are strongly different depending on a particular RE ion [1,2]. To understand the origin of these differences the knowledge of wave functions and energies of the RE levels is of primary importance. These data can be obtained by studying optical transitions within the RE ions and, then, performing the crystal-field (CF) calculations. In this work we have undertaken such investigation for $\text{EuFe}_3(\text{BO}_3)_4$. Far-infrared spectra have also been measured, with the aim to look for peculiarities connected with magnetoelastic and/or magnetoelectric interactions.

Absorption spectra of the europium iron borate were registered in a wide spectral ($30\text{-}23000\text{ cm}^{-1}$) and temperature ($3.5\text{-}300\text{ K}$) regions. Energies of the CF levels of the Eu^{3+} ion were determined. Temperature behavior of spectral lines points to the structural ($T_S=58\text{ K}$) and magnetic ($T_N=34\text{ K}$) phase transitions. The analysis of the spectra in the far-infrared region enabled to obtain the temperature dependence of dielectric constant with anomalies at the points of phase transitions. The anomaly at magnetic ordering can be due to magnetoelastic or magnetoelectric interactions. On the basis of the optical data, CF calculations were performed. CF parameters and wave-functions of the CF energy levels of the Eu^{3+} ion were determined. To analyze the spectral data for the magnetically ordered state, the anisotropic orbitally-dependent exchange Hamiltonian was considered. The reliability of the obtained parameters was checked by modeling the literature data [2] on the magnetic susceptibility of $\text{EuFe}_3(\text{BO}_3)_4$ in both paramagnetic and antiferromagnetic phases.

This work was supported in part by the Russian Foundation for Basic Research (Grant № 10-02-01071) and by the Russian Academy of Sciences under the Programs for Basic Research.

[1] M.N. Popova, JMMM **321**, 716 (2009).

[2] A.M. Kadomtseva, Yu.F. Popov, G.N. Vorob'ev, A.P. Pyatakov, et.al., Fizika Nizkih Temperatur **36**, №6, 640 (2010).

[We-P-36]

Spectroscopic, laser investigations and concentration quenching of two Yb³⁺-doped OH- free calcium aluminosilicate laser glasses

A. Steimacher^{1,2}, M.P. Belançon^{1,2}, A.N. Medina¹, L. Baesso¹, L.H.C. Andrade^{2,3}, S. Lima^{2,3}, R. Peretti², A.M. Jurdyc², A. Brenier², Y. Guyot², G. Boulon^{2*}

¹*Departamento de Física, Universidade Estadual de Maringá,, Maringá, PR, Brazil*

²*Physical Chemistry of Luminescent Materials (LPCML), University of Lyon, UCBLyon1, UMR 5620 CNRS, 69622 Villeurbanne, France*

³*Grupo de Espectroscopia Óptica e Fototérmica, Universidade Estadual de Mato Grosso do Sul, UEMS, Dourados, MS, Brazil*

*E-mail: georges.boulon@univ-lyon1.fr

Rare earths have been introduced into two series of calcium aluminosilicate glasses doped up to 11 wt% Yb₂O₃ prepared under vacuum atmosphere. The first one was prepared with low silica content of 7 wt%(LSCAS) and the second one with high silica content of ~30 wt%(CAS). The interest in these glasses as host materials is because they are OH⁻ free and highly transparent in the spectral range, from ~250 nm to 5 μm, when melted under vacuum conditions. Furthermore, previous work has showed these classes of glasses are a good candidate for solid state laser media hosts due to their thermal, optical and mechanical properties [1]. Laser emission at 1077 nm also was observed with the Nd³⁺-doped LSCAS, which showed efficiency comparable to commercial glass LHG-5[2]. A fluorescent emission at 2.8μm also was reported with Er³⁺-Yb³⁺ co-doped LSCAS samples, interesting for biomedical applications[3]. Moreover, a high value gain cross section, 4.7×10⁻¹⁹ cm² at 635 nm, was recently demonstrated in Ti³⁺-doped LSCAS[4].

The Yb³⁺ ion was chosen as doping to this France-Brazil co-operation supported by COFECUB in France and CAPES in Brazil due to improvements of high performance GaAs and InGaAs pumping laser diodes between 900 and 1100 nm, what has renewed the interest in Yb³⁺-doped materials for applications in high efficiency and high-power diode-pumping laser systems. The optical properties: refractive index, absorption and fluorescence spectra, as well as the Yb³⁺ lifetimes have been investigated at low and room temperature. The results are discussed as a function of Yb₂O₃ concentration and compared between these different glass hosts. ²F_{5/2} → ²F_{7/2} broad emission lines are seen as a result of the multisite distribution. The emission cross section is 1.3x10⁻²⁰cm² in both compounds at 1030nm, higher than in Kigre CB20 glass. Energy level diagrams are achieved from low temperature emission and excitation measurements showing a large splitting of the Stark levels favorable for laser tuneability. Resonance fluorescence line narrowing experiment has been undertaken with the ²F_{5/2} ↔ ²F_{7/2} infrared resonance transition between 965 and 986nm revealing an asymmetrical inhomogeneous distribution for both CAS and LSCAS glasses. Concentration dependence of the fluorescence lifetime shows competition between luminescence quenching and radiative energy transfer mechanisms as in other Yb³⁺-doped laser materials [5-6]. A theoretical approach gives an evaluation of the optimum concentration, higher in LSCAS (8%wt) than in CAS (5%wt) glasses. Successful laser tests performed at 1037nm under laser diode pumping (7W) will be presented.

Finally, no large difference has been observed between the spectroscopic properties of Yb³⁺-doped LSCAS and CAS glasses in contrary of those doped by Ce³⁺ ions where two main distributions have been detected [7].

[1] A. Steimacher, N. G. C. Astrath, A. Novatski, F. Pedrochi, A. C. Bento, M. L. Baesso, A. N. Medina, J Non-Cryst Solids 352 (2006) 3613.

[2] D. F. de Sousa, L. A. O. Nunes, J. H. Rohling, M. L. Baesso, Appl Phys B-Lasers O 77 (2003) 59.

[3] M. L. Baesso, A. C. Bento, L. C. M. Miranda, D. F. de Souza, J. A. Sampaio, L. A. O. Nunes,

J Non-Cryst Solids 276 (2000) 8.

[4] S. M. Lima, J. R. Silva, L. H. C. Andrade, A. Novatski, A. N. Medina, A. C. Bento, M. L. Baesso, Y. Guyot, G. Boulon, Opt. Lett. 35 (2010) 1055

[5] G. Boulon, J. Of Alloys and Compounds, 451 (2008) 179

[6] G. Boulon, Y. Guyot, H. Canibano, S. Hraiech, A. Yoshikawa, JOSA B 25 (2008) 884

[7] L. Andrade, S. Lima, A. Novatski, A. Steimacher, J. Rohling, A. Medina, A. Bento, M. Baesso, Y. Guyot, G. Boulon, Applied Physics Letters 95 (2009) 081104

[Tu-I-4]
**Fluorescence and visible upconversion in heavily doped $\text{LiNd}_x\text{La}_{1-x}\text{P}_4\text{O}_{12}$
nanocrystallines powders**

W. Strek, L. Marciniak, A. Bednarkiewicz, A. Lukowiak, R.J. Wiglusz, D. Hreniak

*Institute of Low Temperature and Structure Research, Polish Academy of Sciences, Wroclaw,
Poland*

The Ln^{3+} stoichiometric tetrphosphate crystals belong to the group of high concentration luminescent materials characterized by reduced concentration quenching of fluorescence due to the large distance between Ln^{3+} ions. In the present work a new method of preparation of Nd^{3+} doped lithium lanthanum tetrphosphate ($\text{LiLa}_{1-x}\text{Nd}_x\text{P}_4\text{O}_{12}$) nanocrystals based on wet is demonstrated. Their structure and morphology were investigated. The influences of Nd^{3+} concentration on luminescence, excitation spectra and luminescence decay profiles were investigated. A concentration dependence of Nd^{3+} fluorescence and excitation spectra was investigated. The role of cooperative interion interactions was discussed. The effect of excitation pumping power on fluorescence and decay curves were studied. The visible anti-Stokes emission was observed and the mechanism of upconversion transitions in $\text{LiNd}_x\text{La}_{1-x}\text{P}_4\text{O}_{12}$ nanocrystalline powders was proposed.

*to be presented at Feofilov Symposium-2010

[Tu-P-5]

Time-resolved spectroscopy of Ce³⁺-doped alkali gadolinium phosphates

G. Stryganyuk^{1,2}, T. Shalapska¹, I. Pashyk¹, A. Voloshinovskii¹, A. Krasnikov³,
S. Zazubovich³

¹*Ivan Franko National University of Lviv, 8 Kyryla i Mefodiya Str., 79005, Lviv, Ukraine*

²*Institute for Scintillation Materials, NAS of Ukraine, 60 Lenin ave., 61001 Kharkiv, Ukraine*

³*Institute of Physics, University of Tartu, Riia 142, 51014 Tartu, Estonia*

Ce³⁺-doped alkali rare-earth phosphates, due to their high light yield, short decay time, and high stability, have promising characteristics for their application in scintillation detectors. In the MRE₄P₄O₁₂-type compounds (M is an alkali ion, and RE is a trivalent rare-earth metal ion), various alkali metals can be utilized in combination with various RE elements; therefore these materials can offer a significant potential for modifying their parameters. An effective way for scintillation efficiency increase is to provide an optimal excitation energy transfer from the host lattice to the luminescence centers. Owing to the effective energy migration through the Gd³⁺ sub-lattice and the subsequent energy transfer from a Gd³⁺ ion towards an adjacent Ce³⁺ center, the luminescence efficiency significantly increases (see, e.g., [1-4]).

The aim of the work was to study the luminescence characteristics of various Ce³⁺-doped alkali gadolinium phosphates, to clarify the processes of energy migration along the Gd³⁺ ions and energy transfer between the Gd³⁺ and Ce³⁺ ions, and to compare the peculiarities of these processes in the phosphates with different alkali metal ions. For that, time-resolved emission spectra and luminescence decay kinetics were measured in the 4.2-300 K temperature range for the Ce³⁺-doped LiGdP₄O₁₂, NaGdP₄O₁₂, and CsGdP₄O₁₂ phosphates.

In all the phosphates studied, the thermally stimulated high-energy shift of the Gd³⁺ emission band is observed, indicating to the thermal population of the higher-energy ⁶P_{5/2} level of the ⁶P_J excited state of Gd³⁺. It improves the resonance conditions among the ⁶P_J levels of a Gd³⁺ ion and, thus, results in the increase of the efficiency of the excitation energy migration along the Gd sub-lattice. Due to the increasing overlap of the Gd³⁺ and Ce³⁺ spectral bands, it also results in the increasing probability of the Gd³⁺ → Ce³⁺ energy transfer. Besides the intense ≈312 nm emission, an additional weak lower-energy vibronic band, appearing due to the interaction with the phosphate group, is observed in the Gd³⁺ emission spectrum. In LiGdP₄O₁₂:Ce and NaGdP₄O₁₂:Ce, the effective Ce³⁺ → Gd³⁺ energy transfer takes place at 4.2-300 K, resulting in the shortening of the decay time of the Ce³⁺ emission [3]. The reverse Gd³⁺ → Ce³⁺ energy transfer becomes possible only at T>150 K, probably, as a result of the thermally stimulated population of the highest ⁶P_{3/2} level of the ⁶P_J excited state of a Gd³⁺ ion. In CsGdP₄O₁₂:Ce, the Gd³⁺ → Ce³⁺ energy transfer prevails at 4.2 K, and its probability increases at T>150 K due to the above-mentioned reason. At 4.2 K, the Ce³⁺ → Gd³⁺ energy transfer takes place as well. At 300 K, the two-dimensional energy transfer processes result in the thermal equilibrium between the Gd³⁺ and Ce³⁺ states in all the phosphates studied.

[1] J. Zhong, H. Liang, H. Lin, B. Han, Q. Su, G. Zhang, *J. Mater. Chem.* 17, 4679 (2007).

[2] J.P. Zhong, H.B. Liang, Q. Su, P. Dorenbos, M.D. Birowosuto, *Chem. Phys. Lett.* 445, 32 (2007).

[3] T. Shalapska, G. Stryganyuk, P. Demchenko, A. Voloshinovskii, P. Dorenbos, *J. Phys.: Condens. Matter*, 21 (2009) 445901 (8 pp).

[4] J. Zhong, H. Liang, Q. Su, J. Zhou, I.V. Khodyuk, P. Dorenbos, *Opt. Mater.* 32, 378 (2009).

[Th-O-52]

Photoinduced complexes in $\text{KTa}_{0.988}\text{Nb}_{0.012}\text{O}_3$ crystals: EPR study

I.N. Subacheva¹, A.A. Rodionov¹, R.V. Yusupov¹, V.A. Trepakov^{2,3}, P.P. Syrnikov²,
A.I. Gubaev⁴, M.Kh. Salakhov¹

¹Kazan Federal University, Kremlevskaya 18, 420008 Kazan, Russia

²Ioffe Physical-Technical Institute, RAS, 194021 St.-Petersburg, Russia

³Institute of Physics, ASCR, 182 21 Prague 8, Czech Republic

⁴Basel University, Klingelbergstr. 50-70, Basel 4056, Switzerland

Polaronic problem in perovskite-like compounds is a subject of permanent interest in connection with the role of polarons in optical, transport properties and structural transformations. Present study of slightly diluted $\text{KTa}_{1-x}\text{Nb}_x\text{O}_3$ (KTN) crystals is a continuation of our previous investigation [1] in which an intense photoinduced polaronic related optical absorption was found both in KTaO_3 (KTO) and KTN crystals. While the properties of the photoinduced centers in KTO were extensively studied with EPR [2, 3], nothing was known about photoinduced EPR of KTN.

Here we report on the experimental observation of the photoinduced EPR spectra in $\text{KTa}_{0.988}\text{Nb}_{0.012}\text{O}_3$ crystals (KTN-1.2). The photoinduced EPR signal in KTN-1.2 consists of two main components: nearly isotropic with $g_{\text{eff}} \sim 2$, and strongly anisotropic one. Signal at $g_{\text{eff}} \sim 2$, similar to that in KTO, reveals presence of several different paramagnetic centers. Spectra of these centers are strongly structured due to hyperfine interaction with the lattice nuclei. This signal originates most probably from single localized photo-carriers – electrons and holes.

Anisotropic spectrum is observed only below 10 K. Analysis of the angular and the temperature dependencies of the spectrum revealed a set of characteristic properties. This signal arises from the axial centers with axes coinciding with the C_4 crystalline axes. Angular dependence of the resonance field of the anisotropic spectrum can be fit well within the model of the axial center with $J = 1$. Obtained parameter values are $g_{\parallel} = 0.82 \pm 0.04$, $g_{\perp} = 0.52 \pm 0.04$, $D = 0.44 \pm 0.03 \text{ cm}^{-1}$. Additionally, thermal stability of the centers was studied using isochronal annealing approach. Observed dependence allowed us to associate the anisotropic photoinduced EPR spectra with the photoinduced absorption in KTN at $\sim 0.8 \text{ eV}$ [1].

Properties of the anisotropic photo-EPR spectrum in KTN-1.2 crystal turned out to be qualitatively similar to that in KTO: the signal is caused by the paramagnetic centers with the axes along the C_4 axes of the crystal. On the other hand – our data by no means can be explained within the frames of the existing models of the photoinduced centers proposed for KTO [2, 3]. The observed features and especially the angular dependence of the resonance field of anisotropic spectrum in KTN-1.2 are inherent to the non-Kramers centers with an integer spin. The simplest models of such photoinduced centers we suggest are bipolarons and excitons. This is consistent with the photoinduced absorption at $\sim 0.8 \text{ eV}$ in KTN, which has been assigned to the Nb^{4+} bipolaron centers in [1].

- [1] Gubaev A. I., Kapphan S. E., Jastabik L., Trepakov V. A. and Syrnikov P. P. *J. Appl. Phys.* **100** (2006) 023106.
- [2] Laguta V. V., Zaritskii M. I., Glinchuk M. D., Bykov I. P., Rosa J. and Jastrabik L. *Phys. Rev. B* **58** (1998) 156.
- [3] Maiwald M. and Schirmer O. F. *Europhys. Lett.* **64** (2003) 776.

[We-I-26]
Inductive-resonant theory of nonradiative transitions in lanthanide and transition metal ions

E.B. Sveshnikova, V.L. Ermolaev

*St. Petersburg State University of Information Technologies, Mechanics, and Optics, St.
Petersburg, 197101 Russia,
E-mail: ermolaev@oi.ifmo.ru*

Inductive-resonant mechanism of nonradiative transitions is based on assumption that these processes are induced by resonant interactions between electronic or vibronic oscillator of excited ion and isoenergetic vibrational oscillators of molecular groups surrounding the excited centre and these processes lead to electronic-vibrational energy transfer [1, 2]. In dipole-dipole approximation this approach makes it possible to calculate the rate constants of nonradiative transitions (k_{nr}) in the ion by the formula analogous to Förster's formula [3]. For such calculation it is necessary to know: the luminescence spectra of the ion from an examined level, the radiative constant (k_r), the vibrational absorption spectra of molecular group surrounding the ion in the range of luminescence spectra and the data on mutual spatial distribution of the ion and group with vibrational absorption. In succeeding years the applicability of *dd* approach of the theory was proved for the lanthanide and transition metal ions in solution, glass and crystal matrices [4, 5]. In the most cases the k_{nr}^{calc} is in the agreement with the k_{nr}^{exp} in the limit of one order of magnitude. The existence of the predicted by us energy transfer to vibrations was proved [6] by the observation of pure vibrational emission from CN⁻ defects in 4.8 μ range occurring as a result of F⁻ center deactivation by CN⁻ defects in halide crystals. Our approach explains in a simple and logic manner the anomalous small k_{nr}^{exp} probability for $^5D_1 \rightarrow ^5D_0$ transition in Eu(III) at energy gap (1750 cm^{-1}) and for $^3P_1 \rightarrow ^3P_0$ transition in Pr(III) (550 cm^{-1}), because this transitions are magnetic dipole while the interaction between the magnetic dipole oscillator of Ln(III) ions and the electric dipole of vibrational absorption should be weak [7]. It was shown that the marked contribution to k_{nr}^{exp} of Eu(III) and Tb(III) in water brings quadruple-dipole interaction of these ions with the vibrations of the nearest molecules [8]. The new proof of applicability of inductive-resonant theory is obtained in paper [9]. An investigation of external solvent effects on τ luminescence of quantum dots (QD) has shown that the effect of toluene is the greatest when the luminescence band of QD coincides with the absorption of C-H vibration second overtone of toluene. In paper [10] the calculation of k_{nr} of Nd(III) $^4G_{7/2}$ and $^4I_{11/2}$ levels in glass and crystal laser matrices was made in *dd* approximation of theory [10]. Authors [10] have demonstrated that the calculated lifetimes of these levels of Nd(III) are in good agreement with experiment when the vibrational linear absorption coefficient of matrix at frequency of transitions under investigation are taken into account. The applicability of *dd* approach of theory was confirmed by data of paper [11] dedicated to k_{nr} calculation of Er(III) $^4H_{13/2}$ level in organic complexes.

- [1]. Sveshnikova E.B., Ermolaev V.L. *Opt. Spectr.* **30**, No 2, 208 (1971)
- [2]. Ermolaev V.L., Sveshnikova E.B. *Chem. Phys. Lett.* **23**, No 3, 349 (1973)
- [3]. Förster Th. *Ann. Phys. N.F.* **2**, No 1-2, 55 (1948)
- [4]. Ermolaev V.L., Sveshnikova E.B., Bodunov E.N. *Physics-Uspekhi.* **39**, No 3, 261 (1996); An erratum for this article: *Physics-Uspekhi.* **40**, 335 (1997)
- [5]. Kamiskii A.A., Aminov L.K., Ermolaev V.L. at al. *Physics and Spectroscopy of Laser Crystals.* Moscow, Nauka, 1986, ch. 7. (in Russian)
- [6]. Ermolaev V.L., Sveshnikova E.B. *J. Luminesc.* **20**, 387-395 (1979)
- [7]. Yang Y., von der Osten W., Lüty F., *Phys. Rev. B.* **32**, No 4, 2724-2726 (1985)
- [8]. Ermolaev V.L., Sveshnikova E.B. *Optics. Spectr.* **95**, No 6, 908-913 (2003)
- [9]. Aharoni A., Banin U., Jortner J. at al. *Phys. Rev. Lett.*, **100**, No 5, 057404-1(2008)
- [10]. Payne S.A., Bibeau C., *J. Luminescence.* **79**, No 3, 143-159 (1998)
- [11]. Quochi F., Orru R., Cordella F. at al. *J. Appl. Phys.* **99**, 053520, (2006)

[We-O-29]

Cathodoluminescence study of Y(Ta,Nb)O₄:Tb³⁺-based powder phosphors

A.N. Trofimov¹, M.V. Zamoryanskaya¹, M.V. Nazarov², S.V. Andreev³, A.A. Zaytsev³

¹Ioffe Physical-Technical Institute, 194021, Saint-Petersburg, Russia, 26 Polytechnicheskaya st.

²Department of Materials Science and Engineering, Gwangju Institute of Science and Technology, 1 Oryong-dong, Buk-gu, Gwangju 500-712, Republic of Korea

³St Petersburg Academic University — Nanotechnology Research and Education Centre

The X-ray phosphors (YTaO₄, YNbO₄) present sufficient absorption in X-ray region and emit in the ultraviolet blue region of the electromagnetic spectrum [1,2]. These luminescent materials are efficient X-ray phosphors for X-ray medical imaging, in which the phosphors are used in films/screen cassettes, and also in electronic detector systems such as computed radiography, computed tomography and fluoroscopy [1-4]. YTaO₄ has three crystal structures; high temperature tetragonal (scheelite, T-structure), low temperature monoclinic (fergusonite, M-structure) and another monoclinic form called M' that can be obtained in appropriate conditions [2,5]. M' structure presents more efficient charge transfer process leading to the superior luminescent emission.

In yttrium niobium-tantalate (Y(Ta,Nb)O₄) phosphors under X-ray excitation, the blue light emission is associated with TaO₄³⁻ and/or NbO₄³⁻ groups from the host crystalline lattice [6]. Adding of rare-earth ions such Eu³⁺, Tb³⁺, Gd³⁺, Sm³⁺, Dy³⁺, Pr³⁺ to the composition leads to partial replacing the yttrium ions in the host crystalline lattice. As a result the luminescent emission appears in longer wavelengths.

We have studied the yttrium tantalate/niobate doped with terbium powders.

Powder	Composition*
YTaO ₄ :Tb	Y _{0.95} Tb _{0.05} TaO ₄
Y(TaNb)O ₄ :Tb	Y _{0.95} Tb _{0.05} Ta _{0.85} Nb _{0.15} O ₄
YNbO ₄ :Tb	Y _{0.95} Tb _{0.05} NbO ₄

* Planned at sample making stage

Yttrium tantalate (YTaO₄), yttrium niobium-tantalate (YTaNbO₄) and yttrium niobate phosphors (YNbO₄) activated with Tb³⁺ were prepared by solid state reaction method from homogeneous mixture consisting of Y₂O₃ (99.9%), Ta₂O₅ (Optipur) and Nb₂O₅ (99%). The oxide precursors for the host lattice and Eu₂O₃ were used in the activator system and Na₂SO₄ (99%) as flux. The mixtures were homogenized with a ball mill, in acetone medium, and dried at 70°C. The phosphor samples were baked at 1200°C for 4 h and slowly cooled to room temperature. Finally, the samples were water washed, dried and then sieved.

Luminescent properties of powders were studied by local cathodoluminescence (CL) method. Powders grains sizes were estimated by SEM. The average composition of powders and composition of certain grains were measured by EPMA. The sizes of crystallites and lattice constants were obtained by XRD.

By CL it was defined that powders are heterogeneous. The SEM and EPMA proved heterogeneousness and showed that the grains of powders differ by size and form size fractions (fig.1) with different compositions. The most homogeneous powder is YNbO₄:Tb. But the average compositions are quite equal to the ones planned at sample making stage.

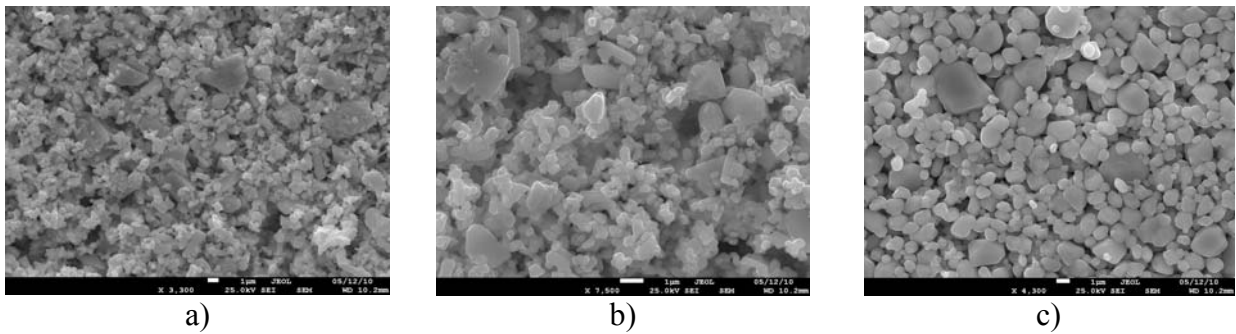


Fig. 1. SEM-images: a) YTaO₄:Tb; b) Y(TaNb)O₄:Tb c) YNbO₄:Tb

It was determined that all samples have the same number of Tb³⁺ emission bands. The emission bands proportion and fine structure of YTaO₄:Tb and Y(TaNb)O₄:Tb are identical, but they differ from the ones of YNbO₄:Tb (fig. 2). The emission spectrum structure of rare-earth ion depends on local symmetry. XRD studies showed that YTaO₄:Tb and Y(TaNb)O₄:Tb have the same crystal structure (lattice parameters differ within error bounds), whereas crystal structure of YNbO₄:Tb notably differs from YTaO₄:Tb and Y(TaNb)O₄:Tb.

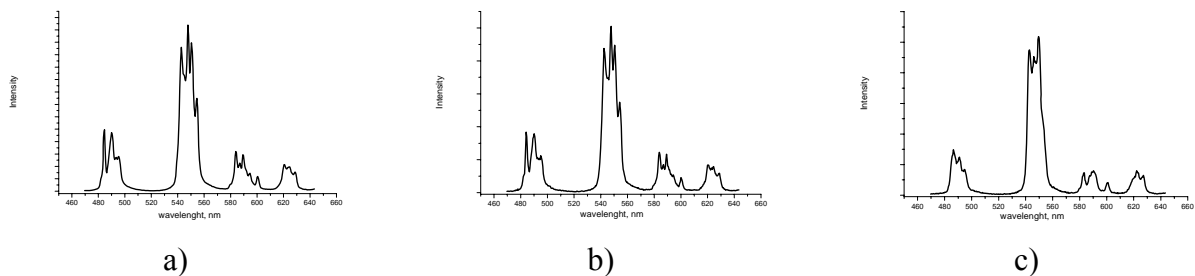


Fig. 2. CL spectra: a) YTaO₄:Tb; b) Y(TaNb)O₄:Tb c) YNbO₄:Tb

The comparison of Tb³⁺ emission bands intensities in equal experimental conditions showed that the sample YTaO₄:Tb have the highest CL intensity. Powders Y(TaNb)O₄:Tb and YNbO₄:Tb have comparable intensities. Measurements of CL decay showed that sample YTaO₄:Tb has the longest decay times of Tb³⁺ emission bands, which means that samples Y(TaNb)O₄:Tb and YNbO₄:Tb have higher probability of nonradiative transition to the ground state. That is why sample YTaO₄:Tb has higher intensity.

So, YTaO₄:Tb powder is the most effective, but very heterogeneous. The powder YNbO₄:Tb has low CL intensity, but is more homogeneous than the others. Adding of moderate quantity of Nb in YTaO₄ matrix (sample Y(TaNb)O₄:Tb) did not change the crystal structure, but increased Tb nonradiative transition probability.

[1] G. Blasse and B.C. Grabmaier, Luminescent Materials, Springer Verlag, Berlin, 1994.
 [2] L.H. Brixner, Mater. Chem. Phys. 16 (1987) 253-281.
 [3] M. Sonoda, M. Takano, J. Miyahara and H. Kato, Radiology, 148 (1983) 833.
 [4] T. S. Curry, J. E. Dowdey and R. C. Murry, Jr., Christensen's Physics of Diagnostic Radiology, Lea and Febiger, 4th edn., 1990.
 [5] G.M. Wolten, The structure of the M'-phase of YTaO₄, a third fergusonite polymorph, Acta Crystallogr. 23 (1967) 939-944.
 [6] G. Blasse and A. Bril, J. Electrochem Soc. 115 (10) (1968), 1067.

[We-O-30]

The formation of stable divalent state of Yb ions in the crystal $\text{Na}_4\text{Y}_6\text{F}_{22}:\text{Ce}^{3+}$, Yb^{3+} after action by intensive UV irradiation

D.I. Tselishev, A.K. Naumov, E.Yu. Koryakina, E.Yu. Gordeev, V.V. Semashko,
S.L. Korableva

Kazan (Volga region) Federal University, Kazan, Russia

In today's world there are active exploratory researches to identify and create new active media for solid-state tunable lasers in the UV spectrum range. Spectroscopic and amplifying properties study shows that fluoride crystals doped with Ce^{3+} ions can be used for this purpose. However, intense coloration of most Ce-activated crystals under the action of pump UV radiation brakes on progress in this area. In this regard, the recent trend in finding ways to suppress the formation of color centers (CC) in the already well-known Ce-activated crystals, which nominally amplify. The most promising method of suppression of the CC formation, at present, is crystallo-chemical [1], there are two approaches exist. In one of them, for these purposes, applies matrix-media variable cation composition. Another approach is Ce-activated crystals co-doped with other ions such as Yb^{3+} for instance. Often for a new UV-active elements creation using both the approaches applies simultaneously for suppressing formation of CC.

Crystal $\text{Na}_4\text{Y}_6\text{F}_{22}:\text{Ce}^{3+}$ (NYF:Ce) was until recently considered as a promising material for a UV-active medium. However, studies of its amplification properties in the "pump-probe" experiments convincingly showed the absence of amplification in this crystal. In these crystals a strong formation of CC by an intensive UV laser radiation were found as a consequence of the large excited state absorption cross section. Moreover with increasing energy density of the pump the individual absorption bands of color centers are bleaching.

When trying to use crystal-chemical approach – co-doping of NYF:Ce by Yb^{3+} ions – to suppress the process of CC formation, crystal shown that long-wave absorption band, which simply can be recorded by the classical spectroscopic methods in crystal NYF:Ce, disappeared. Thus, there was hope that the crystal $\text{Na}_4\text{Y}_6\text{F}_{22}:\text{Ce}^{3+},\text{Yb}^{3+}$ (NYF:Ce,Yb) will amplify UV light. To test this version, a series of pump-probe experiments was made in which laser spark was used as probing radiation source. This source has the continuous spectrum in the region from 200 to 800 nm and the emission duration that repeats the duration of laser pulse. These characteristics of laser spark radiation allowed us to investigate the absorption and luminescence spectra of interconfigurational transitions conditional of RE ions with lifetimes about tens of nanoseconds.

Studies by using this method the crystal NYF:Ce,Yb revealed that the expected amplification in the luminescence region of Ce^{3+} ions is absent, and the absorption spectrum of CC in the long-wave region of the spectrum coincides with that of the crystal NYF:Ce, which registered earlier. Compare with the crystal NYF:Ce in the NYF:Ce,Yb crystal the color centers bleaching begin to appear only at high energy densities the incident UV laser radiation. Absorption spectrum of the crystal NYF:Ce,Yb that were registered over three hours after irradiation by classical spectroscopic method shown, that the long-wavelength part of the CC absorption band was also absented. Thus, we can conclude that in the pump-probe experiment the absorption spectrum of the transient CC was registered.

In addition, in the absorption spectrum of the crystal NYF: Ce, Yb after relaxation all of the CC (about 1000 minutes) besides absorption bands of Ce^{3+} ions in the UV region added intense absorption bands were observed. Their analysis and comparison with literature data showed that these absorption lines belong to the divalent Yb ions [2].

The paper presents results of spectroscopic properties studies of crystals NYF: Ce and NYF: Ce, Yb, before and after exposure to intense UV radiation. In both crystals relaxation times of CC with life times up to several hours were determined. Also it shows the energy density dependence of absorption spectra of transient color centers under different values of the energy density of the incident pump radiation. The result of effect co-doping crystal NYF:Ce by Yb ions on the CC life times, as well as the value of their bleaching under intense pumping, was discussed. The restore transmission at a wavelength of 406 nm in the crystal NYF:Ce³⁺ after termination of pumping radiation was demonstrated. After analyzing experimental data simplified model of the processes that occurs in these crystals under the action of intense laser radiation for crystals NYF: Ce and NYF: Ce, Yb was constructed. On the basis of mathematical model, the cross sections of various transitions of these processes were evaluated and discussed.

This investigation was made in the context and under support of the Federal target program “Scientific and research and educational personnel of innovational Russia”.

- [1] *Spectral-kinetic and photochemical properties of Ce³⁺:Na₄Y_{6-x}Yb_xF₂₂ single crystals*, A.K.Naumov, V.V.Semashko, R.Yu.Abdulsabirov, S.L.Korableva, A.S.Nizamutdinov, E.Yu.Gordeev- in SPIE Proc. Of Int. Reading on Quantum Opt., IRQO'03- 2004 - V.5402. P.430-437.
- [2] *Up and down conversion fluorescence studies on combustion synthesized Yb³⁺/Yb²⁺: MO-Al₂O₃ (M=Ca,Sr and Ba) phosphors*, R.K. Verma et al. - Journal of Luminescence 130 (2010) P.1248–1253.

[We-O-17]

EPR of impurity d-ion complexes in the fluorite type crystals: peculiarities caused by the Jahn-Teller effect on triply degenerated ground orbital state

V.A. Ulanov^{1,2}, M.M. Zaripov², A.D. Siraev¹

¹Kazan State Energetic University, ²Zavoisky Physical Technical Institute RAS

In the fluorite type crystals most of the impurity d-ions, substituting for host lattice cations, form paramagnetic clusters of the type $[\text{MeF}_8]^{k-}(\text{O}_h)$. Some of them occur in the doubly or triply degenerated ground orbital states and, consequently, are the objects displaying the Jahn-Teller effect. As the number of nuclei in the clusters under consideration is 9, some peculiar features in their dynamical properties arise when the impurity d-ions have a triply degenerated ground orbital state.

It was found experimentally by EPR method that practically any Jahn-Teller d-ion in the triply degenerated ground orbital state interacts strongly with lattice vibrations. This interaction leads to a strong deformation of the coordination cube of the d-ion. In the temperature range 4,2-35K, there were observed trigonal (Ag^{2+} in CdF_2 , CaF_2 and SrF_2) and orthorhombic (Cu^{2+} in CdF_2 and CaF_2 , Cr^{2+} in CdF_2 , CaF_2 and SrF_2) static distortions with the central position of an impurity paramagnetic ion. As EPR gave a rich information about parameters of the hyperfine and superhyperfine interactions in the $[\text{AgF}_2\text{F}_6]^{6-}(\text{D}_{3d})$ and $[\text{CuF}_4\text{F}_4]^{6-}(\text{D}_{2h})$ Jahn-Teller complexes, their static molecular structures were determined in details. In these structural investigations a theoretical model of the SHFI parameters was elaborated basing on the MO LCAO approach. It was found that these complexes have adiabatic potentials with a multiwell ground potential sheet. At temperatures $T < 35\text{K}$ the magnetic properties of these complexes could be described by static spin Hamiltonian, but some peculiarities were observed in their EPR spectra at special orientations ($B_0 \parallel \langle 001 \rangle$, $B_0 \parallel \langle 110 \rangle$ and $B_0 \parallel \langle 111 \rangle$). These peculiarities arose due to reorientations of the complex with and without a spin flip.

In some cases the impurity d-ions with triply degenerated ground orbital states were found in the off-center positions of a tetragonal type (Cr^{2+} in BaF_2 and Cu^{2+} in SrF_2 and BaF_2). Due to well resolved hyperfine and superhyperfine structures in the EPR spectra of the $[\text{CuF}_4\text{F}_4]^{6-}(\text{C}_{4v})$ complexes in SrF_2 and BaF_2 crystals, the precise values of the Cu^{2+} off-center shifts were determined (0,95Å in SrF_2 and 1,05Å in BaF_2). As it was found, the potential wells corresponding to the equilibrium positions of the copper and fluorine ions in these off-center complexes were rather deep. As a consequence, at temperatures $T < 100\text{K}$ the tunneling rates were found to be very low. Transitions between these adiabatic wells are accelerated significantly at temperatures $T > 200\text{K}$.

A very interesting type of vibronic interaction demonstrated the paramagnetic centers formed by impurity Ti^{3+} or Ni^{2+} ion and interstitial fluorine F^- . These centers demonstrated vibronic $E \otimes b_2$ and $E \otimes b_1$ interactions, correspondingly, and were produced in the SrF_2 and BaF_2 crystals activated by titanium or nickel in an atmosphere of helium and fluorine. As the interstitial fluorine was found in a tetragonal site, initial symmetry of titanium and nickel associates waited to be C_{4v} . But the symmetries of low temperature magnetic properties of the $[\text{TiF}_4\text{F}_4\text{F}_{\text{int}}]^{6-}$ and $[\text{NiF}_4\text{F}_4\text{F}_{\text{int}}]^{7-}$ clusters were found to be rhombic. The $[\text{TiF}_4\text{F}_4\text{F}_{\text{int}}]^{6-}$ clusters had an effective spin momentum $S = \frac{1}{2}$ and their EPR spectra were observed in a quite wide temperature region (4,2 – 200K). As to the $[\text{NiF}_4\text{F}_4\text{F}_{\text{int}}]^{7-}$ clusters, their EPR spectra could be observed at temperatures $T < 10\text{K}$ only. To account for the properties observed by EPR theoretical models of titanium and nickel clusters were proposed.

[Tu-P-29]

Luminescence study in $\{\text{Bi,Gd}\}_3(\text{Ga,Ti})_5\text{O}_{12}$ single crystalline films

N.V. Vasilieva¹, D.A. Spassky², Yu.V. Ryabchikov³, A.V. Platonova⁴,
V.V. Randoshkin¹, V.N. Kolobanov⁴, V.G. Plotnichenko⁵

¹*Prokhorov General Physics Institute RAS, 119991 Moscow, Russia*

²*Skobeltsyn Institute of Nuclear Physics, M.V. Lomonosov Moscow State University,
119991, Moscow, Russia*

³*Lebedev Physical Institute RAS, 119991 Moscow, Russia*

⁴*Faculty of Physics, M.V. Lomonosov Moscow State University, 119991 Moscow, Russia*

⁵*Fiber Optics Research Center RAS, 119991 Moscow, Russia*

Garnet single crystalline films are used as active optical media for microlasers and also as a material for saturable filters [1,2]. YAG single crystalline films (SCF) doped with rare earth elements and transition metals are extensively used for these applications. However searching for the new compounds with garnet crystal structure for such applications is an actual task. Here we present the results of the investigation of the luminescent properties of $\text{Gd}_3\text{Ga}_5\text{O}_{12}$ (GGG) SCF doped with Ti^{3+} ions.

The luminescence spectra of garnet films were studied using laboratory set-up. Luminescence was excited using xenon lamp with a wavelength 300 nm and 350 nm at a temperature $T = 300$ K. For the luminescence detection LOT-Oriel MS257 spectrograph with a CCD sensor was used. The spectra were corrected for the spectral sensitivity function of the registration route. Epitaxial films were grown by liquid-phase epitaxy in air from a supercooled Bi_2O_3 - B_2O_3 fluxed melts on (111) gadolinium gallium garnet substrates. Seven batches of films were grown from freshly prepared high-temperature solutions containing 0.015, 0.1, 0.5, 1.0, 5.0 and 8.0 mol % TiO_2 and 4.0, 5.0 and 6.0 mol % Gd_2O_3 . It is shown that Bi ions incorporates into the grown SCF therefore forming $\{\text{Bi,Gd}\}_3\text{Ga}_5\text{O}_{12}$ crystals. The maximum of the broad luminescence band of an epitaxial film $\{\text{Bi,Gd}\}_3\text{Ga}_5\text{O}_{12}$ was observed at 480 nm. This band was ascribed to the luminescence of the Bi^{3+} ion.

To the best of our knowledge the luminescence study of $\{\text{Bi,Gd}\}_3(\text{Ga,Ti})_5\text{O}_{12}$ garnet films was performed for the first time. The maximum of the luminescence band of an epitaxial film $\{\text{Bi,Gd}\}_3(\text{Ga,Ti})_5\text{O}_{12}$ has been observed at ~ 483 nm for the low concentrations of TiO_2 at the excitation wavelength 300 nm. With the increase of TiO_2 concentration the band's maximum gradually shifted to the long wavelength region up to 582 nm. The maximum of the luminescence band was observed at 850 nm for an epitaxial film $\{\text{Bi,Gd}\}_3\text{Ga}_5\text{O}_{12}$ under excitation with a wavelength $\lambda = 350$ nm. For an epitaxial film $\{\text{Bi,Gd}\}_3(\text{Ga,Ti})_5\text{O}_{12}$ with concentration 0.015 mol % TiO_2 the luminescence band with maximum at 857 nm was observed, for the SCF with concentration 5 mol % TiO_2 maximum shifted to 592 nm, while for SCF with concentration 8 mol % TiO_2 no luminescence band has been observed under excitation with a wavelength $\lambda = 350$ nm. The nature of the luminescence centers responsible for the observed luminescence and Ti^{3+} concentration effects on the luminescence intensity and spectral distribution are discussed in the presentation.

1. Ferrand B., Chambaz B., Couchaud M. Liquid phase epitaxy: A versatile technique for the development of miniature optical components in single crystal dielectric media // *Optical Materials*, – 1999. - V.11. – P. 101-114.
2. Randoshkin V.V., Vasil'eva N.V., Plotnichenko V.G., Pyrkov Yu.N., Saletzkii A.M., Sysoev N.N., Galkin A.M., Dudorov V.N. Optical absorption in cobalt-containing single-crystal epitaxial films of gadolinium gallium garnets // *Physics of the Solid State—2003*.-V. 45. № 2.- P. 253-258.

[Tu-P-25]

Structural Phase Transformation and Paramagnetic Resonance of the Mn^{4+} , Mn^{2+} , Fe^{3+} , Cr^{3+} and Gd^{3+} Centers in Lanthanum Gallate.

V.A. Vazhenin, V.B. Guseva, A.V. Fokin, A.P. Potapov, M.Yu. Artyomov

*Research Institute of Physics and Applied Mathematics, Ural State University,
620083, Ekaterinburg, Russia*

The interest in investigations of lanthanum gallate and isomorphous $LaMnO_3$ – $LaGaO_3$ solid solutions is connected with the opportunity of preparing solid electrolytes on its base through doping by strontium and transition element ions. Such solid electrolytes are perspective in creation of solid fuel oxygen cells, membranes for oxygen separation and oxygen pumps [1]. Lanthanum gallate is also known as the initial compound for giant magnetoresistance materials [2].

In single crystals of lanthanum gallate slightly doped by manganese we found Mn^{4+} , Mn^{2+} , Fe^{3+} , Cr^{3+} centers in Ga^{3+} position and Gd^{3+} center in La^{3+} position [3-4]. Paramagnetic resonance of these centers at structure phase transition $P_{bmm}(D_{2h}^{16}) \leftrightarrow R\bar{3}c(D_{3d}^6)$ demonstrates the saltatory change of resonance positions, coexistence of phases and temperature hysteresis. Mentioned facts are the evidence of first order structural transformation in $LaGaO_3$.

In two phases of lanthanum gallate we determined spin-Hamiltonian parameters of Fe^{3+} , Mn^{4+} , Cr^{3+} centers. Analysis of orientation behavior of second and fourth rank fine structure parameters let us to determine the rotation angles of oxygen octahedra relative to the perovskite phase structure. The closeness of obtained values with the rotation angles determined by means of the neutron experiments on pure $LaGaO_3$ says about weak deformations of crystal lattice after doping by mentioned ions.

The parameters of the ground state initial splitting of Gd^{3+} center in orthorombic phase was used to obtain the «intrinsic parameters» of the superposition model, which connects the initial splitting parameters with ligand coordinates. The comparison of predictions of two superposition approximations with the experimental results in rhombohedral phases of $LaGaO_3$, $LaAlO_3$, and tetragonal phase of $BaTiO_3$ allowed us draw conclusion about their adequacy.

References:

1. M.S. Khan, M.S. Islam. J. Phys. Chem. B **102**, 3099 (1998).
2. N. Noginova, R. Bah, D. Bitok, V.A. Atsarkin, V.V. Demidov, S.V. Gudenko, J. Phys.: Condens. Matter **17**, 1259 (2005).
3. V.A. Vazhenin, A.P. Potapov, V.B. Guseva, M.Yu. Artyomov. Phys. Solid State **51**, 917 (2009).
4. V.A. Vazhenin, A.P. Potapov, V.B. Guseva, M.Yu. Artyomov. Phys. Solid State **52**, 515 (2010)

[Tu-P-13]
Photoinduced Recharging $Pb^{2+} \rightarrow Pb^{3+}$ in Ferroelectric Lead Germanate

V.A. Vazhenin, A.N. Ivachev, M.Yu. Artyomov, A.P. Potapov

*Research Institute of Physics and Applied Mathematics, Ural State University,
620083, Ekaterinburg, Russia*

The subject of researches [1-5] is holographic recording in ferroelectric $Pb_5Ge_3O_{11}$, where it is shown that the photorefractive sensitivity of these crystals for the slow grating is comparable to that of lithium niobate. The authors [6] obtained evidence of involvement of photoinduced recharging lead host lattice ions in the holographic process, and also defined components of g-tensor for Pb^{3+} ions, parameters of their own and ligand hyperfine interactions with nearby nuclei ^{207}Pb .

In this work, polydomain single crystals of lead germanate doped with Gd, Eu, Fe, Cu, Ag, Si, Cl, F, Br are investigated by the method of paramagnetic resonance. The ions of chlorine, fluorine and bromine were doped into crystals by annealing at a temperature close to the melting point, and formed associations with impurity ions of gadolinium [7]. There is a characteristic EPR spectrum of centres Pb^{3+} after the illumination of samples by xenon lamp or light emitting diode (LED) with an emission peak 410 and 470 nm at a temperature of $100 \div 120$ K. In the case of a xenon lamp spectral intensity saturation occurs within 10 minutes. LED illumination leads to growth of the spectrum for an hour. The maximum concentration of magnetic lead ions is realized in crystals containing fluorine and chlorine, and the minimum - doped with iron.

Increasing the temperature leads to decay (annealing) of Pb^{3+} centres. Measuring the temperature dependence of the decay time allowed us to evaluate the activation energy for this process (0.14 eV). This energy agrees well with the value determined by the authors [6] by measuring the temperature dependence of annealing time by the optical absorption on the transition from the states of Pb^{3+} to the conduction band. An electron-nuclear interaction with more distant nuclei of lead was estimated.

References:

1. W. Krolikowski, M. Cronin-Golomb, B.S. Chen. *Appl. Phys. Lett.* **57**, 7 (1990).
2. X. Yue, S. Mendricks, Y. Hu, H. Hesse, D. Kip. *J. Appl. Phys.* **83** 3473 (1998).
3. X. Yue, S. Mendricks, T. Nikolajsen, H. Hesse, D. Kip, E. Kratzig. *J. Opt. Soc. Am. B* **16**, 389 (1999).
4. S. Mendricks, X. Yue, R. Pankrath, H. Hesse, D. Kip. *Appl. Phys. B* **68**, 887 (1999).
5. O. Gnatovsky, V. Linnik, L. Pryadko. *Semiconductor Physics, Quantum Electronics & Optoelectronics* **4**, 199 (2001).
6. H.J. Reyher, M. Pape, N. Hausfeld. *J. Phys.: Condens. Matter* **13**, 3767 (2001).
7. V.A. Vazhenin, K.M. Starichenko, A.V. Gur'ev, L.I. Levin, F.M. Musalimov. *Sov. Phys. Solid State* **29**, 233 (1987).

[We-P-38]

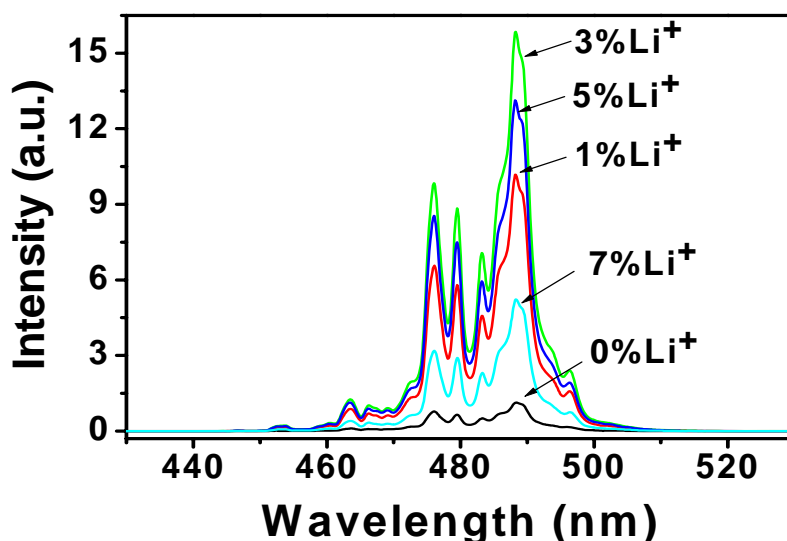
Li-doping Induced Great Enhancement of Upconversion Luminescence in $\text{Y}_2\text{O}_3:\text{Yb}^{3+},\text{Tm}^{3+}$

M. Yin, J. Zhao, X. Wei, Y. Chen, W. Zhang

Hefei National Laboratory for Physical Sciences at Microscale, Department of Physics, University of Science and Technology of China, Hefei 230026, China

Much attention has been centered on the conversion of an IR radiation into visible/ultraviolet spectral range because of its potential applications in a wide range of areas, such as IR sensors, color displays, medical applications, optical storage, and optoelectronics. Among trivalent rare-earth ions, Tm^{3+} is a promising optical activator that opens the possibility for simultaneous blue and ultraviolet emission of laser action. However, after the first report of Auzel in 1966 on the enhancement of upconversion luminescence (UCL) sensitized by Yb^{3+} , to our knowledge, there are no effective routes to improve the UCL by orders of magnitude, which limit the practical application of this kind of upconversion materials. It is therefore imperative to develop more efficient UCL materials.

In this work, $\text{Y}_2\text{O}_3:5\%\text{Yb}^{3+},0.5\%\text{Tm}^{3+}$ with different doping concentrations of Li^+ (0, 1, 3, 5, and 7%) were prepared by a simple sol-gel method. In the synthesis process, the sum of molar quantities of Y^{3+} and Li^+ were strictly kept at 94.5%. The upconversion luminescent properties of the samples were studied under 980 nm excitation. In comparison with $\text{Y}_2\text{O}_3:5\%\text{Yb}^{3+},0.5\%\text{Tm}^{3+}$, a great enhancement of UCL of Tm^{3+} was observed at 300 K for 3% Li-doped powders. To reveal the underlying reason, the temperature dependence of UCL intensity, FT-IR and Raman spectra measurement were carried out. The new phonon induced by Li-doping is observed and is suggested to be responsible for the UCL enhancement. Based on the pertinent phonon-assisted energy transfer rate equations, the conclusion that the phonons with the greatest energy available in Y_2O_3 lattice plays a prominent role in determining the efficiency of multiphonon-assisted upconversion processes is obtained.



UCL spectra of $\text{Y}_2\text{O}_3:5\%\text{Yb}^{3+},0.5\%\text{Tm}^{3+}$ co-doped with 0, 1, 3, 5, and 7% Li^+ ions excited by 980 nm IR-diode laser at room temperature.

[Th-O-39]
Laser-related spectroscopy of Ce³⁺:SrAlF₅ crystals

A.N. Yunusova, A.S. Nizamutdinov, V.V. Semashko, A.K. Naumov, S.L. Korableva, M.A. Marisov

Kazan Federal University, Kremlyovskaja 18, Kazan, 420008, Russia

**E-mail: AzalyU@ya.ru*

Among all UV light sources tunable solid state lasers are most needed system. Opportunity of using of 4f↔5d transition of rare-earth ions in wide-band crystals for UV laser emission was predicted few decades ago [1] but in the doped crystals under pumping condition color centers arise and prevent lasing [2]. Due to color centers formation processes were observed in the SrAlF₅:Ce³⁺ crystals Yb³⁺ ions co-doping were used to suppress them [3].

In this paper spectral-kinetic properties, nonlinear absorption of pumping radiation and net gain characteristic associated with 4f↔5d transitions of Ce³⁺ ions in SrAlF₅ crystals were studied. Trivalent ytterbium co-doping effects on color centers formation processes are studied as well. Besides in the SrAlF₅:Ce³⁺,Yb³⁺ crystals valence reducing of Yb³⁺→Yb²⁺ is find out.

Because of trivalent cerium set on divalent strontium position charge compensation is needed, thus three optical nonequivalent cerium types of centers formation was founded from fluorescence spectra measured at different excitation wavelength at LNT. There is no any energy exchanges between them were observed in the SrAlF₅:Ce³⁺ but in SrAlF₅:Ce³⁺,Yb³⁺ crystal Yb²⁺ ions is an energy donor for all cerium centers and therefore they are fluoresce together. This effects is also exhibit in the results of fluorescence-kinetics measurements and effective Ce³⁺ ions 5d-4f fluorescence lifetimes are vary from 27ns to 60ns depend on studied fluorescence spectral region.

Using pump-probe technique net gain spectrum of SrAlF₅:Ce³⁺,Yb³⁺ crystals due to Ce³⁺ ions 5d→4f transitions were studied for the first time. Net gain value is modest (0.1 cm⁻¹) as far as short-lived color centers still take place even in crystal co-doped by Yb³⁺ ions.

Despite this fact provided chemistry optimization SrAlF₅:Ce³⁺,Yb³⁺ enable to become new effective UV active media.

This investigation was made in the context and under support of the Federal target program “Scientific and research and educational personnel of innovational Russia”.

[1] K.-H. Yang, J. A.DeLuca. UV fluorescence of cerium-doped lutetium and lanthanum trifluorides, potential tunable coherent sources from 2760-3220 Å. – Appl. Phys. Lett., 1977, v.31, P.594 – 596.

[2] D.C.Hamilton Two bad apples.

[3] Semashko V.V., Galyautdinov B.M., Dubinskii M.A., Abdulsabirov R.Yu., Naumov A.K., Korableva S.L., On the improved photochemical stability of solid-state tunable UV material Ce³⁺:LiLuF₄ // Proceedings of the International Conference on LASERS 2000, Albuquerque, NM, STS Press, McLean, VA, 2001, P.668.

[Tu-O-10]

Critical phenomena and femtosecond ordering dynamics associated with electronic and spin ordered phases in YVO₃ and GdVO₃

R.V. Yusupov^{1,2}, D. Mihailovic², C. Colin^{3,4}, G.R. Blake³, T.T.M. Palstra³

¹*Kazan Federal University, Kremlevskaya 18, 420008 Kazan, Russia*

²*Jozef Stefan Institute, Jamova 39, 1000 Ljubljana, Slovenia*

³*University of Groningen, Nijenborgh 4, 9747 AG Groningen, The Netherlands*

⁴*Institut Neel, CNRS & UJF, BP 166, 38042 Grenoble Cedex 9, France*

Results of a systematic study of the electronic and spin excitation dynamics associated with spin and orbital ordering in the complex vanadates YVO₃ and GdVO₃ with ultrafast optical pump-probe reflectance spectroscopy will be presented. Each of the compounds follows a well studied sequence of phase transformations [1,2], but while YVO₃ is found in a single phase state, in GdVO₃ phase separation develops gradually between two spin and orbitally ordered phases below T_N . Experiments were performed with the pump photon energy of ~ 3.10 eV and probe ~ 1.55 eV, both corresponding to the transitions over the Mott-Hubbard gap, in a temperature range of 4.0 - 300 K.

Relaxation dynamics occurs on a different time-scale for each of the ordering transitions, which enables us to unambiguously associate the critical behavior in the dynamics with the observed ordering phenomena. Spin ordering dynamics is observed on two timescales: $\tau_r \sim 2$ ps (risetime) and $\tau_s \sim 300-3000$ ps (decay time), observed below T_N in both compounds. From the temperature-dependence of the dynamics, we observe that in both the G-type and C-type orbitally ordered (OO) phases of YVO₃ spin order develops in a second-order mean-field fashion with the Neel temperature of the C-OO phase found from our data $T_N^C = 83 \pm 7$ K. The orbital order relaxation is associated with the faster components of the reflectivity transients, occurring on the time scales of 25 ± 5 ps in the C-OO and 40 ± 10 ps in the G-OO phases of YVO₃ and 5.3 ± 1.6 ps in the C-OO phase of GdVO₃.

In GdVO₃ we identify the emergence of a new ordered phase within the phase-separated state below 60 K. A new response component with a lifetime of ~ 60 ps is observed below 60 K together with other anomalies in the $\Delta R/R(\Delta t)$ data. This transition takes place under the rare conditions of mesoscopic phase separation, driven presumably with the exchange striction and triggered by lattice instability brought by the elastic strains due to the phase coexistence. This transition was not observed in homogeneous phases of YVO₃, thus it is either a consequence of the phase separation or can only occur in a phase-separated state [3].

[1]. S. Miyasaka, Y. Okimoto, M. Iwama, Y. Tokura. *Phys. Rev. B* **68** 100406 (2003).

[2]. M. H. Sage, G. R. Blake, C. Marquina, T. T. M. Palstra. *Phys. Rev. B* **76** 195102 (2007).

[3]. R. V. Yusupov, D. Mihailovic, C. Colin, G. R. Blake, T. T. M. Palstra. *Phys. Rev. B* **81** 075103 (2010).

[Tu-P-28]

EPR study of the vanadium doped forsterite crystal

R.V. Yusupov¹, I.N. Subacheva¹, A.A. Rodionov¹, N.I. Silkin¹, V.B. Dudnikova², V.F. Tarasov³,
E.V. Zharikov^{4,5}, M.Kh. Salakhov¹

¹*Kazan Federal University, Kremlevskaya 18, 420008 Kazan, Russia*

²*Vernadsky Institute of Geochemistry and Analytical Chemistry of the Russian Academy of Sciences, Kosygina ul. 19, Moscow, 119991 Russia*

³*Zavoisky Physical-Technical Institute of the Kazan Scientific Center of the Russian Academy of Sciences, Sibirskii trakt 10/7, Kazan, 420029 Russia*

⁴*Mendeleev University of Chemical Technology of Russia, Miusskaya pl. 9, Moscow, 125047 Russia*

⁵*Prokhorov General Physics Institute of the Russian Academy of Sciences, Vavilova ul. 38, Moscow, 119991, Russia*

Dielectric crystals doped with the transition metal ions are promising as the active media for the visible and near-IR lasers. In the recent years a possibility of obtaining laser action on forsterite crystals with the impurity of vanadium ions is discussed. Entering the forsterite crystal lattice these ions can possess different oxidation states and occupy different cation sites: either M1 or M2 magnesium positions or the silicon site. M1 and M2 positions are coordinated octahedrally (point groups C_i and C_s , respectively), while silicon is surrounded by oxygen ions forming a distorted tetrahedron (point group C_s).

There are contradicting statements regarding the oxidation state and the site symmetry of the vanadium ions in forsterite in literature. Our intent was to clarify the situation. For this purpose at $T = 10$ K angular dependencies of the X-band EPR spectrum of $Mg_2SiO_4:V$ crystal in three planes perpendicular to the crystallographic axes a , b and c were measured. EPR spectra due to two magnetically-inequivalent centers are observed near $g_{eff} \sim 2$. Spectrum of each center consists of eight hyperfine components typical for the vanadium ions ($I = 7/2$). Fit of the measured angular dependencies of the resonance field allowed us to determine the principal values of g - and A -tensors and corresponding directions relative to crystallographic axes. It turns out that vanadium ions are strongly coupled to the lattice: at $T > 60$ K the EPR spectrum becomes hardly observable due to significant broadening.

Observed EPR spectra arise from the vanadium ions with $S = 1/2$, which corresponds to its tetravalent V^{4+} state. We can claim undoubtedly that the V^{2+} ions are not detected with EPR in the studied crystal. Observation in arbitrary orientation of two magnetically inequivalent centers indicates that vanadium ion occupies either the M2 magnesium position or the silicon site.

Obtained results are in agreement with conclusions of paper [1] that vanadium-doped forsterite crystals grown by the Czochralski technique contain mainly the tetrahedrally coordinated V^{4+} ions.

This work was partially supported by the RFBR grant 09-07-97006 and the grant of the President of the Russian Federation NSh-267.2010.2.

[1] T.F. Veremeichik *et al.*, *Opt. Mat.* **19** 319 (2002).

[We-O-31]

Cathodoluminescence of wide gape crystals doped with rare earth ions

M.V.Zamoryanskaya, A.N.Trofimov, K.N.Guliaeva

Ioffe Physical Technical Institute, St.Petersburg, Russia

Cathodoluminescent method has a number of advantages over traditional optical or luminescent methods. In this case electron beam with energy from 1 to 25 keV excites the optical emission. Such energy of the electron beam is able to excite the optical transitions in wide-gap solid with band-gap more than 5eV (diamonds, oxides and fluoride). The electron beam focuses at less than 1 micron size that provides means for performing local investigation of luminescent properties and getting of cathodoluminescent images. The increasing of electron beam current gives the possibility to change the pumping of emission levels. High sensibility of cathodoluminescence gives the possibility to acquire the low contents of dopants, impurities and defects and to study it's distribution on the sample surface. The region of cathodoluminescence generation depends on the exciting electron energy. It allows obtaining the luminescent spectra from different depths without special training of the samples. Traditionally this method is very popular for study the semiconductors and semiconductors' heterostructures [1]. But it is very effective for insulators investigation too. In this case it is necessary to spray the sample surface by conductive film of carbon or same metals (Al, Cu).

The original cathodoluminescent system used in our experiments [2] allows examining optical characteristics in wide spectral range: from infrared (1 eV) up to ultraviolet (6 eV). There is possibility both to obtain CL images in defocused beam in natural colors (lateral size of such an image is up to 500 μm) and to get CL spectra using focused electron beam 0.1 μm in diameter. Temperature of the sample can be varied in the range from 77 K to 300 K. Moreover our equipment allows to measure time characteristics (rise and decay) of luminescent bands with time resolution about 0.1 μs .

This CL system is connected to electron beam analyzer "Camebax". It lets to combine using of CL system and electron probe microanalysis (EPMA) and enlarges possibilities of solid state investigation. It is very profitable to use both these methods simultaneously when studying laterally inhomogeneous materials.

CL method was successfully used for investigation of oxides ($\text{Y}_3\text{Al}_5\text{O}_{12}$, YAlO_3 , Al_2O_3 , Y_2SiO_5 , YZrO_4) and fluoride (YLiF_4 , BaLiF_3 , KY_3F_{10} , $\text{Na}_{0,4}\text{Y}_{0,6}\text{F}_{2,2}$, $\text{CaF}_2/\text{CdF}_2$) doped with ions of f and d elements. These materials are in use as laser crystals, scintillators, phosphors [3,4,5].

Using of cathodoluminescence technique gives the possibility to investigate the emission from high energy levels of ions (luminescent centers) what couldn't be excited by photoluminescence, the energy transfer between high energy levels, and their time characteristic. On the other hand local cathodoluminescence is applied for studding the homogeneity of the materials (inclusions, distribution of dopants and impurities), valence state of luminescent centers and their local symmetry. It may be very useful for optimization of crystal grow technology.

[1]. V. I. Petrov "Cathodoluminescence Scanning Microscopy"// V. 133 , P. 189

[2]. M.V.Zamoryanskaya, S.G.Konnikov, A.N.Zamoryanski// Instruments and Experimental Techniques, V. 47, N.4, 2004, pp.477-483

[3]. A.N.Trofimov, M.A.Petrova, M.V.Zamoryanskaya// Semiconductors, V41, 2007, pp462-468

[Tu-P-21]

Luminescent properties of lanthanide carboxylates under tunable distortions of Ln^{3+} coordination polyhedron

K. Zhuravlev¹, V. Tsaryuk¹, V. Zolin¹, A. Vologzhanina²

¹ *V.A. Kotelnikov Institute of Radioengineering and Electronics of RAS, 1 Vvedenskii sq., Fryazino Moscow reg., 141190, Russia, vit225@ire216.msk.su*

² *A.N. Nesmeyanov Institute of Organoelement Compounds of RAS, 28 Vavilov str., Moscow, 119991, Russia*

A systematic comparison of the spectroscopic and structural data for series of related dimeric lanthanide carboxylates with 1,10-phenanthroline $\text{Ln}(\text{RCOO})_3 \cdot \text{Phen}$ ($\text{Ln} = \text{Eu}, \text{Gd}, \text{Tb}$): naphthylcarboxylates, trimethylacetates, benzoates, 2-, 3-, and 4-methoxybenzoates, 3,5-dinitrobenzoates, 2-furancarboxylates, phenoxyacetates, acetates, propionates, caproates, 3-nitropropionates was undertaken in search for methods of regulation of quantum yield of the Ln^{3+} luminescence and for paths of control of the excitation energy transfer [1-5]. Some lanthanide carboxylates with 2,2'-bipyridine were also investigated. The influence of gradual distortions of the lanthanide coordination polyhedron (taken as three-capped trigonal prism) derived from X-ray data of succession of compounds [6] on luminescence spectra, lifetimes of $^5\text{D}_0$ (Eu^{3+}) and $^5\text{D}_4$ (Tb^{3+}) electronic states, features of the excitation energy transfer from the ligands to Ln^{3+} ions and efficiency of luminescence was examined. 15 dimeric crystal structures were chosen for this study. To extend the series of compounds investigated the crystal structures of europium propionate and europium and terbium nitropropionates were solved by X-ray diffraction methods.

Relative contributions of the rates of radiative and nonradiative processes to the lifetimes of Ln^{3+} excited states were estimated. An efficiency of various nonradiative processes: multiphonon relaxation, the quenching through ligand-metal charge transfer states in europium compounds, the quenching by back energy transfer from the metastable level of Ln^{3+} ion to the ligand lowest triplet state and the Ln-Ln self-quenching in dimers was analyzed. To estimate contributions of multiphonon relaxation to the lifetimes some compounds with deuterium substituted ligands were investigated. The lifetime of $^5\text{D}_0$ (Eu^{3+}) state in the temperature interval from 77 to 295 K and the lifetime of $^5\text{D}_4$ (Tb^{3+}) state at low temperatures are mainly determined by radiative processes and depend on details of the charge distribution in the nearest surroundings of the Ln^{3+} ion that are connected with distortions of coordination polyhedron. Ln^{3+} polyhedron distortions were obtained from X-ray data [6]. They are primarily caused by the range of the Ln-O bond lengths related to bridging-cyclic carboxylic group that depends on the type and the size of carboxylate anion. At prominent polyhedron distortions in compounds with voluminous carboxylate anions the rates of the radiative processes become higher and the intensity of $\text{Eu}^{3+} \ ^5\text{D}_0 \rightarrow ^7\text{F}_2$ hypersensitive transition increases.

Multiphonon relaxation is the main nonradiative process in europium compounds at 77 - 295 K temperatures and in terbium compounds at low temperatures, but the radiative processes are appreciably prevailing. Dependence of the lifetimes due to natural radiative processes determined from the total integral intensity of europium $^5\text{D}_0 \rightarrow ^7\text{F}_1$ transitions related to the intensity of magnetic-dipole $^5\text{D}_0 \rightarrow ^7\text{F}_1$ transition (see, for example, [7]) on distortions of Eu polyhedron in the sequence of compounds is in agreement with the same dependence obtained from the measured lifetimes, if nonradiative processes are taken into account.

A back energy transfer from $^5\text{D}_4$ state of Tb^{3+} ion to the lowest triplet state related to phenanthroline molecule in most of compounds is the principal nonradiative process contributing noticeably to quenching in terbium compounds at high temperatures. An influence of this process on intrinsic

quantum yield of luminescence can be predominant. In particular, it leads to fourfold decrease in the intensity of terbium benzoate in transition from 77 to 295 K. It was found, that the lifetime of 5D_4 (Tb^{3+}) state and the luminescence efficiency of terbium compounds at high temperatures depend noticeably on the bonding strength of phenanthroline molecule with Ln^{3+} ion.

Thus, to increase the probability of induced electric-dipole transitions, first of all, hypersensitive transitions in the lanthanide carboxylates with heterocyclic diimines, one needs to create substantial distortions of Ln coordination polyhedron through bridging-cyclic carboxylic groups with the help of voluminous carboxylate ligands. At the same time, to decrease the influence of the back energy transfer processes on the quantum yield of luminescence, relatively small changes in the Ln-N bond strengths are sufficient.

The energy of the lowest excited triplet state of the ligands was obtained from gadolinium phosphorescence spectra recorded with time delay. In dimeric carboxylates $Ln(RCOO)_3 \cdot Phen$, a range of the phenanthroline triplet state energy from 20850 to 22100 cm^{-1} was demonstrated in dependence on the type of carboxylate anion. That points to necessity of measurements of the triplet energy in every particular case of analysis of processes of the energy transfer.

Closeness of the radiative (natural) lifetimes of 5D_0 and 5D_4 metastable states of Eu^{3+} and Tb^{3+} ions, respectively, located in the same crystal field was demonstrated. That is, the experimental rate of Eu^{3+} radiative processes can be used for evaluation of the intrinsic quantum yield of luminescence of Tb^{3+} ions, and then, for evaluation of the overall quantum yield.

The work was supported by the Russian Foundation for Basic Research (Grant No. 08-02-00424-a).

- [1]. V. Tsaryuk, K. Zhuravlev, A. Vologzhanina V. Kudryashova, V. Zolin, J. Photochem. Photobiolog. A: Chem. 211 (2010) 7.
- [2]. K. Zhuravlev, V. Tsaryuk, V. Kudryashova, I. Pekareva, J. Sokolnicki, Yu. Yakovlev, J. Lumin. 130 (2010) 1489.
- [3]. K. Zhuravlev, V. Tsaryuk, V. Kudryashova, V. Zolin, Yu. Yakovlev, J. Legendziewicz, Spectrochim. Acta A 72 (2009) 1020.
- [4]. V. Tsaryuk, K. Lyssenko, K. Zhuravlev, V. Zolin, V. Kudryashova, I. Pekareva, Z. Klemenkova, J. Rare Earths 27 (2009) 539.
- [5]. V. Tsaryuk, K. Zhuravlev, V. Kudryashova, V. Zolin, J. Legendziewicz, I. Pekareva, P. Gawryszewska, J. Photochem. Photobiolog. A: Chem. 197 (2008) 190.
- [6]. Cambridge Structural Database System, www.ccdc.cam.ac.uk
- [7]. M.H.V. Werts, R.T.F. Jukes, J.W. Verhoeven, Phys. Chem. Chem. Phys. 4 (2002) 1542.

Contents

<u>D.A. Akhmetzhanov, V.B. Dudnikova, A.A. Konovalov, V.F. Tarasov, E.V. Zharikov</u> Effect of ionizing radiation on structure and valence state of impurity chromium ions in synthetic forsterite as studied by tunable high-frequency EPR spectroscopy	24
<u>L.K. Aminov, A.A. Ershova, S.L. Korableva, I.N. Kurkin, B.Z. Malkin, A.A. Rodionov</u> Super-hyperfine structure of EPR spectra of impurity ions with 4f and 5f electrons in double fluorides LiRF_4 (R=Y, Lu, Tm)	25
<u>L. Andrade, S. Lima, A. Novatski, A. Steimacher, M.P. Belançon, A. Neto, A. Bento, M. Baesso, Y. Guyot, G. Boulon</u> Research of circadian response for white lighting with Ce^{3+} -doped glass phosphor and UV/blue LEDs	26
<u>R.R. Andronenko, S.I. Andronenko</u> EPR study of solid solution $\text{La}_{1-0.33y}\text{Ba}_{0.33y}\text{Mn}_y\text{Al}_{1-y}\text{O}_3$ ($y = 0.02; 0.04; 0.10$)	27
<u>R.R. Andronenko, S.I. Andronenko</u> Spin dynamics and low symmetry effects in Gd^{3+} EPR spectra of single crystal of EuAlO_3	28
<u>S. Anghel, G. Boulon, L. Kulyuk, S. Klokishner, K. Sushkevich</u> Luminescence of co-dope $\alpha\text{-ZnAl}_2\text{S}_4$ spinel type single crystals	29
<u>O.A. Anikeenok</u> First-principles calculations of hyperfine interactions in ions crystals	30
<u>H.R. Asatryan, V.A. Khrantsov, D.V. Kramushchenko, A.A. Gurin</u> Electron paramagnetic resonance of Dy^{3+} ions in a PbGa_2S_4 single crystals	31
<u>H.R. Asatryan, V.S. Vikhnin, T.I. Maksimova, M. Maczka, J. Hanuza</u> Mechanisms of the local structural transition of MnO_4^{2-} molecular ion in the $\text{K}_3\text{Na}(\text{CrO}_4)_2$ ferroelastic	32
<u>V. Aseev, E. Kolobkova, N. Nikonorov, E. Korchagin, V. Golubkov, K. Moskaleva</u> Spectral and luminescent properties and energy transfer of lead-fluorine nanoglassceramics doped with erbium and ytterbium	33
<u>V. Aseev, E. Kolobkova, N. Nikonorov, A. Yasukevich, N. Kuleshov, K. Moskaleva</u> Spectral and luminescent properties of lead-fluorine nanostructured glassceramics doped with erbium	34
<u>A.G. Badalyan, P. Galinetto, A.S. Gurin, M.C. Mozzati, V.A. Trepakov, J. Rosa, L. Jastrabik</u> The Charge Transformation of Chromium Ion Impurity under light and thermal annealing in SrTiO_3 Single Crystals Studied by EPR	35
<u>E.I. Baibekov, I.N. Kurkin, M.R. Gafurov, R.M. Rakhmatullin, G.V. Mamin</u> Coherence times and Rabi oscillations of Cr^{5+} ions in CaWO_4	36
<u>B. Barbara</u> Decoherence in “molecule magnets” and “spin-orbit” qubits	38

<u>V.I.Baryshnikov, A.V.Bolondz, D.V.Sannikova</u>	39
Pulse excitation of cerium doped crystals	
<u>T.T. Basiev, M.E. Doroshenko</u>	40
Spectroscopy and laser oscillations in low phonon crystals and ceramics	
<u>K.N. Boldyrev, B.N. Mavrin, L.N. Bezmaternykh</u>	42
Raman, infrared, and vibronic spectra of YbAl ₃ (BO ₃) ₄	
<u>G. Boulon, W. Zhao, S. Anghel, C. Mancini, D. Amans, T. Epicier, V. Chani, A. Yoshikawa</u>	43
Rare earth dopant segregation in optical ceramics	
<u>T. Chanelière, M. Bonarota, V. Damon, R. Lauro, J. Ruggiero, R.C. Tongning, J.-L. Le Gouët</u>	44
Quantum light storage in rare-earth doped crystals: large multiplexing capacity of Tm:YAG.	
<u>V.A. Chernyshev, A.E. Nikiforov, A.D. Nazemnykh, S.V. Gastev, N.S. Sokolov</u>	46
Calculation of Sm ³⁺ optical spectra in CaF ₂ :Sm strained epitaxial layers on silicon	
<u>V.A. Chernyshev, A.E. Nikiforov, V.P. Volodin</u>	47
Optical spectrum of Yb ³⁺ impurity cluster in CaF ₂	
<u>E.P. Chukalina, M.N. Popova, M.A. Kaschenko, R.V. Pisarev</u>	48
Spectroscopic study of multiferroic TbMn ₂ O ₅	
<u>E.P. Chukalina, D.S. Pytalev</u>	49
Resolved hyperfine structure in optical spectra of KY ₃ F ₁₀ :Ho ³⁺	
<u>Y.A. Dziashko, A.M. Zaitsev, Mengbing Huang, A.A. Gorokhovskiy</u>	50
Micro-luminescence spectroscopy of Xe optical center in diamond	
<u>A.M. Efimov, A.I. Ignatiev, N.V. Nikonorov, E.S. Postnikov</u>	51
Ce(III)- and Ce(IV)-related spectral components observable in the UV absorption spectra of photo-thermo-refractive glass matrices	
<u>M.V. Eremin, J. Deisenhofer, M. A. Fayzullin, Ch. Kant, A. Loidl</u>	53
Exchange-induced magnetic dipole mechanism of magnon sideband in KCuF ₃	
<u>V.L. Ermolaev, E.B. Sveshnikova, S.S.Dudar'</u>	54
Accumulation of excitation energy nanoparticles from Ln(III) complexes at dye molecule admixture.	
<u>M.L. Falin, K.I. Gerasimov, B.Z. Malkin, N.M. Khaidukov</u>	56
Optical and radio frequency optically detected EPR spectroscopy of Sm ³⁺ in Cs ₂ NaYF ₆ cubic crystal	
<u>S.G. Fedorenko, Yu.V. Orlovskii, E.V. Samsonova</u>	57
The many-particle kinetics of the hopping luminescence quenching in disordered solid solutions	
<u>S.P.Feofilov, D.V.Arsentyev, A.B.Kulinkin, R.I.Zakharchenya, T.Gacoin, G.Mialon, R.S.Meltzer, C.Dujardin</u>	59
Gaseous environment-sensitive fluorescence of Ce ³⁺ impurity ions in nanocrystals	

<u>A.S. Galkin, S.A. Klimin, E.P. Chukalina, M.N. Popova, B.V. Mill</u>	60
Optical spectroscopy of the chain nickelate Sm ₂ BaNiO ₅ :crystal-field interactions and magnetic ordering	
<u>S.V.Gastey, V.A.Chernyshev, J.K.Choi, A.V.Krupin, N.S.Sokolov, A.D. Nazemnykh</u>	61
Laser piezospectroscopy of Sm ³⁺ ions in fluorite epitaxial layers	
<u>L.R.Gilyazov, S.I.Nikitin</u>	63
Optical spectroscopy of LaGaO ₃ crystal doped with Mn ions	
<u>L.E. Gonchar, A.E. Nikiforov, Yu.V. Leskova, A.A. Firsin, D.P. Kozlenko</u>	65
Pressure dependence of crystal, orbital, and magnetic structures of LaMnO ₃ and LaMn _{0.5} Ga _{0.5} O ₃	
<u>A.D. Gorlov, D.A. Gorlov</u>	66
Temperature dependences of the second rank parameters b_2^0 and P_2^0 for the odd isotopes Gd ³⁺ in PbMoO ₄ and YVO ₄	
<u>V.V.Gudkov, I.V.Zhevstovskikh</u>	67
Adiabatic potential in ZnSe:Fe ²⁺ crystal reconstructed in an ultrasonic experiment	
<u>K.N. Guliaeva, A.N. Trofimov, M.V.Zamoryanskaya</u>	69
Cathodoluminescent properties of YAG:Nd ³⁺	
<u>V. Hizhnyakov</u>	71
Zero-phonon lines: novel manifestations of vibronic interactions in impurity centers of solids	
<u>L. Hu, M.F. Reid, C.-K. Duan, S. Xia, M. Yin</u>	72
Calculation of crystal-field parameters for 4f and 5d states of lanthanide ions from ab-initio calculations	
<u>R. Hughes-Currie, M.F. Reid, J. Grimm, H.U. Güdel</u>	73
Calculations of energy levels, dynamics, and lifetimes of 4f ¹² 5d states of Tm ²⁺ in SrCl ₂	
<u>S.E. Ivanova, A.M. Tkachuk, A. Mirzaeva, F. Pellé</u>	74
Selfquenching in Tm-doped Sodium-Yttrium double fluoride crystals (Tm:NYF)	
<u>S.E. Ivanova, A.M. Tkachuk, F. Pellé, L.I.Isaenko, M.-F. Joubert, Y. Guyot</u>	75
Luminescence and energy transfer in RE ³⁺ :KPb ₂ Cl ₅ crystals at UV excitonic and RE direct excitation	
<u>S. Ivanova, F. Pellé, A.M. Tkachuk</u>	77
Upconversion absolute efficiency in Er doped Calcium-Yttrium double fluoride crystal	
<u>A.M. Kalashnikova, S.A. Basun, A.S. Moskvina, A.A. Nugroho, T.T.M. Palstra, Th. Rasing, R.V. Pisarev</u>	79
The origin of the 1.6 eV absorption band in the rare-earth hexagonal manganites RMnO ₃ and YMn _{1-x} Ga _x O ₃	
<u>A.M. Karpov, M.G. Zuev</u>	81
Laser spectroscopy of two centre of Eu ³⁺ in silicate with apatite structure	

<u>S.A. Klimin, A.B. Kuzmenko, M.N. Popova, B.Z. Malkin</u>	83
Phonon-assisted magnetic absorption in low-dimensional magnetic systems. Optical data on Gd ₂ BaNiO ₅	
<u>E.Yu. Koryakina, A.K. Naumov, D.I. Tselishev, S.L. Korableva, V.V. Semashko</u>	84
Impact of Yb ³⁺ - co doping on spectroscopic properties dynamic of color centers in KY ₃ F ₁₀ :Ce ³⁺ crystals.	
<u>E.Yu. Koryakina, A.K. Naumov, D.I. Tselishev, S.L. Korableva, V.V. Semashko</u>	86
Spectroscopic properties of color centers in crystals KY ₃ F ₁₀ : Ce and KY ₃ F ₁₀ : Ce, Yb	
<u>T.A.Kudykina, A.I.Pervak.</u>	87
Visible luminescence of nanocrystals	
<u>Ya. V. Kuznetsova, B. E. Burakov, A. N. Trofimov, V. P. Usacheva, M. V. Zamoryanskaya</u>	89
Luminescent properties of Am in yttrium aluminum garnet	
<u>I.I. Leonidov, V.G. Zubkov, A.P. Tyutyunnik, N.V. Tarakina, L.L. Surat</u>	90
Upconversion luminescence in Er ³⁺ /Yb ³⁺ codoped Y ₂ CaGe ₄ O ₁₂	
<u>M. Lezhnina, M. Bentlage, U. Kynast</u>	91
Luminescent Properties of Rare Earth Ions in Nanoscaled Layer Structures	
<u>M. Lezhnina, U. Kynast</u>	92
Rare earth fluoride species in zeolite hosts	
<u>V.I. Lukanin, D.S. Chunaev, A.Ya. Karasik</u>	93
Two-photon picosecond absorption dynamics in MeWO ₄ crystals (Me=Zn, Pb, Ca, Sr, Ba)	
<u>Ch. Lushchik, I. Kudryavtseva, T. Kärner, A. Lushchik, F. Savikhin, E. Vasil'chenko</u>	94
Low-temperature study of intrinsic electronic excitations in wide-gap materials using luminescent RE ³⁺ and Cr ³⁺ impurity ions	
<u>B.Z. Malkin, O.V. Solovyev, V.N. Makhov, G. Stryganyuk, M. Kirm, E. Garcia Villora, K. Shimamura</u>	96
Interconfigurational 4f ⁿ - 4f ⁿ⁻¹ 5d spectra of Pr ³⁺ and Tm ³⁺ in LiLuF ₄ host	
<u>K. Moskaleva, V. Aseev, E. Kolobkova, N. Nikonorov, E. Korchagin, V. Golubkov</u>	97
Upconversion luminescence in ytterbium-sensitized praseodymium-doped LEAD-Fluorine nanoglassceramics	
<u>A.S. Moskvina</u>	98
Cluster theory of the charge transfer excitations in strongly correlated oxides	
<u>I.E. Mumdzhi, S.L. Korableva, S.I. Nikitin</u>	99
Site-selective spectroscopy of BaF ₂ :Yb ³⁺ crystals	
<u>A.Myasnikova, E. Radzhabov, A. Mysovsky</u>	101
Anomalous luminescence in CaF ₂ :Yb ²⁺ crystal from ab initio calculations	

<u>M.V. Narozhnyy, S.A. Klimin, M.N. Popova, T. Lummen, P.H.M. van Loosdrecht, G. Dhalenne</u>	102
Terbium low-lying energy levels in pyrochlore structure (Tbx R1-x)2Ti2O7 studied by optical spectroscopy	
<u>S.I. Nikitin, I.N. Subacheva, R.V. Yusupov</u>	103
Optical studies of the uniaxial stress-induced alignment of Jahn-Teller Cr ²⁺ centers in KZnF ₃ crystal	
<u>N. Nikonorov, V. Aseev, A. Ignatiev, A. Kim, E. Kolobkova, P. Shershnev, A. Sidorov, V. Tsekhomsky</u>	105
New nanoglassceramics doped with rare earth and transition metal ions: optical, spectral and luminescent properties	
<u>A.S. Nizamutdinov, S.A. Kirysheva, V.V. Semashko, A.K. Naumov, S.L. Korableva, E.Yu. Gordeev</u>	107
Pump-probe experiments with CaF ₂ :Ce ³⁺ +Yb ³⁺ crystals	
<u>L. Nurtdinova, V. Semashko, Y. Guyot, S. Korableva, M.-F. Joubert</u>	108
Photoconductivity measurements in Ce ³⁺ -doped fluorides	
<u>I.N. Ogorodnikov, N.E. Poryvay, I.N. Sedunova, A.V. Tolmachev, R.P. Yavetskiy</u>	109
Luminescence and recombination processes in Li ₆ Gd _x Y _{1-x} (BO ₃) ₃ :Eu bulk crystals	
<u>I.N. Ogorodnikov, N.E. Poryvay, I.N. Sedunova, A.V. Tolmachev, R.P. Yavetskiy, V.Yu. Yakovlev</u>	110
A transient optical absorption spectroscopy of Li ₆ Re(BO ₃) ₃ crystals	
<u>Yu.V. Orlovskii, T.T. Basiev, E.V. Samsonova, N.A. Glushkov</u>	111
Energy transfer probe for characterization of luminescent photonic crystals morphology	
<u>A.S. Paklin, A.S. Mysovsky, A.A. Shalaev</u>	113
Experimental and theoretical research of LiF:Cu	
<u>V.A. Panfilov, A.V. Potapov, S.A. Klimin</u>	115
Percolation threshold for magnetic binding in the structure of the Haldane chain nickelates R ₂ BaNiO ₅	
<u>V.V. Pavlov, V.V. Semashko, A.K. Naumov, S.L. Korableva, L.A. Nurtdinova, A.S. Nizamutdinov</u>	116
ESA and activator ions photoionization spectra investigations of Ce:YLF and Ce:LiLuF ₄ single crystals	
<u>C. Pedrini, A. Belsky, A. Petrosyan, R.V. Sargsyan, I. Kamenskikh</u>	118
Parallel between rare earth-trapped exciton and charge transfer in rare earth doped crystals	
<u>F. Pellé, L. Caillat, A. Tadili, B. Hajj, D. Chauvat, J. Zyss</u>	119
Rare earth doped nanoparticles for high resolution imaging	
<u>E.V. Pestryakov, V.V. Petrov, V.I. Trunov, A.V. Kirpichnikov, M.A. Merzliakov, E.N. Galashov, V.N. Shlegel, J.V. Vasiliev</u>	120
Spectroscopic and laser properties of trivalent ytterbium ions in ZnWO ₄ crystal	
<u>R.V. Pisarev</u>	121
Particular features of electronic structure in multiferroic oxides	

<u>R.V. Pisarev, V.V. Pavlov, A.M. Kalashnikova, A.S. Moskvina</u>	123
Near-band gap electronic structure of the tetragonal rare-earth and bismuth cuprates	
<u>M.N. Popova</u>	124
High-resolution spectroscopy of rare-earth orthoborates: crystal-field and anisotropic f-d exchange interactions defects	
<u>K.K. Pukhov, T.T. Basiev, Yu.V. Orlovskii</u>	125
Radiative properties of the nanocrystals doped with lanthanide and transition ions	
<u>L.N. Puntus, K.A. Lyssenko, I.S. Pekareva</u>	127
Influence of the additional excited states on energy transfer processes in lanthanide-containing compounds	
<u>E.A. Radzhabov, E.A. Prosekina</u>	128
5d-4f emission of Nd ³⁺ , Er ³⁺ , Tm ³⁺ , Gd ³⁺ ions in alkaline earth fluorides	
<u>M.F. Reid</u>	129
Structure and dynamics of high-energy states in lanthanide materials	
<u>P.A. Rodnyi, E.I. Gorokhova, S.B. Eron'ko, V.A. Demidenko, S.B. Mikhrin, S.D. Gain</u>	130
Spectral and decay time properties of Pr, Tb, Eu doped Gd ₂ O ₃ ceramics	
<u>A.I. Ryskin, A.S. Shcheulin, A.E. Angervax</u>	131
Color centers in fluorite crystals: the hystory and present state	
<u>K.M. Salikhov, A.A. Sukhanov, V.F. Tarasov, R.B. Zaripov, E.V. Zharikov</u>	132
Anomalous line shape of EPR spectra of impurity Ho ³⁺ ion in synthetic forsterite	
<u>G.S. Shakurov, I.I. Fazlizhanov, V.A. Shustov, A.G. Okhrimchuk, N.V. Lichkova, V.N. Zagorodnev</u>	133
Multifrequency EPR study of Dy ³⁺ ions in RbPb ₂ Cl ₅	
<u>G.S. Shakurov, T.A. Shcherbakova, V.A. Shustov</u>	134
Terahertz EPR-spectroscopy of Fe ²⁺ ions in the natural and synthetic forsterite	
<u>A.S. Shcheulin, T.S. Semenova, M.A. Petrova, L.F. Koryakina, A.E. Angervax, A.I. Ryskin</u>	135
Additive coloration of CaF ₂ :Sm crystals	
<u>R. Shendrik, E. Radzhabov</u>	136
5d-4f emission and scintillation properties of SrF ₂ -Pr ³⁺ and SrF ₂ -Ce ³⁺ crystals	
<u>V.M. Sitdikov, N.V. Nikonorov, A.K. Przhhevuskii</u>	137
Monte-Carlo simulation of energy transfer processes for inhomogeneous activator distribution	
<u>T.Y. Sizova, E.A. Radzhabov</u>	138
The investigation of photochromism in CaF ₂ , SrF ₂ , BaF ₂ .	
<u>A.P. Skvortsov, V.A. Trepakov, N.K. Poletaev, Z Potucek, V.V. Laguta, L. Jastrabik</u>	139
Er centers in KTaO ₃ : optical and EPR spectroscopy study	

<u>V. I. Sokolov, A. V. Druzhinin, N. B. Gruzdev, A. Dejneka, O. Churpita, Z. Hubicka, L. Jastrabik, V. Trepakov</u> Excitons in the thin films of $Zn_{1-x}Mn_xO$ ($x=0-0.06$)	140
<u>V.I. Sokolov, V.A. Pustovarov, A.N. Baranov, P.S. Sokolov, N.B. Gruzdev</u> Photoluminescence of $Zn_{1-x}Ni_xO$ solid solutions with NaCl-type symmetry	141
<u>V.I. Sokolov, V.A. Pustovarov, N.B. Gruzdev, V.T. Surikov</u> Photoluminescence and photoluminescence excitation spectroscopy of ZnO doped with Co and Ni	142
<u>O.V. Solovyev, V.N. Makhov, G. Stryganyuk, M. Kirm</u> Non-Condon optical spectra of impurity centers in crystals at finite temperatures: theory and experiment	143
<u>V.A. Soltamov, I.V. Ilyin, A.A. Soltamova, E.N. Mokhov, P.G. Baranov</u> Identification of the deep level defects in bulk AlN: EPR studies	145
<u>N.P. Soshchin</u> Spectroscopy of an ion Ce^{+3} as probe of the composition multiligande garnets	147
<u>N.P. Soshchin, V.N. Lichmanova, V.A. Bol'shuhin</u> Silicate photoluminophor for conversion of radiation of nitride light-emitting diodes	149
<u>T.N. Stanislavchuk, K.N. Boldyrev, M.N. Popova, B.Z. Malkin</u> Optical and far-infrared spectroscopy of multiferroic $EuFe_3(BO_3)_4$	150
<u>A. Steimacher, M.P. Belançon, A.N. Medina, L. Baesso, L.H.C. Andrade, S. Lima, R. Peretti, A.M. Jurdyc, A. Brenier, Y. Guyot, G. Boulon</u> Spectroscopic, laser investigations and concentration quenching of two Yb^{3+} -doped OH- free calcium aluminosilicate laser glasses	151
<u>W. Strek, L. Marciniak, A. Bednarkiewicz, A. Lukowiak, R.J. Wiglusz, D. Hreniak</u> Fluorescence and visible upconversion in heavily doped $LiNd_xLa_{1-x}P_4O_{12}$ nanocrystallines powders	153
<u>G. Stryganyuk, T. Shalapska, I. Pashyk, A. Voloshinovskii, A. Krasnikov, S. Zazubovich</u> Time-resolved spectroscopy of Ce^{3+} -doped alkali gadolinium phosphates	154
<u>I.N. Subacheva, A.A. Rodionov, R.V. Yusupov, V.A. Trepakov, P.P. Syrnikov, A.I. Gubaev, M.Kh. Salakhov</u> Photoinduced complexes in $KTa_{0.988}Nb_{0.012}O_3$ crystals: EPR study	155
<u>E.B. Sveshnikova, V.L. Ermolaev</u> Inductive-resonant theory of nonradiative transitions in lanthanide and transition metal ions	156
<u>A.N. Trofimov, M.V. Zamoryanskaya, M.V. Nazarov, S.V. Andreev, A.A. Zaytsev</u> Cathodoluminescence study of $Y(Ta,Nb)O_4:Tb^{3+}$ -based powder phosphors	157

- D.I. Tselishev, A.K. Naumov, E.Yu. Koryakina, E.Yu. Gordeev, V.V. Semashko, S.L. Korableva** 159
The formation of stable divalent state of Yb ions in the crystal $\text{Na}_4\text{Y}_6\text{F}_{22}$: Ce^{3+} , Yb^{3+} after action by intensive UV irradiation
- V.A. Ulanov, M.M. Zaripov, A.D. Siraev** 161
EPR of impurity d-ion complexes in the fluorite type crystals: peculiarities caused by the Jahn-Teller effect on triply degenerated ground orbital state
- N.V. Vasilieva, D.A. Spassky, Yu.V. Ryabchikov, A.V. Platonova, V.V. Randoshkin, V.N. Kolobanov, V.G. Plotnichenko** 162
Luminescence study in $\{\text{Bi,Gd}\}_3(\text{Ga,Ti})_5\text{O}_{12}$ single crystalline films
- V.A. Vazhenin, V.B. Guseva, A.V. Fokin, A.P. Potapov, M.Yu. Artyomov** 163
Structural Phase Transformation and Paramagnetic Resonance of the Mn^{4+} , Mn^{2+} , Fe^{3+} , Cr^{3+} and Gd^{3+} Centers in Lanthanum Gallate.
- V.A. Vazhenin, A.N. Ivachev, M.Yu. Artyomov, A.P. Potapov** 164
Photoinduced Recharging $\text{Pb}^{2+} \rightarrow \text{Pb}^{3+}$ in Ferroelectric Lead Germanate
- M. Yin, J. Zhao, X. Wei, Y. Chen, W. Zhang** 165
Li-doping Induced Great Enhancement of Upconversion Luminescence in $\text{Y}_2\text{O}_3:\text{Yb}^{3+}, \text{Tm}^{3+}$
- A.N. Yunusova, A.S. Nizamutdinov, V.V. Semashko, A.K. Naumov, S.L. Korableva, M.A. Marisov** 166
Laser-related spectroscopy of $\text{Ce}^{3+}:\text{SrAlF}_5$ crystals
- R.V. Yusupov, D. Mihailovic, C. Colin, G.R. Blake, T.T.M. Palstra** 167
Critical phenomena and femtosecond ordering dynamics associated with electronic and spin ordered phases in YVO_3 and GdVO_3
- R.V. Yusupov, I.N. Subacheva, A.A. Rodionov, N.I. Silkin, V.B. Dudnikova, V.F. Tarasov, E.V. Zharikov, M.Kh. Salakhov** 168
EPR study of the vanadium doped forsterite crystal
- M.V. Zamoryanskaya, A.N. Trofimov, K.N. Guliaeva** 169
Cathodoluminescence of wide gap crystals doped with rare earth ions
- K. Zhuravlev, V. Tsaryuk, V. Zolin, A. Vologzhanina** 170
Luminescent properties of lanthanide carboxylates under tunable distortions of Ln^{3+} coordination polyhedron

Akhmetzyanov D.A. 24
 Aminov L.K. 25
 Andreev S.V. 107, 157,
 Andronenko S.I. 27, 28
 Anghel S. 29, 43
 Arsentyev D.V. 59
 Asatryan H.R. 31, 32
 Badalyan A.G. 35
 Baibekov E.I. 36
 Baranov P.G. 145
 Baryshnikov V.I. 39
 Basun S.A. 79
 Belançon M.P. 26, 151
 Bentlage M. 91
 Bezmaternykh L.N. 42
 Boldyrev K.N. 42, 150
 Bol'shuhin V.A. 149
 Boulon G. 26, 29, 43, 148
 Burakov B.E. 89
 Chanelière T. 44
 Chauvat D. 119
 Chernyshev V.A. 46, 47, 61
 Chukalina E.P. 48, 49, 60
 Churpita O. 140
 Damon V. 44
 Dejneka A. 140
 Dhallenge G. 102
 Druzhinin A.V. 140
 Dudar' S.S. 54
 Dujardin C. 59
 Efimov A.M. 51
 Eremin M.V. 53
 Eron'ko S.B. 130
 Falin M.L. 56
 Fazlizhanov I.I. 133
 Feofilov S.P. 59
 Fokin A.V. 163
 Gafurov M.R. 36
 Galashov E.N. 120
 Galkin A.S. 60
 Gastev S.V. 46, 61
 Gilyazov L.R. 63
 Golubkov V. 33, 97
 Gordeev E.Yu. 107, 159
 Gorlov D.A. 66
 Gorokhovskiy A.A. 50
 Gruzdev N.B. 140, 141, 142
 Güdel H. U. 73
 Guliaeva K.N. 69, 169
 Gurin A.S. 35
 Guyot Y. 26, 75, 108, 151
 Amans D. 43
 Andrade L. 26, 151
 Andronenko R.R. 27, 28
 Angervax A.E. 131, 135
 Anikeenok O.A. 30
 Artyomov M.Yu. 163, 164
 Aseev V.A. 33, 34, 97, 105
 Baesso M. 26, 148
 Baranov A.N. 141
 Barbara B. 38
 Basiev T.T. 40, 111, 125
 Bednarkiewicz A. 153
 Belsky A. 118
 Bento A. 26
 Blake G.R. 167
 Bolondz A.V. 39
 Bonarota M. 44
 Brenier A. 151
 Caillat L. 119
 Chani V. 43
 Chen Y. 165
 Choi J.K. 61
 Chunaev D.S. 93
 Colin C. 167
 Deisenhofer J. 53
 Demidenko V.A. 130
 Doroshenko M.E. 40
 Duan Chang-Kui 72
 Dudnikova V.B. 24, 168
 Dziashko Y.A. 50
 Epicier T. 43
 Ermolaev V.L. 54, 156
 Ershova A.A. 25
 Fayzullin M.A. 53
 Fedorenko S.G. 57
 Firsin A.A. 65
 Gacoin T. 59
 Gain S.D. 130
 Galinetto P. 35
 Garcia Villora E. 96
 Gerasimov K.I. 56
 Glushkov N.A. 111
 Gonchar L.E. 65
 Gorlov A.D. 66
 Gorokhova E.I. 130
 Grimm J. 73
 Gubaev A.I. 152
 Gudkov V.V. 67
 Gurin A.A. 31
 Guseva V.B. 160
 Hajj B. 119

Hanuza J. 32
 Hreniak D. 153
 Hubicka Z. 140
 Ignatiev A.I. 51, 105
 Isaenko L.I. 75
 Ivanova S.E. 74, 75, 77
 Joubert M.-F. 75, 108
 Kalashnikova A.M. 79, 123
 Kant Ch. 53
 Karpov A.M. 81
 Kärner T. 94
 Khramtsov V.A. 31
 Kirm M. 96, 143
 Kirysheva S.A. 107
 Klokishner S. 29
 Kolobkova E. 33, 34, 97, 105
 Korableva S.L. 25, 84, 86, 99, 107, 108, 116, 159, 166
 Koryakina E.Yu. 84, 86, 159
 Kozlenko D.P. 65
 Krasnikov A. 154
 Kudryavtseva I. 94
 Kuleshov N. 34
 Kulyuk L. 29
 Kuzmenko A.B. 83
 Kynast U. 91, 92
 Lauro R. 44
 Leonidov I.I. 90
 Lezhnina M. 91, 92
 Lichmanova V.N. 149
 Loidl A. 53
 Lukanin V.I. 93
 Lummen T. 102
 Lushchik Ch. 94
 Maczka M. 32
 Maksimova T.I. 32
 Mamin G. V. 36
 Marciniak L. 153
 Mavrin B.N. 42
 Meltzer R.S. 59
 Merzliakov M.A. 120
 Mihailovic D. 167
 Mill B.V. 60
 Mokhov E.N. 145
 Moskvina A.S. 79, 98, 123
 Mumdzhi I.E. 99
 Mysovsky A.S. 101, 113
 Naumov A.K. 84, 86, 107, 116, 159, 166
 Nazemnykh A.D. 46, 61
 Nikiforov A.E. 46, 47, 65
 Nikonorov N.V. 33, 34, 51, 97, 105, 137
 Novatski A. 26
 Nurtdinova L.A. 108, 116
 Hizhnyakov V. 71
 Hu L. 72
 Hughes-Currie R. 73
 Ilyin I.V. 145
 Ivachev A.N. 164
 Jastrabik L. 35, 139, 140
 Jurdyc A.M. 151
 Kamenskikh I. 118
 Karasik A.Ya. 93
 Kaschenko M.A. 48
 Khaidukov N.M. 56
 Kim A.A. 105
 Kirpichnikov A.V. 120
 Klimin S.A. 60, 83, 102, 115
 Kolobanov V.N. 162
 Konovalov A.A. 24
 Korchagin E. 33, 97
 Koryakina L.F. 135
 Kramushchenko D.V. 31
 Krupin A.V. 61
 Kudykina T.A. 87
 Kulinkin A.B. 59
 Kurkin I.N. 25, 36
 Kuznetsova Ya.V. 89
 Laguta V.V. 139
 Le Gouët J.-L. 44
 Leskova Yu.V. 65
 Lichkova N.V. 133
 Lima S. 26, 151
 van Loosdrecht P.H.M. 102
 Lukowiak A. 153
 Lushchik A. 94
 Lyssenko K.A. 127
 Makhov V.N. 96, 143
 Malkin B.Z. 25, 56, 83, 96, 150
 Mancini C. 43
 Marisov M.A. 166
 Medina A.N. 151
 Mengbing Huang 50
 Mialon G. 59
 Mikhlin S.B. 130
 Mirzaeva A. 74
 Moskaleva K. 33, 34, 97
 Mozzati M.C. 35
 Myasnikova A. 101
 Narozhnyy M.V. 102
 Nazarov M.V. 157
 Neto A. 26
 Nikitin S.I. 63, 99, 103
 Nizamutdinov A.S. 107, 116, 166
 Nugroho A.A. 79
 Ogorodnikov I.N. 109, 110

Okhrimchuk A.G. 133
 Paklin A.S. 113
 Panfilov V.A. 115
 Pavlov V.V. 116, 123
 Pekareva I.S. 127
 Peretti R. 151
 Pestryakov E.V. 120
 Petrov V.V. 120
 Pisarev R.V. 48, 79, 121, 123
 Plotnichenko V.G. 162
 Popova M.N. 48, 60, 83, 102, 124, 150
 Postnikov E.S. 51
 Potapov A.V. 115
 Prosekina E.A. 128
 Pukhov K. K. 125
 Pustovarov V.A. 141, 142
 Radzhabov E.A. 101, 128, 136, 138
 Randoshkin V.V. 162
 Reid M.F. 72, 73, 129
 Rodnyi P.A. 130
 Ruggiero J. 44
 Ryskin A. 131, 135
 Salikhov K.M. 132
 Sannikova D.V. 39
 Savikhin F. 94
 Semashko V.V. 84, 86, 107, 108, 116, 159, 166
 Shakurov G.S. 133, 134
 Shalapska T. 154
 Shcheulin A.S. 131, 135
 Shershnev P. 105
 Shlegel V.N. 120
 Sidorov A.I. 105
 Siraev A.D. 161
 Sizova T.Y. 138
 Sokolov N.S. 46, 61
 Sokolov V.I. 140, 141, 142
 Soltamov V.A. 145
 Soshchin N.P. 147, 149
 Stanislavchuk T.N. 150
 Strek W. 153
 Subacheva I.N. 103, 155, 168
 Surat L.L. 90
 Sushkevich K. 29
 Syrnikov P.P. 155
 Tarakina N.V. 90
 Tkachuk A.M. 74, 75, 77
 Tongning R.C. 44
 Trofimov A.N. 69, 89, 157, 169
 Tsaryuk V. 170
 Tselischev D.I. 84, 86, 159
 Ulanov V.A. 161
 Vasil'chenko E. 94
 Orlovskii Yu.V. 57, 111, 125
 Palstra T.T.M. 79, 167
 Pashyk I. 154
 Pedrini C. 110
 Pellé F. 74, 75, 77, 119
 Pervak A.I. 87
 Petrosyan A. 118
 Petrova M.A. 135
 Platonova A.V. 162
 Poletaev N.K. 139
 Poryvay N.E. 109, 110
 Potapov A.P. 163, 164
 Potucek Z. 139
 Przhhevuskii A.K. 137
 Puntus L.N. 127
 Pytalev D.S. 49
 Rakhmatullin R.M. 36
 Rasing Th. 79
 Rodionov A.A. 25, 155, 168
 Rosa J. 35
 Ryabchikov Yu.V. 162
 Salakhov M.Kh. 155, 168
 Samsonova E.V. 57, 111
 Sargsyan R.V. 118
 Sedunova I.N. 109, 110
 Semenova T.S. 135
 Shalaev A.A. 113
 Shcherbakova T.A. 134
 Shendrik R. 136
 Shimamura K. 96
 Shustov V.A. 133, 134
 Silkin N.I. 168
 Sitdikov V.M. 137
 Skvortsov A.P. 139
 Sokolov P.S. 141
 Solovyev O.V. 96, 143
 Soltamova A.A. 145
 Spassky D.A. 162
 Steimacher A. 26, 151
 Stryganyuk G. 96, 143, 154
 Sukhanov A.A. 132
 Surikov V.T. 142
 Sveshnikova E.B. 54, 156
 Tadili A. 119
 Tarasov V.F. 24, 132, 168
 Tolmachev A.V. 109, 110
 Trepakov V.A. 35, 139, 140, 155
 Trunov V.I. 120
 Tsekhomsky V. 105
 Tyutyunnik A.P. 90
 Usacheva V.P. 89
 Vasiliev J.V. 120

Vasilieva N.V. 162
Vikhnin V.S. 32
Vologzhanina A. 170
Wei X. 165
Xia Shangda 72
Yasukevich A. 34
Yin M. 72, 165
Yunusova A.N. 166
Zagorodnev V.N. 133
Zakharchenya R.I. 59
Zaripov M.M. 161
Zaytsev A.A. 157
Zhang W. 165
Zhao W. 43
Zhevstovskikh I.V. 67
Zolin V. 170
Zuev M.G. 81
Vazhenin V.A. 163, 164
Volodin V.P. 47
Voloshinovskii A. 154
Wiglusz R.J. 153
Yakovlev V.Yu. 110
Yavetskiy R.P. 109, 110
Yoshikawa A. 43
Yusupov R.V. 103, 155, 167, 168
Zaitsev A.M. 50
Zamoryanskaya M.V. 69, 89, 157, 169
Zaripov R.B. 132
Zazubovich S. 154
Zhao J. 165
Zharikov E.V. 24, 132, 168
Zhuravlev K. 170
Zubkov V.G. 90
Zyss J. 119

**XIV Международный Феофиловский симпозиум по спектроскопии кристаллов,
активированных ионами редкоземельных и переходных металлов**

Тезисы докладов
(Санкт-Петербург, октябрь, 18-21, 2010)

Технический редактор А.С. Рохмин
Дизайн Е.И. Попова

Редакционно-издательский отдел СПб ГУИТМО
Лицензия ИД №00408 от 05.11.99. Отпечатано на ризографе. Тираж 150 экз.
Заказ № 2259
Подписано в печать 06.10.10